Groundwater Dynamics in Hard Rock Aquifers

Sustainable Management and Optimal Monitoring Network Design

Edited by
SHAKEEL AHMED
RAMASWAMY JAYAKUMAR
ABDIN SALIH

Springer

Groundwater Dynamics in Hard Rock Aquifers

Groundwater Dynamics in Hard Rock Aquifers

Sustainable Management and Optimal Monitoring Network Design

Edited by

Shakeel Ahmed
NGRI, Hyderabad, India

Ramaswamy Jayakumar
UNESCO Office, Beijing, P.R. China

Abdin Salih
UNESCO Office, Tehran, Iran

Springer

A C.I.P. Catalogue record for this book is available from the Library of Congress.

ISBN 978-1-4020-6539-2 (HB)
ISBN 978-1-4020-6540-8 (e-book)

Copublished by Springer,
P.O. Box 17, 3300 AA Dordrecht, The Netherlands
with Capital Publishing Company, New Delhi, India.

Sold and distributed in North, Central and South America by Springer,
233 Spring Street, New York 10013, USA.

In all other countries, except India, sold and distributed by Springer, Haberstrasse 7, D-69126 Heidelberg, Germany.

In India, sold and distributed by Capital Publishing Company,
7/28, Mahaveer Street, Ansari Road, Daryaganj, New Delhi, 110 002, India.

www.springer.com

Cover illustration: Typical dug well in granitic hard rock terrain at Maheshwaram, Andhra Pradesh. Photograph taken by Dr. Shakeel Ahmed.

Printed on acid-free paper

All Rights Reserved
© 2008 Capital Publishing Company
No part of this work may be reproduced, stored in a retrieval system, or transmitted in any form or by any means, electronic, mechanical, photocopying, microfilming, recording or otherwise, without written permission from the Publisher, with the exception of any material supplied specifically for the purpose of being entered and executed on a computer system, for exclusive use by the purchaser of the work.

Printed in India.

Preface

Groundwater is of utmost importance in the arid and semi-arid environment. The areas in such regions are forced to face a variety of problems regarding groundwater as it is the main source of water no matter for any use viz., drinking, domestic, irrigation or industrial particularly for the rural population. The main challenges in hard rock areas in the semi-arid region are the water conservation, management and planning of the water resources. This is further complicated with several complexities of the geological formation. With the semi-arid environment, complex geological settings and over shooting stresses, the aquifer system becomes extremely fragile and sensitive. In spite of a good amount of research in this field, it is still needed to understand the behaviour of such complex system precisely and also apply the result in reasonably larger scales. Therefore, the present research is focused on improving the knowledge on the structure and functioning of the aquifer system in hard rock terrain.

An Indo-French Centre for Groundwater Research (IFCGR: www.ifcgr.net) set-up at the National Geophysical Research Institute (NGRI: www.ngri.org.in) in collaboration with Bureau de Recherche Géologiques et Minières (BRGM: www.brgm.fr), France has realized the need and set goal to study the hard rock aquifers for the groundwater flow and management particularly at local to medium scale. The centre has developed specific methods to:

- determine the geometry and extent of aquifers,
- estimate aquifer parameters and characterize the aquifer system,
- estimate recharge and irrigation returns as input to the aquifer system,
- estimate various parameters at the unmeasured locations and optimal monitoring network design,
- calculate the groundwater balance and simulate the groundwater flow and
- evolve the strategies for sustainable management of the ground water.

With a considerable amount of research and identifiable output, it was thought to share the findings and transfer the knowledge to other organizations and researchers in this field. The research work carried out by taking a pilot area on different aspects of groundwater management have been compiled and presented here in the book. A couple of state-of-the-art papers were included and the gaps were filled by adding a few more articles of relevance. Publication of this book will add value to the present readings in the subject

and complete a milestone in the hard rock hydrogeology. The book starts with a couple of general articles introducing the IHP of UNESCO and water scenarios in India and then the basic knowledge on the hard rock hydrogeology as well as an overview of the work carried out at the Indo-French Centre for Groundwater Research, Hyderabad. The later articles are all technical depicting mostly the case studies on hydrodynamics of the hard rock aquifers with a brief theory on the applications of geostatistical methods as well as Aquifer Modelling.

The editors extend their sincere thanks to all the contributors and IFCPAR, New Delhi as well as UNESCO who have provided funding for the research projects whose results are embedded here. Editors are thankful to Prof. G. de Marsily, Ex-professor of Hydrogeology at the University of Pierre and Marie Curie, Paris, France for critically reviewing the book.

Shakeel Ahmed
Ramaswamy Jayakumar
Abdin Salih

An Introduction to UNESCO's International Hydrological Programme

Abdin Salih*

The United Nations Organization for Education, Science, and Culture (UNESCO) established International Hydrological Programme (IHP) in 1975, as the single intergovernmental programme of the UN system devoted to scientific study of the hydrological cycle and to formulating strategies and policy for the sustainable management of water resources.

IHP was conceived as an evolving programme, ready to adapt to society's needs and transformations. The Programme is implemented in phases of six years, in order to remain prompt in identifying new, emerging problems, alerting decision makers, raising public awareness and providing the necessary resources to respond with action.

The first phase, IHP-I, lasted from 1975 to 1980. IHP-II, on the other hand, was of a shorter duration (1981-1983). This was to enable the Programme to fit in with the timing of the Medium Term Plan of UNESCO.

IHP-I was mainly research-oriented following the International Hydrological Decade. However, in response to the concerns of Member States, the next phases were oriented to include practical aspects of hydrology and water resources. Hence IHP-II (1981-1983) and IHP-III (1984-1989) were planned under the theme Hydrology and the Scientific Bases for Rational Water Resources Management. The theme chosen for IHP-IV (1990-1995) was: "Hydrology and Water Resources Sustainable Development in a Changing Environment". IHP-V (1996-2001) was devoted to the theme: "Hydrology and Water Resources Development in a Vulnerable Environment".

In the development of its various phases, IHP has gone through a profound transformation from a single discipline to a multi-disciplinary programme. Recently, with the increased presence of the social science component, IHP has become a truly inter-disciplinary programme, capitalizing on the recognition that the solution of the world water problems is not just a technical issue.

*Director and Representative, UNESCO Office, Tehran, Iran

UNESCO's intergovernmental scientific cooperative programme in hydrology and water resources is presently the only broadly based science programme of the UN system in this area. It was established because both the international scientific community and governments, realizing that water resources are often the primary limiting factors for the peaceful development in many regions and countries of the world, saw the need for an internationally coordinated scientific programme focusing on water. It has had a prime role as a catalyst in promoting cooperation in water science and water resources management.

Today, integrated water resources management poses scientific, technical, socioeconomic, cultural and ethical challenges. IHP is a multidisciplinary programme at the forefront of assuming these challenges. To this end, IHP is a prominent UNESCO vehicle for meeting the UN Millennium Goals.

The current phase of IHP, IHP-VI, covering the period 2002-2007, is devoted to "Water Interactions: Systems at Risk and Social Challenges". The sixth phase of IHP emphasizes societal aspects of water resources. However, this emphasis should not be interpreted as the replacement of the primary concern: to study the occurrence and distribution of water within the natural environment.

The incorporation of the social dimension underlines the need for improved, more efficient management of water resources and the more accurate knowledge of the hydrological cycle for better water resources assessment. So far, water has been managed in a fragmented way. Surface water and groundwater are considered separately in development activities without due recognition of their interdependence. Water resources in many places are still not managed in conjunction with land resources. Water supply schemes, eventually generating large amounts of waste water in consumer areas, are normally designed and built, especially in developing countries, without the required matching drainage networks and waste water treatment facilities. Quantity is generally managed separately from quality, as is water science and water policy. This fragmentation of approach also impedes coherent hydrological analyses at regional, continental and global scales.

IHP-VI (2002-2007) has been based on the fundamental principle that fresh water is as essential to sustainable development as it is to life and that water, beyond its geophysical, chemical, biological function in the hydrological cycle, has social, economic and environmental values that are inter-linked and mutually supportive.

The launching of IHP-VI coincides with the emergence of a profound paradigm shift in society's approach towards water. As far as the management of this resource is concerned, it is documented in the call for integrated water resources management. Research to support integrated water resources management should also be integrated. This implies not only more inter- and multi-disciplinary approaches but also more co-operation and partnership in executing research programmes. In this regard, water-related activities of

intergovernmental organizations (IGOs) should co-operate and be co-ordinated with the programmes of non-governmental organizations (NGOs). It is expected that this synergy could be the most important basis to successfully implement IHP-VI.

In line with the above-mentioned comprehension of water interactions, technological development of data acquisition and improved modelling of processes and interactions, the relevant IHP-VI topics on hydrologic research, water resources management and education are framed under five themes. The transition and interaction from the global scale to the watershed scale being the overall driving force for the consideration of the complex relationships between water and society and the overall need for knowledge, information and technology transfer.

Theme 1 - Global Changes and Water Resources
Theme 2 - Integrated Watershed and Aquifer Dynamics
Theme 3 - Land Habitat Hydrology
Theme 4 - Water and Society
Theme 5 - Water Education and Training

Two crosscutting programme components: FRIEND (Flow Regimes for International Experimental and Network Data) and HELP (Hydrology for Environment, Life and Policy) have been identified that, through their operational concept, interact with all themes.

Besides the obvious symmetry with FRIEND, HELP is conceived to be funded entirely from extra-budgetary or external financial sources. This structure accounts first of all for the considerably higher financial requirement and longer time scale of HELP projects than for the ones in the regular IHP time and budget framework. However, it is fully considered as an integrated part of IHP-VI (and beyond) as far as scientific objectives, approach and result dissemination is concerned.

A pilot project on "Analyses of Geochemical Contamination in Groundwater including monitoring network design in hard rock aquifer systems" was taken up as part of IHP-VI Theme II - Integrated Watershed and Aquifer Dynamics, in collaboration with Indo-French Centre for Groundwater Research jointly sponsored by National Geophysical Research Institute, India and BRGM of France. Under this project a large number of experiments have been conducted to thoroughly investigate the area. The information gathered from the field has been interpreted by different methods to establish the best and suitable technique to be applied. Extensive application of aquifer modeling and geostatistics were made to make the study versatile. A few new techniques have developed particularly the geostatistical monitoring network design etc. A project on the groundwater management in this weathered-fractured aquifer has been completed and refining of the model with the additional data and for further research particularly unsaturated

zones are continuing. I believe our collaboration with this centre will go a long way in implementing IHP priorities.

UNESCO and IFCGR is planning to create a network of scientists from Asian region and around the world on "Groundwater Monitoring Network Optimization for hard rock areas" to bring all the scientists working in this area together to create a monitoring network design which is the backbone of any development activities in the hard rock aquifer system. I hope through this initiative this region as well the whole world will be benefited in terms of groundwater monitoring in the hard rock aquifer systems.

World Water Assessment Programme is one of the recent initiatives of all UN Agencies in the field of water. This UN-wide programme seeks to develop the tools and skills needed to achieve a better understanding of those basic processes, management practices, and policies that will help improve the supply and quality of global freshwater resources. The United Nations system is complex. It is not easy to explain what each agency and programme does, since each one has its own priorities and procedures. Under this common banner, they have agreed to work together—sharing information, knowledge and know-how—to improve our understanding of the policies and practices that encourage sustainable use of water resources.

We in UNESCO-IHP have now started preparing the themes for IHP Phase VII (2008-2013), and the consultation with member states has started. I request all the scientists and engineers participating in this workshop to consult their respective IHP committees after this training to critically evaluate the priorities and proposals. The Task Force suggests the following four themes for IHP-VII:

Theme I: Global Changes, Watersheds and Aquifers
Theme II: Governance and Socio-Economics
Theme III: Water and Environmental Management
Theme IV: Water Quality, Human Health and Food Security

Finally, the challenge we all have is **"How to put water in the minds of people?"** Let us work together to solve the world's most important problem of water in the coming years. Let me conclude my introduction with a quote from former President J. F. Kennedy **"Anybody who can solve the problems of water will be worthy of two Nobel Prizes, one for peace and one for science".**

About the Editors

Dr. Shakeel Ahmed

Dr. Shakeel Ahmed (born 1958), basically a geophysicist from India, completed his higher studies at Paris School of Mines, France and obtained degrees of DEA and Doctorate as well as Diploma in Geostatistics. Presently serving as Deputy Director of National Geophysical Research Institute, Hyderabad, Dr. Ahmed started his research career by working on an advanced subject of aquifer modelling for groundwater management and geostatistics as well.

He is presently heading the Indian team at the Indo-French Centre for Groundwater Research (IFCGR), an advanced research centre (www.ifcgr.net) where scientists of NGRI, India and BRGM, France are committed for research in hard rock hydrogeology. With about 50 research papers in various journals and many proceedings to his credit, he has edited five published proceedings of international conferences.

Dr. Ahmed is recipient of the Young Scientist Award in physical sciences for the year 1996 from MAAS as well as International Prize of Water Sciences of 2004 awarded by the Cannes Water Symposium, France. He has served as elected secretary of the Indian National Committee of the International Association of Hydrogeologists for about 10 years. Dr. Ahmed is presently associate editor of the *Hydrogeology* journal and member of the editorial board of International Journal of Chemical and Environmental Research.

Dr. Ramaswamy Jayakumar

Dr. R. Jayakumar has obtained Ph.D. in Hydrogeology with post-doctoral experience in conjunctive use of surface and ground water for irrigation. He has specialised in application of remote sensing, GIS and geo-statistics in hydrogeological modelling with a special training in related fields from Osaka City University, Japan. Having worked for the UNESCO, New Delhi, looking after hydrology, and coastal and small islands programmes, he served as a Hydrogeologist with Ford Foundation Project in Anna University, Chennai and later with WS Atkins International Limited, Cambridge, UK in Irrigation Projects funded by Commission of European Communities. At present he is working in UNESCO Beijing office, P.R. China, looking after the Science and Technology programme of UNESCO.

Dr. Abdin Salih

Dr. Abdin Salih, obtained his Ph.D from the Imperial College of Science and Technology, University of London (U.K), 1972. His field of interest is environmental sciences, particularly hydrology (including groundwater), hydraulics, and water/land resources management under arid conditions.

He has worked extensively in renowned universities like University of Padova, Italy; Colorado State University, USA and King Saudi University in Riyadh. He has served as an advisor in many large national water and environmental research projects.

Dr. Salih is a serving member of UNESCO's Advisory Board of the Great–Man-Made River of Libya (1990 to date); and led a multidisciplinary team in 1986-1990 to study and solve the engineering and environmental problems related to the rising groundwater beneath the City of Riyadh (Saudi Arabia). He has contributed over 75 papers and chapters in books, various journals and proceedings of referred conferences and prepared over 30 technical reports. He has served in the editorial board of many national and international journals.

One of his major achievements is the establishment of considerable visibility and remarkable respectability to UNESCO's International Hydrological Programme (IHP) and to its Man and the Biosphere (MAB) programme. Since June 1999 till date, he has been serving as Deputy Secretary of the IHP at UNESCO's Headquarters in Paris. In this capacity, he participated in the shaping of the phase six of IHP (2002-2007) and contributed to many new initiatives, including the UN-wide World Water Assessment Programme, the establishment of the IHE of Delft as a UNESCO-IHE Institute of Water Education, and the Regional Centres in Cairo, Tehran and Chile. He has also been instrumental in securing extra-budgetary contributions to IHP, particularly the over $2.3 millions Flanders Fund in Trust Support to FRIEND/Nile, Palestinian Territories, South Africa and Chile projects. Since January 2003 he continues to hold the post of Director of UNESCO Tehran Office.

Contents

Preface *v*

An Introduction to UNESCO's International Hydrological Programme
Abdin Salih *vii*

About the Editors *xi*

1. Hydrogeological Research in India in Managing Water Resources
K.D. Sharma and Sudhir Kumar 1
2. Nature of Hard Rock Aquifers: Hydrogeological Uncertainties and Ambiguities
B.B.S. Singhal 20
3. Overview of the Hydrogeology of Hard Rock Aquifers: Applications for their Survey, Management, Modelling and Protection
P. Lachassagne 40
4. Geophysical Characterization of Hard Rock Aquifers
N.S. Krishnamurthy, Subash Chandra and Dewashish Kumar 64
5. Application of Remote Sensing and GIS in Groundwater Exploration
S.K. Nag 87
6. Pumping Tests: Planning, Preparation and Execution
K. Subrahmanyam and Haris H. Khan 93
7. Various Pumping Tests and Methods for Evaluation of Hydraulic Properties in Fractured Hard Rock Aquifers
J.C. Maréchal, B. Dewandel, K. Subrahmanyam and R. Torri 100
8. Analyses of Aquifer Parameters from Different Hydraulic Tests and Their Scale Effect
J.C. Maréchal, Faisal K. Zaidi and B. Dewandel 112

9. Upscaling of Slug Test Hydraulic Conductivity Using Discrete Fracture Network Modelling in Granitic Aquifers
Dominique Bruel, Faisal K. Zaidi and C. Engerrand 123
10. Groundwater Balance at the Watershed Scale in a Hard Rock Aquifer Using GIS
J.C. Maréchal, L. Galeazzi and B. Dewandel 134
11. Water Budgeting and Construction of Future Scenarios for Prediction and Management of Ground Water under Stressed Condition
Faisal K. Zaidi, Benoît Dewandel, Jean-Marie Gandolfi and Shakeel Ahmed 142
12. Applying Geostatistics: Basic Knowledge and Variographic Analysis with Exercises
P.S.N. Murthy, Tanvi Arora and Shakeel Ahmed 150
13. Kriging for Estimating Hydrogeological Parameters
Shakeel Ahmed and K. Devi 172
14. Application of Geostatistics in Optimal Groundwater Monitoring Network Design
Shakeel Ahmed, Dewashish Kumar and Aadil Nabi Bhat 179
15. Reconstruction of Water Level Time Series in an Aquifer Using Geostatistical Technique
Dewashish Kumar and Shakeel Ahmed 191
16. Governing Equations of Groundwater Flow and Aquifer Modelling Using Finite Difference Method
Shazrah Owais, S. Atal and P.D. Sreedevi 201
17. Simulation of Flow in Weathered-Fractured Aquifer in a Semi-Arid and Over-Exploited Region
Shakeel Ahmed and P.D. Sreedevi 219
18. Regional Simulation of a Groundwater Flow in Coastal Aquifer, Tamil Nadu, India
L. Elango and C. Sivakumar 234
19. Hydrogeology of Hard Rock Aquifer in Kashmir Valley: Complexities and Uncertainties
G. Jeelani 243

Index *249*

1 Hydrogeological Research in India in Managing Water Resources

K.D. Sharma and Sudhir Kumar

National Institute of Hydrology, Roorkee 247667, India

INTRODUCTION

India is a vast country with a total geographical area of about 3.28×10^6 km^2. Due to diversified geological, climatological and physiographic setup, groundwater situations in different parts of the country are divergent. Uneven distribution of surface water in space and time, man's interference, and over-exploitation of groundwater have caused regional imbalances in the supply and demand of water both in the alluvial tract of north India and in the hard rock formations of Peninsular India. The total annual water resources of India are about 1960 km^3. The utilizable water resource is 1140 km^3 (690 km^3 from surface water and 450 km^3 from groundwater). The present utilization is 750 km^3 (500 km^3 from surface water and 250 km^3 from groundwater). The projected demand for the year 2025 is 1050 km^3 indicating that by that point of time the total available water resources have to be put to use.

Groundwater has to fulfill about 33% of the water demand by the year 2025. Availability of groundwater varies from free flowing wells in parts of Indo-Gangetic plains to deep aquifers (>100 m) in Rajasthan depending on the hydrogeological conditions. Also, availability of groundwater in hard rock areas depends on the thickness of weathered material and fractures and fissures.

In view of the above, there is a need to understand the distribution and occurrence of groundwater in different hydrogeological situations. In this article, the hydrogeological setup of the country and occurrence of groundwater in different geological formations have been presented. Also, the research carried out in the areas of groundwater recharge, water quality and remote sensing and GIS have also been included.

WATER RESOURCES OF INDIA—AVAILABILITY AND DEMANDS

The present population of India is about 105 billion. It has mainly tropical climate but certain parts of the country in the west and in the peninsular region have semi-arid to arid climate.

India is bestowed with large resources of surface water and groundwater. However, their distribution both in space and time is highly variable due to the monsoon type of climate. The average annual rainfall is of the order of 1170 mm which brings about 4000 km^3 of water and about 200 km^3 flows in from the neighbouring countries. Evapotranspiration rates are high causing a total loss of about 1820 km^3 of water to the atmosphere. A water balance prepared by the National Commission of Agriculture is given in Fig. 1. The total water resources of all the river basins in the country are about 1869 km^3. Due to topographic limitations, only about 690 km^3 of water is considered as utilizable flow, out of which at present only about 500 km^3 is being used. The rest presently flows down unused either through surface flow or via groundwater to the oceans.

The maximum utilization of surface water is in Indus, Krishna, Kaveri, Sabarmati and Mahi river basins, while that in Ganga, Brahmaputa, Mahanadi and Narmada is low. Out of 1869 km^3 annual surface water potential, as much as 585.6 km^3 or 31.1% is in Brahmaputra Basin where due to non-availability of sufficient irrigable land only 24 km^3 is considered utilizable.

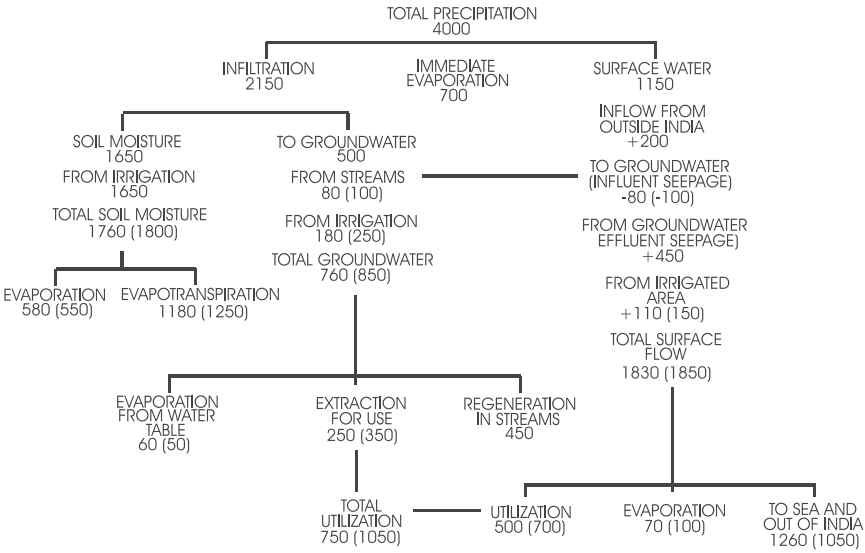

Figure 1. Approximate annual water resources of India in 2000 and 2025 AD (in km^3). The values in brackets are those anticipated for 2025 AD (Singh, 1997).

The river Brahmaputra carries more water per unit area of the basin than any other river in the world and is also one of the major sediment transporting rivers of the world, second only to the Yellow River of China.

The utilizable annual water resources of India are about 1140 km^3 out of which 690 km^3 is from surface water and 450 km^3 from groundwater sources. The utilization for the year 2000 and the projected annual demands of water for the year 2025 are given in Table 1.

Table 1: Estimates of Annual Water Demand and Water Distribution in India (in km^3)

Sl. No.	*Purpose*	*Year 2000*	*Year 2025*
Annual Water Demand			
1.	Domestic use	33	52
2.	Industrial	30	120
3.	Energy	27	71
4.	Irrigation	630	770
5.	Other uses	30	37
	Total	750	1050
Annual Water Distribution			
	Surface water	500	700
	Groundwater	250	350

(*Source:* Singh, 1997)

Table 1 indicates that out of total water utilized in the country, 84% is used for irrigation, about 4.4% for drinking and municipal use, 4% for industry, 3.6% for energy development and the remaining 4% for other purposes. Table 2 also shows that nearly the entire utilizable water resources of the country would be required to be put to use by the year 2025.This is mainly on account of increased demand of water for irrigation required to grow more food grain for the increasing population which is estimated to reach about 1.25 billion by the year 2025. Even at present there are indications of over-exploitation of groundwater as manifested by the lowering of water table in several areas. Therefore, there is an urgent need for chalking out suitable strategies for planning, development, conservation and management of available water resources in an optimal way.

GROUNDWATER RESOURCES

The assessment of water resources of the country dates back to 1949, Dr. A.N. Khosla (1949) estimated the total average annual run-off of all the river systems in India as 1674 km^3 (167.4 million hectare meter [Mham]), based on empirical formula which included both the surface and groundwaters. Since then various Working Groups/Committees/Task Force, constituted by Government of India, have made attempts to estimate the groundwater

resources of the country. But, due to paucity of scientific data and incomplete understanding of the parameters involved in recharge and discharge processes, all these estimations were tentative and at best approximation.

The National Commission on Agriculture (1976) assessed the total groundwater resources of the country as a whole, taking into account the total precipitation, its distribution, evaporation from the soil, and sub-soil percolation. The groundwater recharge was worked out from the total quantity of water that percolated into the soil. The Commission assessed the groundwater resources as 670 km^3 (67 Mham), excluding soil moisture. The usable groundwater resource was assessed as 350 km^3 (35 Mham), of which 260 km^3 (26 Mham) was considered as available for irrigation. It further worked out the ultimate irrigation potential from groundwater as 400,000 km^2 (40 Mha) based on utilizable groundwater resource of 260 km^3 (26 Mham) and an average requirement of 0.65 hectare meter depth of groundwater to irrigate a cropped hectare, in contrast to 0.90 hectare meter of surface water, as conveyance losses are higher in the latter case.

This was the first exercise for conversion of the volume of groundwater to the area to be irrigated. The water requirement of crops was based on the average depth of gross irrigation application at the source per crop hectare.

The first attempt to estimate the groundwater resources on scientific basis was made in 1979. Agriculture Refinance and Development Corporation constituted a High Level Committee, Ground Water Over Exploitation Committee to recommend definite norms, for groundwater resources computations. Based on these norms the State Governments and the Central Ground Water Board computed the gross groundwater recharge as 467.90 km^3 (46.79 Mham) and the net recharge (70% of the gross) as 324.9 km^3 (32.49 Mham). This committee had, however, recommended that the methodology be revised with increasing availability of data.

Subsequently, Government of India constituted another committee to go into various aspects of the problems of the groundwater development. This committee examined in depth a large volume of hydrogeological and related data generated by the Central Ground Water Board through nation-wide surveys, exploration and 12 water balance projects, completed till then, and area oriented studies carried out by the State Ground Water Organizations. The Ground Water Estimation Committee came up with a revised methodology for assessment of groundwater potential and evolved new norms in 1984. Based on these norms the annual replenishable groundwater resources of the country were worked out to be 453.30 km^3 (45.33 Mham). Keeping a provision of 15% (69.8 km^3) for drinking, industrial and other uses the utilizable groundwater resource for irrigation was computed 383.40 km^3 (38.34 Mham) per year. The ultimate irrigation potential in terms of area based on the state-wise assessment was estimated as 80.38 Mha. In this assessment, the irrigation requirement varies from 0.36 m/ha in Uttar Pradesh to 1.20 m/ha in Assam. Even in individual states, a range of values of

irrigation requirement was considered viz. 0.36 to 0.937 m for Tamilnadu, 0.4 to 0.75 m for Maharashtra, etc.

Ministry of Water Resources, Government of India, revised the groundwater resources in 1995. According to the report, the total rechargeable groundwater resources in the country are computed as 43.19 m.ha.m. The available groundwater resource for irrigation is 36.08 m.ha.m, of which the utilizable quantity is 32.47 m.ha.m. The utilizable irrigation potential of the country has been estimated as 64.05 m.ha., based on crop water requirement and availability of cultivable land. The stage of groundwater development is estimated as 55.23% based on irrigation potential created in the country (35.38 m.ha.). Basin wise groundwater potential is given in Table 2.

Table 2: Basin-wise Ground Water Potential of India

Sl. No.	*Name of Basin*	*Total Replenishable Ground Water Resources (km^3)*
1.	Brahmai with Baitarni	4.05
2.	Brahmaputra	26.55
3.	Cambai Composite	7.19
4.	Cauvery	12.30
5.	Ganga	170.99
6.	Godavari	40.65
7.	Indus	26.49
8.	Krishna	26.41
9.	Kutch and Saurashtra Composite	11.23
10.	Madras and South Tamil Nadu	18.22
11.	Mahanadi	16.46
12.	Meghna	8.52
13.	Narmada	10.83
14.	Northeast Composite	18.84
15.	Pennar	4.93
16.	Subarnarekha	1.82
17.	Tapi	8.27
18.	Western Ghat	17.69
	Total	431.42

In order to establish changes in groundwater levels, Central Ground Water Board has established a network of about 15,000 stations covering various parts on the country. In addition to these, State Ground Water departments are also monitoring the water levels in their respective States. The observations for the year 1980-2000 indicate a decline of about 4 m during this period covering almost all the States. In the capital city of Delhi, a decline of more than 5 m has been reported. The overall decline in water table is due to greater demand of water for irrigation, domestic and industrial uses as well as decreasing groundwater recharge as a result of urbanization. As the pace

of development is not uniform, there are areas, which are greatly affected while in other parts the problem is not so severe.

In view of the recurring problems of drought, Government of India has launched an Accelerated Programme of Groundwater Exploration and development. Under this programme, tube wells are being drilled as "sanctuary wells", which will be used only during the drought period, as a crisis management measure exclusively for drinking water needs.

HYDROGEOLOGICAL SETUP

India is a vast country having diversified geological, climatological and physiographic setup, giving rise to divergent groundwater situations in different parts of the country. The rocks, which control the movement of groundwater, vary in age from Archean to Recent and also vary widely in composition and structure. The landforms vary from rugged mountains of the Himalayas to flat alluvial plains of rivers and coastal tracts, and the aeolian deserts of Rajasthan. The rainfall also varies from <100 mm in parts of Rajasthan to >10,000 mm in Meghalaya. The topography and rainfall virtually control the surface runoff and consequently the groundwater recharge. Fig. 2 shows the major aquifers in India.

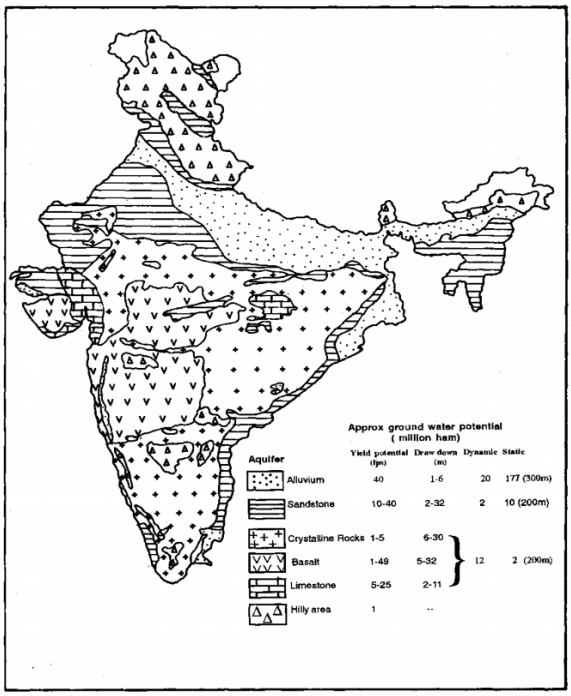

Figure 2. Distribution of major aquifers in India (*Source:* Raju, 2003).

The large alluvial tract in the Sindhu-Ganga-Brahmaputra plains, extending over a distance of 2000 kms from Punjab in the west to Assam in the East, constitute one of the largest and most potential groundwater reservoirs in the world. These aquifer systems are extensive, thick, hydraulically interconnected and moderate to high yielding. To the north of this tract all along the Himalayan foot hills, lies the linear belt of Bhabar piedmont deposits, and the Tarai belt down slope with characteristic auto flowing conditions.

Hydrogeologically alluvial formation consists of unconsolidated sand, silt and clay with occasional beds of gravel extending to a depth of more than one km at some places. In a narrow belt in the north, at the foot of the Himalayas, artesian aquifers, under free flowing conditions exist at a depth of 50 to 100 m. Possibilities of deep confined aquifers as a potential source of water is indicated from deep drilling carried out for oil exploration at some places (Jones, 1987). The area is also bestowed with good rainfall and recharge conditions. Ground water is mainly used for irrigation in addition to domestic and other uses. Tube well irrigation is being practiced in this area from the last more than one hundred years.

The next older formation of Cenozoic age consisting of unconsolidated to semi-consolidated sandstone and shale occupy parts of coastal areas and also in the northeast. Under favourable conditions these formations form artesian aquifers as in parts of Cambay basin in the west and Neyveli in Tamilnadu in South India.

The main volcanic suite of rocks is represented by Deccan Traps occupying an area of more than 500,000 km^2 in the western and central parts of the country. A number of basaltic flow units are identified of age varying from Upper Cretaceous to Lower Eocene. Main source of groundwater is from the weathered, fractured and vesicular horizons. At places different layers of basalt form a multi-aquifer system. Parts of this area has semi-arid climate due to which recharge is limited and availability of groundwater is poor.

The Gondwanas are represented by semi-consolidated sandstone, shale and coal beds, which were deposited in the structurally controlled faulted basins. They are fresh water deposits of age varying from Permo-Carboniferous to Late Jurassic. They also form multi-aquifer system. Uncontrolled mining has resulted in the flooding of mines causing great loss of life of miners.

Most part of Peninsular India is occupied by a variety of hard and fissured formations, including Crystalline, trappean basalt and consolidated sedimentaries (including carbonate rocks), with patches of semi-consolidated sediments in narrow intracratonic basins. Rugged topography and compact and fissured nature of the rock formations combine to give rise to discontinuous aquifers, with limited to moderate yield potentials. The near

surface weathered mantle forms the all important groundwater reservoir, and the source for circulation of groundwater through the underlying fracture systems. In the hard rock terrain, deep weathered pediments, low-lying valleys and abandoned river channels generally contain adequate thickness of porous material, to sustain groundwater development under favourable hydrometeorological conditions. Generally, the potential water saturated fracture systems occur down to 100 m depth, and in cases yield even up to 30 litres per second (Ips). The friable semi consolidated sandstones also form moderate yielding aquifers, and auto flowing zones in these formations are not uncommon. Shallow large diameter dug-wells and small diameter bore-well s are the main source of water supply for domestic and irrigation purposes. The yield characteristic of wells varies widely. Over exploitation of groundwater has caused considerable lowering of water table. Recent studies have indicated the presence of potential aquifers at deeper levels due to the presence of deep-seated fractures along lineaments. These lineament zones are found to be highly productive for construction of bore-well s (Singhal and Gupta, 1999).

Consolidated sedimentary formations viz., sandstone, shale and limestone of Pre-Cambrian age occur as isolated basins in different parts of the country. The permeability of the rocks is usually poor. Limestone is usually massive and lack in the development of secondary porosity due to the lack of solution activity except in some parts of western and Peninsular India.

The coastal and deltaic tracts in the country form a narrow linear strip around the peninsula. The eastern coastal and deltaic tract and the estuarine areas of Gujarat are receptacles of thick alluvial sediments. Though highly productive aquifers occur in these tracts, salinity hazards impose quality constraints for groundwater development. In this terrain, groundwater withdrawal requires to be regulated so as not to exceed annual recharge and not to disturb hydro-chemical balance leading to seawater ingress.

The high relief areas of the northern and northeastern regions occupied by the Himalayan ranges, the hilly tracts of Rajasthan and peninsular regions with steep topographic slope, and characteristic geological set-up offer high run-off and little scope for rainwater infiltration. The groundwater potential in these terrains are limited to intermontane valleys. Distribution of hydrogeological units in India is given in Table 3.

Table 3: Distribution of Hydrogeological Units in the country and their potential

Geologic Age	*Stratigraphic Unit*	*Rock Formation*	*States/Hydrogeological Characters*
Consolidated Formations			
Jurassic Upper Cretaceous to Eocene	Rajmahal Traps, Deccan Traps.	Basalts, Dolerites, Diorites and other acidic derivatives of Basaltic magma.	Occur in West Bengal, Bihar, Madhya Pradesh, Gujarat, Maharashtra, Andhra Pradesh and Karnataka. Hydrogeological characteristics almost similar. Fractured and Vesicular basaltic layers and inter-trappean sedimentaries are productive. Yield up to 5 lps. Storativity: 1 to 4%. Hydraulic conductivity 5 to 15 m/day. Unconfined shallow aquifers and leaky-confined/ confined deeper aquifers.
Pre-Cambrian	Cuddapahas Delhi and Equivalent Systems.	(a) Consolidated Sandstones, Shales, Conglomerates. (b) Limestones, Dolomites (c) Quartzites, Marbles (d) Intrusive Granites and Malani Volcanics.	Occur in all States. These formations are devoid of primary porosity. Weathering and denudation, structural weak planes and fractures impart porosity and permeability in the rock mass. Solution cavities (caverns) in carbonate rocks at places, give rise to large ground water storage/circulation. The ground water circulation is generally limited within 100 m depth. Storativity value of unconfined aquifer is generally low (0.2% to 3%). Hydraulic conductivity varies widely depending on fracture incidence (2 to 10 m/day). Leaky confined/confined aquifers may be present in layered formations. Granites and granite-gneisses are the most productive aquifers. Yield range 2 to 10 lps and more.
Archaean	Archaean Complex Dharwars, Aravalis and Equivalent formations.	(a) Granites, Gneisses, Charnokites and Khondalites (b) Schists, Slates, Phyllites Granulites. (c) Banded Haematite Quartzites (Iron ore series)	

(Contd.)

(*Contd.*)

Geologic Age	*Stratigraphic Unit*	*Rock Formation*	*States/Hydrogeological Characters*
Semi-consolidated Formations			
Tertiary		(a) Nummulitic Shales and Limestones (b) Carbonaceous Shales (c) Sandstones (d) Shales (e) Conglomerates (f) Ferrugineous (g) Sandstones (h) Calcareous Sandstones (i) Pebble Beds (j) Boulder-Conglomerate (k) Sands (l) Clays	The hydrogeological potential of these formations is relevant only in the valley areas. Lower Siwaliks and their equivalents in Himachal Pradesh, Jammu and Kashmir, Assam, Punjab, Haryana, Uttar Pradesh and Sikkim generally do not form potential aquifers. The Upper Siwaliks have moderate groundwater potential in suitable topographic locations. Tertiary sand stones of Rajasthan, Gujarat, Kutch, Kerala, Orissa, Tamil Nadu, Andhra Pradesh, West Bengal and North Eastern States have moderate to moderately good yield potentials up to 28 lps. Possess moderate primary porosity and hydraulic conductivity.
Upper Carboniferous to Jurassic	Gondwanas	(a) Boulder-Pebble Beds (b) Sandstones (c) Shales	Occur in Bihar,. Maharashtra, Andhra Pradesh, Orissa, Madhya Pradesh, Gujarat, Rajasthan and Tamil Nadu.
	Jurrasic of Kutch and Rajasthan Baghbeds Lametas and Equivalents.	(a) Coal Seams (b) Sandstones (c) Calcareous Sandstone (d) Shales (e) Quartzites (f) Limestones	These formations do not have wide regional distribution, Possess moderate primary porosity and hydraulic conductivity. Karstified limestones are good water yielders. Friable sandstones in Barakars and Kamthis (Lower Gondwana) and their equivalent formations possess moderately good potential. Yield up to 14 lps.

(*Contd.*)

(*Contd.*)

Pleistocene to Recent	(a) Fluvio Glacial deposits	(a) Mixed Boulders, Cobbles, Sands and Silts	The morainic deposits occupy valleys and gorges in interior Himalayas. Karewas (Kashmir Valley) are lacustrine deposits displaying cyclic layers of clayey, silty and coarser deposits with intervening boulder beds. Locally significant hydrogeological potential.
	(b) Glacio-Lacustrine deposits	(b) Conglomerates, Sands Gravels, Carbanaceous shales and Blue Clays.	
	(c) Piedmont and Himalayan Foot Hill deposits	(c) Boulders, Cobbles, Pebble Beds, Gravels, Sands, Silt and Clays.	The Bhabhar piedmont bell contains many productive boulder–cobble gravel-sand aquifers. The water table is deep. Forms recharge zone for deeper aquifers of alluvial plains in south. Tarai belt is down-slope continuation of Bhabhar aquifers. The deeper confined aquifers display flowing artesian conditions. Shallow water table yields up to 28 lps.
	(d) Alluvial Plains (Older and Newer Alluvium)	(d) Clays and Silts, Gravels and Sands of different mix. Lenses of Peat and Organic matter, Carbonate and Siliceous Concretions (Kankar).	Occur widespread in the Indo-Ganga-Brahmaputra alluvial plains. Form the most potential groundwater reservoirs with a thick sequence of sandy aquifers down to great depths. The unconfined sand aquifers sometimes extend down to moderate depth (125 m). Deeper aquifers are leaky-confined/confined. The older alluvium is relatively compact. The unconfined aquifers generally show high storativity (5 to 25%) and high transmissivity (500 to 3000 m^2/day).

(*Contd.*)

(*Contd.*)

Geologic Age	*Stratigraphic Unit*	*Rock Formation*	*States/Hydrogeological Characters*
Unconsolidated Formations			
			The deeper confined aquifers generally occurring below 200 to 300 m depth have low storativity (0.005 to 0.0005) and transmissivity (300 to 1000 m^2/day). Highly productive aquifers yield up to 67 lps and above. The potentials of peninsular rivers alluvium are rather moderate with yield up to 14 lps. But the alluvial valley fill deposits of Narmada, Tapi, Purna basins, 100 m thick, sustain yield upto 28 lps. The quality of ground water at deeper level is inferior. (Storativity 4×10^{-6} to $1.6 \times 1.0^{-2)}$ and transmissivity 100 to 1000 m^2/day). Thick alluvial sequences in deltas of major rivers on the eastern coast and in Gujarat estuarine tracts. Hydrogeological potential is limited by salinity hazards.
	(e) Aeolian deposits (sandstones)	(e) Very fine to fine sand and silt.	The aeolian deposits occurring in West Rajasthan, Gujarat, Haryana, Delhi and Punjab have moderate to high yield potentials; are well sorted and permeable; lie in arid region; natural recharge is poor and water table is deep.

(*Source:* CGWB, 1995)

GROUNDWATER RECHARGE STUDIES

Groundwater recharge has been measured at many locations in India by the tritium tagging or tritium injection method. The method is based on the assumption that the soil water in the unsaturated zone moves vertically downward as discrete layers. Water added on the surface either as precipitation or irrigation will move downwards by pushing the older water beneath and this in turn will push the still older water further below, thereby the water from the unsaturated zone is added to the groundwater reservoir. This flow mechanism is known as the piston flow. Therefore, the vertical movement of the injected tritium can be monitored in the soil column. The position of the tracer is indicated by a peak or a maximum in the tritium activity versus depth plot. However, molecular diffusion, dispersion and aquifer heterogeneties may cause broadening of the peak. The methodology provides spot measurements of natural recharge.

This method has been used by a number of workers in different hydrogeological environments in India. Measurements have been carried out for the last more than 25 years in 35 watersheds, water basins and administrative blocks by various research workers (Table 3).

Natural recharge rates obtained from the tritium injection method were compared with other methods e.g. water level fluctuation and groundwater modelling. The recharge rates calculated from tritium injection method range from 24 to 198 mm/yr. or 4.1 to 19.7% of the local average seasonal rainfall depending upon the hydrogeological and climatic conditions (Table 4). The replenishable groundwater potential of India, for normal monsoon years based on tritium injection method, is calculated as 476×10^9 m^3 per year.

Table 4: Rainfall recharge measurements in India using tritium injection method

SI.. No.	*Basin/watershed/ Blocks*	*Main rock types*	*Rainfall (mm yr^{-1})*	*Natural recharge derived*		
				Median (mm yr^{-1})	*Mean (mm yr^{-1})*	*Rainfall (%)*
1.	Punjab	Alluvium	460	35	56	12.2
2.	Haryana	Alluvium	470	43	70	14.9
3.	Western Uttar Pradesh	Alluvium		174	195	19.7
4.	Churu district, Rajasthan	Alluvium	491	67	62	12.6
5.	Godavari-Puma basin, Maharashtra	Basalt	652	50	56	8.6
6.	Lower Maner basin, Warangal and Karimnagar dists. Andhra Pradesh	Sandstone and shale	1250	103	117	9.4
7.	Neyveli basin, Tamilnadu	Sandstone	1398	150	181	12.9
8.	Neyveli basin, Tamilnadu	Alluvium	1004	50	161	16.0
9.	Noyil basin, Tamilnadu	Granite, Gneiss	715	35	69	9.6

(after Rangarajan and Athavale, 2000)

Studies in the hard rock terrains covered with black cotton soil in basaltic terrain and red lateritic soil in granitic areas indicate that a minimal rainfall of about 246 mm and 412 mm are required for initiation of deep percolation in red and black cotton soils respectively. However all of this will not be available for utilization as part of it will be lost to base flow and effluent seepage to surface drainage system. This also does not include other sources of recharge such as return flow from irrigation.

WATER QUALITY

In addition to the problem of inland salinity, overexploitation of groundwater has resulted in seawater intrusion in coastal areas. This problem is more severe in the coastal parts of Gujarat, Orissa, Tamilnadu and Kerala. Further, higher concentration of fluoride, iron and arsenic is reported from some areas. Higher concentration of fluoride (more than the permissible limit of 1.5 mg/lit) is reported from parts of Andhra Pradesh, Tamilnadu, Rajasthan and Uttar Pradesh. The cause of high fluoride in these areas is geogenic i.e. due to the dissolution of fluoride bearing minerals. At some places, deflouridation plants are installed to remove high concentration of fluoride.

The occurrence of arsenic in groundwater, reported in recent years from parts of West Bengal, has caused great concern. In West Bengal, life of more than five million people is at risk due to high As in groundwater and already about half a million people suffer from various arsenic related diseases. Similar problem is reported from the neighbouring country of Bangladesh where high concentration of arsenic (0.3 to 1.1 mg/lit) is reported from shallow alluvial and deltaic aquifers in the depth range of 15 to 75 m below the ground surface. The permissible limit of arsenic in drinking water in India is 0.05 mg/lit, while the WHO has put a limit of 0.01 mg/lit.

Studies in West Bengal by the scientists of the Bhaba Atomic Research Center (BARC) and CGWB show that groundwater from shallow unconfined aquifers (depth 20 to 80 m) has low dissolved oxygen, negligible SO_4 and higher concentration of As (0.5 to 1.0 mg/lit or more), and bicarbonate; pH being above 7. In most of the areas the arsenic concentration is localized. Higher concentration of As is in areas where clay pockets predominate. Isotope data indicate modern recharge to the shallow aquifer. Groundwater in deeper semi-confined to confined aquifers (>100 m) contains negligible amount of As and is much older in age (5000 to 13,000 years) indicating that these are palaeowaters. Surface water in these areas does not have any arsenic.

The cause of high arsenic in groundwater of both India and Bangladesh is somewhat controversial. Some workers attribute it to the presence of arsenic bearing pyrite in the clay, silt and peat formations interbedded with alluvial aquifers. Lowering of water table, due to excessive withdrawal of groundwater, has resulted in the oxidation and leaching of As from the sediments.

According to other scientists, arsenic, which is adsorbed on the iron hydroxide surface, is released to groundwater under reducing conditions (Mukherje et al., 2001). They have also argued that detrital pyrite or arsenopyrite is absent from the aquifer in these areas.

Studies by the CGWB in West Bengal have indicated the presence of arsenic-free aquifers in the depth range of 200 to 250 m below ground level which can be tapped by constructing deep tube wells. Mitigation is difficult given the scale of the problem as well as social and economic factors. Options include use of deep groundwater (>150 m), use of disinfected groundwater from dug-wells, rainwater harvesting, and treatment of contaminated groundwater and surface water.

Groundwater having more than the maximum permissible limit of 1.0 mg/lit of iron is reported from high rainfall areas in eastern states and northeastern states. It is attributed to the dissolution of iron oxides in laterites and other iron bearing minerals. Iron-removal plants are installed at some places to provide safe drinking water in these areas.

The problem of acid mine drainage especially from high sulphur Tertiary coals of Assam in northeastern India is quite acute. In this area the problem is aggravated due to high rainfall of the order of 400 cm/yr. The mine drainage water is highly acidic (pH = 2.3 to 4.0) and contains more than 3000 mg/lit of sulphate and about 300 mg/lit iron.

Dumping of industrial waste and sewage into surface water-courses cause widespread pollution resulting in large number of deaths due to water-borne diseases.

GROUNDWATER AUGMENTATION THROUGH ARTIFICIAL RECHARGE

The artificial recharge is being practiced for augmentation of groundwater reservoir and to provide sustainability to groundwater development in India. The schemes for artificial recharge are being implemented in different hydrogeological situations by CGWB and many State Groundwater Departments. A few case studies from different hydrogeological setups are given herein under:

Basaltic Terrain—Maharashtra

Over-exploitation of groundwater for orange cultivation has depleted the groundwater resources in parts of Amravati district, Maharashtra. Hydrogeological studies have brought out that the watershed WR-2 covering 488 km^2 area has surplus monsoon runoff of about 98.9 million cubic metres (MCM) which can be conserved through simple artificial recharge structures like percolation tanks and check dams (cement plugs). The efficiency of these structures constructed at suitable locations with appropriate design in case of percolation tanks is 91% and for cement plugs 94%. The benefited

area in case of percolation tanks with gross storage capacity varying from 71 to 220 thousand cubic metres (TCM) varied from 60 to 120 hectares (ha) during 1997-98 and benefits extended up to 1.5 km down stream of percolation tanks. In case of cement plugs with storage capacity varying from 2.10 TCM to 7.42 TCM varied from 3 to 15 ha during 1997-98.

Alluvial Aquifers Bordering Mountain Front—Maharashtra

The prominent regional aquifer system for Tapi Alluvial basin paralleling Saturn Mountain front is being extensively developed to meet the water requirement of cash crops like banana and sugarcane. This has led to decline of water levels by more than 8-10 metres during last 10-15 years. Large number of wells have either gone dry or their yields have declined. The Central Ground Water Board carried out artificial recharge studies in TE-17 watershed in Jalgaon district. The sub-surface storage potential of watershed five metres below ground level was assessed as 85 million cubic metres (MCM) compared to surplus monsoon runoff of 29.7 MCM. Artificial recharge techniques like recharge through percolation tanks, recharge through existing dug-wells, recharge shafts and through injection tubewells were experimented. Percolation tanks in Bazada formation of Saturn foothills were found to be highly efficient with efficiency as high as 97% and capacity utilization going up to 400%. The zone of benefit extended to 5 km with benefited area up to 400 ha.

Percolation Tanks in Hard Rocks in South India

Artificial recharge by percolation tanks is an ancient practice of water conservation especially in the hard rock terrains of India. Hundreds of such tanks are constructed every year in drought prone areas to augment groundwater recharge from permeable river beds by constructing check dams/ dykes. Rate of infiltration from these tanks depend on local hydrogeological conditions, topography and storage characteristics of the tank. Studies in granites and basaltic terrains of South India indicate that the rate of recharge from percolation tanks vary from 9 to 12 mm/day. The rate of infiltration decreases with time due to silting. In ephemeral and seasonal streambeds, recharge rates are comparatively high due to the reworking/removal of silt during the dry period. Evaporation losses from the tanks are also high, being about 4 to 6 mm/day (Muralidharan and Rangarajan, 2001).

Coastal Area—Saurashtra, Gujarat

After detailed hydrogeological surveys and groundwater draft estimation, artificial recharge through pressure injection and surface spreading methods was experimented in the alluvial area around Kamliwara in the Central Mehsana. Source water for the test was drawn from the phreatic aquifer

below the Saraswati riverbed. Since groundwater was used for artificial recharge, the injection water was devoid of silts and other impurities and chemically compatible with the water in aquifer getting recharged. The pressure injection experiment was conducted continuously for about 250 days with an average injection quantity of 225 cubic metres per day. During the recharge cycle, a rise in water level of five metres in the injection well (apparent built up of 11 m) and 0.6 to 1.0 m in wells 150 metres away from the injection well were observed.

In Mehsana area, artificial recharge experiments through spreading method were also conducted using canal water. A spreading channel of 3.3 metres width, 400 m length with 1 in 1 side slope was constructed and in which the canal water was fed for 46 days. The recorded build up in water level of 1.4 to 2 m was observed up to 15 m from the recharge channel and about 20 cm at distance of 200 m. The recharge rate of 260 cubic metres per day was estimated using an infiltration rate of 17 cm/day. Dissipation in recharge mound (1.42 m) was observed in 15 days.

Studies on control of salinity in the coastal Saurashtra using spreading and injection method have indicated that the recharge pit and the injection shaft can effect recharge at the rate of 192 and 2600 cubic metres per day respectively. Canal water was used for recharge studies.

Alluvial Areas of Ghaggar River Basin—Haryana

Central Ground Water Board, with the assistance of UNDP, carried out artificial recharge studies involving recharge through injection well in Kurukshetra District along Ghaggar river in Haryana. After construction and development of injection well, recharge experiment was conducted with a recharge rate of 40 LPS for 389 hours and with 22 LPS for another 24 hours. The experiment demonstrated that the hydrogeological conditions of the area are favourable for artificial recharge through injection method. The canal water quality was found to be suitable for injection.

REMOTE SENSING AND GIS APPLICATIONS

Since late 60's many attempts have been made to explain spatial variability of groundwater occurrence in different terrain conditions using aerial photography and remote sensing. Ghosh and Singh (1975) have identified the control of palaeochannels on the occurrence and movement of groundwater in Rajasthan. Under National Drinking Water Mission, ISRO has identified and mapped favourable zones for groundwater exploration (ISRO, 1988).

Groundwater cannot be seen directly from the remote sensing data; hence its presence is inferred from identification of surface features, which act as an indicator of groundwater (Das et al., 1997; Ravindran and Jeyram, 1997).

Many researchers have used remote sensing and GIS techniques successfully for demarcating the groundwater potential zones in diverse

geological setup (Raj and Sinha, 1989; Champati et al., 1993; Krishnamurththy et al., 1996; Saraf and Chaudhary, 1998; Shahid et al., 2000).

Department of Space have recently completed a project under drinking water mission in five states of the country (NRSA, 2000). Under this project different thematic maps—viz., geology, geological structures, geomorphology and recharge conditions have been prepared and the said maps have been integrated in GIS for demarcation of potential groundwater zones.

Jaiswal (2003) has developed an approach for identifying groundwater prospect zones in hard rock areas. The approach is based on information extracted on lithology, geological structures, landforms, landuse map prepared from remotely sensed data and drainage network, soil characteristics slope of terrain from conventional methods and studying all these data in GIS environment.

CONCLUDING REMARKS

India is a vast country with diverse hydrogeological conditions. Distribution and availability of groundwater depends on the type of aquifers. A lot of work has been done on exploration of groundwater and understanding the hydrogeological setup of the country. Modern techniques like isotopic tracers are being used to study the groundwater recharge and groundwater movement in different conditions. Remote sensing and GIS is also being used to identify the groundwater prospect zones.

REFERENCES

CGWB, 1995. *Ground Water Resources of India*. Faridabad, 147 pp.

CGWB, 2000. *Guide on Artificial Recharge to Ground Water*. Faridabad, 93 pp.

Champati Ray, P.K., Dave, V. and Roy, A.K., 1993. Groundwater Investigation Using Remote Sensing and GIS Technique- A case study in Manbazar-II Purulia-9 (WB). Proceeding of National Symposium (ISRS)-Remote Sensing Applications for Resources Management, Guwahati, India. 25-27, November, 1993.

Das, S., Behera, S.C., Kar, A., Narendra, P. and Guha, S., 1997. Hydrogeomorphological Mapping in Groundwater Exploration Using Remotely Sensed Data-A case study in Keunjhar district, Orissa. *Journal of the Indian Society of Remote Sensing*, **25:** 247-260.

Ghose, B. and Singh, S. 1975. Geomorphology of Prior and Present Drainage Networks and Their Control on Groundwater in Sandstone Formations, Jodhpur district, *Annual Report*, CAZRI, Jodhpur.

Jaiswal, R.K., Mukherjee, S., Krishnamurthy, J. and Saxena, R., 2003. Role of remote sensing and GIS technique for generation of groundwater prospect Zones Towards Rural Development—An approach. *International Journal of Remote Sensing*, **24:** 993-1008.

Jones, P.H., 1987. Deep Aquifer Exploration Project in the Ganges and Bengal Basins in India (Unpublished report), 54 pp.

Khan, M.A. and Moharana, P.A., 2002. Use of Remote Sensing and Geographic Information System in the Delineation and Characterization of Groundwater Prospect Zones. *Journal of the Indian Society of Remote Sensing*, **30:** 131-141.

Krishnamurthy, J., Venkatesa Kumar, N., Jayaraman, V. and Manivel, M., 1996. An Integrated Approach to Demarcate Groundwater Potential Zones through Remote Sensing and Geographic Information System. *International Journal of Remote Sensing*, **17:** 1867-1884.

Mukherje, P.K. et al., 2001. Arsenic-rich Phases in Aquifer Sediments from Southern West Bengal. *Journal of Geological Society of India*, **58:** 173-176.

Muralidharan, D. and Rangarajan, R. 2001. Replenishent of unconfined Hard Rock Aquifer and Improvement of Percolation Tank Efficiency. *In:* Singhal, D.C. et al. (Eds.) Proceedings International Symposium on Emerging Trends in Hydrology, **II:** 113-124.

National Institute of Hydrology, 1992. Hydrological Developments in India since Independence: A Contribution to Hydrological Sciences, Roorkee

NRSA, 2000. Rajiv Gandhi National Drinking Water Mission: Technical guidelines for preparation of groundwater prospects maps. NRSA/AD/GG/GD/TR:1/2000. NRSA, Department of Space, Hyderabad, India.

Raj, S. and Sinha, A.K., 1989. An Integrated Approach for the Delineation of Potential Groundwater Zones using Satellite Data: Case study, Udaipur District, Rajasthan. Asia-Pacific *Remote Sensing Journal*, **2:** 61-64.

Raju, K.C.B., 2003. Water conservation in Hard Rock Areas: A necessity. *In:* Singhal, B.B.S. and Verma, O.P. (Eds.), 2003. *S & T Inputs for Water Resources Management*. DST's Spl. Vol. 3, Indian Geological Congress, Roorkee. 173-195.

Ravindran, K.V. and Jeyaram, A., 1997. Groundwater Prospects of Shahbad tehsil, Baran district, eastern Rajasthan: A remote sensing approach. *Journal of the Indian Society of Remote Sensing*, **25:** 239-246.

Saraf, A.K. and Choudhary, P.R., 1998. Integrated Remote Sensing and GIS Approach for Groundwater Exploration and Identification of Artificial Recharge Sites. *International Journal of Remote Sensing*. **19:** 1825-1841.

Shahid, S., Nath, S.K. and Roy, J., 2000. Grounwater Potential Modelling in a Soft Rock Area Using a GIS. *International Journal of Remote Sensing*, **21:** 1919-1924.

Singh, B., 1997. Water Resources Development in India—A perspective. *In:* Singhal, D.C. et al. (Eds.) Proceedings International Symposium on Emerging Trends in Hydrology, **I:** 1-17.

Singhal, B.B.S. and Gupta, R.P., 1999. *Applied Hydrogeology of Fractured Rocks*. Kluwer Academic Publishers, Dordrecht, The Netherlands. 324 pp.

Singhal, B.B.S. and Verma, O.P. (Eds.), 2003. S & T Inputs for Water Resources Management. Indian Geological Congress, Roorkee. DST's Spl. Vol. 3, 232 pp.

2 Nature of Hard Rock Aquifers: Hydrogeological Uncertainties and Ambiguities

B.B.S. Singhal

Retired Professor, Department of Earth Sciences
Indian Institute of Technology, Roorkee 247 667, India

INTRODUCTION

The term hard rock was perhaps originally coined by drillers to indicate poor drillability of these rocks. Hard rocks are characterized by insignificant primary (intergranular) porosity and primary permeability. However, weathering and fracturing can impart secondary porosity and permeability to varying extent. Usually, crystalline (igneous and metamorphic) rocks are included in this group. As the hydraulic properties of these rocks are mainly controlled by fracturing, these are also referred as fractured rocks. Unlike sedimentary rocks, the hard rocks generally represent anisotropic and heterogeneous media.

Hard rocks widely occur in various parts of the world and cover about 20% of the land surface. In India, over two third of the surface area totalling about 2.40 million sq. km. is occupied by hard rocks regions and nearly 50% of the replenishable resources of groundwater occur in these rocks. In certain parts of the hard rock terrains in India, as in the Western Ghats and in Assam, rainfall is high (about 400 cm per year) but over a greater part of the area, rainfall is poor and these are drought prone areas e.g. Central Maharashtra, Telengana area of Andhra Pradesh and some parts in Karnataka and Rajasthan. In these semi-arid areas availability of groundwater is quite problematic.

In the past, the hard rocks were neglected as a possible source of groundwater. This was mainly due to their low permeability and high cost of drilling. However, in recent years, geo-hydrological investigations have indicated that the rocks everywhere are not so unpromising. Moreover, rapid methods of drilling by down-the-hole hammer have also facilitated the

groundwater investigations and development work. Systematic geo-exploration has also increased the rate of success in water well drilling in hard rock areas.

Studies on the hydrogeology of hard/fractured rocks are being pursued for different purposes and with widely differing objectives, such as:

(i) Development of safe groundwater supplies for domestic and irrigation purposes.
(ii) Contaminant migration studies, in order to estimate the movement of pollutants through fractures etc.
(iii) Tapping of geothermal resources involving estimation of extractable amount of hot fluids from the natural geothermal gradients.
(iv) Development of petroleum and gas reservoirs.
(v) Underground nuclear waste disposal.
(vi) Construction of underground rock cavities for storing water, oil and gas etc. and underground passages such as tunnels.
(vii) In several other geo-technical problems, e.g. stability of rocks, slopes and seepage from dams and tunnels, triggering of earthquakes etc.

All the above studies require a clear understanding and proper description of' the hydrological characteristics of these rocks. A comparison of the hydrogeological characteristics of porous and hard (fractured) rock aquifers is given in Table 1.

Table 1: Comparison of Granular and Fractured Hard Rock Aquifers

Aquifer Characteristics	*Aquifer Type*	
	Granular Rock	*Fractured Rock*
Effective porosity	Mostly primary	Mostly secondary through joints, fractures etc.
Isotropy	More isotropic	Mostly anisotropic
Homogeneity	More homogeneous	Less homogeneous
Flow	Laminar	Possibly rapid and turbulent
Flow predictions	Darcy's law usually applies	Darcy's law may not apply, cubic law applicable
Recharge	Dispersed	Primarily dispersed with some point recharge
Temporary head variation	Minimal variation	Moderate variation
Water quality variation	Minimal variation	Greater variation

ROCK DISCONTINUITIES AND FRACTURES

Hard rocks are characterized by various types of rock discontinuities of various scales varying from few mm size joints to major fault zones and lineaments. The main rock discontinuities are foliation, fractures (joints), faults and lineaments.

Foliation is a characteristic feature of metamorphic rocks. Along a fault, relative movement of rock mass takes place while long discontinuities extending over several km are termed as lineaments. Fracturing is caused by tectonic stresses, residual stresses, contraction-cooling and desiccation, unloading and weathering.

Fractures and other discontinuities are the most important geological structures from the hydro-geological point of view as they facilitate storage and movement of fluids through them. On the other hand, some discontinuities, e.g. faults and dykes may also act as barriers to groundwater flow.

A number of factors including stress, fracture geometry and temperature etc. control the groundwater flow through fractures. For example, fracture aperture and flow rate are directly interrelated, non-parallelism of walls and wall roughness leads to friction losses, hydraulic conductivity of fractures is inversely related to normal stresses and depth because normal stress tends to close the fractures and reduce the hydraulic conductivity. Fractures parallel to the maximum compressive stress tend to be open, whereas those perpendicular to this direction tend to be closed.

Experience in the hard rock areas of Scandinavian countries and in India indicate that tensional fractures are more open and transmissive than shear fractures, as the latter are held closed by a component of normal stress. This hydro-tectonic model was originally suggested by Larsson.

As fracture geometry and their hydraulic properties greatly depend on stress distribution, palaeo-stress and in situ stress analysis is important. Studies in the hard rock areas of Norway have also indicated the importance of post-glacial isostatic rebound on well yields (Banks et al., 1996).

In addition to stress distribution, interconnectivity of fractures, fracture aperture and other fracture properties are also important from permeability point of view. Fracture permeability reduces with increasing temperature. As temperature increases with depth, thermal expansion in rocks takes place, which leads to reduction in fracture aperture and corresponding decrease in permeability. Further, the fracture permeability also decreases by cementation, filling and weathering etc.

Sheeting joints developed in granitic rocks due to weathering and unloading impart higher hydraulic conductivity horizontally. However at deeper level vertical fractures may be the main cause of groundwater flow where K_h/K_v may be less than one.

In view of the above, from hydrogeological point of view, including movement of contaminants, it is extremely important to study the structure of rock mass and quantify the pattern and nature of fractures etc.

Fractures, lineaments and faults can be studied in the field outcrops, and by aerial photographs, remote sensing as well as from bore hole surveys. Fractures have certain orientation, spacing, aperture, length etc. which are studied in rock outcrops in the field. Several sets of fractures are often

developed in a rock mass. The number of sets of fractures in an area can be statistically determined by contouring the pole points and in rose diagram.

As weathering will affect surface exposures and their fracture network, bore hole data will provide complementary information for the interpolation of fracture network and its attributes at depths. Later, this is compared with the data obtained from hydraulic tests on bore holes to get an idea about the hydraulic attributes related to the fracture set volumes. The combination of all these data helps generating the calculated hydraulic attributes of fracture networks for numerical modelling of fracture aquifers.

Studies in many crystalline rock terrains world over has shown that highly transmissive fractures occur locally as clusters in a near-horizontal form embedded within an extensive network of less transmissive fractures (Fig. 1).

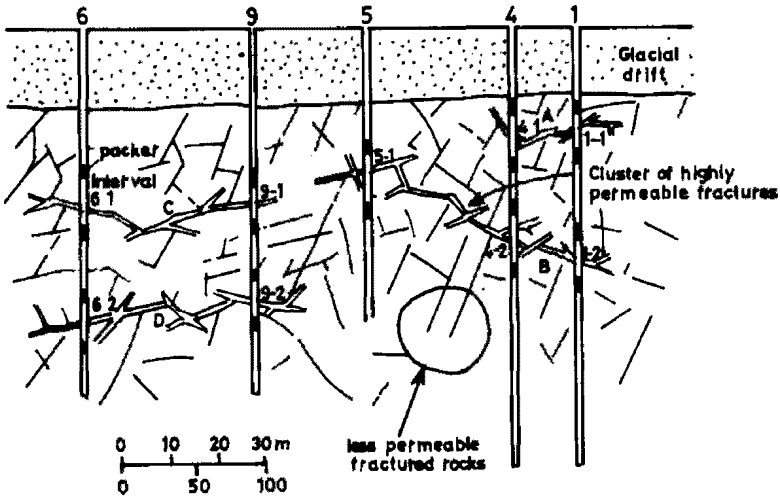

Figure 1. Vertical cross section and conceptual model of the US Geological Survey's fractured rock research site near Mirror Lake, New Hampshire. Four clusters of highly permeable fractures labelled A-D occur in the less permeable fractured rocks. Borehole packers are closed sections (after Rutqvist and Stephansson, 2003).

The weathered zone is also an important source of groundwater in hard rock terrain. In many developing countries in Asia and Africa, large diameter dug-wells tap water from this zone. The thickness of the weathered zone depends on the geomorphological, climatic and lithological conditions. Electrical resistivity and seismic refraction methods are quite helpful in estimating the thickness of this zone.

GROUNDWATER FLOW

The characterization and prediction of flow and transport through fractured hard rock mass is extremely difficult as the geometry of the flow and path

in these rocks is often very complex and heterogeneous depending upon the fracture characteristics as discussed earlier. In fractured rocks, the groundwater movement mainly takes place along discontinuities, i.e. joints, fractures and shear zones. The interconnections between rock discontinuities and their spacing, aperture size and orientation decide the porosity and permeability of such rock masses. Open joints and fractures which are not filled with weathered or broken rock material form potential passage for groundwater movement but their permeability is greatly reduced when filled with clayey material such as smectite or montmorillonite. These filling materials form fracture skin which also influence the movement of solutes from the fractures into the porous matrix.

Flow through Single Fracture

The Darcy's law for flow in a single fracture can be written as:

$$V = K_f I \tag{1}$$

where K_f is the hydraulic conductivity of the fracture, defined by

$$K_f = \frac{\gamma a^2}{\mu\, 12} \tag{2}$$

where a is the fracture aperture, γ is the specific weight of water and μ is the viscosity. The hydraulic conductivity (K), and permeability (k) are related by the expression

$$K = \frac{\gamma}{\mu} k \tag{3}$$

Therefore, the permeability of the fracture, k_f , can be defined as:

$$k_f = \frac{a^2}{12} \tag{4}$$

By combining equations (1) and (2), the average velocity ($\overline{V}_\alpha$) in the fracture expressed by a single parallel plate model is given by

$$\overline{V}_\alpha = \frac{\gamma a^2}{12\mu} \frac{dh}{dl} \tag{5}$$

Here it is assumed that the fracture walls are impermeable. In terms of transmissivity of fracture, T_f, equation (4) can be written as:

$$T_f = \frac{\gamma}{\mu} \frac{a^2}{12} - K_f a \tag{6}$$

Many researchers also defined T_f as the hydraulic conductivity of fracture. The volumetric flow rate per unit plate (fracture) width (Q_f) will be

$$Q_f = \left(\frac{\gamma a^3}{12\mu}\right) I \tag{7}$$

Equation (7) is referred as the cubic law which is valid for laminar flow through parallel wall fractures with smooth surfaces. In natural conditions, these assumptions usually do not hold good. The validity of cubic low is discussed by several researches, viz. Lee and Farmer, 1993.

Under field conditions, it is usually difficult to determine the representative distance between the fracture walls. At low applied stress, when the fractures are open, the parallel plate approximation for fluid flow through fracture may be valid. However, due to stress the contact area between fracture surfaces will increase and, therefore, variation in fracture aperture should be considered.

Flow Models

Depending on the porosities and permeabilities of the fractures and the matrix blocks, the fractured rock formations can be classified into (a) purely fractured medium, (b) double porosity medium, and (c) heterogeneous medium (Fig. 2). In a purely fractured medium, the porosity and permeability is only

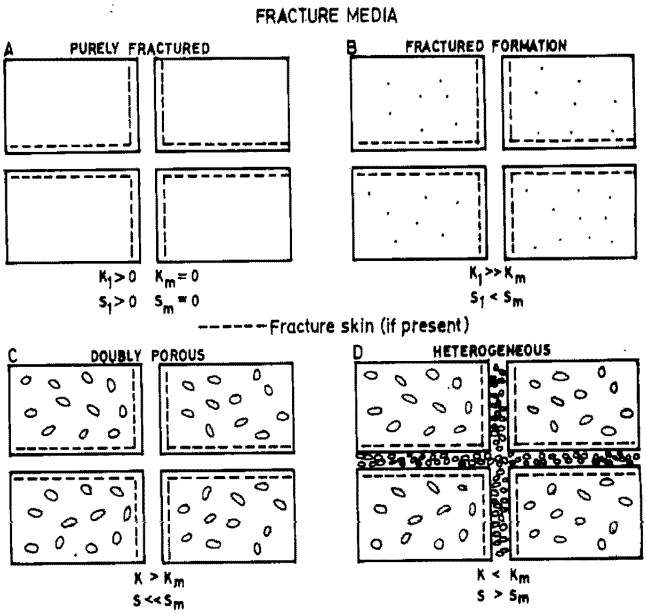

Figure 2. Hydrogeological classification of fractured media (after Streltsova, 1975). K_f and K_m are the hydraulic conductivities of the fractures and the matrix, respectively. S_f and S_m represent the fluid storativities of the fractures and the matrix. A: purely fractured media. B: fractured formation. C: double porosity medium. D: heterogeneous formation. In cases B, C, and D, the fracture coating or "skin" may be hydrogeologically significant.

due to interconnected fractures while blocks are impervious. In double (dual) porosity medium, both fractures and matrix blocks contribute to groundwater flow but fractures are the main contributors. In a situation, when fractures are filled with clay or silty material, the fracture permeability is considerably reduced and such a medium is termed as heterogeneous.

In fractured rocks, the concept of porous medium can be applicable where the fractures are interconnected and the density of conductive fractures is high. When these conditions are not met, alternate conceptualizations must be used.

Some of the models describing flow in a fractured medium are:

1. Double porosity model.
2. Equivalent porous medium (EPM) model.
3. Discrete fracture network model.

It may be mentioned that various models require knowledge about characteristic features of individual fractures and thereby account for the heterogeneity. Therefore, careful mapping of fractures by surface and subsurface measurements is important. The level of details depends on the purpose for which the model is being developed. A greater accuracy is required for modelling solute transport as the heterogeneity of the fracture system greatly influences the travel time and solute concentration. It is also important to estimate the hydraulic properties of different fracture sets. Studies indicate that fractures parallel to the maximum compressive stress tend to be open, whereas those perpendicular to this direction tend to be closed (Anon, 1996).

The choice of modelling strategy depends on information desired. The choice of simulation model should depend on conceptual model . If necessary hydrogeological data are lacking, sophisticated numerical models can not be justified. In case sufficient data is not available, simple epm model can be used for flow but not for transport.

Double Porosity Model

Double porosity model is also known as *dual porosity model*. The behaviour of a fractured aquifer for regional groundwater investigations can be represented by a double-porosity model. The concept of double porosity model has been explained in detail by Streltsova-Adams (1978) and Gringarten (1982). The model assumes two regions—the porous block and the fracture, which have different hydraulic and hydromechanic characteristics. Three types of distributions of matrix block are considered—horizontal slabs (strata-type), spherical blocks, and cubes (Fig. 3). The fissured medium with horizontal fractures has been considered to be analogous to alternate aquifer-aquitard system (Boulton and Streltsova, 1978). The block consists of fine pores which are separated from fractures. The blocks supply fluid to the

fractures and act as uniformly distributed source. Such an approach with some modifications has been also used by several researchers in analyzing the behaviour of fractured oil reservoir (Anon, 1996).

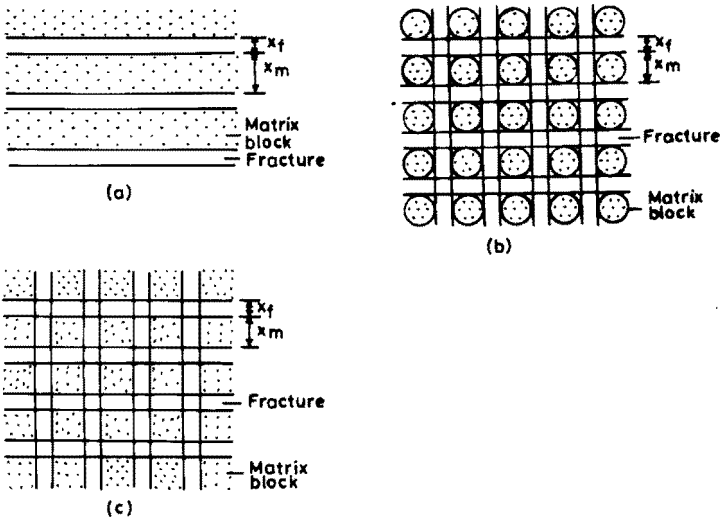

Figure 3. Types of double porosity aquifers: (a) Horizontal fractures and matrix blocks; (b) Spherical matrix blocks, and (c) Cubical matrix blocks.

In the double-porosity model, the porous blocks have high primary porosity but low hydraulic conductivity while the adjacent fractures have although low storativity but high conductivity. The difference in pressure between the porous blocks and the fractures lead to flow of fluid from porous to adjacent fractures. Due to difference in the permeabilities of fracture and blocks, flow mechanism is different during early, long and intermediate times of pumping.

The characteristics of a double (dual) porosity aquifer system are given in terms of K_f, K_m, S_f, and S_m, where subscripts f and m are for fractures and matrix respectively. The other two parameters are storativity ratio (ω) and the transmissivity ratio (λ). Storativity ratio (ω) is the ratio of fissure to total system (blocks plus fissures) storativities and can be expressed as

$$\omega = \frac{S_f}{S_f + S_m}\beta \tag{8}$$

where S_f and S_m are the storativities of fractures and blocks respectively, and β is a factor depending on matrix block geometry which is taken to be equal to 1 for strata type. The transmissivity ratio, or interporosity flow coefficient (λ) (dimensionless) is given by:

$$\lambda = a\, r_w^2 \frac{K_m}{K_f} \tag{9}$$

where a is the shape factor parameter depending on fracture and matrix geometry and r_w is well radius.

Equivalent Porous Medium Model

This is also known as equivalent continuum model. Here it is assumed that flow in a large volume of fractured medium can be similar to that of a porous medium especially when fracture density is high. In such cases conventional pumping test methods can be used.

Discrete Fracture Network Models

Network models use fracture characteristics and heterogeneity of rocks mass based on field data. The hydraulic behaviour of a discrete fracture aperture, length, density, orientation, connectivity of fractures and fracture filling material is discussed later.

Two-dimensional and three-dimensional fracture network models have been suggested by Lee and Farmer (1993). These models evaluate flow in fractures or fracture sets with synthetic distributions of apertures, orientations, spacings and dimensions and take into account various surface roughness, flow channelling, and mixing phenomena at fracture intersections. The application of these theoretical models to natural systems has been limited. These models are useful where the area of interest is small—as in the study of the effect of radionuclide transport through fractures as a result of nuclear waste storage in geological formations over a long period of time. The disadvantages of the discrete modelling are that statistical information about fracture characteristics may be difficult to obtain.

HYDRAULIC CONDUCTIVITY OF FRACTURED MEDIA

In fractured rocks, a distinction can be made between hydraulic conductivity of fracture, K_f and of intergranular (matrix) material, K_m. As fractures form the main passage for the flow of water, the hydraulic conductivity of fractured rocks mainly depends on the fracture characteristics, e.g. aperture, spacing, stress, infilling (skin), connectivity etc. as discussed below.

Relationship of Hydraulic Conductivity with Fracture Aperture and Spacing

The relationship between hydraulic conductivity (K_f) of a single plane fracture with aperture (a) is given by equation:

$$K_f = \frac{\gamma a^2}{12\mu} \tag{10}$$

The equivalent hydraulic conductivity of a rock mass, (K_s) with one parallel set of fractures is expressed by:

$$K_s = \frac{a}{s} K_f + K_m = \frac{\gamma a^3}{12 s \mu} + K_m \tag{11}$$

where s is fracture spacing. Usually K_m is very low except when rock is porous and/or fractures are filled with impervious material.

The range of hydraulic conductivity of fractured rocks from some areas in Europe and USA is given in Fig. 4.

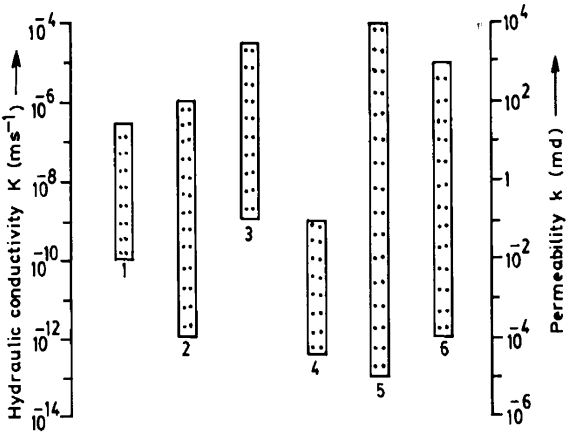

Figure 4. Range of hydraulic conductivity (K) and permeability (k) in some crystalline rocks estimated from in situ borehole tests (based on data from Brace, 1984; Black, 1987). 1. Granite batholith, Monticello, SC, USA; 2. Altnabreac, Scotland; 3. Carynnen, Cornwall, UK; 4. HDR, Cornwall, UK; 5. Deep drilling in northern Switzerland; 6. Four sites in Sweden.

Relationship of Permeability with Depth

The decrease in permeability with depth in fractured rocks is usually attributed to reduction in fracture aperture and fracture spacing due to increased stress. Although, a decrease in permeability with increasing depth is demonstrated from several places, this decrease may not be systematic, especially at greater depths (>50 m). The permeability can also vary several order of magnitude at the same depth (Fig. 5). Higher permeabilities at shallow depths (<50 m) can be attributed to greater influence of surficial phenomena like weathering etc. and development of sheeting joints due to unloading. Further, fractures at the same depth below the ground surface but with different orientations may be subjected to different stresses and, therefore, may have different permeability.

Sheeting joints developed at shallow depths in granitic rock terrains are more open thereby imparting higher hydraulic conductivity horizontally which imparts a greater heterogeneity. However, at deeper levels vertical fractures are the main cause of permeability. Lee and Farmer (1993) have suggested values of K_h/K_v ranging from 1 to 10.

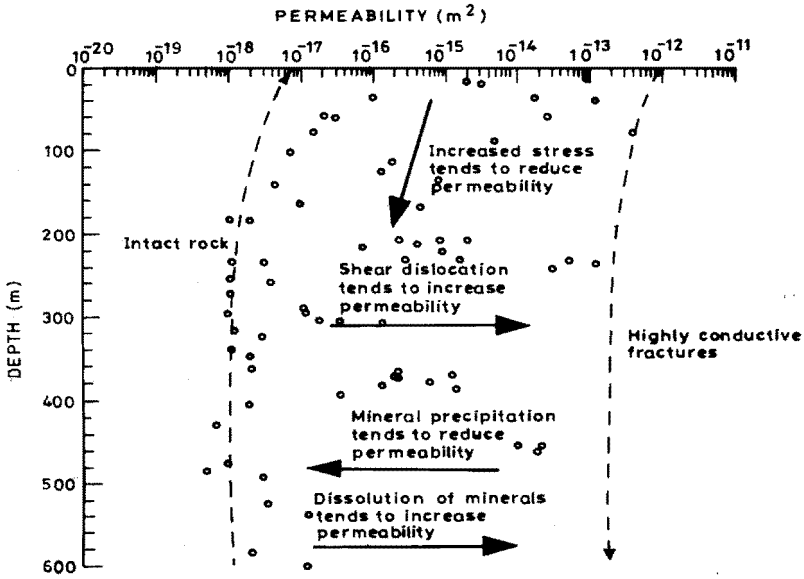

Figure 5. Permeability estimated from short-term well tests in fractured crystalline rocks of Sweden (after Rutquist and Stephansson, 2003)

Even at depths of more than 1000 m, appreciable permeability are reported in fractured rocks. For examples, Fetter (1988) reported higher permeabilites from fractures at depths of 664 to 1669 m in granitic rocks of Illinois, USA. Recent studies under the Continental Deep Drilling Project in Germany (Kessels and Kuck, 1995) and HDR experiments in the Rhine Graben, France (Gerard et al., 1996) also showed existence of good hydraulic interconnection between adjacent boreholes through fractures even at a depth of more than 3000 m.

On the basis of above discussion, it may be summarized that although, generally in fractured rocks a decrease in permeability with depth is observed at several places but there is not much justification of such a universal rule. Therefore, site-specific studies are necessary to establish any such variation.

Permeability is also influenced by mineral precipitation and dissolution (Fig. 5).

Influence of Temperature on Permeability

Significant changes in rock temperature can occur due to natural weather conditions viz. alternate freezing and thawing and due to man-induced changes. Formation of ice in fractures will cause freezing and thawing. It further causes extension of fractures and can also block the movement of water producing pressure buildups. The influence of temperature on

permeabilities is important for disposal of radioactive waste and in harnessing geothermal energy. An increase in temperature will cause a volumetric expansion of the rock material leading to reduction in fracture aperture and an overall decrease in rock permeability. Studies at Stripa mine in Sweden demonstrated a reduction in permeability of granites by a factor of three when temperature was increased by 25°C by circulating warm water.

METHODS OF AQUIFER PARAMETER ESTIMATION

Hydraulic properties of an aquifer can be estimated in laboratory and in the field. However, values obtained in the laboratory from rock samples are not representative of the formation.

Table 2 gives a list of commonly used field methods. The choice of a particular method depends on the purpose of study. For small scale problems, as in geotechnical investigation, seepage of water to mines and tunnels and contaminant transport, packer tests, slug tests and tracer tests are preferred. Cross-hole pneumatic injection tests are recommended for detailed investigation on a local scale (Illman and Neuman, 2003). For estimation of aquifer parameters and groundwater development and management on a regional scale, pumping test method should be used.

Table 2: Field test methods for the estimation of hydraulic characteristics of hard rock aquifers

Purpose of Investigation	*Size of area under Investigation*	*Distribution of Fractures*	*Test Method*
Geo-technical investigations; mine drainage; waste	A few km^2	Random	Packer (Lugeon) test, slug test, tracer injection test
		Systematic fractures of 1, 2 or 3 sets	Modified packer test, cross-hole hydraulic test; tracer injection
Groundwater development; water	> 100 km^2	Random and closely	Pumping test
Geothermal and petroleum reservoirs	A few km^2	Random	Well interference test, tracer injection test

In hard rocks, as the geometry of the fractures will greatly influence the flow characteristics and pumping test data, structural analysis is significant in the planning of pumping tests and interpretation of test data. Reader may refer to Kruseman and deRidder (1990), Singhal and Gupta (1999) and Lloyd (1999) for a detailed account of the pumping tests and interpretation of data. The effect of scale of measurement on permeability values is depicted in Fig. 6.

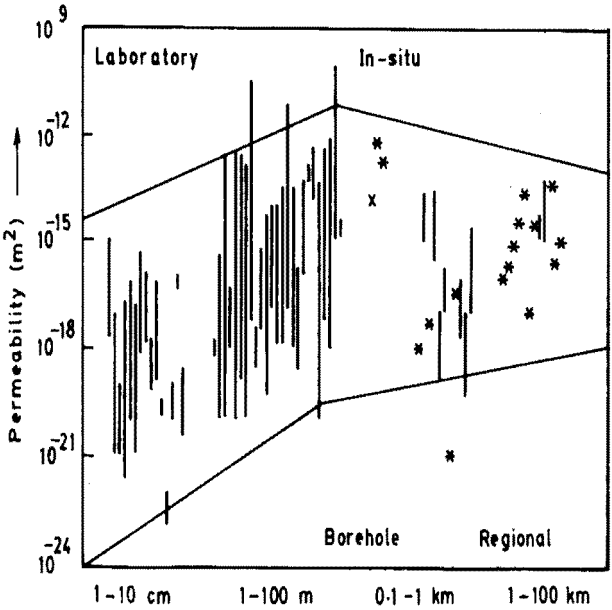

Figure 6. Variation in permeability values of crystalline rocks as a function of scale of measurement. Bars mark the permeability range based on several reported values, and stars represent single values (after Clauser, 1992).

In a recent study, Shapiro (2003) has shown that although the hydraulic conductivity measured from borehole tests in individual fractures varies over more than six orders of magnitude (10^{-10} to 10^{-4} ms^{-1}), the magnitude of the bulk hydraulic conductivity of the rock mass was the same from aquifer tests over 10's of metres and kilometre-scale estimates inferred from groundwater modelling. In contrast, the magnitude of the formation properties controlling chemical migration viz. dispersivity and matrix diffusion increases from laboratory size tests to field tests on kilometre scale.

Most of the earlier work on well hydraulics was based on porous homogeneous media. However, as the hard rock aquifers have varying degree of heterogeneity, due to the complexity of geometry of fracturing, the conventional well flow equations developed for homogeneous porous aquifer will not adequately describe the drawdown response in fractured aquifers.

Theis' method, although originally developed for porous and homogeneous media, can be used for fractured rock aquifers with due care if the correct part of the time-drawdown curve is matched with the Theis' type curve.

Experience in South Africa has shown that the estimated values of S in fractured rocks decrease with increase in the distance of observation well from pumping well (Fig. 7). Such a behaviour is explained by the rapid release of water from larger fractures near the pumping well while the pressure gradient between the small and larger fractures will be smaller away from the pumping well. Further, a variation is noted only at the early time of

pumping. As the system reaches close to steady condition, S will approach a uniform value.

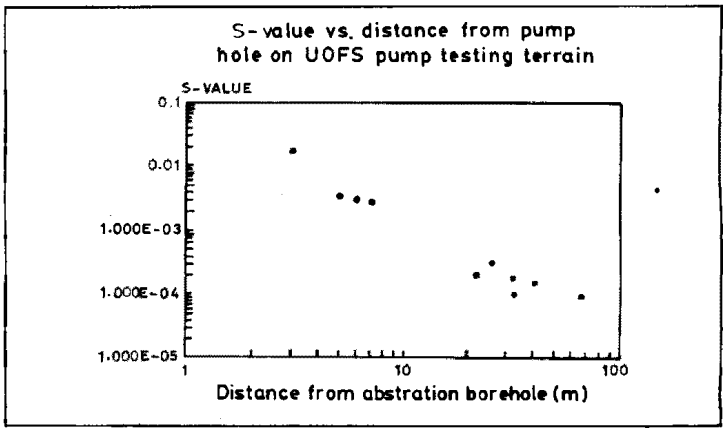

Figure 7. Variation of estimated S-values in relation to the distance between the observation and pumping borehole as obtained in the fractured-rock aquifer on the University of the Orange Free State (UOFS) campus (after Lloyd, 1999).

FACTORS AFFECTING WELL YIELD

Drilling of a successful well for groundwater in hard rocks is to a great extent a matter of chance. Groundwater exploration in hard rock formations should be carried out with due considerations to lithological, structural and geomorphological setting of hard rock formations. Plotting of structural data viz. poles of joints and foliation planes on Schmidt's equal area net is useful in the design and orientation of wells in such rock formations. Shape of cone of depression and base flow from streams are of help in determining the relative role of different fracture planes as groundwater conduits.

As fractures tend to close with depth, an overall decrease in well yield with depth is reported from various crystalline terrains. The optimum depth of wells is regarded between 50 and 100 m (Table 3). Although generally lithologies do not have any significant influence on well yield but coarse-grained rocks viz. pegmatites are more permeable. Fine grained and micaceous rocks viz. phyllites and schists have poor yield. Weathered granites usually have lower permeabilities as compared with fractured rocks due to the development of secondary clay minerals. Lineament zones are more productive for the construction of bore-wells.

In areas underlain by hard crystalline and meta-sedimentaries viz., granite, gneiss, schist, phyllite, quartzite, etc., occurrence of groundwater in the fracture system has been identified down to a depth of 60 m and even up to 200 m locally. In most of the granite-gneiss country, the weathered residuum serves as an effective groundwater repository. It has been found that the deeper

Table 3: Data on optimum depth of wells in different regions and rock types

Region	*Rock type*	*Optimum depth (m)*
Cyprus	Gabbro	170-200
Satpura hills, India	Granite gnesiss and schist	45-60 and 45-75
Northern Carolina, USA	Granite	75-90
Kararnoja, Uganda	Gneiss and schist	30-92
Zimbabwe	Greenstone and gneiss	40-80
Norway	Granite and gneiss	40-60

fracture systems are generally hydraulically connected with the weathered saturated residuum. The yield potential of the crystalline and meta-sedimentary rocks shows wide variations. Through 10 cm to 15 cm diameter bore-wells, the fractured system generally yields from 10 m^3/hour and up to 100 m^3/hour in the vicinity of structurally disturbed areas (Table 4).

Studies in different parts of the world indicate that the following factors can be related to well yields (Banks et al., 1996; Singhal and Gupta, 1999; Moore et al., 2002, Faillace, 2003; Henriksen, 2003).

- Rainfall regime and intensity.
- Size of the drainage area up-gradient of the well.
- Distance to the nearest water body.
- Well proximity to major fractures and lineaments.
- Narrow alluvial valleys in hard rock terrain and underlying weathered and fractured hard rocks can be a potential source of water supply.

Table 4: Yield of bore-wells in crystalline rocks

Rocks type	*Region*	*Well yield (m^3 h^{-1})*	*Well depth (m)*
Granite-gneiss	Southern and eastern India	3-10	15-80
Granite-gneiss, Charnockite	Tamilnadu, South India	6-18.3	0-70
Granite and gneiss	Kwara, Nigeria	9.5	50-75
Granite and gneiss	Victoria, Zimbabwe	4.1	20-30
Gneiss (fractured)	Maharashtra, India	48	164
Granodiorite and Gabbro (fractured)	Lee Valley, USA	3.5-23	60-150
Pegmatite (fractured)	Karnataka, India	110	42
Quartz vein (fractured)	Bihar, India	55	137
Marble	Sri Lanka	2.4-24	
Quartzite	Sri Lanka	6-28.8	
Schist	Connecticut, USA	4.16	33.4
Slate	Slate Maine, USA	3.42	

- Topography and geomorphology have distinct influence on transmissivities and well yields. Steep slopes and sites on hill tops should be avoided for constructing bore-wells.
- Lithology doesn't appear to have any appreciable influence on well yield (Fig. 8)

Experience of water well drilling in hard rock terrains indicate that even in geologically promising areas, the yield of bore-wells may not be satisfactory. Proper design and development of bore holes is very important. A bore hole should be oriented so that it intercepts the maximum number of fractures, preferably perpendicular to the hydraulically open fractures. Further, techniques of artificial yield enhancement such as hydraulic fracturing or explosives will greatly improve well yield by creating a network of interconnected fractures (Singhal and Gupta, 1999).

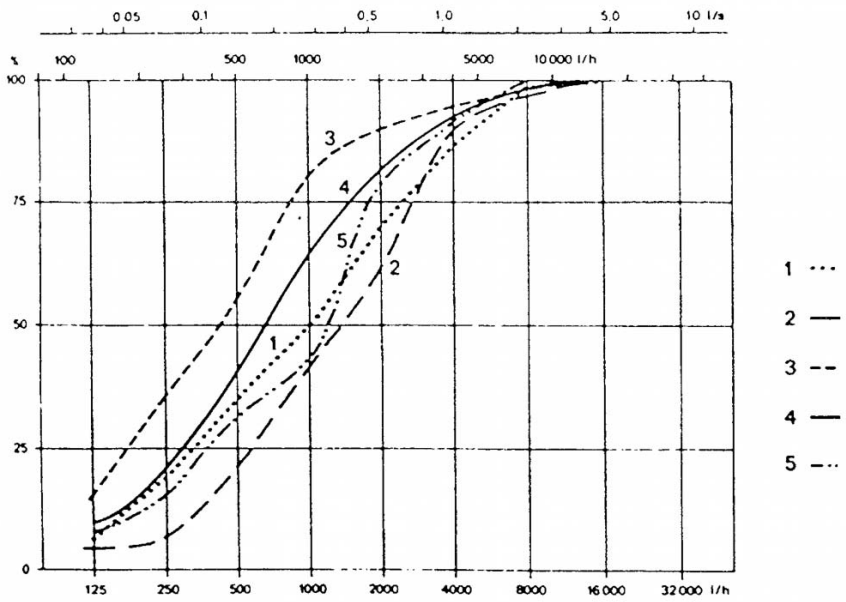

Figure 8. Distribution of well yields for different rock types in the Central Scandinavian area (after Banks et al., 1996) 1: syn-orogenic granites. 2: post-orogenic granite. 3: post-orogenic gabbros and dolerites. 4: gneisses. 5: Caledonian mica schists.

ESTIMATION OF AQUIFER RECHARGE

Quantitative estimates of recharge to aquifers and changes in groundwater storage is important to manage the development of groundwater resources and to know the amount of groundwater that can be withdrawn without exceeding recharge.

The hard rock terrain usually poses a different set of problems unlike porous rock areas, viz. rapid variation in hydraulic characteristics (*T* and *S*), both laterally and vertically. Demarcation of the boundaries of the groundwater basin in a hard rock terrain is also problematical. The watershed may be taken as a unit for recharge estimation as the watershed boundary is likely to be a no flux boundary for groundwater also. The watershed may further be divided into various hydrogeologically homogeneous units depending upon their hydrogeological characteristics.

In hard rocks the most common methods for recharge estimation are (Lloyd, 1999):

- Water balance estimate
- Chloride profile method
- Chloride mass balance
- Hydrograph method
- Cumulative Rainfall Departure method
- Tritium injection method

The residence time of groundwater in hard rock aquifers varies from few years in shallow weathered horizon to several thousand years in deeper fractured zones as revealed from isotopic data (Gale et al., 1982; Sukhija and Rao, 1983; Silar, 1996). This indicates slow recharge of deeper fractures.

GROUNDWATER QUALITY

In crystalline (igneous and metamorphic) rocks the groundwater flow is mainly through fractures. Therefore, the contact area between water and rock matrix is less than in porous media. Further, the crystalline rocks contain usually silicate minerals which have comparatively low solubility. Therefore, in general groundwater in these rocks has relatively low salinity (TDS < 500 mg/l). However, in arid and semi-arid regions, groundwater may have high salinity. In some eastern and western African countries, where arid conditions prevail, groundwater in crystalline rocks is brackish to saline with TDS in the range of 2000 to 6000 mg/l (Faillace, 2003).

At some places, as in parts of Andhra Pradesh and Rajasthan in India, groundwater in acidic igneous rocks (granites and pegmatite) and mica schists has fluoride contents more than the permissible limit (1.5 mg/l), which is mainly due to the presence of fluoride-bearing mineral, viz apatite, fluorite, biotite and hornblende in rocks. Among other trace elements, iron and manganese are common as a result of weathering of biotite and hornblende bearing rocks. In mafic and ultramafic rocks, chromium is quite prominent.

A vertical zonation in the water quality has also been reported from several crystalline rock terrains. Shallow groundwaters are usually of Ca-HCO_3 type. With increasing depth salinity increases (TDS = 5000-50,000 mg/l) and water at depths greater than 500 m tends to be of the Na-HCO_3 type and Na-Ca-Cl type (Gascoyne and Kamineni, 1996; Bae et al., 2003).

The quality of groundwater in deep-seated crystalline rocks is not only of geochemical interest but is also of importance for the disposal of radioactive waste and tapping of geothermal power.

CONTAMINANT TRANSPORT AND WASTE DISPOSAL

Hydrogeological studies in fractured rocks are also required to find suitable sites for the disposal of hazardous waste material and site selection of landfills etc. The transport of hazardous dissolved contaminants, especially radio nuclides and other hazardous waste, in the subsurface, especially in complex environments through highly deformed and fractured rocks is quite complicated. Under such situations the contaminants undergo rapid transport through fractures and the movement of solutes into the high-porosity low-permeability matrix by chemical diffusion. Sorption by very large surface area of the matrix will retard the transport of reactive contaminants.

Dense non-aqueous phase liquids (DNAPLs) are also an important class of groundwater contaminant. DNAPLs, released on ground surface underlain by fractured rocks, migrate under the influence of gravitational and viscous forces while capillary forces retard their forward movement.

Local industries, such as tanneries in South India using Cr (iv) and textile industries using large salt concentration for dyeing, cause point source contamination. Use of fertilizers and human and animal excreta are the main cause of nitrate contamination especially in shallow groundwaters. However, at greater depths, nitrate is reduced by denitrifying bacteria.

Special care is required for the disposal of high level radioactive waste (HLW) produced from nuclear reactors for power production, weapons manufacturing and research. Crystalline rocks including salt, shale and clay beds, being impervious, are regarded to be suitable host rocks for HLW disposal in repositories at depths of more than few hundred metres.

Most of the waste from nuclear power plants and nuclear weapons consists of radioactive isotopes, which are long-lived and, therefore, require several thousands of years of isolation from the environment. Therefore, the safety requirements of such repositories pose considerable technical, social and political challenges. The movement of dissolved radio nuclides in groundwater through fractures is a matter of great concern. It has to be demonstrated that the disposal of HLW will not have any adverse effect on the environment and human health so that such programmes are acceptable to the public. This has led to the establishment of Underground Research Laboratories (URLs) for detailed hydrogeological and geotechnical studies in different parts of the world viz., USA, Canada, Europe, Japan and Korea.

In USA, a repository for the disposal of HLW is proposed at the Yucca Mountain in Nevada in the unsaturated (vadose) zone within basaltic tuffs at a depth of about 350 m below the ground surface and 225 m above the water table. The area is located in a desert environment having an annual

rainfall of about 15 cm. Conceptual models for flow in the variably saturated fractured rocks at the Yucca Mt. are developed. However, doubts have been created about the safety of the proposed repository. If all goes well, the repository is expected to accept waste in 2010.

In India, the deep abandoned gold mine in the Pre-Cambrian crystalline rocks (amphibolites) in the Kolar Gold Field is regarded to be a potential repository for the disposal of HLW (Bajpai, 2004).

REFERENCES

Anon, 1996. Rock Fractures and Fluid Flow: Contemporary understanding and applications. National Academy Press, Washington, D.C.

Bae, D., Koh, Y.K., Kim, K.S., Kim, C.S. and Kim, G.Y., 2003. The Hydrogeological and Hydrochemical Conditions of Deep Groundwater System in Yuscong Granite Area, Korea. *In:* Krasny J., Hrkal, Z. and Bruthans, J. (eds.) IAH Symposium on Groundwater in Fractured Rocks, Prague, p. 25-26.

Bajpai, R.K., 2004. Recent Advances in the Geological Disposal of Nuclear Wastes Worldwide and Indian Scenario, *Jour. Geol. Soc. Ind*, **63(3):** 354-356.

Banks, D. et al., 1996. Permeability and Stress in Crystalline Rocks. Terra Nova, pp. 223-235, Blackwell Services Ltd.

Black, J.H., 1987. Flow and Flow Mechanisms in Crystalline Rocks. *In:* Fluid Flow in Sedimentary Basins and Aquifers, (eds) J.C. Goff and B.P. Williams, Geol. Soc. Spl. Publ. 34, pp. 185-200.

Boulton, N. and Streltsova, T.D., 1978. Unsteady Flow to a Pumped Well in an Unconfined Fissured Aquifer. *Jr. of Hydro*., **35:** 257-269.

Brace, W.F., 1984. Permeability of Crystalline Rocks: New in-situ measurements. *J. Geophys. Res.* **89 (B6):** 4327-4330.

Clause, C., 1992. Permeability of Crystalline Rocks, EOS, *Trans. Am. Geophys. Union*, **73:** 233-238.

Faillace, C., 2003; Hydrogeology of Hard Rocks in Some Eastern and Western African Countries. IAH Symposium on Groundwater in Hard Rocks, Prague, pp.4-6

Gale, J.E. et al., 1982. Hydrogeologic Characteristics of a Fractured Granite. *In:* Papers of the Groundwater in Fractured Rock Conference. AWRC Conference Series No.5, Canberra, pp. 95-108.

Gascoyne, M. and Kamineni, D.C., 1993. The Hydrogeochemistry of Fractured Plutonic Igneous Rocks in the Canadian Shield, Memoir 24th Congress of IAH, Oslo, pp. 440-449.

Gerard, A., 1996. European Hot Day Rock Research Project at Soultz-Sous-Forets. 30th IGC, Abstracts, Vol.1, Beijing, pp. 385.

Gringarten, A.C., 1982. Flow Test Evaluation of Fractured Reservoirs. *In:* Recent Trends in Hydrogeology, Geol. Society of America, Special paper 189, pp. 237-263.

Henriksen, H., 2003. The Role of Some Regional Factors in the Assessment of Well Yields from Hard Rock Aquifers of Fennoscandia. *Hydrogeology Jr.*, **11(6)**: pp. 628-645.

Illman, W.A. and Neuman, S.P., 2003. Steady-state Analysis of Cross-hole Pneumatic Injection Tests in Unsaturated Fractured Tuffs, *Jour. of Hydrology*, **281:** 36-54.

Kessels, W. and Kuck, J., 1995. Hydraulic Communicator in Crystalline Rock Between the Two Boreholes of the Continental Deep Drilling Project in Germany. *Intl. Jour. Rock Mech.Min. Sc.* and Geotech. Abstacts, **32(1):** 37-47.

Kruseman, G.P. and de Ridder, N.A., 1990. Analysis and Evalution of Pumping Test Data, 2nd edition, Intl. Inst. for Land Reclamation and Improvement, Wageningan, Bulletin 11, p 200.

Lee, C.H. and Farmer, I. 1993. Fluid Flow in Discontinuous Rocks. Chapman and Hall, London, pp 169.

Lloyd J.W., 1999. Water Resources of Hard Rocks Aquifers, Studies and Reports in Hydrology, 58, UNESCO.

Moore, R.B., Schwarz, G.E., Clark Jr., S.F., Walsh, G.J. and Degnan, J.R., 2002. Factors Related to Well Yield in the Fractured Bedrock Aquifer of New Hampshire. USGS Professional Paper 1660, Denver, Colorado.

Rutqvist, J. and Stephansson, O., 2003. The Role of Hydromechanical Coupling in Fractured Rock Engineering. *Hydrogelo. Jr.,* **11:** 7-40.

Shapiro, A.M., 2003. The Effect of Scale on the Magnitude of the Formation Properties Governing Fluid Flow Movement and Chemical Transport in Fractured Rocks. Proc. Symp. on Groundwater in Fractured Rocks, Prague, pp. 13-14.

Silar, J., 1996. Groundwater Residence Time in Crystalline Rocks. *In:* Hardrock Hydrogeology of the Bohemian Massif, Acta Karlova, Czech Republic, vol. 40, pp. 279-288.

Singhal, B.B.S. and Gupta, R.P., 1999. Applied Hydrogeology of Fractured Rocks. Kluwer Academic Publishers, Dordrecht. The Netherlands, pp 400.

Streltsova-Adams, T.D., 1975. Well Hydraulics in Heterogeneous Aquifer Formations, *In:* Hydroscience, Vol. 11, Academic Press, pp. 357-423.

Sukhija, B.S. and Rao, A.A., 1983. Environmental Tritium and Radiocarbon Studies in the Vedavati river basin, India. *J. Hydro*., **60:** 185-196.

3 Overview of the Hydrogeology of Hard Rock Aquifers: Applications for their Survey, Management, Modelling and Protection

P. Lachassagne

Resource Assessment, Discontinuous Aquifers Unit, Water Division, BRGM, French Geological Survey, 1039, rue de Pinville, 34000 Montpellier, France

INTRODUCTION

Hard rocks (granites, metamorphic rocks) occupy large areas throughout the world (Africa, South and North America, India, Korea, several areas in Europe, etc.). Their groundwater resources are modest in terms of available discharge per well (from less than 2-3 m^3/h up to 20 m^3/h), compared to those in other types of aquifers (sedimentary, karstic or volcanic aquifers). They are, however, geographically widespread and therefore well suited to scattered settlement, and small to medium size cities. These resources contribute largely to the economic development of such regions, especially in arid and semi-arid areas where the surface water resource is limited.

However, these aquifers are considered as highly heterogeneous. For example, two neighbouring wells may exhibit very contrasted behaviours: one of them yielding several cubic metres per hour, the other being of very low discharge. As a consequence, for most authors, their hydrodynamic properties feel quite unpredictable at the local scale and they are thus considered as "discontinuous aquifers". Moreover, their properties also seem to be unpredictable at the catchment scale.

Significant advances have recently been made in our knowledge of the structure and functioning of hard rock aquifers. Their hydrodynamic properties appear to be mainly related to the existence of ancient weathering profiles. The spatial distribution of such weathering profiles, or their remains after

erosion, can now be mapped, even at the catchment scale. Thus, this newly developed approach enables to regionalize hard rock aquifers properties, and to find numerous practical applications: from the mapping of groundwater potential on a regional scale, through well siting techniques and methods, to water resources management at the watershed scale, crucial in areas where ground water is heavily exploited.

These recent research results and their practical applications are summarized within the present paper.

STRUCTURE AND HYDRODYNAMIC PROPERTIES OF HARD ROCK AQUIFERS

The Classical Concept of Discontinuous Aquifer

The "hard rock" aquifers, or "fissured aquifers", that are present near the surface (within the first 100 m below ground surface) are considered as "discontinuous aquifers", as a consequence of their discrete hydraulic conductivity. In fact, during a drilling, the first significant water bearing zones appear within the fresh (hard) rock. The well intersects an impermeable rock that is only very locally (along a few centimetres or decimetres) showing significantly permeable zones. Most of the wells exhibit a few of these water strikes (from 0 to 4 or 5 water bearing zones).

The classical concept of discontinuous aquifer has been developed during the seventies, mainly on the basis of the results of the large drilling campaigns performed in Africa (Detay et al., 1989). It considers that these water bearing zones are tectonic open fractures (Fig. 1).

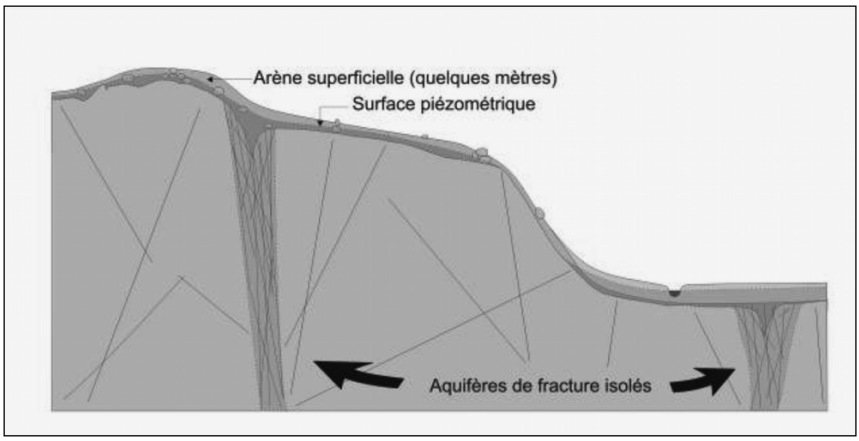

Figure 1. The classical concept of discontinuous aquifer [translation - upto bottom: superficial and consolidated weathering cover (a few metres), piezometric level, aquifers in isolated fractures].

Several authors noticed a decrease of the occurrence of such water bearing zones with depth (within the first 100 m below the ground surface) and attributed it to the "closure" of these tectonic fractures, as a consequence of the increase of the lithostatic strain. These concepts influenced in the past, and still presently influence the methodologies used in such areas, for instance for water well sitting.

The New Concept of Continuous Stratiform Aquifer due to the Weathering Processes

Most of the areas where metamorphic or plutonic rocks do outcrop are stable areas, emerged since a long time, that were thus exposed during very long periods (several tens of millions years) to the weathering processes, under rather humid climates. The outcropping rocks thus generally comprise a several tens of metres thick superficial weathered layer, where it has not been eroded. This superficial layer corresponds to a laterite type weathering profile (Dewandel et al., 2006).

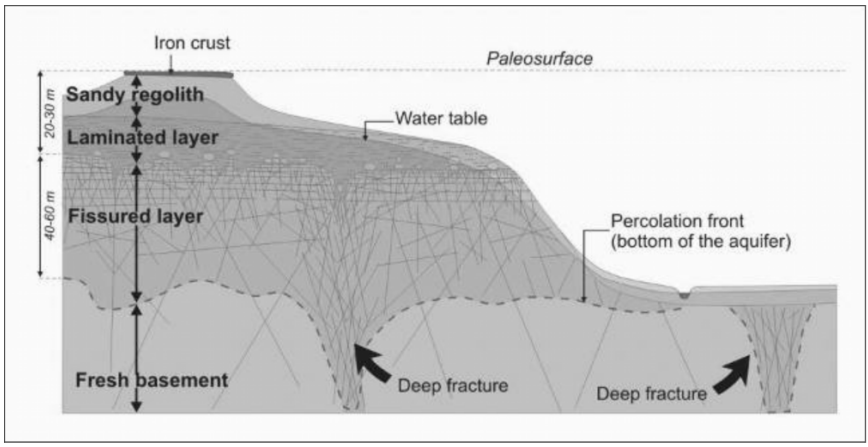

Figure 2. Stratiform conceptual model of the structure and the hydrogeological properties of hard rock aquifers (after Wyns et al., 2004).

From recent results (see for instance Dewandel et al., 2006; Wyns et al., 2004), a typical weathering profile (Fig. 2) comprises the following layers that have specific hydrodynamic properties. All together (where and when saturated with ground water), these various layers constitute a composite aquifer. From the top to bottom, the layers are the following (Fig. 2):

- The laterite (or iron or bauxitic crust) that can be absent, due to erosion or rehydration of hematite in a latosol (for iron crusts), or resilicification of gibbsite/boehmite into kaolinite (for bauxitic crusts).

- The *saprolite or alterite, or regolith* (Fig. 3), a clay-rich material, derived from prolonged in situ decomposition of bedrock, a few tens of metres thick (where this layer has not been eroded). The saprolite layer can be divided into two sub-units: the alloterite and the isalterite.
  - The alloterite is mostly a clayey horizon where, due to the volume reduction related to mineralogical weathering processes, the structure of the mother rock is lost.
  - In the underlying isalterite, the weathering processes only induce slight or no change in volume and preserve the original rock structure; in most of the cases this layer takes up half to two thirds of the entire saprolite layer. In plutonic rocks, such as granites, the base of the isalterite is frequently laminated; this layer is thus named the 'laminated layer'. It is constituted by a relatively consolidated highly weathered parent rock with coarse sand-size clasts texture and a millimetre-scale dense horizontal lamination crosscutting the biggest minerals (e.g., porphyritic feldspars), but still greatly preserving the original structure of the rock.

    Because of its clayey-sandy composition, the saprolite layer can reach a quite high porosity, which depends on the lithology of the parent rock (bulk porosity is mainly between 5 and 30%; Compaore et al., 1997; Wyns et al., 2004), and displays generally a quite low permeability, about 10^{-6} m/s. Where this layer is saturated, it mainly constitutes the *capacitive function of the global composite aquifer.*

Figure 3. Saprolite (grus and laminated grus) in granites (Jeonju area, South Korea).

- The *fissured layer* (Fig. 4) is generally characterized by fresh (hard) rock cut by a dense horizontal fissuring in the first few metres and a depth-decreasing density of subhorizontal and subvertical fissures (Cho et al., 2003; Maréchal et al., 2003; Maréchal et al., 2004; Wyns et al., 2004). Several processes such as cooling stresses in the magma, subsequent tectonic activity or lithostatic decompression were invoked to explain the origin of these fissures. However, it has been demonstrated that fissuring results from the weathering process itself (Cho et al., 2003; Dewandel et al., 2006; Wyns et al., 2004). Swelling of certain minerals results in a local increase of volume that favours cracks and fissuring. In granitic rocks, the most sensitive mineral to swelling is biotite. Where the rock texture is relatively isotropic (in granite for example), the generated fissures are orthogonal to the lower constraint vector (σ_3), and thus subparallel to the topographic surface contemporaneous with the weathering process (Fig. 4 left). In highly foliated rocks (i.e., gneisses or schists) the orientation of the fissures can be also controlled by the rock structure. The intensification of this horizontal fissuring at the top of the layer constitutes the overlying laminated layer.
  The fissured layer mainly assumes the *transmissive function of the global composite aquifer* and is drawn from most of the wells drilled in hard rock areas. However, the covering saprolite layer may have been partially or totally eroded, or may be unsaturated. In these cases, the fissured layer assumes also the capacitive function of the composite aquifer; e.g., in French Brittany 80 to 90% of the groundwater resource is located in the fissured layer (Wyns et al., 2004).
- *The fresh unfissured basement* is permeable only locally, where tectonic fractures are present. The hydraulic properties of such fractures have been investigated in various studies, particularly in details when the purpose of these studies is the storage of nuclear waste (Neuman, 2005). Even if these tectonic fractures can be as permeable as the fissures induced by the weathering processes described here above, in most of the geological contexts, their density with depth is much more lower than within the fissured layer (Cho et al., 2003). At the catchment scale, and for water resources applications, the fresh basement can then be considered as impermeable and of very low storativity (Maréchal et al., 2004).

In addition to rock mineralogy, the development of such thick weathering profiles requires specific climatic conditions: mainly significant rainfall, in order to ensure mineral hydrolysis and, on the second order, quite high mean temperatures to favour the kinetics of the process. Its development also requires long periods of time under stable tectonic conditions (a few millions to a few tens of millions years), the latest duration leading to profiles a few tens of metres thick. In addition, relatively flat topography is required to avoid the erosion of weathering products (saprolite), and also to favour

Figure 4. The fissured layer in granites (left: Margeride, Lozère, France)and in metamorphic rocks (right: Gokseong area, South Korea).

water infiltration. Thus, such profiles cannot develop in regions of sharp topography where the erosion rate is higher than the one of weathering.

An important consequence of this weathering process is that, from the hectometre scale to the regional one, these layers are parallel to the paleo-weathering surfaces (paleo-landscape) contemporaneous with the weathering phase and thus appear as stratified layers (Fig. 2; Wyns et al., 2004; Lachassagne et al., 2001). Moreover, geological features (faults, dykes, etc.) or contrasts in rock mineralogy or structure can locally modify the characteristics (mineralogy, thickness, etc.) of the weathering profile. These contrasts lead to differential weathering and in some cases to the development of positive topographic anomalies such as inselbergs.

More complex weathering profiles can result from multiphase weathering and erosion processes. In Korea for instance at least two main phases of weathering have been identified (Cho et al., 2002; Fig. 5):

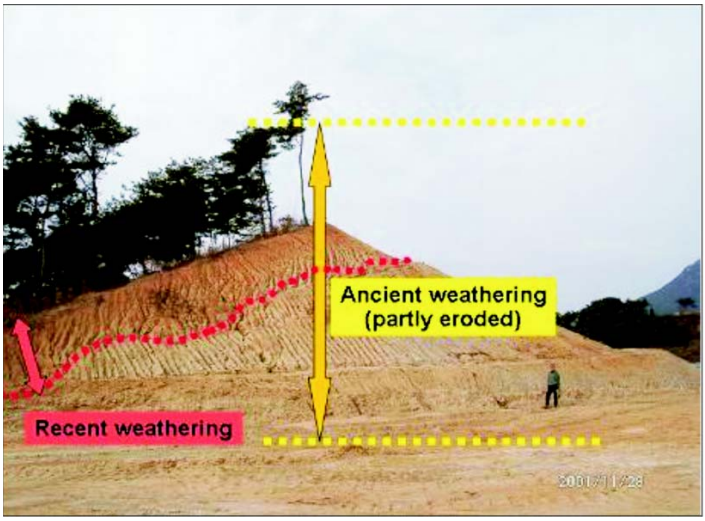

Figure 5. Red recent weathering, related to the present topography, intersecting an old weathering profile (Namwon area, South Korea).

- *an "ancient" one* which deeply affects hard rocks (up to more than 50 m) and results in a typical weathering profile, similar to those observed in other regions of the world (Africa, South America, Europe, etc.); from bottom to top, it comprises:
  - the *unweathered hard rock*,
  - the *fissured horizon*, and,
  - above, the *saprolite* in metamorphic rocks and *grus* in granites, including a laminated horizon in the lower part. The upper part of the original weathering profiles (mottled horizon and iron crust) has not been observed. As a consequence of its position at the top of the original profile, it has probably been removed by erosion,
- *a more recent one* which only affects the rocks (and the ancient weathering profile) within their first metres below the topographic surface. It is clearly posterior to the previous weathering phase(s) as it crosscuts all the horizons of the previously described weathering profile. It is probably quite recent as it clearly follows the actual topographic surface.

  This recent weathering phase didn't develop a thick fissured layer. It is thus of low hydrogeological interest.

In *southern India* (Dewandel et al., 2006), the non-laminated saprolite is very thin (1-3 m) and is almost constant in thickness while it should be thicker in the plateau areas than in the valleys if the weathering had occurred earlier than the erosion that shaped the present topography. The thickness of the laminated layer (10-15 m) is disproportionate compared to that of the non-laminated saprolite, while in the classical weathering profile (Fig. 2) the laminated layer occupies only one third to half of the entire saprolite layer. The thickness of the fissured layer is small compared to that of the saprolite (ratio of ~1 instead of ~2). Moreover, the laminated layer presents preserved fissures, which are usually not observed in the classical model.

In fact, the weathered zone appears to be composed of an old, probably Mesozoic, weathering profile (Fig. 6a), where only a part of the fissured layer has been preserved. An erosion phase, probably due to regional uplift, thus caused the erosion of the entire saprolite layer and a part of the fissured layer (Fig. 6b). Then, at least one more recent weathering phase, the latest being probably still active, is responsible for the saprolitisation of this truncated profile and explains the development of 1-3 metres non-laminated saprolite locally capped by an iron crust, and the lamination of a large part of the ancient fissured layer (Fig. 6c). The profile structure is thus controlled by a multiphase weathering process that was induced by the geodynamic history of the Indian Peninsula.

This (or these) more recent weathering phase(s) was (were) efficient enough to hydrogeologically rejuvenate the old weathering profile through the apparition of new permeable weathering induced fissures.

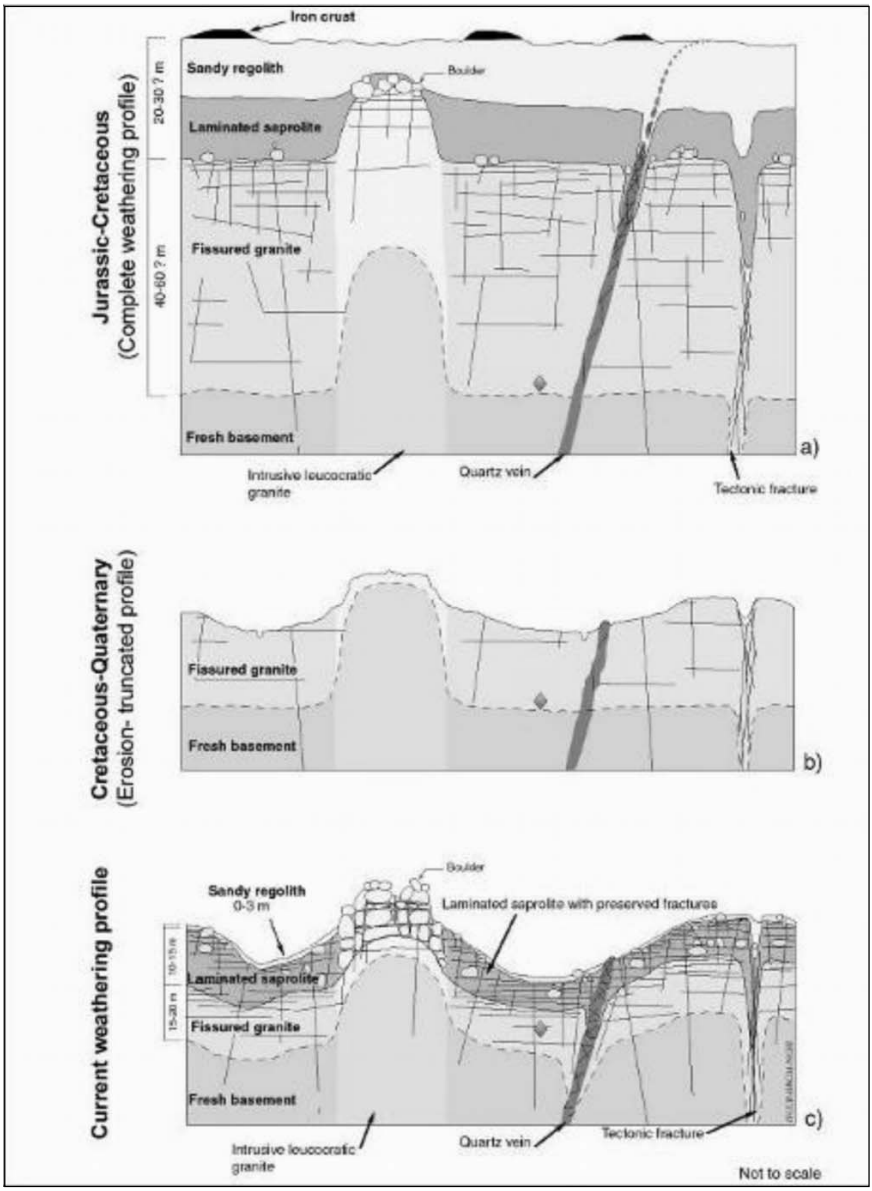

Figure 6. Multiphase weathering conceptual model observed in southern India (vertical scale exaggerated) from Dewandel et al., 2006.

Hydrodynamic Properties of the Fissured Layer

Recent research works confirm that the fissured layer of the weathering profile plays a major role from a hydrodynamic point of view. For example,

the statistical analysis of several hundreds existing well yields from Korea (Cho et al., 2003) reveals no evidence to suggest a relationship between well yield and tectonic fracturing (Fig. 7).

Conversely, a marked relationship is observed (Cho et al., 2003) between the well's specific yield (yield [m^3/day] divided by well depth [m] below the base of the saprolite) and its depth below the base of the saprolite (the first water bearing zone always appears below this horizon), shown as a "classical" sharp decrease with depth (Fig. 8). The most interesting point is that this relationship is well expressed for wells drilled in zones where a weathered cover (saprolite and/or fissured layer) is preserved (Fig. 8), but is not consistent where the weathering profile has been totally eroded. It thus appears that the weathered cover, and thus its lower part, the fissured layer, plays a determining role in terms of the transmissive properties of the hard rocks and not only in term of their water-retention capacity. The weathered-fissured horizon, which develops within the uppermost tens of metres of the "fresh" basement substratum, is clearly due to the weathering processes. Thus, well yields are statistically much higher in regions where a weathered cover (alterites + fissured layer or fissured layer only) is preserved than in places where these horizons have been eroded.

Despite providing different absolute values of specific yield, similar results are obtained for granite and metamorphic rocks.

The underlying fresh basement substratum is permeable only very locally due to tectonic fracturing. Despite local significant yields from certain fractures, the overall specific yield is lower than that measured in the weathered-fissured horizon (Fig. 8).

The *hydrodynamic properties* (permeability, storativity, anisotropy, fissures density, double porosity, scale effects) of the *fissured layer* of a granite aquifer have been characterized in details in southern India, within a multiphase weathering profile (*see* previous subsection) using hydraulic tests at different investigation scales. Slug tests, injection tests, flowmeter tests, and pumping tests are interpreted using various analytical solutions (Table 1) specific for fractured media (Maréchal et al., 2004 and Dewandel et al., 2006). A first comprehensive hydrodynamic model of the fissured layer has then been proposed.

The application of flowmeter profiles during injection tests determines the vertical distribution of the most conductive fissure zones (CFZ) and their hydraulic conductivities (Fig. 9c). The geometric mean of available data (19 flowmeter tests) is $K_{CFZ} = 8.8 \times 10^{-5}$ m/s (according to the geometry of the well and the observed drawdowns, the sensitivity of the flowmeter limits the identification of fissure zones to those with a hydraulic conductivity higher than 1×10^{-5} m/s; hydraulic transmissivity $T > 5 \times 10^{-6}$ m^2/s). The rather narrow range of hydraulic conductivities (which do not exceed 2.10^{-3} m/s) suggests a similar genesis for all of them, namely the weathering processes.

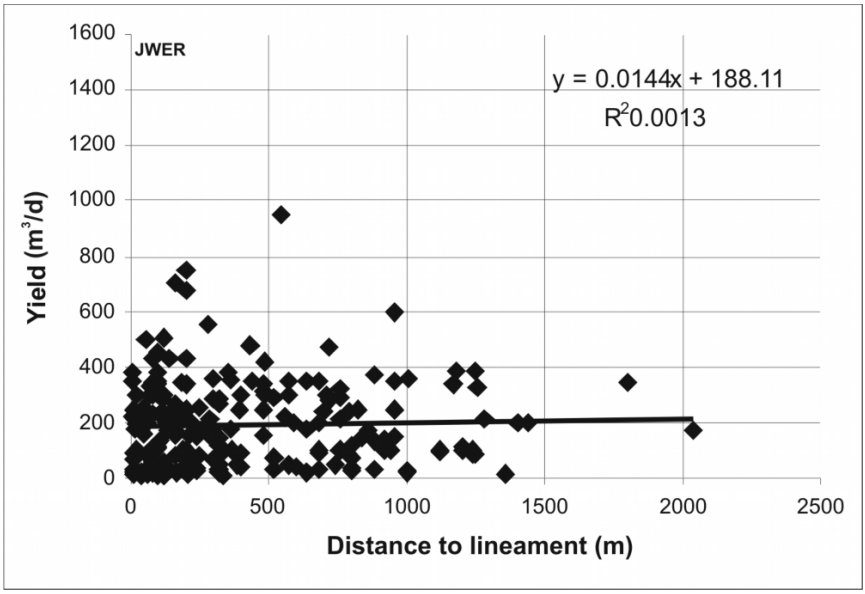

Figure 7. Example of the distribution of well yields as a function of the distance to lineaments (from Cho et al., 2003).

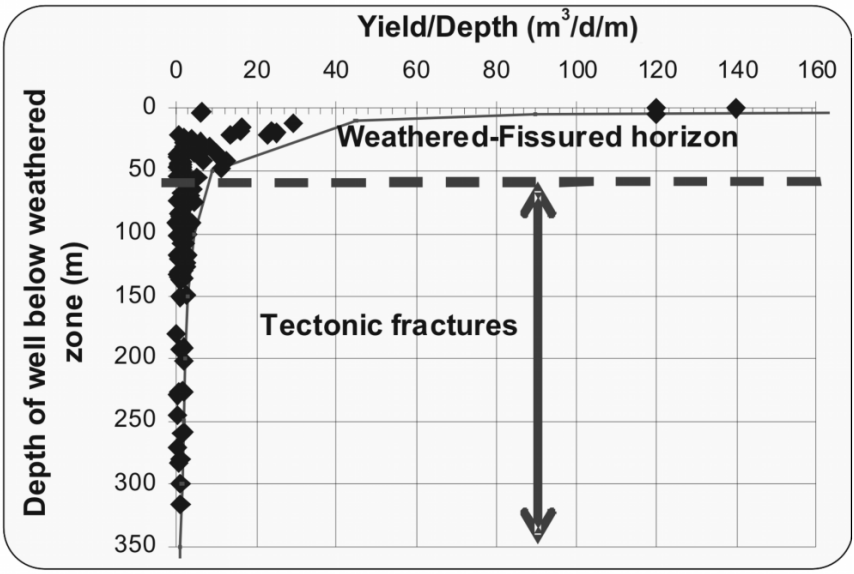

Figure 8. Example of the vertical distribution of specific yields as a function of depth for wells drilled in zones with a weathering cover (Jeonju Wanju area, Korea, Jurassic granites) (from Cho et al., 2003).

Table 1: Characteristics of the techniques used for the interpretation of hydraulic tests on the Maheswaram experimental catchment (Southern India) (from Maréchal et al., 2006).

Hydraulic test	*Interpretation method*	*U/C*[1]	*T/S*[2]	*Parameters obtained*	
Slug test	Solution for unconfined aquifers	U	T	Local permeability	Scale effect
Injection test	Usual Dupuit (1848, 1863) solution	U	S	Permeability	
Flowmeter test	Usual Dupuit (1848, 1863) solution for confined aquifers corrected for unconfined aquifers	U	S	Permeability and density of CFZ[3]	
Pumping test	Double porosity (Warren and Root, 1963)	C	T	Bulk permeability and storage of blocks and fractures	
Pumping test	Anisotropy (Neuman, 1975)	U	T	Permeability and storage, degree of permeability anisotropy	
Pumping test	Single fracture (Gringarten, 1974)	C	T	Radius of fractures	
Pumping test	Fractional dimension flow (Barker, 1988)	C	T	Flow dimension, generalized transmissivity and storage	

[1] Hypothesis on aquifer property in the analytical solution (u: unconfined, c: confined)
[2] Analytical solution type (t: transient, s: steady-state)
[3] CFZ: conductive fracture zones

The vertical distribution of the CFZ (Fig. 9a) shows the occurrence of conductive fractures both within the bottom of the saprolite (unusually preserved fissures) and within the first 20 m of the underlying fissured layer, with higher concentrations of fissures within its first metres (the curve on Fig. 9b shows that observations between -6 and +24 metres can be considered as representative, the percentage of investigated wells being higher than 50%—for a given aquifer portion, ratio between the number of available observations and the total 19 possible measurements). The low number of observations at shallow depths suggests that the apparent decrease in fractures density above 15 metres is an artefact due to lack of observations. Consequently, in such a context, it can reasonably be assumed that the fissured layer extends above the upper limit of observations, which is consistent with field and well geological observations.

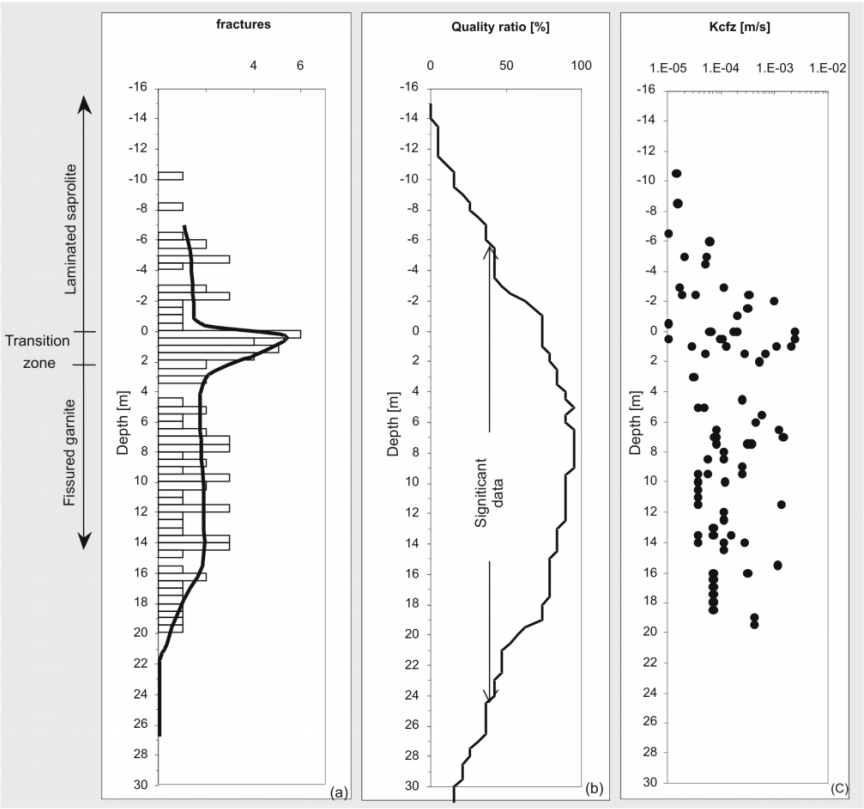

Figure 9. Interpretation of flowmeter-measurement profiles (19 wells) by 0.5-metre-thick aquifer portions performed in the Maheswaram (southern India) experimental watershed. (a) Number of identified hydraulically conductive fissures zones (CFZ). (b) Quality of observation (see definition in the text). (c) Hydraulic conductivity of CFZ (from Dewandel et al., 2006).

The bottom of the weathered-fractured layer is better constrained thanks to the quality of the available observations. The number of fractures starts to decrease between 14 and 16 metres (Fig. 9a) and is followed by an absence of fractures below 20 metres while the quality ratio of observations remains high down to 24 metres. This depth roughly corresponds to the top of the fresh basement as identified by geological observations during the drilling of the wells, and also to a sudden decrease in drilling rates at this depth.

The comparison of the characteristics of the Maheshwaram aquifer, resulting from a multiphase weathering process, with the ones of aquifers where the landscape mainly results only from a single main weathering phase (Dewandel et al., 2006), leads to a generalized 3-D geological and hydrogeological conceptual model of granitic aquifers (Fig. 10).

The hydrodynamic properties of the fissured layer are thus controlled by the distribution, the hydraulic conductivity, the anisotropy of hydraulic conductivity and the connectivity of the fissures (Maréchal et al., 2004). It thus constitutes an anisotropic medium. It is the most permeable layer of the entire weathering profile and assumes most of the transmissive function of the aquifer.

The global hydraulic conductivity of this layer appears to be a result of the number of conductive fissures intersected by the considered well, and not the result of a higher hydraulic conductivity of a single (or more) conductive fissure (Maréchal et al., 2004). Indeed, the hydraulic conductivity of the conductive fissure zones belonging to this layer is relatively similar regardless of the case study location in the world; it ranges between 10^{-6} and 10^{-4} m/s. Thus, it appears that granitic rocks exposed to weathering are affected by similar weathering processes that induce similar fissure hydraulic conductivities.

As the hydraulic conductivity of this layer closely depends on the density of the conductive fissures, the variations in hydraulic conductivity from one well to another are explained by the variability in hydraulically conductive fissure density itself and not by the variability of fissure hydraulic conductivity. Moreover, the hydraulic conductivity of the fissures does not significantly decrease with the depth (Fig. 9). The apparent decrease in hydraulic conductivity toward the base of this layer, largely observed worldwide, reflects only a downward decrease in density of the weathering-induced fissures (Fig. 10).

The presence of two main fissure sets, a horizontal and a subvertical one, recognized both from geological observations and from pumping test interpretation (Maréchal et al., 2004), ensures good connectivity between the fissures and induces an anisotropy of hydraulic conductivity (vertical anisotropy ratio close to 10; $K_{horiz} >> K_{vert}$), which is in agreement with the qualitative geological observations.

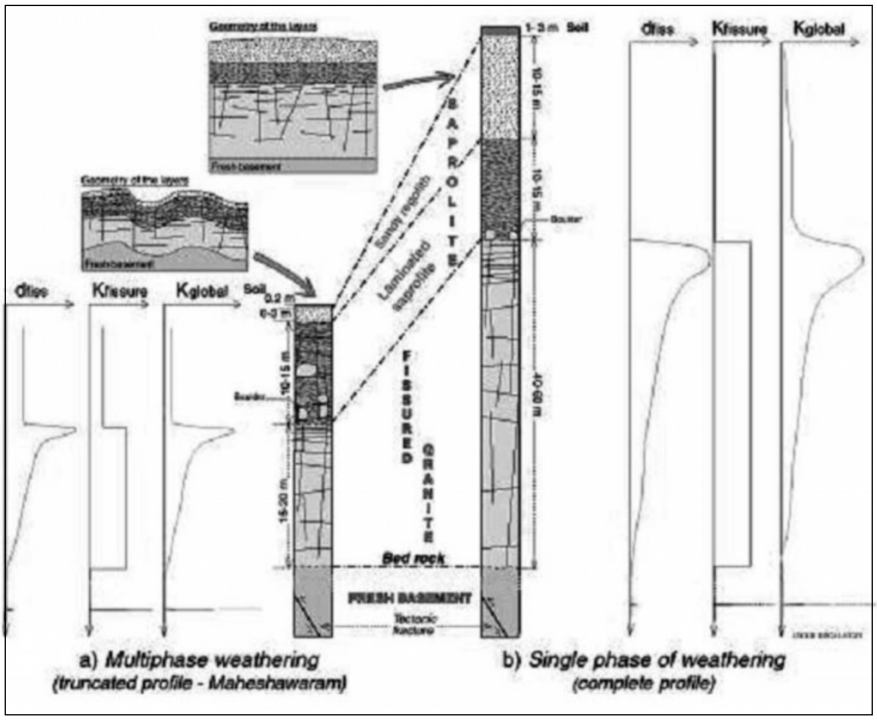

Figure 10. Generalized 3-D geological and hydrogeological conceptual model of granite aquifers controlled by single or multiphase weathering. (a) Maheshwaram (southern India) multiphase weathering and (b) Classical profile - single weathering - (idealized profile). Dfiss: density of conductive fissures, Kfiss: hydraulic conductivity of fissures and Kglobal: equivalent hydraulic conductivity of the layer (from Dewandel et al., 2006).

The effective porosity of the fissured layer is relatively low, about 10^{-2}, and is mainly (90%) ensured by the low permeability fissure zones affecting the blocks (block permeability, including very low permeability fissure zones: 5×10^{-8} m/s), while the conductive fissure network contributes only 10% to the effective porosity (Maréchal et al., 2004).

The top of the fissured layer is characterized by a few metres-thick high density fissured zone, named the 'transition zone' (density: 0.7-0.5 m^{-1}) (Figs 9 and 10). This zone, 2-metre-thick in the case of the young rejuvenated weathering profile studied in Maheshwaram, can reach more than 12 metres in the case of old thick weathering profiles (French Brittany, Wyns et al., 2004). The hydraulic conductivity of the fissures belonging to this transition zone is comparable to that of the deeper part of the fissured layer. This transition zone is the more permeable part of the fissured zone, thus of the entire weathering profile.

MAPPING THE LAYERS CONSTITUTING THE HARD ROCK AQUIFERS

The formation of the fissured layer is, therefore, closely related to the development of the alterites, and hence to the weathering front. An important consequence of this process is that, at the catchment scale, these weathered layers are parallel to the paleo weathering surfaces (paleo landscape) contemporaneous with weathering. At the local scale (from about 10 to about 100 m), it can be influenced by lithological or structural variations, the latter being well-known to basement hydrogeologists and geophysicists who use them to site water wells: the presence of fractures enables water to circulate or diffuse, causing a local deepening of the base of the alterites.

These ancient surfaces have been affected by erosion processes posterior to the main weathering phase. Therefore, the saprolite and the fissured layer make up stratiform beds whose geometry at the regional scale can be linked to the more or less good preservation of paleoweathering surfaces. On the basis of the knowledge of this genetic principle, it is quite easy to map, at the watershed scale (Lachassagne et al., 2001; Dewandel et al, 2006):

- the altitude of:
  - o the limit between the saprolite (laminated layer) and the fissured layer,
  - o the base of the fissured layer,
- and thus to respectively compute the residual thickness of:
  - o the saprolite,
  - o the fissured horizon.

In most cases, the geometry of the base of the saprolite is determined at first, through the combined use of well data, geophysical data if any, and specific field surveys. Since the surface of the base of the saprolite is, in many places, cut by the present-day ground surface, notably near valleys, it is relatively simple, in the field, to determine the position of the saprolite/weathered-fissured layer interface.

On the basis of observations of the thickness of the fissured layer (observations on outcrops, statistical treatment of existing well data), the altitude of its base can also be directly computed from one of the alterite base. The altitudes of (i) the saprolite/fissured layer interface and (ii) fissured layer/fresh rock interface can therefore be subtracted from that of the present ground surface, as inferred from Digital Elevation Model (DEM) data, in order to compute the residual thickness of respectively the saprolite and the fissured layer. In regions where the paleosurface(s) have partly been preserved from erosion, slope analysis from DEM data can also be used for the elaboration of such maps.

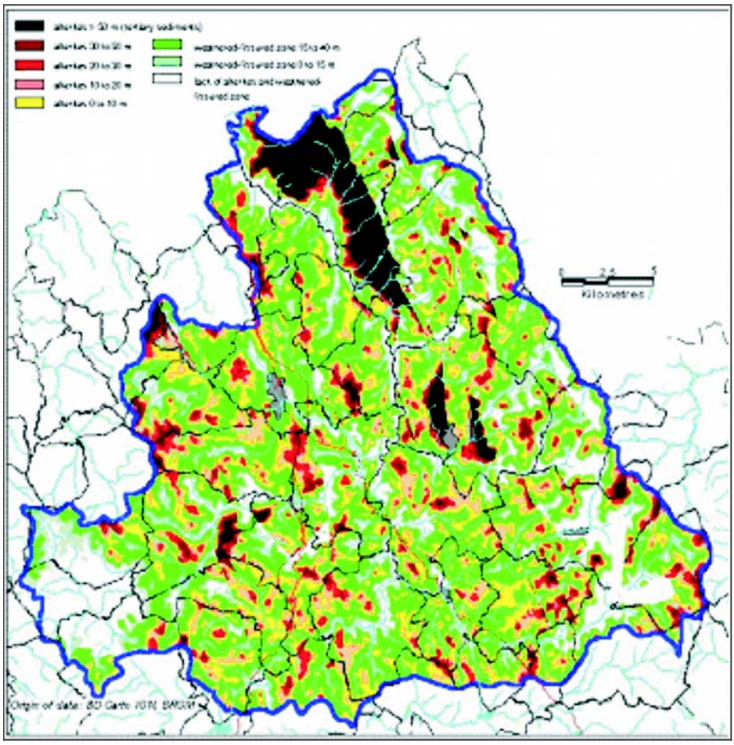

Figure 11. Lozère part of the Truyère river catchment (700 km^2, Massif Central, France): thickness of the saprolite (increasing thickness from yellow to red and black) and the fissured layer (green colours) (from Lachassagne et al.,2001).

Figure 11 displays an example of such a map obtained in France, Truyère river catchment, Massif central, 730 km^2 (Lachassagne et al., 2001), in a region where no data from wells was available. The interface between the saprolite and the fissured layer was systematically sought along roads and trails, following routes perpendicular to the slopes. About 700 km of roads and trails, distributed as evenly as possible over the study area (about one linear km per km^2), were reconnoitred. These field studies were accomplished in two weeks. Based on observed or inferred interfaces, as well as on available surveying data, the contour lines of the bottom of the alterites were plotted. The observation grid was tightened in the zones where the bottom of the saprolite is cut by vertical slip faults subsequent to the weathering (for the most part these faults were contemporary to the formation of Oligocene grabens). The contour lines of the bottom of the saprolite were then digitized, turned into a figure field and interpolated in order to create a grid that can be overlain on the DEM. The thickness of the saprolite layer was then calculated by subtracting the altitude of the bottom of the saprolite from that

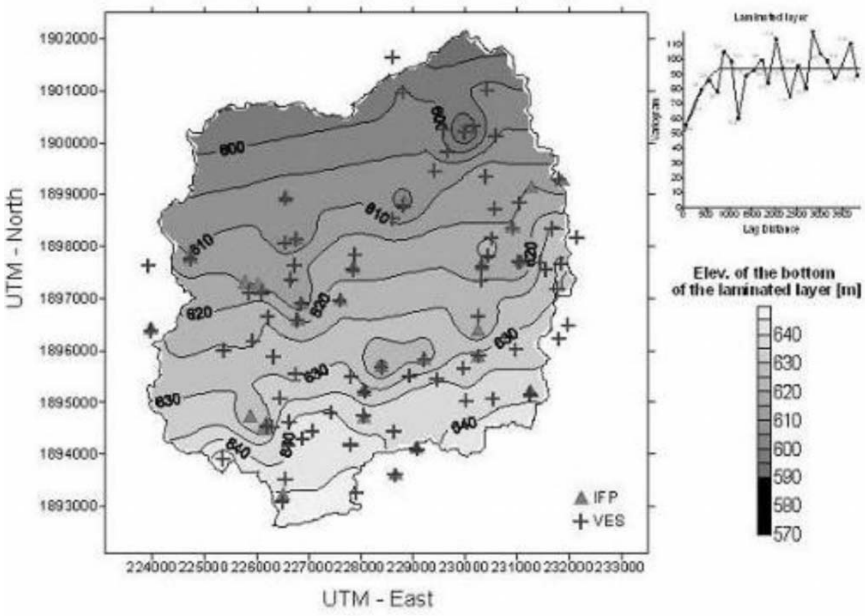

Figure 12. Krigged map (45 bore-well lithologs—IFP—and 80 VES interpretations) of the elevation (in m amsl) of the base of the saprolite (base of the laminated layer) on the 60 km^2 southern India Maheswaram catchment (from Dewandel et al., 2006). The plot in the right corner shows the variogram used for krigging.

of the ground surface. Although the time spent on field surveying was kept to a minimum, measurements done later showed that the uncertainty concerning the altitude of the bottom of the saprolite (generally better than 10 m) was consistent with this regional approach.

Figure 12 displays an example of a similar map obtained on the southern India Maheswaram catchment (Dewandel et al., 2006), mainly from geophysical data (Vertical Electric Soundings), and well data (lithologs). It was completed by observations on outcrops (dug-wells).

APPLICATIONS

The main research results obtained these last years on hard rock aquifers and the main practical applications of these results for the development, the management and the protection of their water resource are summarised in Table 2.

Table 2: Main scientific results on hard rock aquifers and corresponding main hydrogeological applications

Scientific results	*Applications*
1. Knowledge of the structure of hard rock aquifers and particularly *demonstration of the relationship existing between their permeability and the weathering processes* they were submitted to in the past. The hydrodynamic properties of the main permeable layer (the *fissured horizon*), 50 metres thick approximately, located below the *saprolite*, are due to the development of weathering-induced fissures (sub-horizontal in granites) caused by the strain induced in the rock by the swelling of some minerals (especially biotite). Hard rock thus comprises two kinds of permeability: a fissure permeability related to weathering and a fracture permeability related to tectonic fracturing. *Most of the water wells, particularly those used for village's hydraulics or irrigation, are tapping the weathering induced fissures.* These results have been demonstrated in numerous regions of the world.	1.1. *Mapping of hard rock aquifers, potentialities evaluation at large areas scale* (several hundreds, thousands, or tens of thousands km^2), on the basis of (i) the susceptibility of the various kinds of hard rocks to the weathering processes (development of an efficient fissured layer, mainly as a consequence of the rocks' mineralogical composition), (ii) the state of the weathering profiles erosion (iii) the depth to the water table, etc. (Fig. 13) (Lachassagne et al., 2001). 1.2. *Mapping and location of the areas* (a few km^2 to tens of km^2) *favourable for field hydrogeological prospecting* (before the implementation of geological or geophysical investigations). (Lachassagne et al., 2001). 1.3. *Hard rock aquifers vulnerability maps*
2. Characterisation of the *hydrodynamic properties of the fissured horizon* (thickness, density and orientation of the various kinds of fractures, anisotropy, permeability, storage properties, etc.). Specially designed for hard rock aquifers *pumping tests* ("tool box") and interpretation. (Maréchal et al., 2004; Dewandel et al., 2006)	2.1. *Long term forecast of high yield wells* 2.2. *Parameters for the deterministic modelling* of hard rock aquifers.
3. Development of *geophysical methods* (especially PMR[1]) for the *characterisation of the thickness and the hydrodynamic properties* – especially specific yield – of the main constitutive layers (alterites, weathered horizon) of hard rock aquifers. (Wyns et al., 2004)	3.1. Evaluation of the *groundwater storage* within the aquifers. (Fig. 14). 3.2. Evaluation of the *durability of diffuse source pollutions* within the aquifer.

(Contd.)

(Contd.)

Scientific results	*Applications*
4. Development of a methodology for the assessment of *regional scale hard rock aquifers groundwater budget*, with specific applications to over-exploited, semi-arid area, aquifers. (Maréchal et al., 2006), that can take into account the spatial distribution of the weathering layers and the spatial variations of their hydrodynamic properties (namely their specific yield) in X-Y and with depth.	4.1. Evaluation of the *sustainable water resource* of aquifers (annual recharge, irrigation return flow, water budget, relationships with surface waters, catchment scale efficiency of artificial recharge, etc.) (Maréchal et al., 2006) (Fig. 15). 4.2. *Decision Support Tools* for hard rock aquifers management (Dewandel, Gandolfi et al., 2006)
5. Building-up of a methodology for the *discretized modelling of hard rock aquifers* (Lachassagne, Ahmed et al., 2001)	5.1. Deterministic modelling of hard rock aquifers at well to catchment scale (resource evaluation, pollutant transfers, etc.). (Durand et al., 2004) 5.2. Decision Support Systems for hard rock aquifers management
6. *Radon methodology*. Development and validation of the radon method, setting up of the field and lab measurements protocols, temporal and spatial variability of the radon signal, etc. (Lachassagne and Pinault, 2001; Lachassagne et al., 2001)	6.1. *"High yield" water well siting* located on both weathering-induced fissures and tectonic fractures 6.2. *Integrated prospecting methodology* including geology, remote sensing, radon, geophysics
7. *Hydrogeochemical tools* designed for hard rock aquifers (major elements, traces, isotopes) (Négrel and Lachassagne, 2000; Pauwels et al., 2001)	7.1. Comprehension of the *functioning of the aquifers* (protection, management, etc.) 7.2. *Groundwater quality* (fluoride, arsenic and metallic elements, nitrates, etc.)

[1.] PMR: Proton Magnetic Resonance (or Nuclear Magnetic Resonance)

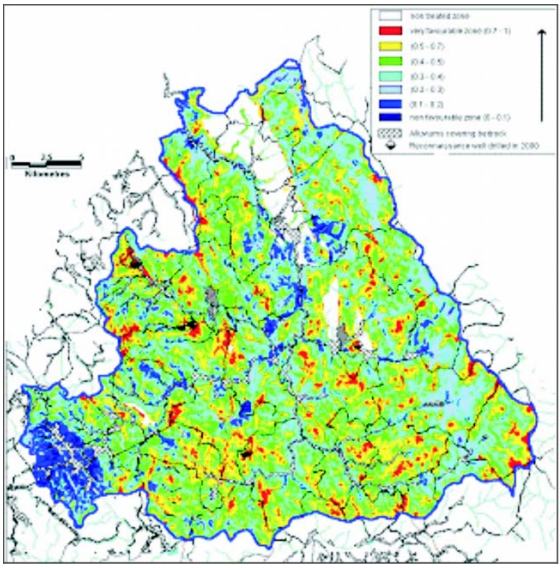

Figure 13. Example of a map of groundwater potential (obtained from multivariate analysis integrating the thickness of the weathering profile - cf. Fig. 11) on the Lozère part of the Truyère river catchment (700 km^2, Massif Central, France). Dark blue to red: increasing groundwater potential.

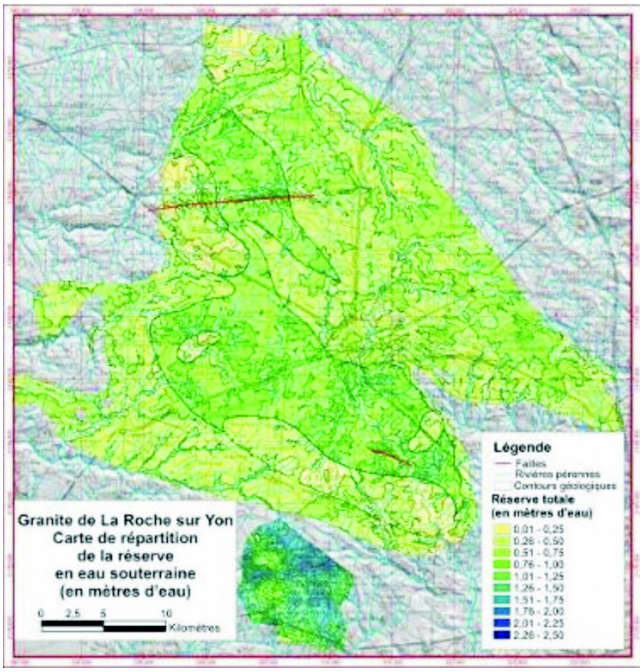

Figure 14. Map of groundwater reserves (in metres of water). La Roche Sur Yon Granite (Vendée, France).

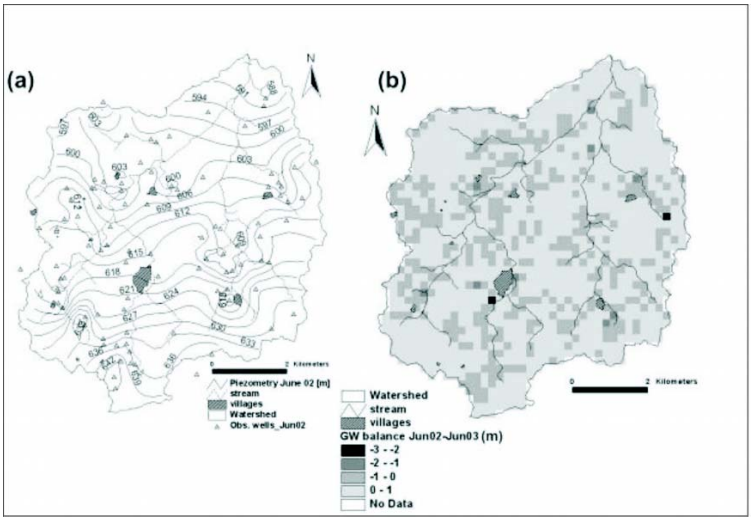

Figure 15. (a) Water table map and (b) annual (June 02 to June 03) groundwater budget expressed as water table fluctuations for the southern India Maheswaram catchment (from Maréchal et al., 2006).

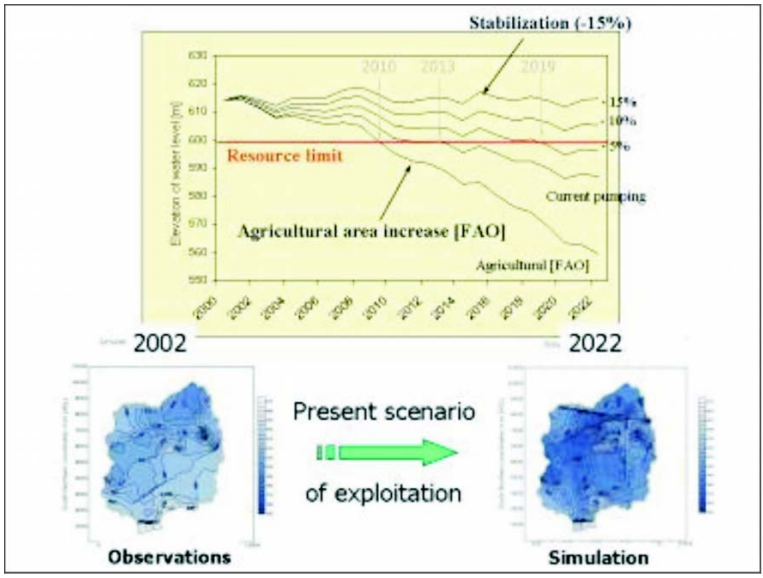

Figure 16. Example of an output of a DST (from Dewandel, Gandolfi et al., 2006). Predicted evolution of groundwater reserves for different agricultural policy scenarios. Maheswaram southern India catchment. Upper graph: –5%, –10%, –15%: 5, 10 and 15% reduction of groundwater withdrawal for irrigation; FAO: increased withdrawal in order to meet the production objectives of FAO scenarios. Lower graph: current water level in the aquifer (2002) and predictions for 2022 if increase in withdrawal for irrigation continues according to the current trend.

CONCLUSION

Significant advances have recently been made in our knowledge of the genesis, geometry and functioning of hard rock aquifers. The hydrodynamic properties of these aquifers appear to be mainly related to weathering processes. The weathering profile, up to more than 100 m thick, is mainly composed of two superposed layers, the saprolite, playing a capacitive role, and the underlying fissured layer that assumes the transmissive function. All together and where saturated with ground water, these two layers constitute a composite aquifer.

The spatial distribution of such weathering profiles (single or multiphase), or their remains, can be mapped at the catchment scale on the basis of various types of data: digital elevation model, observations on outcrops, drilling cuttings and geophysical measurements. Then, the spatial distribution of the hydrodynamic properties of granite type aquifers can also be mapped. A precise geological mapping not only of lithology but also of the weathering structure thus appears to be a prerequisite for groundwater management in hard rock areas.

These newly developed geological and hydrogeological concepts, that enable to regionalize hard rock aquifers properties, can answer several key issues: (i) evaluation of aquifer potentialities from large to small (a few hectares) areas; as a consequence, it helps in defining the characteristics of field surveys (geophysics, radon, etc.) and well siting, (ii) elaboration of water budget at the catchment scale, taking into account the piezometric level fluctuations in the various layers, (iii) input data for numerical modelling of the aquifer, (iv) elaboration of vulnerability maps, (v) guidelines for aquifer protection, for town and country planning (siting of landfill, quarry), etc.

Such a geological and hydrogeological model now requires to be adapted to the geological contexts of weathered metamorphic rocks. The mapping methodology is also to be developed for applications at a larger scale, 1,000 to 10,000 km^2, through the integration of techniques such as remote sensing and spectrometric and radiometric aerial surveys.

REFERENCES

Cho, M., Choi, Y.S., Ha, K.C., Kee, W.S., Lachassagne, P. and Wyns, R. (2002). Paleoweathering covers in Korean hard rocks: A methodology for mapping their spatial distribution and the thickness of their constituting horizons. Applications to identify brittle deformation and to hard rock hydrogeology. *KIGAM Bulletin*, **6(2):** 12-25.

Cho, M., Choi, Y., Ha, K., Kee, W., Lachassagne, P. and Wyns, R. (2003). Relationship between the permeability of hard rock aquifers and their weathering, from geological and hydrogeological observations in South Korea. *In:* Krāsny, J., Hrkal, Z. and Bruthans, J. (Eds.), International Association of Hydrogeologists

IAH Conference on "Groundwater in fractured rocks", Prague 15-19 September 2003.

Compaore, G., Lachassagne, P., Pointet, T. and Travi, Y. (1997). Evaluation du stock d'eau des altérites. expérimentation sur le site granitique de Sanon (Burkina-Faso). *In:* IAHS (Edited), Rabat IAHS conference. IAHS Publication. IAHS, Rabat, pp. 37-46.

Detay, M., Poyet, P., Emsellem, Y., Bernardi, A. and Aubrac, G. (1989). Development of the saprolite reservoir and its state of saturation: Influence on the hydrodynamic characteristics of drillings in crystalline basement (in French). *C. R. Acad. Sci.* Paris 1989, Série II, (t. 309), 429-436.

Dewandel, B., Gandolfi, J.M., Ahmed, S. and Subrahmanyam, K. (2006). A Decision Support Tool for sustainable Groundwater Management in semi-arid Hard-Rock areas with variable agro-climatic scenarios. *Current Sciences of India* (Submitted).

Dewandel, B., Lachassagne, P., Maréchal, J.C., Wyns, R. and Krishnamurthy, N.S. (2006). A generalized 3-D geological and hydrogeological conceptual model of granite aquifer controlled by single or multiphase weathering. *Journal of Hydrology*, **330:** 260-284.

Durand, V. et al. (2004). Modeling hard rock aquifers taking in account the geometry and hydrodynamic properties of weathered and fissured horizons: Plancoët, Brittany, France, *EGS, 2004, Strasbourg, France*.

Lachassagne, P., Ahmed, S., Golaz, C., Maréchal, J.-C., Thiery, D., Touchard, F. and Wyns, R. (2001). A methodology for the mathematical modelling of hard rock aquifers at catchment scale based on the geological structure and the hydrogeological functioning of the aquifer. *In:* XXXI IAH Congress "New approaches characterizing groundwater flow". "Hard Rock Hydrogeology" session, Munich, Germany, 10th-14th September 2001, Wohnlich, S. Eds.' AIHS: Munich, Germany, 2001.

Lachassagne, P. and Pinault, J.-L. (2001). Radon-222 emanometry: A relevant methodology for water well siting in hard rock aquifer. *Water Resources Research*, **37(12):** 3131-3148.

Lachassagne, P., Wyns, R., Bérard, P., Bruel, T., Chéry, L., Coutand, T., Desprats, J.-F. and Le Strat, P. (2001). Exploitation of high-yield in hard-rock aquifers: Downscaling methodology combining GIS and multicriteria analysis to delineate field prospecting zones. Ground Water, **39(4):** 568-581.

Maréchal, J.C., Dewandel, B., Ahmed, S., Galeazzi, L. and Zaïdi, F.K. (2006). Combined estimation of specific yield and natural recharge in a semi-arid groundwater basin with irrigated agriculture. *Journal of Hydrology* (in press).

Maréchal, J.C., Dewandel, B. and Subrahmanyam, K. (2004). Use of hydraulic tests at different scales to characterize fracture network properties in the weathered-fractured layer of a hard rock aquifer, *Water Resources Research*, **40(11):** doi 10.1029/2004WR003137.

Maréchal, J.C., Wyns, R., Lachassagne, P., Subrahmanyam, K. and Touchard, F. (2003). Anisotropie verticale de la perméabilité de l'horizon fissuré des aquifères de socle: concordance avec la structure géologique des profils d'altération, *C.R. Geosciences*, **335:** 451-460.

Neuman, S.P. (2005). Trends, prospects and challenges in quantifying flow and transport through fractured rocks. *Hydrogeology Journal*, **13(1):** 124-147.

Négrel, P. and Lachassagne, P. (2000). Geochemistry of the Maroni River (French Guyana) during low water stage: implication for water rock interaction and groundwater characteristics. *Journal of Hydrology*, **237:** 212-233.

Pauwels, H., Lachassagne, P., Bordenave, P., Foucher, J.-C. and Martelat, A. (2001). Temporal variability of nitrate concentration in a schist aquifer and transfer to surface waters. *Applied Geochemistry*, **16(6):** 583-596.

Wyns, R., Baltassat, J.M., Lachassagne, P., Legtchenko, A. and Vairon, J. (2004). Application of proton magnetic resonance soundings to groundwater reserves mapping in weathered basement rocks (Brittany, France). Bulletin de la Société Géologique de France, **175(1):** 21-34.

4 Geophysical Characterization of Hard Rock Aquifers

N.S. Krishnamurthy, Subash Chandra and Dewashish Kumar

IFCGR, National Geophysical Research Institute
Hyderabad-500007, India

INTRODUCTION

Geophysics plays a major role for characterizing the hard rocks for groundwater studies. The qualitative and quantitative application has increased since past few years due to rapid development and advancement in microprocessors and associated numerical modelling solutions. Although geophysics has ability to probe deep earth interior (say >1000 m), but its application for groundwater studies is usually restricted to depths less than and around 250 m below the surface. These include mapping the depth and thickness of aquifers, mapping aquitards or confining layers, locating fractures and fault zones and mapping contamination to the groundwater such as that from saltwater intrusion. The theoretical and practical background to geophysics has been extensively reviewed and can be studied in standard texts on the subject, for example Kearey & Brooks (1991); Telford et al. (1976); Parasnis (1979); Dobrin (1976); Grant and West (1965); Reynolds (1997); Miller et al. (1996); Murali et al. (1998); etc.

IMPORTANCE OF FRACTURES IN HARD ROCK AREAS

Fractures often serve as major conduits for movement of water and dissolved chemicals through hard rocks in the underground. The geological structure normally encountered in hard rock areas of places such as in India is granite or granite gneiss overlain by a variable thickness of weathered material. The latter is a regolith produced by the in-situ weathering of the basement rock (Acworth, 1987). The regolith normally grades into solid unfractured basement over several tens of metres, although often the boundary between the two

may be fairly sharp. Hydrogeologically the weathered overburden has a high porosity and contains a significant amount of water, but, because of its relatively high clay content, it has a low permeability. The bedrock on the other hand is fresh but frequently fractured, which gives it a high permeability. But as fractures do not constitute a significant volume of the rock, fractured basement has a low porosity. For this reason a good borehole, providing long term high yields, is one which penetrates a large thickness of regolith, which acts as a reservoir, and one which additionally intersects fractures in the underlying bedrock, the fractures providing the rapid transport mechanism from the reservoir and hence the high yield. Boreholes which intersect fractures, but which are not overlain by thick saturated regolith, cannot be expected to provide high yields in the long term. Boreholes which penetrate saturated regolith but which find no fractures in the bedrock are likely to provide sufficient yield for a hand pump only.

HARD ROCK AQUIFER CHARACTERISTICS

The most significant features of the hard rock aquifers are: 1. A topographical basin or a sub-basin generally coincides with ground water basin. Thus, the flow of ground water across a prominent surface water divide is very rarely observed. 2. The aquifer parametres like Storativity (S) and Transmissivity (T) often show erratic variations within small distances. 3. The saturated portion of the mantle of weathered rock or alluvium or laterite, overlying the hard fractured rock, often makes a significant contribution to the yield obtained from a dug-well or bore-well. 4. Only a modest quantity of ground water, in the range of one cu.m. to a hundred cu.m. or so per day, is available at one spot. 5. Draw down in a pumping dug-well or bore-well is often almost equal to the total saturated thickness of the aquifer.

STUDY AREA

The case studies shown in this part are from the geophysical studies carried out in the Maheshwaram watershed having an area of about 60 km^2, situated at about 30 km south of Hyderabad, India. It lies in between geographical coordinates having 17° 06′ 20″ to 17° 11′ 00″ North latitudes and 78° 24′ 30″ to 78° 29′ 00″ East longitudes and forms part of Survey of India toposheet 56K/8. The geology of the Maheshwaram watershed is mainly granites of Archean age intersected by dolerite dykes and quartz veins. They have undergone variable degrees of weathering with depths extending up to even 20 m followed by fracturing at many places. The dyke located in the extreme northern part strikes east-west with about 15 m width. Another dyke exposed about 1 km south of the first one, strikes N60°E-S60°W with a width of about 20 m at places. A quartz vein of about 20 m width with a strike of ENE-WSW is exposed in the drainage divide in the southern boundary of the watershed. Ground water in the area occurs under water table conditions

in the weathered granite and in semi-confined conditions in the fractured granites. The depth to water level varies from 11 m to 20 m. The yield of the bore-wells range from 1000 gph to 5000 gph. The high yielding bore-wells are either recharged by the irrigation tanks or tapping the deeper fractures. The yield of the bore-wells in the vicinity of the dolerite dykes is high as they are tapping thick fractured zone. The area comprises thin soil cover of sandy loam and clayey soils and is underlain by granites. These granites are medium to coarse grained and of pink and grey colour.

GEOPHYSICAL METHODS

Several geophysical methods are available for groundwater exploration. Most of the available geophysical methods have been applied here to study the aquifer system of a hard rock granitic terrain. A brief description of the methods is given here.

Electrical Resistivity Technique

Electrical resistivity technique is the most commonly applied method among all the geophysical methods for groundwater exploration, because of the large variation of resistivity for different formations and the changes that occur due to the saturated conditions. Resistivity is defined as the resistance offered by a unit cube of material for the flow of current through its normal surface. If L is the length of the conductor, and A is its cross-sectional area, then the resistance is defined as

$$R = \rho \frac{L}{A}$$

where ρ is constant of proportionality and is called as resistivity. In MKS system the unit of resistivity is ohm-metre (Ωm).

In the case of an inhomogeneous medium, the resistivity measured is called as the apparent resistivity. The apparent resistivity of a geologic formation is equal to the true resistivity of a fictitious homogeneous and isotropic medium. Resistivity of rock formations varies over a wide range, depending on the material, density, porosity, pore size and shape, water content and quality, and temperature. There are no fixed limits for resistivities of various rocks: igneous and metamorphic rocks yield values in the range 10^2 to 10^8 ohm m while sedimentary and unconsolidated rocks, 1 to 10^4 ohm.m.

Generally for measuring the resistivities of the surface formations, four electrodes are required. A current of intensity I is introduced between one pair of electrodes, called as current electrodes, named as A and B and some times as $+I$ and $-I$ denoting source and sink respectively. The potential difference produced as a result of current flow is measured with the help of another pair of electrodes, called as potential electrodes and represented by

M and N. There are different electrode arrangements for measuring the potential difference, which are uniquely used as different purposes in exploration techniques. The most commonly used arrangements are Wenner and Schlumberger configurations.

Wenner Array: Wenner configuration consist a system of earth resistivity measurements with four collinear equally-spaced point electrodes on the ground surface. The two current electrodes A and B and two potential electrodes M and N are placed at surface at equal distance '*a*' as shown here. Current *I* is passed into the ground through A and B and the potential difference is measured through M and N.

```
A      M   O   N       B
↑_____↑___.___↑_______↑
  ← a →← a →← a →
```

The geometrical factor (K) for this array is $2\pi a$ and apparent resistivity is given by

$$\rho_a = 2\pi a\ (\Delta V/I\ )$$

Schlumberger Array: The Schlumberger array also uses four collinear point electrodes but measure the potential gradient at the mid point. In this array the current electrodes are spaced much farther apart than the potential electrodes, usually five times or more as shown here.

```
A              M   O   N              B
↑____________↑___.___↑_____________↑ where L ≥ 5(l)
                ← 2(l) →
←- - - - - - - - - - 2L - - - - - - - - - - - →
```

The geometrical factor for this array is

$$K = \pi\{(AB/2)^2\text{-}(MN/2)^2\}/MN$$

Or $$K = \pi\ (L^2 - l^2)/2l$$

Apparent resistivity $\rho_a = K(\Delta V/I)$, where A and B are the current electrodes, M and N are the potential electrodes, L = half spacing of current electrodes and l = half of spacing of potential electrodes.

Resistivity Profiling

Electrical profiling is used to determine the lateral inhomogeneities up to a particular depth and thereby a particular section of the subsurface is mapped along a profile. This method is highly useful in mineral exploration where the detection of isolated bodies of anomalous resistivity is required and in groundwater exploration to determine the linear features in the subsurface, which control the movement of ground water. In resistivity profiling, the electrode system moves as a whole from one station to other along a line, known as profile or traverse. For a given spacing, the electrode system has

its depth of investigation. For higher electrode spacings, the depth of investigation will be more.

When the apparent resistivity observations for all stations on a traverse and for all such traverses spread over the entire area of the survey are made, the resistivity values are plotted at their respective positions over a map. After this, the contours of equal resistivity values for particular electrode spacing are drawn and are called as equi-resistivity or contour maps. Thus the representation is in the form of linear maps for several electrode spacings or contour maps for a particular assumed depth section. The resistivity highs/lows are marked to give an idea about the epicentral location of the target (resistive or conductive zone) and its lateral extent. The resistivity profiles taken across two dykes are shown in Fig. 1. The results show low resistivities at shallow depths and high resistivities at deeper depths over the dyke thus indicating the conductive nature due to weathering/fracturing of the dyke in upper parts and hence suggests that this dyke is not acting as barrier for the ground water to flow at shallow depths, whereas in deeper levels, the dykes may be acting as barriers.

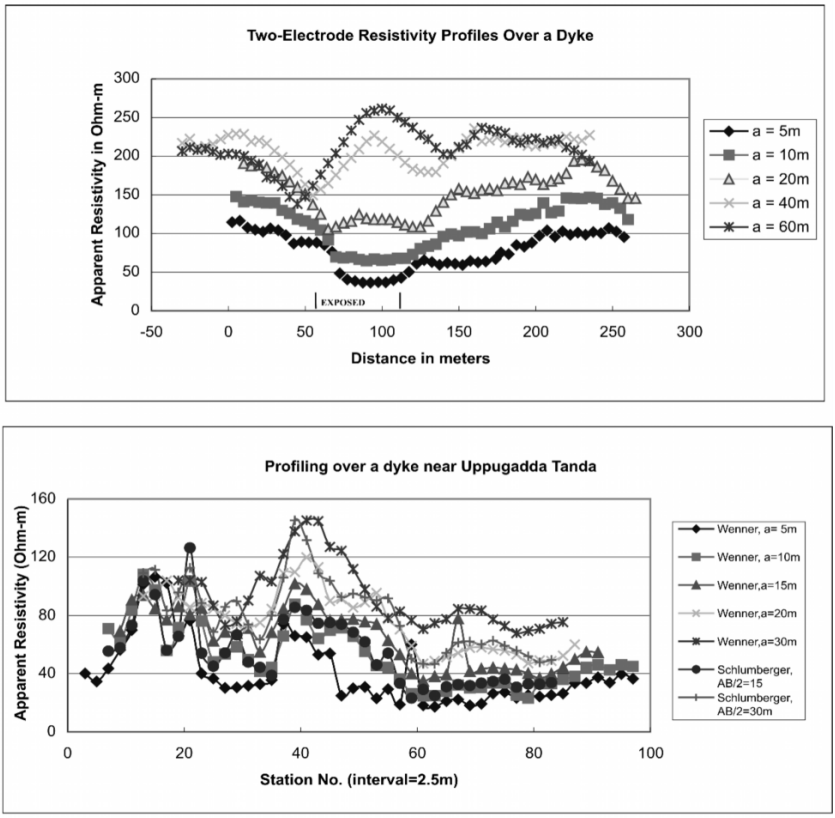

Figure 1. Resistivity profiles in Maheshwaram watershed.

Resistivity Sounding

Vertical Electrical Sounding is applied whenever a depth section is to be determined at a particular place and, in this method, increase in the depth of investigation can be obtained by gradually increasing the distance between the current electrodes such that current penetrates deeper and deeper into the ground. This method gives the information about depth and thickness of various subsurface layers and their resistivities.

The field procedure of a sounding is to use a fixed centre with expanding electrodes. The Wenner and Schlumberger layouts are particularly suited to this technique. But Schlumberger array has some advantages. There are always some naturally developing potentials (self-potential, SP) in the ground, which have to be eliminated and nullified. The potential difference developed, due to the experimentally impressed current, should be taken into consideration. For different spacings, the apparent resistivity of the ground for particular array can be calculated.

Interpretation of Sounding Data

The apparent resistivity is plotted against half current electrode spacing on a double logarithmic paper and the curve so obtained is called sounding curve. To get the layer parametres (resistivity and thickness) of the subsurface, these sounding curves are to be interpreted and there are mainly two types of interpretational techniques: Indirect methods and direct methods.

In the indirect methods, the field curve is compared with a set of theoretical curves, also called as master curves, for different known layered parametres prepared in advance. Several albums of master curves are available which include among others Compagne Generale de Geophysique (1963), Flathe (1963), Orellana and Mooney (1966) and Rijkswaterstaat (1969). These are computed from the expression for surface potential (Stefanesco et al., 1930).

$$V = \frac{\rho_1 L}{2\pi}\left[\frac{1}{r} + 2\int_0^\infty K(\lambda) J_0(\lambda r)\, d\lambda\right]$$

where r = distance of the measuring point from current source, ρ_1 = resistivity of surface layer, $K(\lambda)$ = Stefanesco kernel function determined by thickness and resistivity of surface layer, $J_0(\lambda r)$ = Bessel function of zero order and first kind and λ = Integration variable, a real number with dimensions of inverse length. When a match of the field curve is obtained with the theoretical curve, one can get the layer parametres in terms of resistivity and thickness of the subsurface layers.

In direct methods, one can get the layer parametres from the field curve itself by using the computer code available. Quite often, it is possible that the field curve may not match with the available master curves. In the absence of a proper set of master curves that simulates the geological situation, one has to compute a theoretical sounding curve that best fits the field

situation to get the proper layer parametres. In some codes, one requires giving an initial guess model and the curve is interpreted by an iterative process and in another type of direct methods, the field curve is interpreted without the necessity of an initial model.

The method of automatic iterative interpretation given by Zohdy (1974) is based on the similarity in shape existing in many cases between apparent resistivity curves and Dar Zarrouk curves. Zohdy (1989) has developed an algorithm for automatic iterative interpretation of field sounding curve, where no initial guess model of the layered earth are required to be given as initial model. Based on the field curve an initial model is assumed. Then first thickness parametres are changed according to an algorithm till minimum root mean square error is obtained. Later, layer resistivities are changed according to an algorithm till another minimum is obtained in RMS error. Using equivalence principle the layers can be suppressed finally.

When the layer parametres are obtained in terms of resistivities and thicknesses, these can be inferred in terms of lithology of the subsurface by knowing the geology of the area and correlation of resistivities with various formations from a known place.

The resistivity data collected in Maheswaram watershed was interpreted using a computer programme based on the inversion algorithm of Jupp and Vozoff (1975), which uses digital filter theory (Ghosh, 1971a, b). The iterative method successively improves the initial model given, until the error measure is small and the parametres are stable with respect to a reasonable change in the model parametres. Figure 2 is an example of a sounding curve interpreted by the above method.

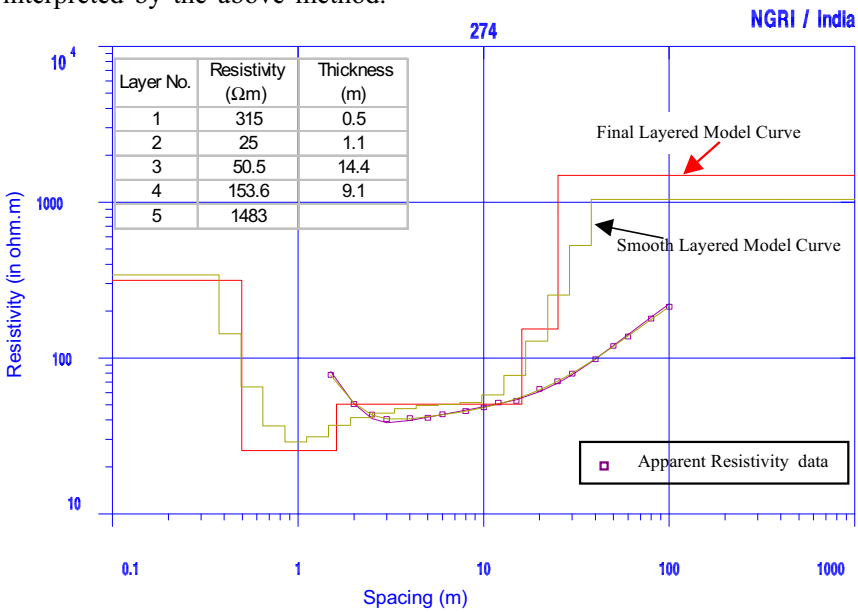

Figure 2. Resistivity sounding interpreted showing the field and computed curves.

It may be necessary to mention that a parameter model derived either by conventional or computer method may not be unique because of an inherent limitation, namely the phenomenon of equivalence resulting in a range of models fitting the same sounding curve. Another limitation is the simplified assumption of horizontal, homogeneous and isotropic model layers, which is never the case in nature. It is, therefore, very essential to gather the hydrogeological knowledge of the area and correlate the sounding data obtained near existing wells with lithology for a reliable interpretation.

Multi Electrode Resistivity 2-Dimensional Imaging (MER2DI)

The improvement of resistivity methods using multielectrode arrays has led to an important development of electrical imaging for subsurface surveys (Griffiths and Turnbull, 1985; Griffiths et al., 1990; Barker, 1992; Griffiths and Barker, 1993). Such surveys are usually carried out using a large number of electrodes, 24 or more, connected to a multi-core cable. A laptop micro-computer together with an electronic switching unit is used to automatically select the relevant four electrodes for each measurement. Apparent resistivity measurements are recorded sequentially sweeping any quadruple (Current and Potential Electrodes) within the multi-electrode array. MER2D data can be interpreted with the help of RES2D inversion software and finally a true

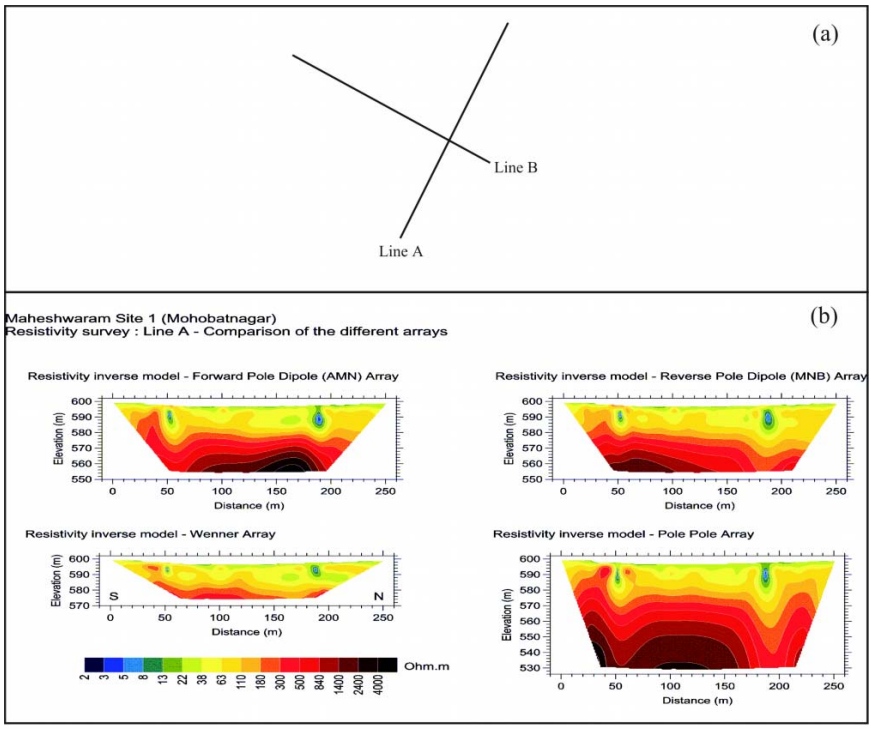

Figure 3. (a) Profile layout and (b) Comparison of different arrays along Line A in Mohabatnagar.

resistivity cross-section can be obtained. As a result, high-definition pseudo-section with dense sampling of apparent resistivity variation at shallow depth (0-100 m) is obtained in a short time. It allows the detailed interpretation of 2D resistivity distribution in the ground (Loke and Barker, 1996).

Figure 3 shows comparison of different configurations along a profile. As seen from the resistivity image, the following are observed.

- The pole-dipole arrays bring rather distorted images at depth. The resistivity of the bedrock is overestimated at the end opposite to the current electrode.
- Only the pole-pole array has sufficient depth of investigation to effectively image the bedrock with resistivity higher than 1500 Ohm.m.
- But with respect to Wenner configuration the image at the surface is much poorer. For instance, the lateral extension at shallow depth of the two conductive anomalies is clearly detected with the Wenner array, but is not seen with the pole-pole array.
- From another point of view, the high depth of investigation of the pole-pole array is counter balanced by a large model uncertainty.

MER2D data interpreted with the help of RES2D inversion software and model uncertainty obtained along two profiles in Mohabatnagar are shown in Fig. 4 and described below. As seen in Fig. 4, there are two clear conductive faults respectively located at distance 55 m and 190 m along line A. The second fault located at 190 m from the profile and at a depth of 20 m seems to be more prominent compared to the first one, located at 55 m. The second one presents a lateral extension at shallow depth. The prominent anomaly also corresponds to large weathered thickness of resistivity 100 Ωm. There is a clear bedrock raise with a resistivity of around 600 Ωm, to the surface at distance 45 m. The second conductive anomaly corresponds to a lineament detected on aerial photography. All the other anomalies observed at depth are not corresponding to geomorphological features. The presence of conductive body at the surface raises the uncertainty of the model at depth. The same anomaly was also prominent in other configurations like Wenner, and pole-pole array and the basement upliftment is more prominent in the pole-pole array with extension of conductive zone about 40 m, which could indicate the fracture in granite.

The bedrock presents a regular deepening from the eastern to the western part along line B (Fig. 4). No faults are detected as interpreted from the inverse model. The result shows low resistivity of 60-100 Ωm, which indicates the weathered fractured granite. At the surface a conductive area is located between distances 160 and 270 m. This conductive area is not corresponding to the black shrinking clayey soils of the paddy fields but to the reddish clayey soils covering the end of a gentle hill slope.

In addition to this, the intrusive lineaments like dykes or quartz veins, which behave resistive to the groundwater flow, can be taken as an indicative tool for exploring the groundwater potential zones. The contact zones of the intrusive material and the host material become weak because of their

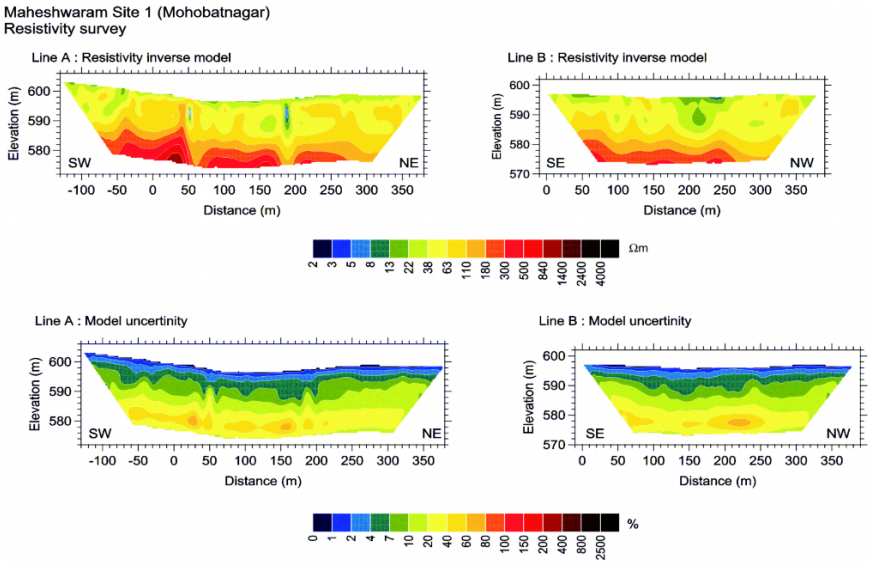

Figure 4. MER2DI Section along Line A and Line B (Mohabatnagar).

formation by cooling and crystallization at different times, development of cracks and fractures at the time of intrusion in the host material, and weathering of the contact zone due to water entrance through the fractures. Even the intrusive bodies may get weathered due to the fracture development and hence become good groundwater potential zones. With this idea Electrical Resistivity Tomography (ERT) was carried out at Kothur quartz vein (~25 m thick) in Maheshwaram watershed. The resistivity image (Fig. 5) has revealed the weathering effect at the contact zone, which was confirmed by the drilling of the bore-well. The top red coloured patch is the impression of high resistive quartz vein; however at coming further deeper it has shown low resistivity, which is nothing but the weathering and fracturing effect. The deepening of the weathering front can be clearly seen (as low resistivity) on either side of the quartz vein.

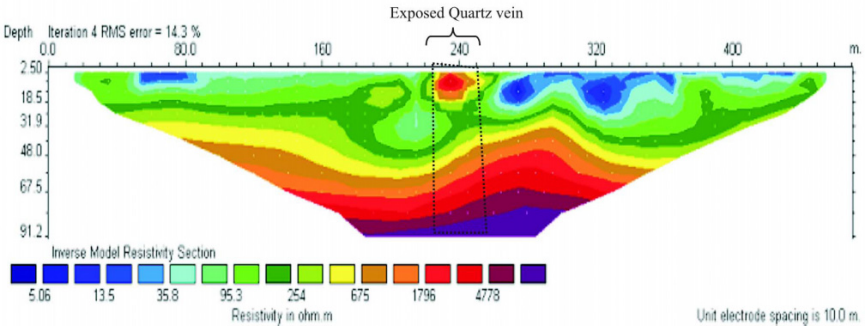

Figure 5. ERT across a quartz vein near Kothur, Maheshwaram watershed.

Magnetic Method

Magnetic methods are based on the observation of anomalies in the magnetic field of the earth that are caused by magnetic susceptibility of different rocks. As dolerite dykes are very common features in hard rock and important for groundwater flow, these methods are very useful to delineate even the buried dykes. Magnetic surveys are classified as grid and profile survey depending upon the density and geometrical distribution of the points of observation. Measurements with a magnetometer are taken 2 to 4 times at a station and their average value is considered to that station. The time of measurement is also noted for every observation since the magnetic field does not remain constant with time and hence necessary correction is applied for each station value by having repeat observations at base station.

Different types of instruments are available for magnetic surveys e.g. Schmidt type or by compensation as in Torsion magnetometer, Induction type of instrument, Fluxgate magnetometer, Proton precession magnetometer, Optical absorption magnetometer or the high sensitivity atomic resonance magnetometer etc. Magnetic systems consist of a permanent magnet, which can be deflected under the influence of geomagnetic field. The value of the magnetic field is determined by the deflection as in Schmidt type or by compensation as in Torsion magnetometer. Induction types of instruments consist essentially of an induction coil operated by a motor in the earth's magnetic field. The electromotive force developed in the coil due to intersection of force of the earth's magnetic field is a measure of the field. Instruments with sensitive fluxgate elements consist of a coil with core made of an alloy whose magnetic permeability strongly depends on the minor changes in the external magnetic field. The change in the electromagnetic parametres of the sensitive element determines the intensity of the earth's magnetic field.

Proton precession magnetometer consists of a container of water with a coil wound around it. When a strong magnetic field is applied in a direction approximately perpendicular to the earth's field, the protons will align parallel to the applied field. At this stage if the field is suddenly cut off, the protons start processing, inducing a small e.m.f. in the coil which is a measure of the earth's field. Optical absorption magnetometer or the high sensitivity atomic resonance magnetometer is the latest type. There are three types namely, the metastable helium, rubidium or cesium magnetometer. All these magnetometres make use of optical pumping technique. They are highly sensitive and also enable the measurement of the vertical gradient of the earth's magnetic field employing two magnetometres kept separated vertically apart from each other. One example of a magnetic profile carried out across a dyke in Maheswaram watershed is shown in Fig. 6.

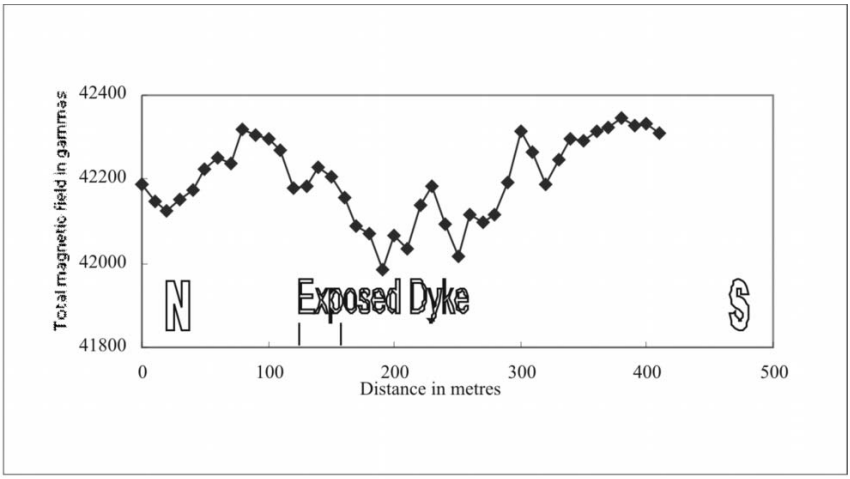

Figure 6. Magnetic traverse across a dyke.

Magnetic Resonance Sounding (MRS)

The initial idea of transforming the well-known proton magnetometer into a tool for water prospecting from the surface is ascribed to R.H. Varian (Varian, 1962). This idea was further developed and put into practice much later by a team of Russian scientists under the guidance of A.G. Semen. The Institute of Chemical Kinetics and Combustion (ICKC) of Russian Academy of Sciences fabricated the first version of the instrument for measurements of magnetic resonance signal from subsurface water ("Hydroscope"). The basic principle of operation of the Magnetic Resonance Sounding or the hitherto called surface Proton Magnetic Resonance (PMR) method for groundwater investigation is similar to that of the proton magnetometer. They both assume records of the magnetic resonance signal from a proton-containing liquid (for example, water or hydrocarbons). However, in the proton magnetometer, a special sample of liquid is placed into the receiving coil and only the signal frequency is a matter of interest. In MRS, a wire loop 100 m in diameter is used as a transmitting/receiving antenna and the water in the subsurface behaves as the sample. Thus, the main advantage of the MRS method, compared with other geophysical methods is that the surface measurement of the PMR signal from water molecules ensures that this method only responds to the subsurface water. Used routinely in Russia and tested in other countries (Shirov et al., 1991; Goldman et al., 1994; Lieblich et al., 1994) the method has demonstrated its potential.

The wire loop/antenna is laid out on the ground, normally in a circle with a diameter between 10 and 200 m, depending on the depth of aquifers; it may also be laid out in a "figure of eight" in order to improve S/N ratio (Trushkin et al., 1994). A pulse of alternating current then energizes the antenna

$$i(t) = I_0 \cos(\omega_0 t),\ 0 < t \leq \tau \quad (1)$$

where I_0 and τ are respectively the pulse amplitude and duration. The frequency of the current ω_0 is equal to the Larmor frequency of the protons in the geomagnetic field $\omega_0 = \gamma H_0$ with H_0 being the magnitude of the geomagnetic field and γ the gyromagnetic ratio for the protons (physical constant).

The pulse causes precession of the protons around the geomagnetic field, which creates an alternating magnetic field that can be detected using the same antenna after the pulse is terminated ("free induction decay" method). In practice, the PMR response recording is possible after an instrumental delay ("dead time").

Equipment

The parametres of currently available surface PMR equipment, such as Hydroscope (ICKC, Russia) and NUMIS (IRIS Instruments, France), do not permit measurements of the very short signals (less than 30 ms) corresponding to 'bounded' water in the subsurface. Thus, the vertical distribution of the water content deduced from the MRS data corresponds to the location and amount of 'free' water in the aquifers. Free water distribution in the subsurface is a solution of integral equation. Like many other ill-posed problems, the inversion is sensitive to field measurement errors caused by external electromagnetic interference such as electrical discharges in the atmosphere, magnetic storms, and all kinds of electrical currents through the subsurface. Interference may also be due to cultural noise produced by power lines, electrical generators and engines. In addition, the electrical conductivity of the subsurface (the operational frequency is between 1.5 and 2.8 kHz) not only attenuates the signal, but also has an effect on the kernel of the integral equation. Knowledge of this effect is important for the practical application of the method and for the data interpretation. Although further research is required to establish a precise relationship between the decay times of the PMR signal and the hydrogeological parametres of water in a porous medium, the studies show that PMR application allows to assume, with sufficient accuracy, that the decay time for bounded water is less than 20-30 ms and that for free water is between 30 and 1000 ms.

The transmitting antenna usually consists of a 100 m diameter loop laid on the ground, allowing a depth of investigation of the order of 100 m. The Larmor frequency varies between 0.8 and 3.0 kHz depending on the amplitude of the local Earth's magnetic field. The energizing current in the loop will reach intensities of 200-300A during pulses of a few tens of milliseconds. The relaxation field of the protons is measured in the same loop, after the energizing current is turned off. The voltage measured in the loop is of the order of a few tens to a few thousands nanovolts. Stacking is used to enhance the signal. To reduce the noise, 'figure-of-eight' shaped antenna is used

which gives a maximum depth of investigation of about 40 m. One example of a sounding in Maheswaram watershed is shown in Fig. 7.

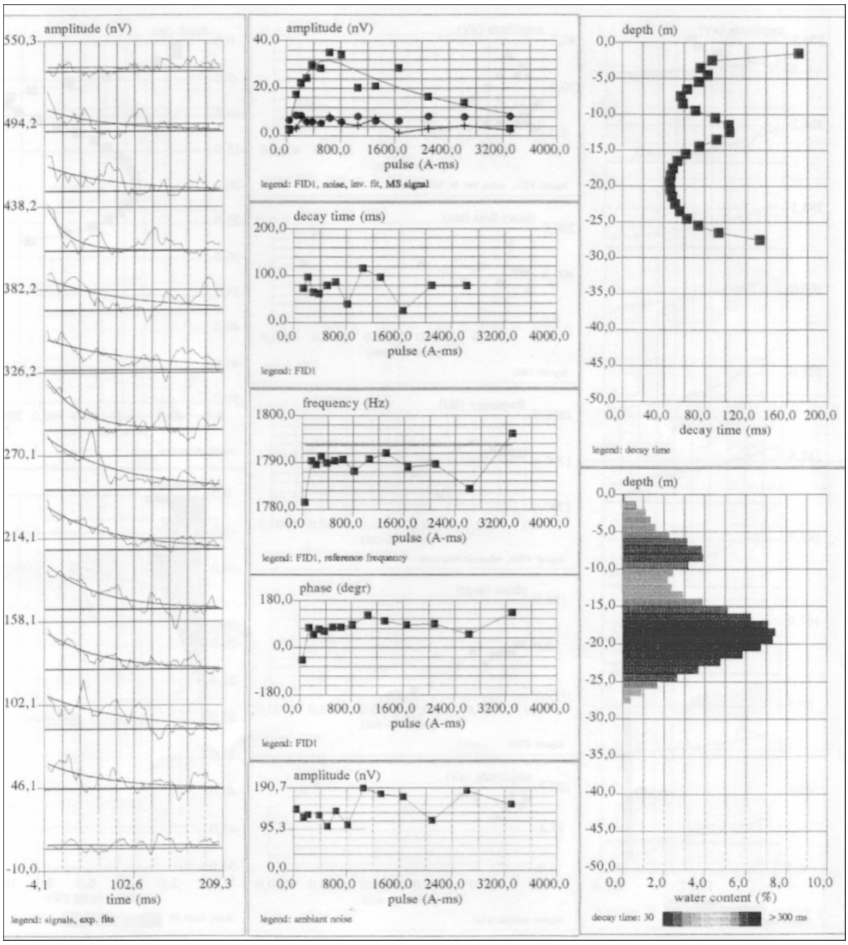

Figure 7. PMR sounding result at IPMR 10.

- To the left, the raw data time series for each value of the pulse parameter (the pulse parameter increases from bottom to top of the page).
- In the centre, measured and reconstructed amplitude, decay time, frequency, and phase of the PMR signals ambient noise versus the pulse parameter.
- To the right, the result of amplitude and decay time data inversion, i.e. water content and decay time distribution versus depth.

The cross section, as shown in Fig. 8a, summarizes the water content and decay time deduced from inversion of the PMR data at Mohabatnagar. The maximum thickness of the water saturated weathered zone was found to be about 25 m on PMR-10. The upper portion of the main part of IPMR13 may

be due to alluvial deposits. The underlying probable weathered zone increases from almost non-existent on IPMR 13 to reach the thickness of 20 m for a maximum depth of 30 m on IPMR10 (Fig. 8). This deepening of the weathered zone may be related to the fracture zone in the vicinity of IPMR10. A relatively long signal decay time reveals a small amount of clay in the weathered zone. Higher water content and a longer decay time suggest that more water is stored in this area than in KB Tanda area.

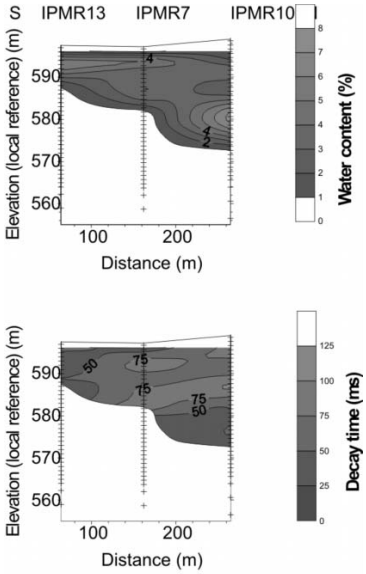

(a)

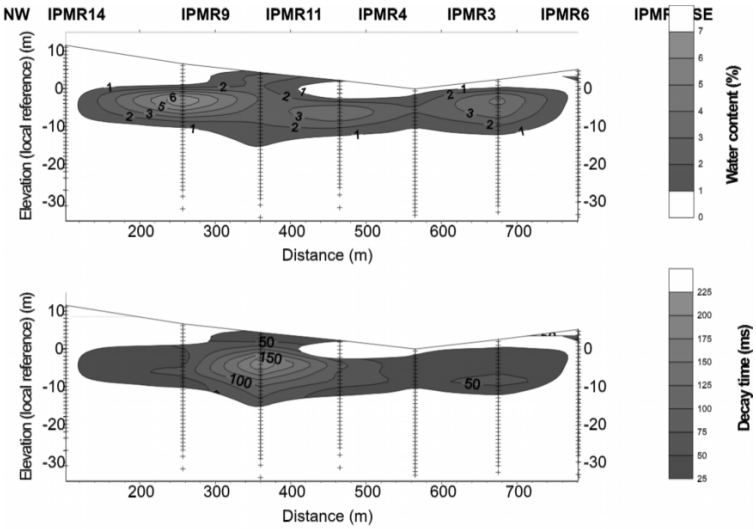

(b)

Figure 8. 2D sections from PMR soundings.

IPMR13a and IPMR13b measured at the same place but at right angles, show very different water contents and depths, which could be explained by the presence of 2D or 3D structures that are not revealed in the same manner by both soundings. Due to a low signal to noise ratio, it may also be possible that the IPMR13b result are erroneous.

The cross-section presented in Fig. 8b summarizes the water content and decay time deduced from inversion of PMR soundings at KB Tanda. The higher water content and longer decay time suggest that the largest amount of water is stored in the northwestern part of the profile (IPMR9, IPMR11). The maximum thickness of the water-saturated weathered zone was found to be about 15 m. A relatively short decay time and low water content (IPMR3) is most probably caused by a greater amount of clay or silt in the weathered zone. The low water content and almost waterless areas, as observed on IPMR14 and IPMR8 can be attributed to unweathered zones (fresh rocks).

WELL LOGGING

Geophysical well logging provides information on the geologic framework and the groundwater system at disposal sites. Log data can be used to plan the location of pits, trenches and monitoring wells. They can provide specific information on completion problems in monitor or injection wells. Logging provides more continuous data on the vertical and lateral distribution of effluent from waste than can be obtained from samples at a lower cost. Logs can also be used for monitoring changes in water quality. In order to plan a cost effective remediation programme, a thorough understanding of the hydrogeologic system is necessary and much of the needed information can be obtained economically from well logs.

Self-Potential (SP) Logging: The SP log is a measurement of the natural potential differences or self-potentials between an electrode in the borehole and a reference electrode at the surface. The development of SP in bore-wells is contributed mainly due to the differences in salinity and other parametres between the fluid filling the borehole i.e. mud or water and the quality of formation water. The diffusion of ions of different salts from one medium to another and flow potentials generate spontaneous polarization. Normally, clay/shaly rocks produce positive anomalies while porous, permeable layers such as sands, fractured sandstone, and compact sandstone give rise to negative anomalies. The interpretation of SP logs mainly consists of identification of different lithological horizons and marking their boundaries. This is usually done in conjunction with the resistivity logs.

Point Resistance (PR) Logging: One of the simplest and very useful logging methods measuring resistivity variations is called as the point resistance (PR) logging method. In this technique, the resistance between two electrodes (one of them is kept on the surface and the other is moved

in the bore-wells) is measured and is invariably used in conjunction with SP logging. Measurement of ground resistance serves more as an indicator of the probable order of resistivity rather than for determining the actual resistivity of formations. The compact zone shows high resistance while the others is indicated by lower values. The PR log has some advantages such as: 1. The anomaly highs or lows are proportional to the resistivity of the formation. 2. Very thin beds with different resistivities can be identified provided the borehole diametres are not very large compared to sonde diameter. 3. The measurement and interpretation of PR logs is simple.

Resistivity Logging: The most commonly used electrode arrangement is normal or potential sonde in which one current electrode and two potential electrodes are located on the sonde. The other current electrode is kept on the surface. The curves obtained by potential or normal resistivity logs are symmetrical in form in which the maximum indicates the layer with the higher resistivity, and the minimum indicates a layer with lower resistivity.

Gamma Ray Log: The gamma ray log is a record of a formation's radioactivity. The radiation emanates from naturally occurring uranium, thorium and potassium. Most rocks are radioactive to some degree. Igneous and metamorphic rocks are more so than sedimentary rocks. However, amongst sedimentary rocks, shales have by far the strongest radiation. It is for this reason that the simple gamma ray log has been called the 'shale log'. A high gamma ray value frequently means shale. Quartzite shows no radioactivity. Sandstones usually show low gamma ray values.

The various well logging techniques used in IFP-19 at Maheswaram watershed are shown in Figs. 9 and 10. The geological sequence encountered while drilling is the top weathered and semi-weathered layer followed by fractured granite underlain by compact granite at a depth of about 36 m. The resistivity sounding result shows a resistivity of 292 Ωm for the semi-weathered zone followed by fracture granite from 16-30 m with a resistivity of 496 Ωm, underlain by bed-rock. Self-Potential, Point Resistance, Temperature log, Short Normal, Long Normal and Gamma logs were done in this well. S.P. and Temperature logs do not indicate any anomalous zone. The SN and LN logs indicate low resistivity around 31 m and the PR log indicates a low resistance around 32 m.The apparent resistivity as observed against weathered zone are 110 Ωm and 600 Ωm by SN and LN respectively whereas against fractured zone are 220 Ωm and 1200 Ωm. The gamma log indicates high activity below 22.5 m onwards, which is in the range of 500 cps compared to that above 22.5 m which is in the range of 300 cps or less. This high activity can be activated to a fractured zone. Combining all these results showed that there is a clear fracture zone around 25 m as shown in Fig. 10. All the electric logs indicate that the bedrock occurs at a depth of 38 m.

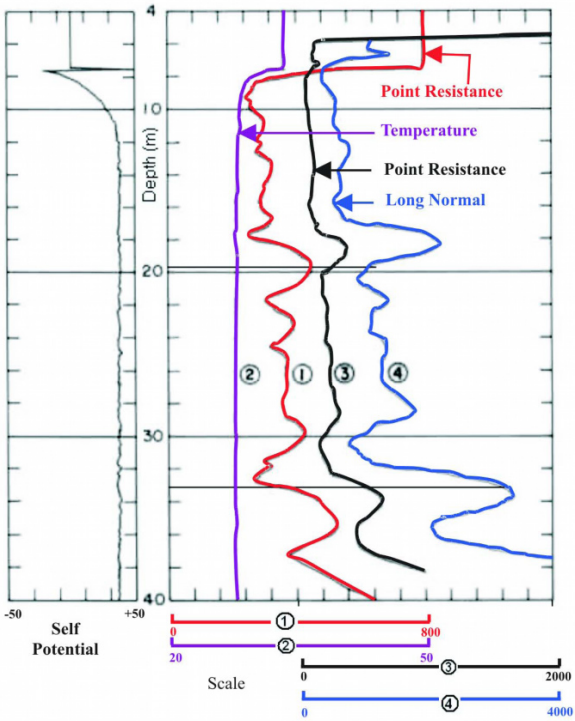

Figure 9. Geophysical Well Logs at IFP-1.

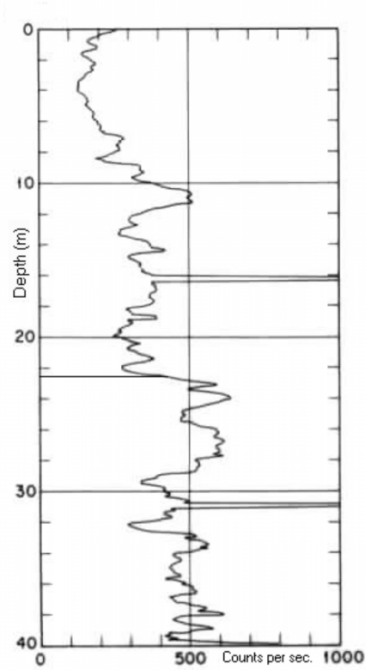

Figure 10. Gamma Log at IFP-1.

SELF POTENTIAL (SP) METHOD

Certain natural or spontaneous potentials occurring in the underground caused by electro-chemical or mechanical activity are called self-potentials. These potentials, when associated with groundwater at geologic contacts, bioelectric activity zones etc., are known as electro-kinetic or streaming potentials. Streaming Potentials generated by subsurface water flow are the source of the great majority of SP anomalies of groundwater interest. In a porous or fractured media, the relative movement between solid matrix and electrolyte (groundwater) causes an electrical potential at the interface, called zeta potential. If the water movement were brought by a hydraulic gradient (ΔP), a difference of electric potential E, called streaming potential, would result between any two points in the direction of motion. The following relation can be observed.

$$E = C \times \Delta P$$

where C, the streaming potential coefficient is dependent on a number of parametres like resistivity, dielectric constant and viscosity of fluid in the rock, the zeta potential, the grain size, the water path and others (Ahmed, 1964; Parkhomenko, 1971; Bogoslovsky and Ogilvy, 1973). The presence of a pressure gradient in the sub-surface, however, is not a sufficient condition to ensure the existence of an electric potential on the surface. As defined by Fitterman (1979), it is necessary to have a pressure gradient parallel to a boundary that separates regions of different streaming potential coefficients. An electric field equivalent to that by a surface distribution of current dipoles along the boundary is developed. The equipment required is extremely simple, consisting merely of a pair of non-polarisable electrodes (to eliminate electrode polarization effect) connected by a wire to a millivoltmeter of high impedance (greater than 108 ohms, so that negligible current will be drawn from the ground during the measurement). The procedure for carrying out the field studies is described by Krishnamurthy et al. (2001).

MISE-À-LA-MASSE METHOD

Schlumberger first attempted the mise-à-la-masse method in 1920. Only very limited case histories are available for this method (Parasnis, 1967, 1979; Ketola, 1972). The idea is to use a subsurface conductive mass (in this case water bearing fracture) as energisation point. The conductor is energized by a point source by lowering one current electrode in borehole below the water table. The other current electrode is kept on the surface at far off place (infinity). Potential on the surface is mapped in a grid pattern by keeping one electrode fixed as the reference electrode on the surface and moving the other potential electrode along the various profiles. The mise-à-la-masse equipotential maps are prepared by normalizing the potential values for 1A current (i.e, units are volts/amp).

Figure 11 shows Mise-à-la-masse and SP equipotential map near borehole no. 265. This bore-well drilled up to 42 m struck water at a depth of 23 m in pink granite and has static water level at 21.18 m. The drill log of existing bore-well indicates minor fractures between 15.84 and 32.90 m and fractured pink granite from 32.90 to 37.50 m. Well developed fractures with high density from 32.90 to 37.50 m substantially increased the yield of the well to 100 lpm. The current electrode in the bore-well was lowered down to depth of 37 m. Mise-à-la-masse map shows a well-developed trend of high equipotential zone in N-S direction along the central profile across the borehole. This indicates the extension of the fractures in N-S direction. SP map also shows similar trend in N-S direction. Two bore-wells (BW-1 and BW-2), one each on southern and northern side of the existing bore-well recommended on the basis of the Mise-à-la-masse measurements intercepted fractures at nearly the same depth as in borehole no. 265. A bore-well (BW-3) recommended on hydrogeological consideration in NW of existing bore-well did not intercept any fracture. This confirms the extension of fracture in N-S direction only.

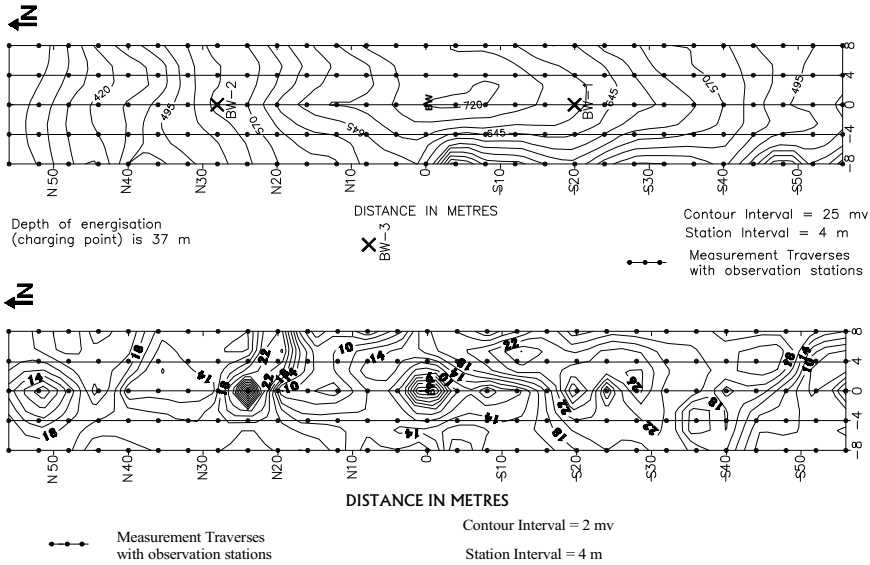

Figure 11. Mise-à-la-masse (above) and SP equipotential map (below) at IFP-11.

CONCLUSION

Many geophysical techniques have been applied to groundwater investigations with some giving more success than others. For resource mapping, it is not the groundwater itself that is the target of the geophysics rather it is the geological situation in which the water exists. Potential field methods, gravity

and magnetics, have been used to map regional aquifers and large-scale basin features. Seismic methods have been used to delineate bedrock aquifers and fractured rock systems. Electrical and electromagnetic methods have proved particularly applicable to groundwater studies as many of the geological formation properties that are critical to hydrogeology such as the porosity and permeability of rocks can be correlated with electrical conductivity signatures. Most geophysical techniques have been used for groundwater characterization but once again it is with the electrical and electromagnetic methods that the greatest success has been shown in directly mapping and monitoring contaminated and clean groundwater. The use of geophysics for groundwater studies has been stimulated in part by a desire to reduce the risk of drilling dry holes and also a desire to offset the costs associated with poor groundwater production.

REFERENCES

Acworth, R.I., 1987. The Development of Crystalline Basement Aquifers in a Tropical Environment. *Quarterly Journal of Engineering Geology*, **20:** 265-272.

Ahmed, M.V., 1964. A Laboratory Study of Streaming Potentials: *Geophysical Prospecting*; **12(1):** 49-64.

Barker, R.D., 1992. The Offset System of Resistivity Sounding and its use with a Multicore Cable. *Geophysical Prospecting*, **29:** 128-143.

Bogoslorsky, V.A. and Ogilvy, A.A., 1973. Deformations of Natural Electric Fields Near Drainage Structures: *Geophysical Prospecting*; **21(4):** 716-723.

Compagne Generale De Geophysique, 1963. Mater Curves for Electrical Sounding, 2nd Revised Edition, Eaeg, The Hague, The Netherlands.

Dobrin, M.B. 1976. Introduction to Geophysical Prospecting. New York, Mcgraw-Hill, pp. 630.

Eddy-Dilek, C.A., Hoekstra, P., Harthill, N., Blohm, M., and Phillips, D.R., 1996. Definition of a Critical Confining Zone Using Surface Geophysical Methods. SAGEEP, pp. 387.

Fitterman, D.V., 1979. Calculation of Self-Potential Anomalies Near Vertical Contacts: *Geophysics*; **44(2):** 195-205.

Flathe, H., 1963. Five Layer Master Curves for the Hydrogeological Interpretation of Geoelectrica Resistivity Measurements above a Two Storey Aquifer, *Geophysical Prospecting*, **11:** 471-508.

Ghosh, D.P., 1971a. The Application of Linear Filter Theory to the Direct Interpretation of Geoelectrical Resistivity Sounding Measurements, *Geophysical Prospecting*, **19:** 192-217.

Ghosh, D.P., 1971b. Inverse Filter Coefficients for the Computation of Apparent Resistivity Standard Curves for a Horizontally Stratified Earth, *Geophysical Prospecting*, **19:** 769-775.

Goldman, M., Rabinovich, B., Rabinovich, M., Gilad, D., Gev, I. and Schirov, M., 1994. Application of Integrated Nmr-Tdem Method in Ground Water Exploration in Israel. *Jour. Appl. Geophys*, **31:** 27-52.

Grant, F.S. and West, G.F., 1965. Interpretation Theory in Applied Geophysics. Mcgraw-Hill, New York.

Griffiths, D.H., Turnbull J. and Olayinka, A.I., 1990. Two Dimensional Resistivity Mapping with a Computer Controlled Array. *First Break*, **8:** 121-129.

Griffiths, D.H. and Turnbull, J., 1985. A Multi Electrode Array for Resistivity Surveying. *First Break* **3:** 16-20.

Griffiths, D.H. and Barker, R.D., 1993. Two-Dimensional Resistivity Imaging and Modeling in Areas of Complex Geology. *Journal of Applied Geophysics,* **29:** 211-226.

Jupp, D.L.B. and Vozoff, K., 1975. Stable Iterative Methods for the Inversion of Geophysical Data. *Geophysical Journal of The Royal Astronomical Society*, 957-976.

Kearey & Brookes, 1991. An Introduction to Geophysical Exploration.

Ketola-Matti, 1972. Some Points of View Concerning Mise-À-La-Masse Measurements. *Geoexploration*, **10(1):** 1-21.

Krishnamurthy, N.S., Ananda Rao., V., Negi, B.C., Kumar, D., Jain, S.C., Ahemed, S. and Dhar, R.L., 2001. Electrical Self Potential and Mise-À-La-Masse Investigation in Maheshwaram Watershed, Andhra Pradesh, India. NGRI Technical Report No. NGRI-2001-GW-314.

Lieblich, D.A., Legchenko, A., Haeni, F.P. and Portselan, A., 1994. Surface Nuclear Magnetic Resonance Experiments to Detect Subsurface Water at Haddam Meadows, Connecticut. Proceedings of the Symposium on the Application of Geophysics to Engineering and Environmental Problems, March 27-31, 1994, Boston, Massachusetts, 2, pp. 717-736.

Loke, M.H. and Barker, R.D., 1996. Rapid Least-Squares Inversion of Apparent Resistivity Pseudosections by a Quasi-Newton Method. *Geophysical Prospectings* **44:** 499-524.

Miller, P.T., Mcgeary, S. and Madsen, J.A., 1996. High-Resolution Seismic Reflection Images of New Jersey Coastal Aquifers. Sageep, pp. 55.

Murali, S., Patangay, N.S., 1998. Principles and Applications of Groundwater Geophysics, AEG, Hyderabad, India.

Orellana, E. and Mooney, H.M., 1966. Master Tables and Curves for Vertical Electrical Sounding over Layered Structures. Interciencia, Madrid, Spain.

Parasnis, D.S., 1979. Principles of Applied Geophysics. Chapman and Hall. pp. 275.

Parasnis, D.S., 1967. Three-Dimensional Electric Mise-À-La-Masse Survey of an Irregular Lead-Zinc-Copper Deposit in Central Sweden. *Geophysical Prospecting*, **15:** pp. 407-437.

Parkhomenko, E.I., 1971. Electrification Phenomena in Rocks. Plenum Press; New York; 285.

Rangarajan, R. and Prasada Rao, N.T.V., 2001. Technical Report No. NGRI-2001-GW-298

Reynolds, 1997. An Introduction to Applied and Environmental Geophysics, 1st Ed. Wiley.

Rijkswaterstaat, The Netherlands, 1969. Standard Graphs for Resistivity Prospecting. European Association of Exploration Geophysicists, The Hague.

Schirov, M., Legchenko, A. and Creer, G., 1991 New Direct Non-Invasive Ground Water Detection Technology for Australia. *Expl. Geophys*., **22:** 333-338.

Stefanesco, S.S. et al., 1930. Sur La Distribution Electrique Potentielle Author D'une Prise Ae Rerre Ponetuelle Dans Unterrain A Couches Horzontales Homogens Et Isotropes. *Journal Physique Et Radium Sieres*, **7:** 132-141.

Telford, W.M., Geldart, L.P., Sheriff, R.E. and Keys, D.A., 1976. Applied Geophysics. Cambridge University Press.

Trushkin D.V., Shushakov, O.A. and Legchenko, A.V., 1995. Surface NMR applied to an electroconductive medium. *Geophys.Prosp*., **43:** 623-633.

Varian, R.H., 1962. Ground Liquid Prospecting Method and Apparatus. US Patent 3019383.

5 Application of Remote Sensing and GIS in Groundwater Exploration

S.K. Nag

Department of Geological Sciences
Jadavpur University, Kolkata-700032, India

INTRODUCTION

Remote sensing and GIS methods permit rapid and cost effective natural resource survey and management. Moreover, remotely sensed data serve as vital tool in groundwater prospecting (Sharma and Jugran, 1992; Chatterjee and Bhattacharya, 1995; Tiwari and Rai, 1996; Ravindran, 1997; Horton, 1945). The remote sensing data helps in fairly accurate hydrogeomorphological analysis and identification and delineation of land features (Kumar and Srivastava, 1991). With sufficient ground data, hydrological characteristics of geomorphological features can be deciphered. Groundwater occurrence being subsurface phenomenon, its identification and location is based on indirect analysis of some directly observed terrain features like geological and geomorphic features and their hydrologic characters. Satellite remote sensing provides an opportunity for better observation and more systematic analysis of various geomorphic units, lineament features, following the integration with the help of Geographical Information System to demarcate the groundwater potential zones. Therefore, an integrated approach, including studies of lithology, hydrogeomorphology and lineament, has been taken up, using remote sensing and GIS techniques, for a proper assessment of groundwater potential zones in the study area.

METHODOLOGY

For the groundwater resource development in an area the following methodology may be undertaken which integrates remotely sensed data. The groundwater resource development in the study area involves lithological, hydro-geomorphological and lineament thematic maps generation. The Survey

of India toposheets may be used for the preparation of base map. The methodology of generation of thematic maps such as lithology, hydro-geomorphology and lineaments of the study area requires visual interpretation of satellite remote sensing data. Identification and delineation of various units on the thematic maps are based on the colour, tone, texture, size, pattern and association. All the thematic maps are verified during the field checks. The thematic details thus finalized are transferred to the base map prepared from the Survey of India toposheets. A typical method used in GIS modelling is to compute numerical values for each spatial feature in a theme and classify the numerical values on an interval basis known as Weighted Index Overlay Analysis.

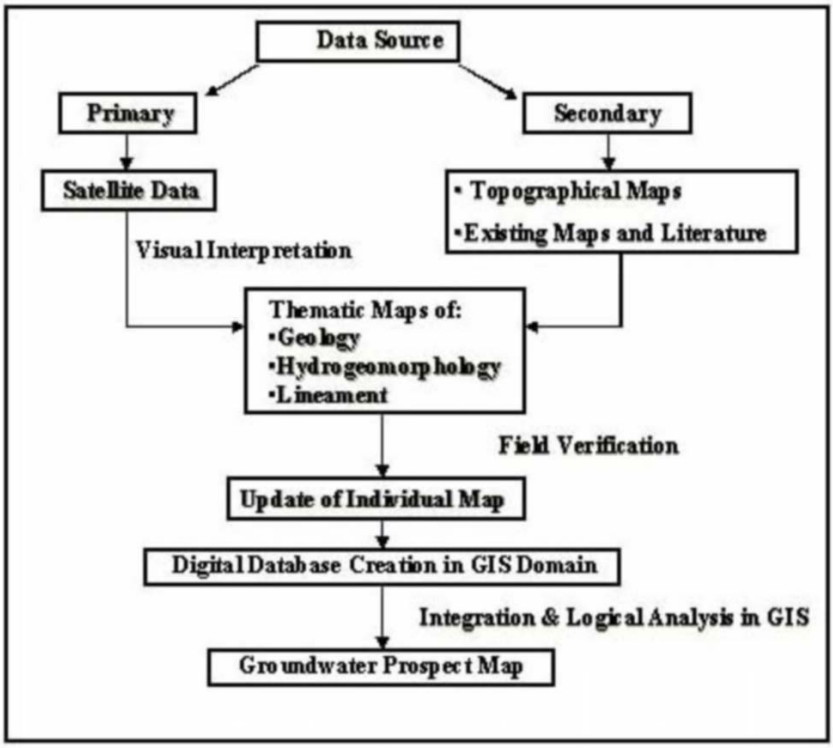

Flow Chart

HYDROGEOMORPHOLOGY

The hydrogeomorphology in the hard rock terrain is highly influenced by the lithology and structures of the underlying formations. The area is characterized by a dominant rocky terrain and a number of erosional and depositional hydrogeomorphic features, which are manifested by hills, uplands and undulating surfaces. The significant hydrogeomorphic units, commonly identified on the basis of their image characteristics, include buried pediments

(shallow), buried pediments (medium) and valley fills. Depositional processes also develop landform namely valley fill. The weathered pediments buried under soil cover represent the features formed by the involvement of both erosional and depositional process.

Buried Pediments (Shallow) [BPS]

This unit is basically a pediment zone and consists of very low weathered zone. A flat and smooth surface of buried pediment consists of shallow overburden of weathered derivative material. Groundwater prospects are moderate to poor, but open wells yield good amount of potable water after monsoon (Shah, 2001).

Buried Pediments (Medium) [BPM]

These units are moderately weathered with their thickness greater than that of the shallow pediments. A flat and smooth surface of buried pediment with moderately thick overburden of weathered derivative material. Groundwater prospects are also good to moderate.

Valley Fills [VF]

Valley fills are linear depressions present in between the hill ranges and occupy the lowest reaches in topography, commonly filled with pebbles, cobbles, gravel, sand, silt and other detrital material. The groundwater potential ranges from moderate to good. These valleys are developed along the fractures and such places can be exploited for groundwater through deep bores. In general, it is observed that adequate recharge source of groundwater is met within valley fillings. Hence, in such places, the groundwater is considered to be moderately better with adequate source of water. This has very good porosity and permeability but some time presence of clay may make it impermeable.

The details of various geomorphic units and their groundwater bearing prospects are given in Table 1.

Table 1: Hydrogeomorphology and groundwater prospects of various geomorphic units

Geomorphic Units	*Description*	*Water Prospects*
Valley Fill	Accumulation zone of colluvial materials derived from surrounding uplands; shallow to deep; fine loamy to clayey soils.	Good
Buried Pediment (Medium)	Gently sloping topography; very deep, clayey to fine loamy soils.	Moderate
Buried Pediment (Shallow)	Nearly flat to gently sloping topography, shallow to moderately deep, loamy soils followed by regolith zone.	Poor

LINEAMENT STUDY

In the hard rock areas, the movement and occurrences of groundwater depends mainly on the secondary porosity and permeability resulting from folding, faulting, fracturing etc. The most obvious structural features that are important from the groundwater point of view are the lineaments. The lineaments are linear or curvilinear feature pattern and play a vital role, particularly in geomorphic and structural analysis. The lineaments like joints, fractures etc., developing generally due to tectonic stress and strain, provide important clue on surface features and are responsible for infiltration of surface run off into sub-surface and also for movement and storage of groundwater (Subba Rao et al., 2001). Photolineaments generally represent the surface traces of fractures in bedrocks, projected more or less vertically upwards to the erosion surface by various mechanisms (Srinivasan, 1988). A systematic mapping effort needs to be conducted to perform the lineament trace analysis. By visually interpreting the satellite imageries, the lineaments of the study area are picked up and traced on the basis of tonal, textural, soil tonal, vegetation, topographic and drainage linearities, curvilinearities and rectilinearities (Lillesand, 1989; Drury, 1990; Gupta, 1991).

The remote sensing data, which offer synoptic view of large area, helps in understanding and mapping the lineaments both on regional and local scale. The lineament analysis of the area from remotely sensed data provide important information on subsurface fractures that may control the movement and storage of groundwater. To determine the lineament density in the study area, the total study area is subdivided in a number of grids of dimension 1 km × 1 km. Density of the lineaments of a single grid is obtained from the values of the total length of the lineaments in a single grid (ΣL). Calculation of the density of the lineaments in the area involves the ratio of ΣL to A. By calculating the value of $\Sigma L/A$ for each grid and locating the value at the centre of that grid, the density of the lineaments of the study area is calculated. These values are joined by isolines to prepare a lineament density map using GIS software.

The main advantages in using remote sensing techniques for groundwater exploration are: quick and less expensive way of getting information on the occurrence of groundwater, aids to select promising areas for further groundwater exploration thus reducing field work and provides information on prospects in one map.

WEIGHTED INDEX OVERLAY ANALYSIS (WIOA)

It is a simple and straightforward method for a combined analysis of multi-class maps. The efficacy of this method lies in that the human judgement can be incorporated in the analysis. A weight represents the relative importance of a parameter vis-à-vis the objective. WIOA method takes into consideration the relative importance of the parameters and the classes belonging to each

parameter. There is no standard scale for a simple weighted overlay method. For this purpose, criteria for the analysis should be defined and each parameter should be assigned importance (Saraf and Chowdhury, 1998).

RESULTS AND DISCUSSION

Groundwater occurrence is influenced by the climate, physiography, drainage and geology of the area. Geomorphological mapping allows an improved understanding of watershed management, groundwater exploration, land use/ land cover planning etc. Analysis of remotely sensed data along with Survey of India topographical map, collateral information and limited ground checks help in establishing the baseline information for groundwater targeting of the area. Furthermore Remote Sensing techniques are efficient means of obtaining land use/land cover information more accurately at a faster rate with less manpower and with greater cost efficiency. Measurement of land cover based on information obtained from satellite imagery can also be greatly expedited through computer analysis.

The main advantages in using remote sensing techniques for groundwater exploration are: quick and inexpensive way of getting information on the occurrence of groundwater, aids to select promising areas for further groundwater exploration thus reducing field work and provides information on prospects in one map. This type of information is very helpful in the areas where more emphasis is on groundwater for the irrigation and drinking purposes.

REFERENCES

Chatterjee, R.S. and Bhattacharya, A.K., 1995. Delineation of the Drainage Pattern of a Coal Basin Related Inference Using Satellite Remote Sensing Techniques. *Asia Pacific Remote Sensing J*, **1:** 107-114.

Gupta, R.P., 1991. Remote Sensing Geology. Springer-Verlag, Germany, pp. 356.

Horton, R.E., 1945. Erosional Development of Streams and their Drainage Basins: Hydrophysical approach to quantitative morphology. *Geol. Soc. Am. Bull.*, **56:** 275-370.

Kumar, Ashok and Srivastava, S.K., 1991. Geomorphological Unit, their Geohydrological Characteristics and Vertical Electrical Sounding Response near Munger, Bihar. *J. Indian Soc. Remote Sensing*, **19(4):** 205-215.

Lillesand, T.M., 1989. Remote Sensing and Image Interpretation. John Wiley and Sons, U.S.A., pp. 721.

Revindran, K.V., 1997. Drainage Morphometry Analysis and Its Correlation with Geology, Geomorphology and Groundwater Prospects in Zuvari Basin, South Goa, Using Remote Sensing and GIS. Proc. Nal Sym-remote sensing for natural resource with special emphasis on water management, held at Pune during Dec. 4-6, 1996, pp. 270-296.

Saraf, A.K. and Chowdhury, P.R., 1998. Integrated Remote Sensing and GIS for Groundwater Exploration and Identification of Artificial Recharge Sites. *International Journal of Remote Sensing*. **19(10):** 1825-1841.

Shah, P.N., 2001. Hyrogeomorphological Mapping for Evaluation of Groundwater Prospect Zones in Mirzapur District, Uttar Pradesh, India using IRS-1A, LISS-II Geocoded Data, Spatial Information Technology. Remote sensing and Geographical Information Systems, Vol. II, pp. 447-453.

Sharma, D. and Jugran, D.K., 1992. Hydromorphological Studies around Pinjaur-Kala Amb area, Ambala district (Haryana), and Sirmur district (Himachal Pradesh), *J. Indian Soc. Remote Sensing*, **29(4):** 281-286.

Srinivasan, P., 1988. Use of Remote Sensing Techniques for Detailed Hydrogeological Investigations in parts of Narmadasagar Command Area, MP (India). *Photonirvachak (Journal of the Indian Society of Remote Sensing)*, **16(1):** 55-62.

Subbu Rao, N. et al., 2001. Identification of Groundwater Potential Zones Using Remote Sensing Techniques in and around Guntur town, Andhra Pradesh, India. *J. Indian Soc. Remote Sensing*, **29(1&2):** 69-78.

Tiwari, A. and Rai, B., 1996. Hydrogeomorphological Mapping for Groundwater Prospecting Using Landsat-MSS images—A Case Study of Part of Dhanbad District. *J. Indian Soc. Remote Sensing*, **24(4):** 281-285.

6 Pumping Tests: Planning, Preparation and Execution

K. Subrahmanyam and Haris H. Khan

National Geophysical Research Institute
Hyderabad - 500007, India

INTRODUCTION

The most important aspect of groundwater studies in an area is to determine how much groundwater can be safely withdrawn and also for management of the available source. This determination involves

(i) Transmissibility and storage coefficients of the aquifers
(ii) The lateral extent of aquifers and the nature of the boundary conditions
(iii) The effect of future developments on recharge and discharge

All the above information can be obtained by conducting pumping tests in the field. A pumping test involves the bailing out of water through a pumping well (Pw) and the measurement of water level changes induced in one or more observation wells (Ob well/s) located in the vicinity of the pumping well. In general, two types of tests are conducted in the field. A long duration test known as the aquifer performance test (APT) is for obtaining the characteristic features of the aquifer. The second type of test, step-draw down test (SDT) is for determining the optimal capacity of the well and to install proper pumping equipment. A step-draw down test is conducted with different pumping rates in three or five stages, each stage being of the same duration. The specific capacity versus the yield relationship is determined on a designed production well.

Since a pumping test is a costly proposition, an attempt has been made in the following paragraphs to briefly discuss the most important aspects of selection of a test site, preparation and procedures to accomplish the tests.

SELECTION OF TEST SITE

The factors to be considered before selecting a test site could be: (a) topography, (b) geology of the area, (c) porosity and permeability, (d) joints and faults and folds, (e) proximity to tanks, rivers, springs, lakes, unlined channels and (f) existing pumping wells.

As the aquifer parametres have to be utilized for effective planning and management of the groundwater in an area, it is very essential that the wells be so selected that they do not fall near contact zones of formations. The movement of water in hard rocks is through joints, fractures and cracks which are interconnected. Wells that tap the highly jointed rocks or along fault plane produce very high yield in comparison to surrounding areas. When the rocks are folded into anticlines and synclines, the synclines are favourable spots for groundwater storage in the pervious layers, while if a well taps the anticlines, it may not yield, since the crest forms a groundwater divide. Thus a judicious selection for a pumping test site should be made. The water levels in confined aquifers are subject to immediate changes in pressure heads caused due to heavy traffic passing nearby the test sites, such as railway lines or heavy road trucks.

In addition to the above factors, adequate subsurface investigations prior to performance of an aquifer test are to be determined for ascertaining the lithological character, thickness of aquifer, location of aquifer boundaries, character of bed overlying and underlying the aquifer, nature of barrier or recharge boundaries if any, direction of groundwater flow, water table gradients and regional water level trend. The thickness of aquifer, and the features of the overlying and underlying beds can be ascertained during the drilling of the bore-well. The depth vs. yield of the various formations could be collected from the data recorded during drilling. If the main aquifer is bounded by any partially permeable formations, then adequate care has to be exercised for sealing of the inflows by inserting a suitable packer assembly. It is also very important to dispose off the pumped water preferably through pipeline to a distant place so that it does not return back and cause interference with the water level changes in wells. Gradient of the water table should be low and, preferably, the boundary conditions of the aquifer should be clearly defined and simple.

Abstraction Well (Pumping Well - PW)

The diameter of the well should be able to accommodate pumping equipment and sufficient length of casing must be inserted to avoid collapsing of loose material if any. The length of the casing of the screen should at least be 70% of the aquifer thickness, so that it does not become a partially penetrating well.

Observation Well (Ob Well)

To measure drawdown within the cone of depression caused by discharging well. As a general rule, the observation wells should be placed at a distance of 1.5 to 2.0 times the thickness of the aquifer. More than one observation well, if available, would also give the directional inhomogeneities, if any.

The position of observation wells should be considered with respect to: (a) type of aquifer, (b) hydraulic conductivity, (c) well penetration, (d) geohydrologic boundaries, (e) discharge and (f) stratification. Observation wells should not be located near a recharge area, as the data from these wells may not reflect actual storage coefficient

The operation for pumping test involves prior information at the test site:

(a) measurement of static water level (before pumping begins), the depth below a measuring point or ground level
(b) the lithological characteristics and the details of well depth, length of casing inserted, the discharge of the well (say at the time of drilling)
(c) general water table, the performance of nearby wells.

EQUIPMENT REQUIRED

A truck-mounted test-pumping unit should comprise a submersible pump (with three-phase motor) and a (diesel) power generating set (since uninterrupted power may not be available at the test site as in most parts of India) and tripod/hydraulic arrangement for smooth lowering of pump and pipes. The pump and power unit for a pumping test should be capable of operating continuously at constant discharge rate for longer periods of time. Suitable measurement devices for time, discharge and water level. The time intervals may be best noted through a stopwatch, and if several wells have to be monitored then all the watches have to be matched to a common time.

Measurement of Water Level

Best device is automatic water level recorder since this gives a continuous record of changes in water level measurements. The other types of devices in usage are (a) chalked steel tape, (b) whistle tape, (c) hollow cylinder, (d) digital tape and (e) electrical tape. These can be used accurately for measurement in the observation wells since the water levels are not disturbed by changes in pumping rate and inflows into the well (as in the case of fractured rocks).

Since the water levels decline at a faster rate during the early stages of pumping, it is required that the frequency of measurements is high in the beginning of the test. The yield test is generally run for 10-15 hours continuously and till constant draw down is maintained in the well. Thus, the specific capacity of the well is its yield per unit draw down and for the given pumping period. This may also vary with the wet and dry seasons.

Measurements in Pumping well and Observation well

Time since pump started (minutes)	*Time intervals (minutes)*
0-5	1-5
5-60	5
60-120	10
120-360	(or till shut down) 20

Discharge Measurements

A pumping test requires correct measurement of discharge of the pumped well at a constant discharge rate. The flow rate is measured at regular intervals of time and adjustments made to keep it constant through deployment of (a) integrating type of water meter installed in the pipe, (b) Orifice meter and (c) 90° V-notch. Small discharges can also be measured by recording the time taken to fill a known volume of container.

Discharge through a 90° V-notch

$Q = 1.38\ H^{2.5}$, where H = head in m and Q = discharge in m^3/sec.

Head H (cm)	*Discharge Q (lpm)*
2	4.7
4	26.5
6	73
8	149
10	255
12	414
15	725
20	1490
25	2580
30	4060

Estimation of Flow from Horizontal Pipes

A fairly close determination of the flow from full open pipes may be made by measuring the distance the stream of water travels parallel to the pipe in falling 12 inches vertically.

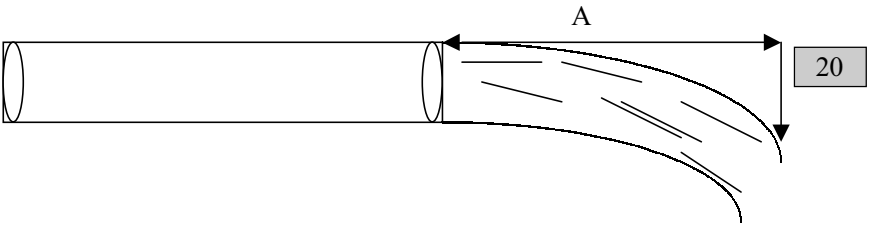

The flow in gallons per minute equals the distance (A) in inches multiplied by a constant k obtained from the following table.

Internal diameter of pipe (")	*k*
2.0	3.3
2.5	5.1
3.0	7.3
3.5	10.0
4.0	13.1
4.5	16.5
5.0	20.4
5.5	24.7
6.0	29.4
6.5	34.5

Approximate flow from pipe running full in gallons per minute

	Horizontal Distance (A)									
Dia-pipe	*12″*	*14″*	*16″*	*18″*	*20″*	*22″*	*24″*	*26″*	*28″*	*30″*
2″	41	48	55	61	68	75	82	89	96	102
3″	90	105	120	135	150	165	180	195	210	225
4″	150	181	207	232	258	284	310	336	361	387
6″	352	410	470	528	587	645	705	762	821	880

Minimum period of pumping test - at least 6 to 8 hrs or till a good response of the Aquifer is achieved.

Preparation, Compilation and Analysis of Data

Time to be expressed in days

Water level to be reduced to draw down in metres

Either time-draw down or distance-draw down data

Correction of observed draw down for variation in barometric pressure, changes in tidal height, rate of pumping changes in adjacent wells.

Type of aquifer

Suitable methods for analysis to be applied depending upon type of aquifer

The two important aquifer parameters in relation to groundwater flow are the transmissivity (T) and the Storage Coefficient (S). Pumping tests are the most practical and direct methods of determining these parameters. Some of the constraints in performing these tests are, however, the cost towards conducting the tests, and the availability of observation wells near the

discharge wells. Theis (1935) has shown that transmissivity could be calculated from the recovery water level data and this method is often used in estimating transmissivity from single bore-wells. From the time-drawdown data of an observation well located at a distance 'r', the aquifer parametres can be determined. The other data required for the computation are the drawdown from the observed data, the time factor and the constant discharge of the pumped well. The type curve and the data curve (plotted on double logarithmic paper) are matched and the following data are noted from a common match point. (No attempt is made to elaborate the theoretical aspects of the method.) Another method has been described by Jacob, which involves plotting of observed data on a semi-logarithmic paper and fitting the data to straight line. Both transmissivity and storage coefficient can be determined.

Theis Method

$T = Q/4\pi s\ w\ (u);\ u = r^2\ S/4Tt$

from match point

where $s = 0.174$ m, $t = 5.2 \times 10^{-2}$ day, $w(u) = 1.0$, $1/u = 100$, $u = 0.01$ and $r = 130$ m

Jacob's Straight-line Method

$$T = 2.30\ Q/4\ \Delta s; \qquad S = \frac{2.25\,T\,t_0}{r^2},$$

where 'T' is the transmissibility (m^2/day), 'Q' is the discharge in m^3/day, Δs is log cycle difference in drawdown (m), 'S' is the storage coefficient, 't_0' time intercept on the zero-drawdown axis ($s = 0$) and 'r' is the distance between pumping well and observation well.

Selection of Pump Sets

The selection of proper pumping set is important to ensure yields from wells and factors to be considered are:

(a) finished inside diameter and total depth of the well
(b) yield from the well, the desired pumping rate and hours of pumping per day
(c) the lowest pumping water level (in dry season)
(d) the total head on the pump
(e) the power required

CONCLUSIONS

The chapter provides practical tips for carrying out the pumping tests that are at one hand important experiments in groundwater hydrology and on the other hand quite cumbersome and to be handled with utmost care to obtain

a useful result. A number of relevant literatures exist and they are listed for further reading and consultation.

REFERENCES

Deulleur, J.W., 1998. The Handbook of Groundwater Engineering. CRC Press, 992 pp.

Fetter, C.W., 1994. Applied Hydrogeology. Prentice Hall, Englewood Cliffs, NJ.

John, E. Moore and Moore, E. Moore, 2002. Field Hydrogeology. CRC Press, 195 pp.

Jonathan, D. Istok, Karen, J. Dawson, Jack, F. Yablonsky and Istok, D. Istok, 1991. Aquifer Testing: Design and Analysis of Pumping and Slug Tests. Lewis Publishers, 344 pp.

Kruseman, G.P. and de Ridder, N.A., 1991. Analysis and Evaluation of Pumping Test Data (2d ed.): Publication 47, International Institute for Land Reclamation and Improvement, The Netherlands, 377 pp.

Roscoe Moss Company, 1990. Handbook of Ground Water Development. Wiley - IEEE, 512 pp.

Todd, D.K., 1980. Groundwater Hydrology. John Wiley and Sons, Inc., New York, NY, 664 pp.

Vedat, Batu, 1998. Aquifer Hydraulics: A Comprehensive Guide to Hydrogeologic Data Analysis, Wiley - IEEE, 752 pp.

Walton, William C., 1990. Groundwater Pumping Tests, Design and Analysis. Lewis Publishers, 216 pp.

Watson, I. and Alister D. Watson, 1993. Hydrology: An Environmental Approach. CRC Press, 750 pp.

Willis, D. Weight and John L. Sonderegger, 2001. Manual of Applied Field Hydrogeology, McGraw-Hill Professional, 608 pp.

7 Various Pumping Tests and Methods for Evaluation of Hydraulic Properties in Fractured Hard Rock Aquifers

J.C. Maréchal, B. Dewandel, K. Subrahmanyam[1] and R. Torri

Water Department, Unit "Water Resources, Discontinuous Media", BRGM, Montpellier, France

[1]Indo-French Centre for Groundwater Research, National Geophysical Research Institute, Uppal Road, Hyderabad, 500 007, India

INTRODUCTION

Large tracts of South India are underlained by hard crystalline rock terrain (granite, gneiss, basalt, etc.). The area is also classified as semiarid to arid, generally prone to drought conditions, requiring optimal management of groundwater resources against increasing demands of water for various activities (agricultural, industrial, domestic). Estimating the hydraulic characters of water bearing layers is an essential part of groundwater studies. The most effective way of determining these characteristics is to conduct and analyse in-situ hydraulic tests. One of the early records of pumping tests on a large scale in India was done by Vincent and Sharma (1978). The study indicates that well losses comprise a significant portion of the total drawdown in a number of low- and high-yielding wells. Karanth and Prakash (1988) observed that the transmissivity values (T) obtained by slug-tests are more than pump test values for low T values, and that they vary from negligible up to a factor of about three for higher T values. Pradeep Raj et al. (1996), from hydrological tests on dug wells in the crystalline rocks, estimated a range of T values from 26.5 to 56.36 m^2/d, for the weathered zone based on interpretation made by Papodopulos and Cooper method (Papadopulos and Cooper, 1967). Ballukraya (1997), from a study in Karnataka, postulates that the yield fluctuation in the pre- and post-monsoon periods is largely dependent

on recharge that is restricted to about 60 m depth. All these studies considered hard rock aquifer as isotropic and homogeneous, which is not the case as demonstrated below.

The fresh unaltered massive hard rock is not water bearing, but the (i) weathered zone and (ii) fissured and jointed zones are productive. In general, the weathered horizon, when it is water saturated, is poorly transmissive with high storage while the fissured and jointed zones are poorly capacitive, but highly transmissive. The problem of flow through fractures or a fractured environment is primarily a problem of flow through a dual-porosity media, which includes the porous matrix and the fractured network. These two components are hydraulically interconnected and cannot be treated separately. The degree of interconnection between these two media defines the character of the entire flow domain, and is a function of the hydraulic properties of each of them. These properties include matrix hydraulic conductivity and fracture-network distribution, orientation, apertures, connectivity and, thus, bulk hydraulic conductivity. They will also determine the heterogeneity and anisotropy of the whole aquifer. The complexity of flows through fractures makes inadequate the use of classical techniques such as Theis and Jacob methods for the interpretation of hydraulic tests. Basically, in hard rock context, assumptions (homogeneity and isotropy) attached to such methods are not coherent with the reality. Thus, there is a need for alternative techniques for the evaluation of aquifer parameters able to involve the specificity of hard rock aquifers.

Four different methods are presented below, for the interpretation of pumping tests, well adapted to the complexity of groundwater flows in hard rock aquifers. The method of Neuman (1975) is suited for unconfined anisotropic aquifers while Gringarten method (Gringarten and Witherspoon, 1972) was developed for the case of a single (horizontal) fracture intersecting the pumping well. These methods are complementary because they deal both with anisotropy at the observation and at pumping wells respectively. The Warren and Root (1963) method takes into consideration the heterogeneity of the medium, allowing the introduction of a double porosity aquifer (transmissive fractures and capacitive matrix). Finally, the fourth method - Barker theory (Barker, 1988)—opens the way for the assessment of the flow dimension and of the degree of connectivity between the fractures. All these methods are incorporated and illustrated on observations obtained from pumping tests carried out in the same study area.

The Maheshwaram watershed located in India (Andhra Pradesh, Ranga Reddy District) is the main study area of the Indo-French Centre for Groundwater Research (French Geological Survey/National Geophysical Research Institute). This watershed, located at 30 kilometres away from Hyderabad, covers a surface of about 55 km^2 and is mainly constituted by Archean granites. The weathering profiles are observable through many dug wells earlier used by the farmers for irrigation. Profiles are generally truncated

by erosion: under a few decimetres of red soils, the alterites are thick with less than five metres. A high density of horizontal fractures is observed in the fissured zone (Maréchal et al., 2005). Vertical fractures with a tectonic origin are also present. Due to the overexploitation of groundwater resources, water levels are far below ground level and the alterites are dry while only the fissured zone is saturated. This specificity was used to realise pumping tests with the objective to test the four interpretation methods mentioned above and thus to characterise the hydrodynamic properties of the fissured layer only.

ANISOTROPY OF PERMEABILITY USING NEUMAN METHOD AT OBSERVATION WELLS

On a bi-logarithmic plot (Fig. 1), the drawdown curves at observation wells IFP-1/1 and IFP-1/2 during pumping tests at IFP-1 well have a complex shape, difficult to interpret with classical methods (Theis, for example). Drawdown curves are composed by three parts: the first one, at short times, with strong slopes, is followed by an intermediate period during which water level stabilisation occurs, and a third part for long times shows a new increase in slopes.

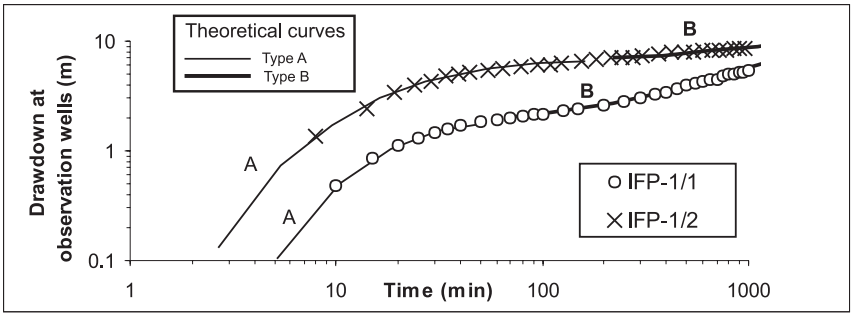

Figure 1. Adjustment of drawdown in observation wells IFP-1/1 and IFP-1/2 using Neuman theoretical curves of types A and B.

The theory initially developed by Boulton (1970), to interpret some special curves obtained in observation wells, takes into account the notion of "delayed yield from storage in unconfined aquifers" (Boulton and Pontin, 1971). It was improved by Neuman (1972) who developed an analytical solution adapted to anisotropic unconfined aquifers, where K_r is the radial permeability parallel to the aquifer extension and K_z is the vertical permeability. Neuman method considers an unconfined and infinite aquifer. When a constant discharge rate is pumped in a complete well, the water comes for one part from the storage in the aquifer and for the other part from gravitational drainage at the free surface. The Neuman solution, under abacus, gives reduced

drawdowns in an observation well located at a radial distance r from the pumping well, $s_{DN} = \frac{4\pi T}{Q}$ as a function of:

Reduced time $t_z = \frac{Tt}{Sr^2}$ for type A curves;

Reduced time $t_y = \frac{Tt}{S_y r^2}$ for type B curves;

where T is the transmissivity of the aquifer, S the storage coefficient, S_y the specific yield, t the time since the starting of pumping. The interpretation using this method consists in fitting the observed drawdowns on the abacus constituted by two types of curves: type A curve for early times and type B curve for later times. Both curves are characterised by the same parameter $\beta = \frac{r^2 K_D}{b^2}$, which is a function of the permeability anisotropy $K_D = \frac{K_z}{K_r}$, the thickness of the aquifer b and the distance r between the observation and pumping wells.

The application of this method (Table 1a) to the observation wells IFP-1/1 and IFP-1/2 leads to the evaluation of transmissivities, storage coefficients (S) and specific yields (S_y). Very similar values are obtained in each observation wells for T_A and T_B showing the coherence of the interpretation of this pumping test using Neuman method. The values obtained for specific yields are consistent with other ones deduced both from indirect methods by Magnetic Resonance soundings (Wyns et al., 1995) and from direct methods by adjustment of water levels fluctuations using a global model (Engerrand, 2002).

Table 1a: Transmissivity and storage parameters obtained by adjustment of drawdown

Observation well	*Pumping well*	*r (m)*	T_A *(m²/s)*	T_B *(m²/s)*	T_A/T_B *(-)*	T_{AB} *(m²/s)*	*S (-)*	S_y *(-)*
IFP-1/1	IFP-1	28	1.76E-05	1.96E-05	0.90	1.86E-05	7.0E-05	1.7E-03
IFP-1/2	IFP-1	27.5	1.71E-05	1.76E-05	0.97	1.74E-05	3.7E-05	1.5E-03

T_A: transmissivity obtained by adjustment on type *A* curve, T_B: transmissivity obtained by adjustment on type *B* curve, T_{AB}: average of T_A and T_B.

The determination of K_D needs the knowledge of the aquifer thickness b. Flowmeter measurements during injection tests in eight wells of the basin have shown that the fresh basement does not contain any conductive fracture. It is namely the case in pumping well IFP-1. Thus, the top of this layer was chosen as the bottom of the aquifer. As for classical methods, the uncertainty on the value of r makes difficult any interpretation of drawdown in pumping wells. The results of this interpretation, included in Table 1b, show an anisotropy of the permeability tensor, in accordance with geological

observations: horizontal permeability is systematically higher than vertical one. This result is consistent with the observation of many horizontal fractures in dug wells.

Table 1b: Permeability and anisotropy degree determined at observation wells using Neuman method

Observation well	β *(-)*	*r (m)*	*b (m)*	K_r *(m/s)*	K_Z *(m/s)*	K_D *(-)*	$1/K_D$ *(-)*
IFP-1/1	1.00	28	21.8	8.5E-07	5.2E-07	0.606	1.7
IFP-1/2	0.20	27.5	21.8	8.0E-07	1.0E-07	0.126	8.0

HORIZONTAL FRACTURE INTERSECTING THE PUMPING WELL USING GRINGARTEN METHOD

Flowmeter vertical profile in IFP-9 (Maréchal et al., 2005) shows that only one fracture is conductive (at 29 metres depth) and is saturated during the whole pumping test. Moreover, the analysis by Neuman method arises the existence of hydraulic anisotropy due to the existence of horizontal fractures (Marechal et al., 2005). Thus, the method developed by Gringarten and Ramey (1974) for a vertical well intersecting a single horizontal fracture in an anisotropic aquifer (Fig. 2), applicable to the pumping well, is well adapted to the hydrogeological context of IFP-9 well.

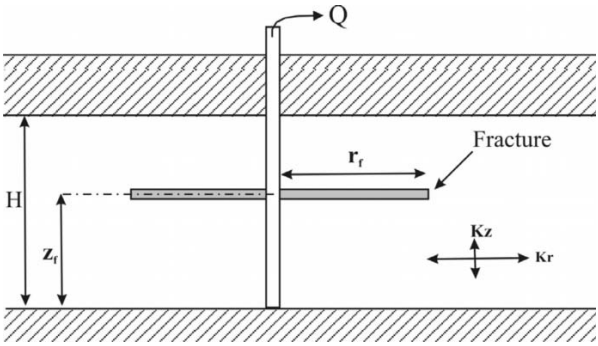

Figure 2. Schematic section of the Gringarten aquifer model (one single horizontal fracture).

The complexity of the analytical solution necessitates an interpretation through the adjustment of observed drawdown on theoretical curves (known as master curves) giving the reduced drawdown in a pumping well as a function of reduced time for various geometrical configurations represented by the parameter H_{DG}, when the fracture is located at the centre of the aquifer $\left(\frac{z_f}{H} = 0.5\right)$, with

$$t_{DG} = \frac{K_r t}{S_s r_f^2},\ s_{DG} = \frac{4\pi\sqrt{K_r K_z}\, r_f s}{Q} \text{ and, } H_{DG} = \frac{H}{r_f}\sqrt{\frac{K_r}{K_z}}$$

where z_f is the distance between the fracture and the bottom of the aquifer, and H the aquifer thickness. K_r, the permeability along the radial direction parallel to the fracture, can be interpreted as the permeability increased by the existence of the horizontal fracture. K_z, the vertical permeability, represents the matrix permeability, S_s the specific storage coefficient, t the time since the pumping started, r_f the radius of the horizontal fracture, s the drawdown and Q the pumping discharge rate.

Adjustment of observed drawdowns by Gringarten theoretical curves (Fig. 3) leads to high value of H_{DG}, suggesting a high permeability anisotropy. Difference between observations and theoretical curve at short times is attributed to well losses in the pumping well. Knowing the geometry of the case (i.e. the thickness H of the aquifer), supposing the distance z_f between the bottom of the aquifer and the fracture equal to half H and using the value determined by Maréchal et al. (2005) using Neuman method for S_s (9.7×10^{-5} at IFP-9), the hydrodynamic properties of the aquifer are evaluated (Table 2): K_r the horizontal permeability, K_z the vertical permeability and the radius r_f of the horizontal fracture. It is observed that the anisotropy of the aquifer is shown in the pumping wells while estimated fracture radius is coherent with field observations.

Table 2: Permeability, anisotropy degree and radius of the horizontal fracture determined at pumping wells using Gringarten method

	Known parameters					*Parameters determined by adjustment*				
Pumping Well	H (m)	*Fissure*	z_f (m)	$\frac{z_f}{H}$ (–)	S_s* (1/m)	H_{DG} (–)	r_f (m)	K_r (m/s)	K_z (m/s)	$\frac{K_r}{K_z}$ (–)
IFP-9	7.3	F9/1	4.0	0.55	9.7E-05	5	3.4	2.9E-05	5.2E-06	5.5

*S_s is the average of specific storage coefficient determined for each site using Neuman method at observation wells.

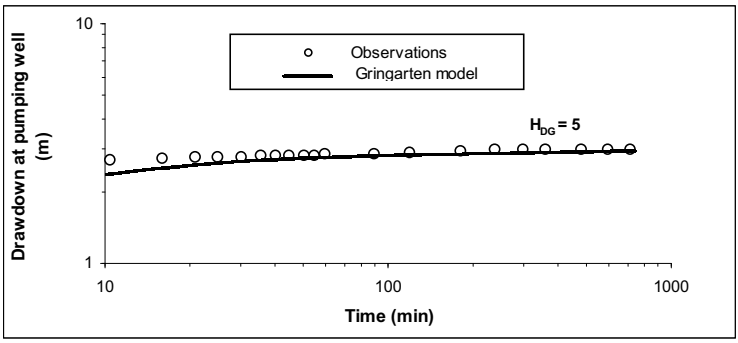

Figure 3. Adjustment of drawdown in pumping well IFP-9 using Gringarten theoretical curves.

DOUBLE POROSITY MODEL USING WARREN AND ROOT METHOD

Due to the fact that blocks separated by fractures compose hard rock aquifers, one method allowing describing such behaviour is proposed. This method derives from the conceptual double porosity model developed by Barenblatt et al. (1960). The concept (Fig. 4) supposes a confined aquifer constituted by two media: the fractures, transmissive but poorly capacitive, and the matrix, capacitive but poorly transmissive. Each medium is characterised by its hydraulic properties. K_f and S_f are the permeability and the storage coefficient of the fracture medium respectively and K_m and S_m are the permeability and the storage coefficient of the matrix respectively. The flow, radial to the pumping well, is only controlled by the transmissivity of fractures (flow from matrix to pumping well is nil, $K_f >> K_m$) and the fractures network drains the matrix where the flow is stationary (spatial variation of the hydraulic head is neglected). The expression of the drawndown is:

$$s(r, t) = \frac{Q}{4\pi T_f} F(u^*, \lambda, \omega);$$

$$u^* = \frac{T_f t}{(S_f + \beta S_m) r^2}$$

$$\lambda = \alpha r^2 \frac{K_m}{K_f} \text{ and}$$

$$\omega = \frac{S_f}{S_f + \beta S_m}$$

where λ is interporosity flow coefficient (dimensionless), $\alpha = 4n(n + 2)/l^2$ shape factor, parameter characteristic of the geometry of the fractures and aquifer matrix where n (dimensionless) is the number of fracture sets (n = 1, 2, 3; see Fig. 4), l the width of matrix blocs (in metre), β, a factor, for early time analysis equal to zero and for late time analysis equal to 1/3 (orthogonal system, n = 2, 3) or 1 (n = 1), r a radial distance from the pumping well, T_f the fractures transmissivity ($T_f = H K_f$; H: aquifer thickness), Q the pumping rate and t the time.

This method is well illustrated at pumping well IFP-16. The logarithmic derivatives of drawdowns in IFP-16 have the typical shape of a double porosity aquifer (Fig. 5a): (i) well effects and flow trough fractures to pumping well, (ii) transitional period: the "U" illustrates the contribution of the matrix flow through fractures to the pumping (note that in most cases the "U" of

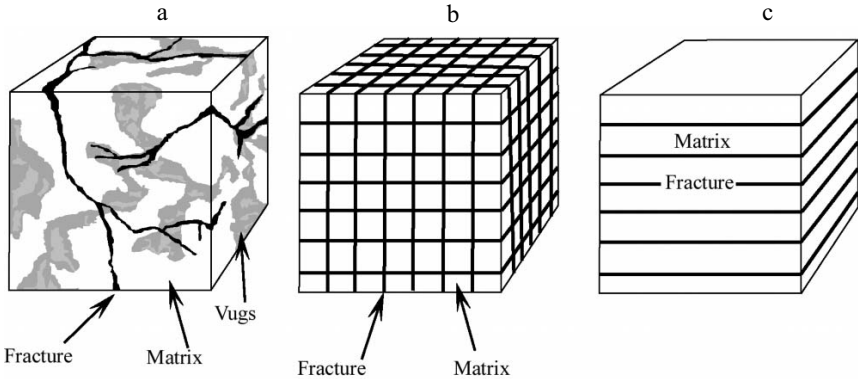

Figure 4. Double porosity model. (a): naturally fractured rock formation, (b) and (c) Warren and Root idealised fractured system; (b) orthogonal fractures network (n = 3) and (c) horizontal fractures network (n = 1).

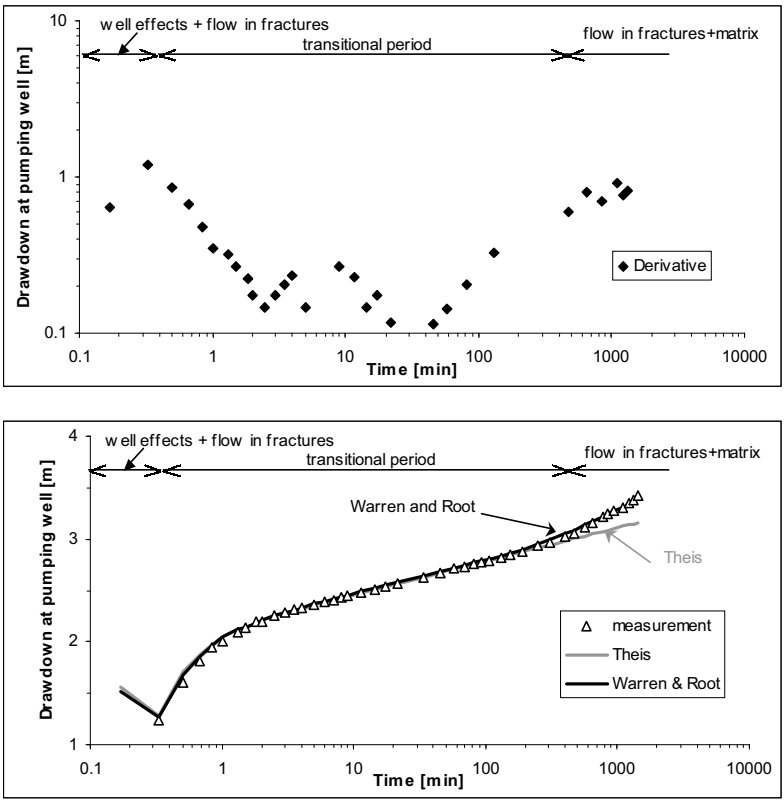

Figure 5. Interpretation at pumping well IFP-16 using a double porosity model. (a) logarithmic derivative at IFP-16 and (b) adjustment of drawdown using Warren and Root (double porosity) and Theis method.

derivatives is often masked by well effects) and (iii) flow in fractures and matrix. The application of Warren and Root method is then justified for this data set (Fig. 5b). For the interpretation, according to flowmeter measurements and geological observations, $n = 3$ and $l = 1$ m were used. The hydraulic conductivity of fracture network $K_f = 5.3 \times 10^{-5}$ m/s and that one of matrix $K_m = 7.76 \times 10^{-8}$ m/s. On Fig. 5b is also presented the interpretation using Theis method, which cannot properly interpret the drawdown after 470 min of pumping. This shows the limit of such models for hydraulic tests in hard rock terrain, and consequently the necessity to use more sophisticated models.

CONNECTIVITY AND FRACTIONAL DIMENSION FLOW USING BARKER THEORY

In fractured aquifer, flow properties are controlled by the fractures distribution. Barker model (9) takes account of the dimension of the flow, which results from the distribution and connectivity of the conductive fractures (Fig. 6). This theory is a generalisation of the Theis theory considering a radial flow, n-dimensional, into a homogeneous, confined and isotropic fractured medium characterised by a hydraulic conductivity K_f and specific storage S_{sf}. This Generalised Flow Model introduces the fractional dimension of flow, n, which characterises the variation law of flow section according to distance

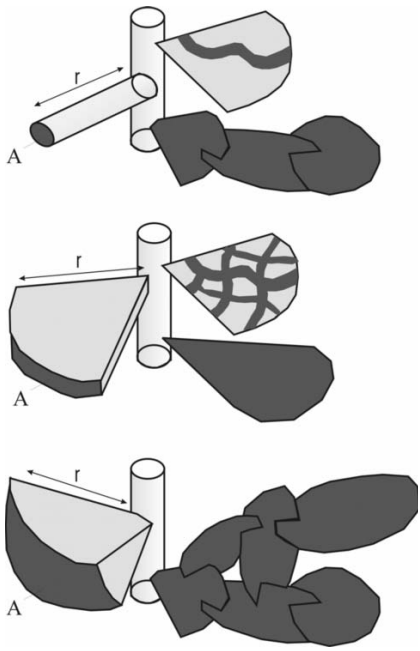

Figure 6. The concept of flow dimension (from Black, 1994).

from the pumping well. Values of n vary from 0 to 3, when $n = 3$ the flow is spherical (Fig. 6), cylindrical when $n = 2$ (that corresponds to Theis model) and linear when $n = 1$. Parameter n can take any values, entire or not, revealing the complex geometry of the flow. Expression of transient drawdown in the aquifer ($s(r,t)$) is given as following:

$$s(r,\ t) = \frac{Q r^{2-\mathrm{n}}}{4\pi^{\frac{\mathrm{n}}{2}} K_{\mathrm{f}} b^{3-\mathrm{n}}} \Gamma\left(\frac{n}{2} - 1, u\right), \quad u = \frac{S_{\mathrm{sf}} r^2}{4 K_{\mathrm{f}} t}$$

where $\Gamma(a,\ x) = \int_{\mathrm{x}}^{\infty} e^{-\mathrm{t}} t^{\mathrm{a}-1} dt$ is the incomplete gamma function, r the radial distance from the pumping well, Q the pumping rate and t the time.

This method has been applied to pumping well IFP-9 (Fig. 7). The generalised transmissivity $K_{\mathrm{f}} b^{3\text{-n}}$ is evaluated: 1.66×10^{-4} $\mathrm{m}^{1.5}/\mathrm{s}$. The flow dimension is equal to 2.5, and thus corresponds to an intermediate flow between cylindrical (like Theis) and spherical. The flow seems to be generated by one sub-horizontal fractures network, or only one single horizontal fracture

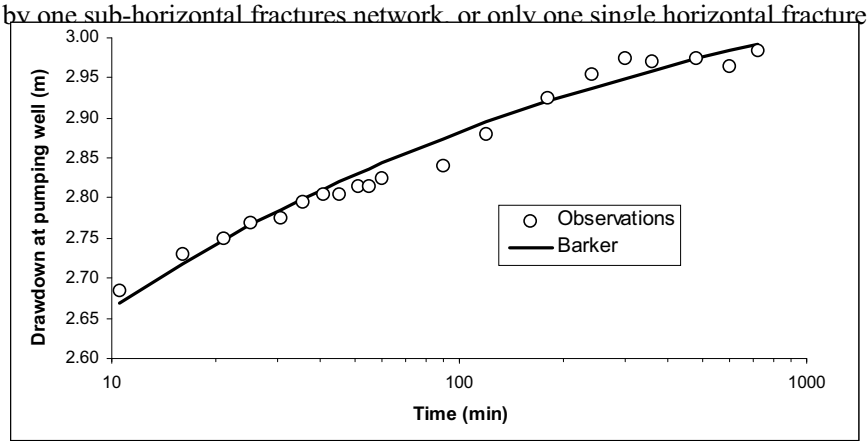

Figure 7. Adjustment of drawdown at pumping well IFP-9 using Barker theory.

as suggested by flowmeter tests, connected to a second fracture network probably sub-vertical to vertical.

CONCLUSIONS

Aquifer tests in hard rock terrain (granite, gneiss, basalt) make inadequate the use of classical techniques such as Theis or Jacob methods and need specific methods allowing taking into account the complexity of groundwater flow. The methods adopted in the present paper consider the heterogeneity and the anisotropy of the media: anisotropy of permeability (Neuman, 1975),

single horizontal fracture intersecting the pumping well (Gringarten and Witherspoon, 1972), double porosity behaviour (Warren and Root, 1963) or connectivity and fractional dimension flow (Barker, 1988). These methods are successfully applied to case studies in Archean granites and allow to characterise the complexity of flows through fractures. These techniques should be widely used by scientists and engineers for fractured aquifer characterisation (structure, anisotropy, heterogeneity) and evaluation (permeability, storage, water supply).

REFERENCES

Ballukraya, P.N., 1997. Groundwater Over-exploitation: A Case Study from Moje-Anepura, Kolar district, Karnataka. *J. Geol. Soc. India*, **50:** 277-282.

Barenblatt, G.E., Zheltov, I.P. and Kochina, I.N., 1960. Basic Concepts in the Theory of Seepage of Homogeneous Liquids in Fissured Rocks. *Jour. of Applied Math. (USSR)*, **24(5):** 1286-1303.

Barker, J.A., 1988. A Generalized Radial Flow Model for Hydraulic Tests in Fractured Rock. *Water Resour. Res.*, **24:** 1796-1804.

Black, J.H., 1994. Hydrogeology of Fractured Rocks - A Question of Uncertainty about Geometry. *Appl. Hydrogeol.*, **3:** 56-70.

Boulton, N.S. and Pontin, J.M.A., 1971. An Extended Theory of Delayed Yield from Storage Applied to Pumping Tests in Unconfined Anisotropic Aquifers. *J. Hydrol.*, **14:** 53-65.

Boulton, N.S., 1970. Analysis of Data from Pumping Tests in Unconfined Anisotropic Aquifers. *J. Hydrol.*, **10:** 369-378.

Engerrand, C., 2002. Hydrogéologie des socles cristallins fissures à fort recouvrement d'altérites en régime de mousson: Etude hydrogéologique de deux basins versants situés en Andhra Pradesh (Inde). Ph D thesis, University Paris VI, 2002.

Gringarten, A.C. and Ramey, H.J., 1974. Unsteady-state Pressure Distribution Created by a Well with a Single Horizontal Fracture, Partially Penetrating or Restricted Entry. *Trans. Am. Inst. Min. Eng.*, **257:** 413-426.

Gringarten, A.C. and Witherspoon, P.A., 1960. A Method of Analysing Pump Test Data from Fractured Aquifers. Percolation through Fissured Rock, Deutsche Gesellschaft fur Red and Grundbau, Stuttgart, 1972, T3B1-T3B8. *J. Appl. Math. Mech*. (Engl. Transl.), **24(10):** 1796-1804.

Karanth, K.R. and Prakash, V.S., 1988. A Comparative Study of Transmissivity Values Obtained by Slug Tests and Pump Tests. *J. Geol.Soc. India*, **32:** 244-248.

Maréchal, J.C., Wyns, R., Lachassagne, P. and Subrahmanyam, K., 2004. Vertical Anisotropy of Hydraulic Conductivity in the Fissured Layer of Hard Rock Aquifers due to the Geological Structure of Weathering Profiles. *Journal of the Geological Society of India*, **63:** 545-550.

Neuman, S.P., 1975. Analysis of Pumping Test Data from Anisotropic Unconfined Aquifers Considering Delayed Gravity Response. *Water Resour. Res.*, **11(2):** 329-342.

Neuman, S.P., 1972. Theory of Flow in Unconfined Aquifers Considering Delayed Response of the Water Table. *Water Resour. Res.*, **8(4):** 1031-1045.

Papadopulos, I.S. and Cooper, H.H., 1967. Drawdown in a Well of Large Diameter. *Water Resour. Res.*, 241-244.

Pradeep Raj, Nandulal, L. and Soni, G.K., 1996. Nature of Aquifer in Parts in Granitic Terrain in Mahbubnagar District, Andhra Pradesh. *J. Geol. Soc. India*, **48:** 299-307.

Uhl, Vincent, W. Jr. and Sharma, G.K., 1978. Results of Pumping Tests in Crystalline Rock Aquifers. *Groundwater*, **16:** 192-203.

Warren, J.E. and Root, P.J., 1963. The Behaviour of Naturally Fractured Reservoirs. *Eng. J.*, **3:** 245-255.

Wyns, R., Baltassat, J.M., Lachassagne, P., Legchenko, A., Vairon, J. and Mathieu, F., 2004. Application of SNMR Soundings for Groundwater Reserves Mapping in Weathered Basement Rocks (Brittany, France). *Bulletin de la Société Géologique de France*, **175(1):** 21-34.

8 Analyses of Aquifer Parameters from Different Hydraulic Tests and Their Scale Effect

J.C. Maréchal, Faisal K. Zaidi[1] and B. Dewandel

Hard Rock Aquifer Unit, BRGM, Montpellier, France
[1]National Geophysical Research Institute, Hyderabad, India

INTRODUCTION

Slug test is based on the principle of the analysis of the rate of water level fluctuation in a well after a certain volume of water (slug) has been suddenly added or removed from the well. However one limitation of conducting slug tests in this manner is that if the tests are being conducted for environmental monitoring purposes it is not advisable to inject or take out a certain volume of water in the well as it may disturb the ambient water quality or it may produce hazardous wastes. To overcome this problem, it is common to insert an iron cylinder of a known volume in the well. The length of the cylinder may vary from 1 to 1.5 metres with a cord tied to one end which facilitates the cylinder to be lowered quickly below the water level and later to be quickly raised above the water level. This instantaneous lowering and raising of the slug in the bore-well causes a cone of depression or suppression which can be related to a pumping or injection tests. The corresponding changes in water levels are recorded in the bore-well with the help of a water level recorder. With this record of the rate of recovery or recession of the water level, the transmissivity or the hydraulic conductivity of the borehole can be measured (Kruseman and de Ridder, 1994). Generally slug tests can yield good results of hydraulic conductivity for formations which have low permeability. For highly permeable formations, such as alluvial aquifers, slug tests cannot be very successful as the disturbance in water level created by the slug dissipates very fast in the formation and it is difficult to measure the corresponding water level changes. Of course the development of automatic water level recorders with the capability of taking regular

measurements every few seconds have solved the problem to a great extent even for highly permeable formations.

In the recent times where the hard rock aquifers have been subjected to over exploitation, there has been a considerable decline in the water level to a extent that the weathered portion is completely dry and the water is limited to the fissured/fractured zone. In such situations if pumping tests are carried out it will not represent the true aquifer parameter, as the zone of investigation will be reduced due to further drop in water level because of pumping. In these cases slug tests and injections tests can give a better picture of the aquifer parameter as the zone of investigation increases because there is an increase in water level when a slug is lowered in the bore-well during a slug test or when water is injected in the bore-well during the course of an injection test.

Flow meter tests when coupled with injection tests helped in determining the conductive fissure zones within the aquifer and thus help in the characterization of the hydraulic properties of the aquifer in the vertical direction.

SLUG TESTS

Context

Hydraulic parameters in saturated zone of aquifer are required to be determined for the purpose of modelling groundwater flows in Maheshwaram watershed. In this regard slug tests were carried out in all 25 IFP wells for the pre-monsoon period in 2002. The slug tests data were interpreted using Bouwer & Rice method to estimate the hydraulic conductivity in the wells. In addition, slug tests were performed on six IFP wells during 2001 and were interpreted using de Marsily method (for transmissivity and storage coefficient) and the same were reinterpreted using Bouwer & Rice method to compare the results.

To have a completed data base of the hydraulic conductivities of all the observation wells present in Maheshwaram, seven more slug tests were carried out in the newly drilled wells by NGRI during July 2003. All the tests were interpreted using Bouwer & Rice method.

Principle and Theory

The principle consists of analyzing the rate of water level fluctuation in the well after a certain volume ("slug") of water is suddenly removed/added from/to the well. Emerging/submerging a cylinder in the water brings about this sudden fluctuation (fall/rise) of water level. Instantaneously, it creates a cone of depression/pression, which corresponds to pumping/injection test. The chosen interpretation method is the one proposed by Bouwer & Rice (1976) for slug tests in unconfined aquifers with completely or partially penetrating wells. In addition to experiment measurements (water level

monitoring with time), parameters needed are basically in relation with the geometry of the well (length of casing, radius of well, water level in the well).

The calculation is based on the Thiem equation of steady state flow to a well. The equation of Bouwer & Rice (equation 1) gives K, which is calculated from recovery/drawdown of the water level in the well after suddenly removing/adding a slug of water from/in the well (Fig. 1).

$$\text{Bouwer \& Rice equation: } K = \frac{r_c^2 \ln(R_c / r_w)}{2L} \frac{1}{t} \ln \frac{y_o}{y_1} \tag{1}$$

K is the hydraulic conductivity [m/s], y is the vertical distance between water level in the well and equilibrium water table before the test [m]—y_0 at $t = 0$ and y_t at t, t is the time [s], R_e is the effective radius over which the head loss y is dissipated in the flow system [m], r_w is the well radius [m], r_c is the casing radius [m], L is the height of the portion of well through which water enters [m]. R_e only depends on the geometry of the well and the flow system. Pre-established curves allow evaluation of ln (R_e/r_w) using an abacus (Bouwer and Rice, 1976) giving parameters as function of L/r_w.

Field data should fit on a straight line when they are plotted as $\ln y_t = f(t)$. So the expression $(1/t) \ln y_0/y_t$ is the slope of the corresponding straight line.

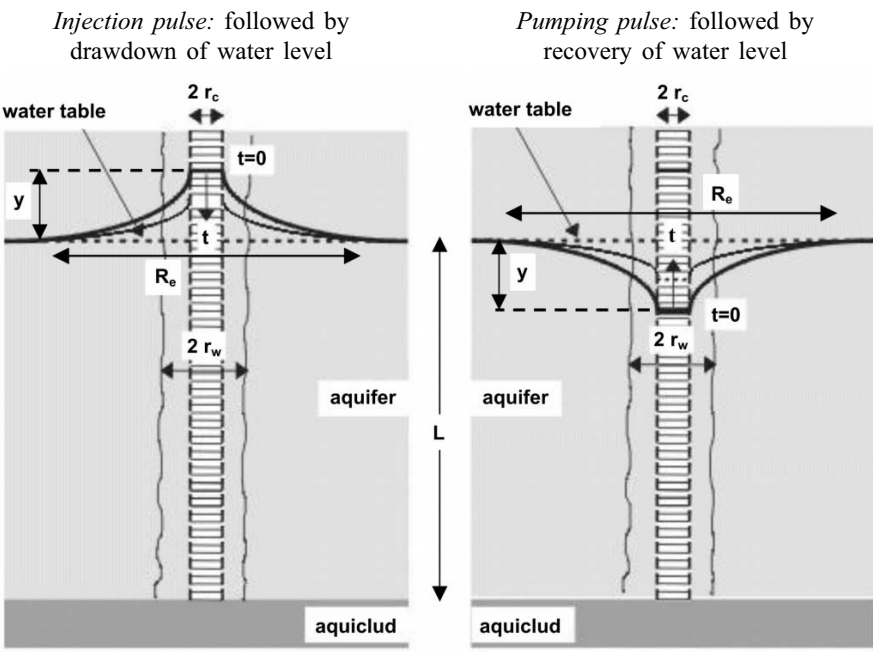

Figure 1. Injection pulse and pumping pulse.

Well Geometry and Aquifer Thickness

In Bouwer & Rice slug test method, the well and aquifer geometries are required for calculation of K (Fig. 2). Thus the aquifer thickness should be well known before analysis and interpretation of slug test.

In these slug tests campaigns, the aquifer geometry has been determined from the geological observations during well drillings. The bottom of the aquifer corresponds to the top of the massive granite layer. This is supported by flowmeter tests, which show that transmissive fractures exist only above the fresh basement (massive grey granite). For data processing, well thickness in massive grey granite (below aquifer zone) is not used for calculation of K. Water in this well portion is considered as "dead water".

The different well parameters required for the determination of the parameter R_e are L, H and D detailed in Fig. 2. L is the height of the portion of well through which water enters, H is the total height of the well in the aquifer and D is the aquifer thickness ($L \leq H \leq D$). In fact, there are four cases for the geometry of bore-wells. Both extreme cases are illustrated in Fig. 2. If the well is partially penetrating, H is inferior to D; if the well is completely penetrating, H is equal to D. In Maheshwaram, in most of the cases, the wells are fully penetrating thus $H = D$.

The value of L is dependent on the casing depth: if the casing reaches the water table, L is inferior to H. On the contrary, if the casing doesn't reach the water table, $L = H$.

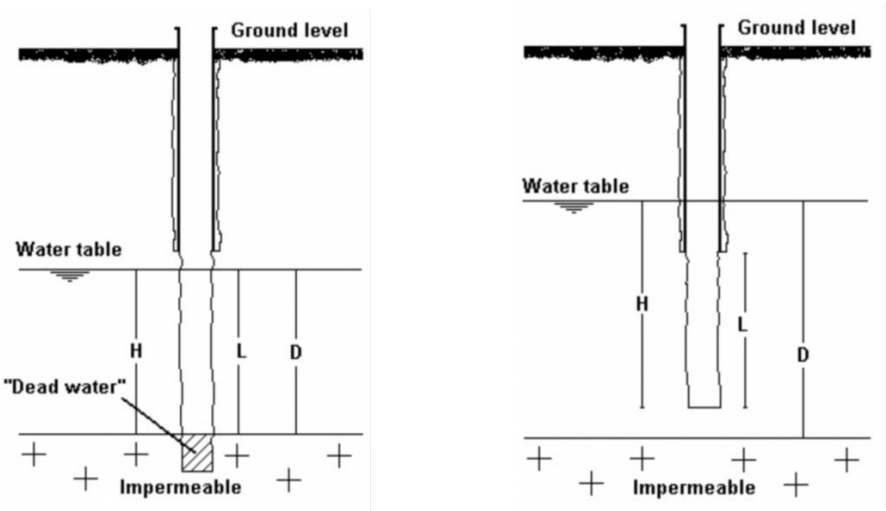

Figure 2. Different geometries of observation wells.

Field Procedure

A slug test cycle comprises two pulses: the injection pulse and the pumping pulse (Fig. 3).

Injection pulse: The rapid insertion of the slug in the bore-well causes a sudden increase in water level and it is followed by a gradual fall in order to reach the static water level.

Pumping pulse: Similarly when the slug is removed suddenly there is a sudden fall in the water level and then gradually the water level tries to regain its initial position.

The time taken to reach the initial water level during the injection and pumping pulses is a direct function of the permeability of the formation. Data have been recorded using Madofil (automatic water table recorders) and is coupled with manual measurements which help in calibration and checking of Madofil data.

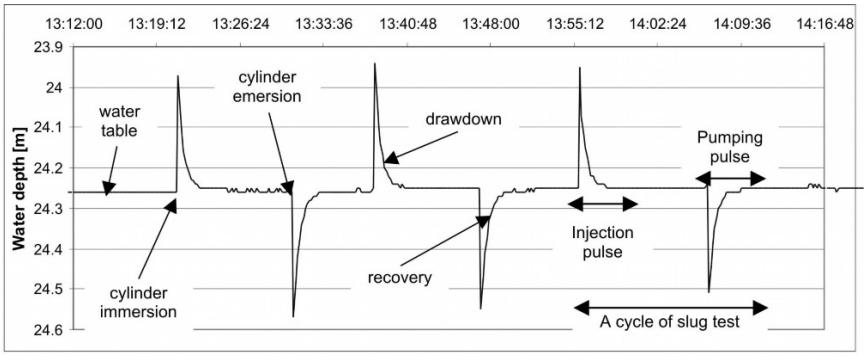

Figure 3. Madofil slug test data.

Data Processing and Interpretation

The recording of the drawdown and the recovery were verified to ensure the quality of data acquisition. Each test is a cycle of rise and fall in the water level and in the ideal condition, the water level should come back to its original position (making $y = 0$). Also the drawdown and recovery curves should be smooth without any noise.

The field records of water level through Madofil (the automatic water level recorder) have not shown any noise in recording but in a few cases, a definite trend of water level decline/increase (of the order of 10 cm) was observed which is much beyond the accuracy of Madofil (1 cm). This trend phenomenon is the consequence of pumping in farmer bore-wells or recovery in wells close to observation wells.

Thus a trend line was fitted on recorded values of water level and corresponding shift was made so that the water level at the end of the experiment reaches its original value. Figure 4 shows this correction graphically for a typical test.

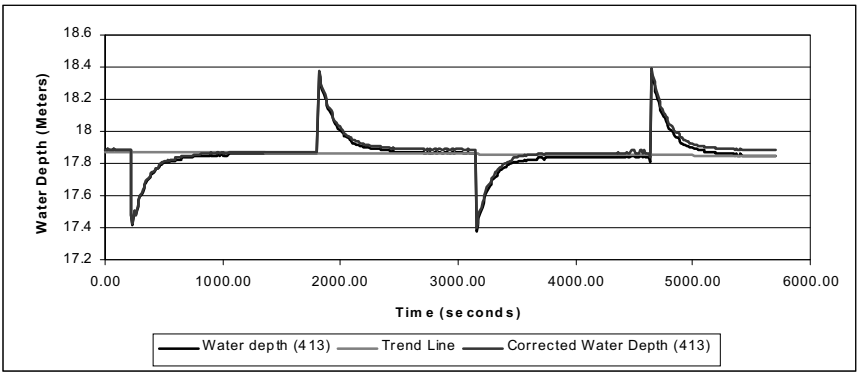

Figure 4. Recorded and corrected water level data.

Data recorded by Madofil are water depths (from well head) with time. Data processing consists of determining y (vertical distance between water level and static water level) for every recorded value. The plot of field data as $\ln y_t = f(t)$ is fitted by a straight line (Fig. 5). According to the equation of Bouwer & Rice (equation 1), hydraulic conductivity is calculated from the slope of this straight line and the geometry of the well.

For each test, two K's are determined: one average K injection and one average K pumping (respectively averages of all K's of injection pulses and all K's of pumping pulses) are distinguished. A geometrical average of all these K's gives a representative hydraulic conductivity in the well.

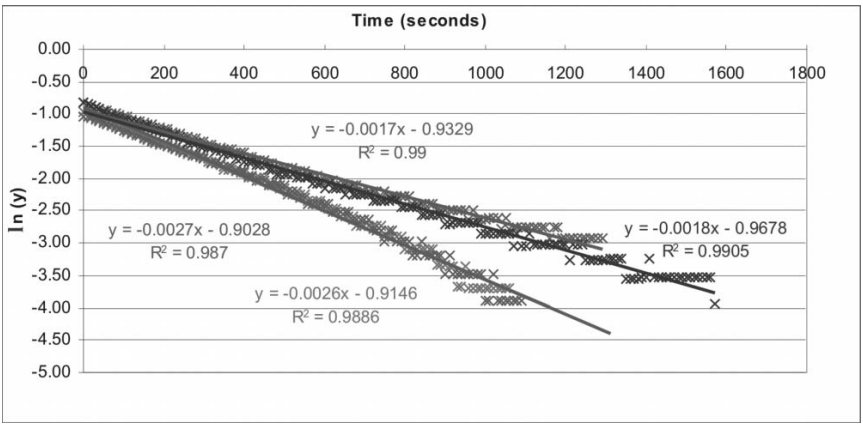

Figure 5. Plot of ln (y) versus t for OB 1-2 well.

INJECTION AND FLOWMETER TESTS

Injection Tests

With the aim of determining the hydraulic conductivity before monsoon with different methods and to characterize the hydraulic properties of the fractured aquifer in the vertical direction (weathered and fissured zones), a new hydraulic tests campaign was carried out between May and July 2002 in the Maheshwaram watershed. In the continuation of slug tests campaigns (March 2001 and March-April 2002), eight flowmeter tests have been coupled with injection tests of short duration. The 2003 campaign was carried out during monsoon period on the seven wells drilled by NGRI during that period.

Injection tests were interpreted according to Theis method with ISAPE software. Concerning flowmeter tests, the determination of hydraulic conductivities of the wells and each located fractures was based on the Dupuit equation.

Principle

Since flowmeter measurements require a water flow (pumping or injection test) into the bore-well, injection tests of short duration have been coupled with flowmeter tests. For each well, the field procedures were identical: the water was available from water tanker of 6 m^3. Water from the tanker is injected into the bore-well with a constant discharge and the experiment is carried out for a period of 25 to 75 minutes depending on the flow rate.

The main problem during these tests was to maintain a constant discharge. At the head of installation, the valve of water tanker wasn't reliable. Therefore, a drum, which controlled a permanent load, was installed in the middle of the water circuit. The obtained permanent load in the drum has given a constant discharge through the pipe inside the bore-well.

Water level in the bore-wells were recorded with the help of Madofil (automatic water level recorder) and with a follow-up of manual measurements for helping in calibration and checking up of the Madofil data. Each recording includes a buildup of water level during the injection of water and then a drawdown that begins when the injected flow is stopped.

Data Processing and Interpretation

Injection tests of short duration are interpreted by Theis method, which is based on the principle of unsteady state radial flow to the well, in confined or unconfined aquifer (if hydraulic head variations are low). The other assumptions include that the aquifer is homogeneous and isotropic with infinite extent and constant thickness.

Theis equation

$$h(r, t) = \frac{Q}{4\pi T}\int_0^u \frac{e^{\frac{-1}{u}}}{u}du\ ,\ u = \frac{4Tt}{r^2 S} \tag{2}$$

$$h(r, t) = \frac{Q}{4\pi T}W(u) \tag{3}$$

where $W(u)$ is the Theis' well function, i.e., exponential integral of order 1 ($E_1(1/u)$), which is known and tabulated. The "Theis curve" is drawn as a function of the parameter u. The h is hydraulic head [m], r: well radius [m], t: time [s], Q: pumping flow rate [m^3/s], T: transmissivity [m^2/s], and S: storage coefficient [-].

Storage coefficient cannot be evaluated when there is no observation well and if the test duration is short. In fact, the storage coefficient is more representative of the well effects and storage of fractures in the vicinity of the bore-well than the real storage of aquifer if the test is of a short duration. Thus, in the report, storage values are not presented. Concerning transmissivity, values are valid in the nearby area of the well and characterize locally the fractures that are intercepted by the bore-well.

Properties and Functions of ISAPE Software

One of the advantages of ISAPE software is to consider variable injection flow rates and depletion effect (the injection pipe empties back to the well once the injection is stopped) allowing a more accurate determination of transmissivity and storage coefficient.

Principle is to fit a theoretical curve, calculated from Theis well function (equation 3) on the experimental curve (Fig. 6) determined from the field. In most of the cases, transmissivity is determined from the buildup (during injection) and the drawdown (after injection), but when discharge control was difficult at the beginning of the test (variations of water level), the aspect of the buildup curve doesn't allow fitting the theoretical model and the fit on the drawdown has always been privileged.

In an easy way, injection tests have been interpreted like pumping tests transforming buildup in drawdown and drawdown in recovery; T and S values are not affected. The three required parameters to be controlled are the flow rate, the well radius and the buildup recording.

Hydraulic Conductivity

Injection tests help in determining the transmissivity of the aquifer, while flowmeter tests give a measure of the hydraulic conductivity. For having a detailed comparison the results of these two methods, hydraulic conductivity must be determined from results of injection tests, using the thickness of aquifer evaluated from geological observations during well drilling. The

bottom of the aquifer was chosen at the top of the massive granite layer. Flowmeter tests show that transmissive fractures only exist above this fresh basement.

Flowmeter Tests

The location of hydraulically conductive fissures was obtained using vertical profiles of flowmeter measurements. In order to increase the vertical extension of the investigated zone, the measurements are done during injection tests and not pumping. A water tanker is brought to the site and water is directed to a drum connected to the well through a pipe with a valve. A constant head is maintained in the drum thanks to overflowing water flow. This allows injecting constant flow rate. During the injection at constant rate Q when a pseudo steady state is reached, the flowmeter, which measures the vertical flow within the screen, is lowered close to the bottom of the bore-well and a measurement of velocity is obtained. The flow meter is then raised a few decimetres, another reading taken, raised another few decimetres, and so on. As illustrated in the lower portion of Fig. 6, the final result is a series of data points giving vertical discharge $Q(z)$ within the screen as a function of depth z. Just above the top of the screen the meter reading should be equal to Q, the steady injection rate that is measured independently on the surface with a water meter. The procedure may be repeated several times to ascertain that readings are stable.

As usually assumed, one considers the aquifer as a series of horizontal layers. The difference between two successive meter readings constitutes the net radial flow (q_{rj}) entering each layer of the aquifer:

$$q_{\mathrm{rj}} = \frac{Q_{\mathrm{i}+1} - Q_{\mathrm{i}}}{e} \tag{4}$$

where e is thickness of the layer.

Then, the Dupuit formula for a confined aquifer and horizontal flow to a well is applied to each layer, leading to the estimation of the layer hydraulic conductivity:

$$K_{\mathrm{i}} = \frac{q_{rj}}{2\pi\Delta h}\ln\frac{R}{r} \tag{5}$$

where Δh is the drawdown, R the investigation radius and r the well radius.

The aggregated permeability of the profile is obtained:

$$K_{\mathrm{p}} = \frac{\sum_{j=1}^{n} K_j e_j}{\sum_{j=1}^{n} e_j} \tag{6}$$

Interpretations of long duration pumping test carried out in the area have shown that aquifers are unconfined. Consequently, flowmeter conductivities, calculated for confined condition, need to be corrected. A correction factor is applied to the obtained conductivities in order that the aggregated conductivity of the well is equal to the global conductivity, K, using the Dupuit formula for unconfined aquifer for the injection tests.

$$K = Q\frac{\ln(R/r)}{\pi\Delta h(2\Delta h + H)} \tag{7}$$

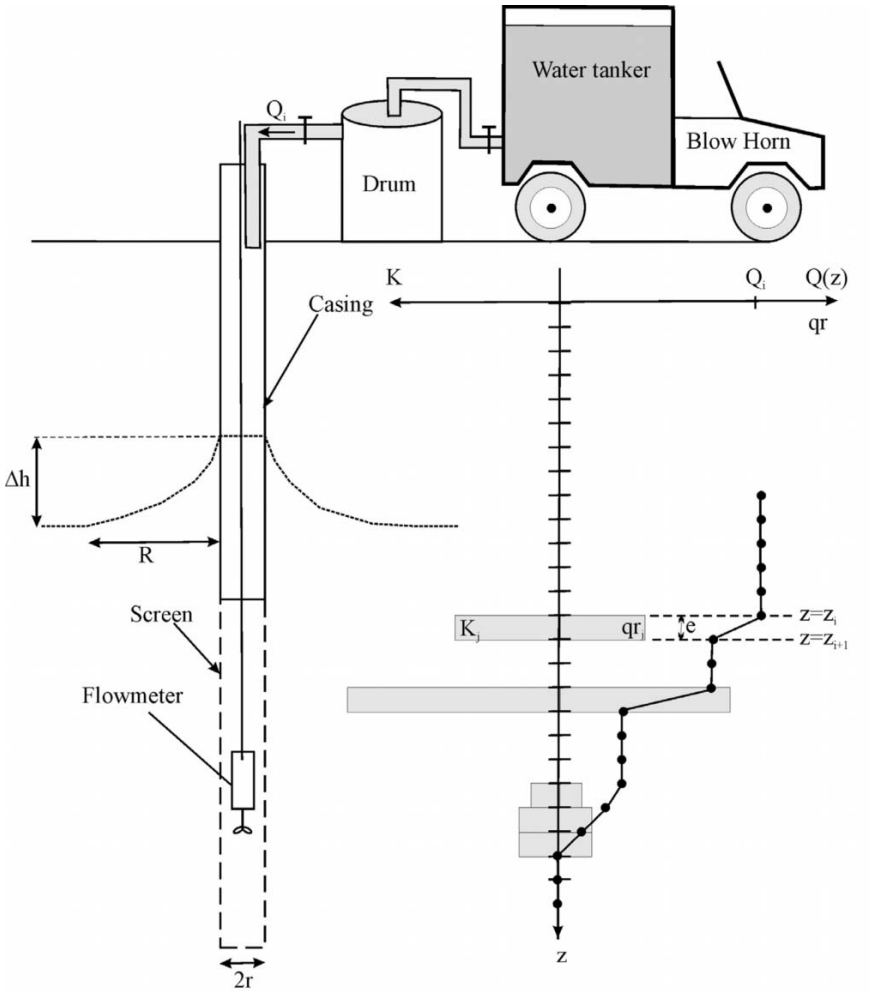

Figure 6. Injection and flowmeter tests.

REFERENCES

Ahmed, S. and Gupta, C.P., 1989. Stochastic Spatial Prediction of Hydrogeologic Parameters: Use of cross-validation in Krigings. *In:* Proc. of Internat. Groundwater Workshop, Hyderabad, India, Feb.-March, 1989 (Gupta et al. eds.), Oxford & IBH, Vol III, pp. 77-90.

APGWD, 1977. Studies on hydrologic parameters of groundwater recharge in water balance computations, Andhra Pradesh. Government of Andhra Pradesh Ground Water Department, Hyderabad, Research series no. 6, pp. 151

De Marsily, G., 1986. Quantitative Hydrogeology. Academic Press, Orlando.

FAO, 1990. Irrigation and Drainage Paper no. 56, Crop Evapotranspiration, Chapter 6.

Kruseman, G.P. and de Ridder, N.A., 1994. Analysis and Evaluation of Pumping Test Data, 2nd Edition, Publication 47, International Institute for Land Reclamation and Improvement, PO Box 45, 6700 AA Wageningen, The Netherlands.

Lachassagne, P., Wyns, R., Bérard, P., Bruel, T., Chéry, L., Coutand, T., Desprats, J.F. and Le Strat, P., 2001. Exploitation of High-yield in Hard-rock Aquifers: Downscaling Methodology Combining GIS and Multicriteria Analysis to Delineate Field Prospecting Zones, *Ground Water*, **39(4):** 568-581.

Monteih J.L., Huda, A.K.S. and Midya, D., 1989. Modelling Sorghum and Pearl Millet—Rescap: A Resource Capture Model for Sorghum and Pearl Millet. *In:* Modelling the growth and development of Sorghum and Millet. Research Bulletin no. 12. International Crop Research Institute for the semi-Arid Tropics, pp. 30-40.

NRSA, 2003. Land Use/Land Cover of Maheshwaram Watershed, Ranga Reddy district, Andhra Pradesh, Using Remote Sensing and GIS Techniques. Land Use Division, Land Use and Urban Studies Group, RS and GIS application area, National Remote Sensing Agency, Department of Space, Government of India, Hyderabad.

9 Upscaling of Slug Test Hydraulic Conductivity Using Discrete Fracture Network Modelling in Granitic Aquifers

Dominique Bruel, Faisal K. Zaidi[1] and C. Engerrand

Centre de Géosciences, Ecole des Mines de Paris
35 rue St Honoré, 77300 Fontainebleau, France
[1]NGRI, Uppal Road, Hyderabad-500 007, India

INTRODUCTION

The Indian sub-continent is underlain by hard rocks aquifers that are devoid of primary porosity and occupy more than two thirds of the landmass. These aquifers are highly vulnerable to pollution and resource depletion because they are the most heavily exploited by the population for agriculture, industry and domestic needs. These hard rocks aquifers, in general, consist of three layers: the weathered zone that can be considered as a porous media, the fissured/fractured zone, which is heterogeneous, and the fresh basement which is generally devoid of any openings unless and until some deep seated tectonic fractures are present. Aquifers in such geological settings are, therefore, of very variable quality, inherently to the heterogeneous nature of the fracture networks. Due to the adaptation of the latest drilling technology in India during the last few decades, ground water has been exploited on a large scale. But this uncontrolled exploitation of the resource has resulted in an alarming decline in water levels. The characterization of the flow and storage of ground water in these systems is a challenging task since flow and transport processes are very different from those occurring in the porous matrix. Furthermore there is an extremely high degree of contrast between the hydraulic conductivity of the fractures within short distances. An estimation of the groundwater resources is only possible through an estimation of flow and storage parameters in the fracture systems but it is anticipated that the responses of pumping tests performed in well field cannot be analyzed through classical aquifer-testing methods that assume a homogeneous aquifer.

STUDY AREA AND AVAILABLE DATA

For the above mentioned reasons, a joint Indo-French Collaborative Project on groundwater research was launched in 1999 (Ahmed & Ledoux, 1999) and a number of field investigations were conducted in a watershed in Maheswaram mandal, about 30 km south of Hyderabad, Andhra Pradesh, India. Some historical data of rainfall, water levels in wells and land-use were available from the Groundwater Department but much of the field investigations were jointly performed by the scientists involved in the project. The studies included the base-line data generation of well inventory, preparation of geomorphological maps based on aerial photographs and satellite imageries, geophysical investigations for the delineation of the extension of weathering in dykes, and across lineaments, mapping of the weathering profiles, drilling of wells at specific locations for regular monitoring of water levels, conducting hydraulic tests of short (30 minutes) duration to mid and long duration (4 to 6 hours, 18 hours), and the monitoring of a hydrometeorological station. Under the present project, about 25 piezometers have been drilled in the entire watershed to carry out the hydrological tests and for monitoring water levels and quality parameters. This considerable but necessary amount of data will form the basis for the preparation of a model so that future scenarios of water balance could be established for the management of the limited resource. This paper mainly deals with the results of slug tests and the related subjects. Figure 1 shows the set of normalized slug test responses which will be used later.

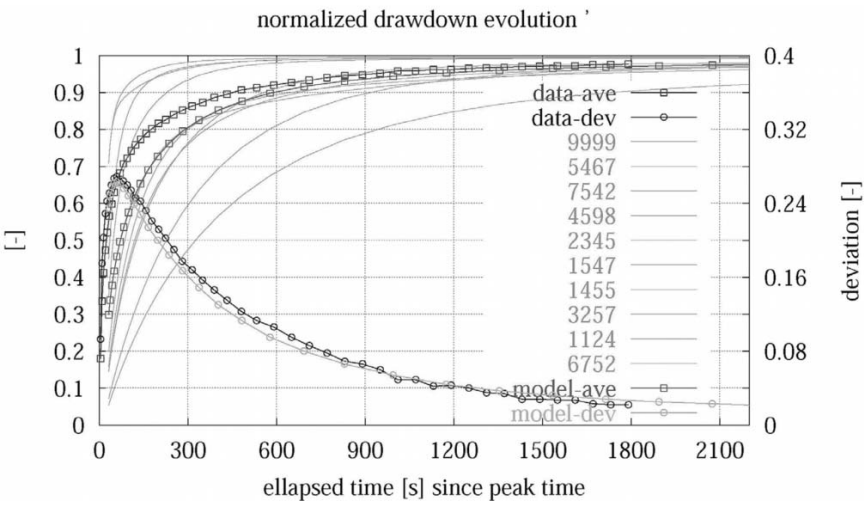

Figure 1. Slug tests responses, normalized versus the initial water level change. Superimposed is the average value observed at a given time and the standard deviation measuring the spreading of the responses at that particular time (three poor responses have been discarded).

THE DISCRETE FRACTURE NETWORK APPROACH

Conceptual Model

Discrete fracture network approaches have been developed in the past few years to handle the question of fluid and mass transport in fractured heterogeneous systems where discontinuities are likely to exist at many scales. Various conceptual approaches were proposed to describe the geometry of network of discontinuities, and capture the uneven nature of flow and solute transfer within a single fracture. 2D flow as well as channel models in random or structured network of planar fractures were investigated and tested against a variety of in situ experiments. Different softwares now exist with most of these capabilities (i.e. NAPSAC developed by AEA Tech in UK, FRACMAN package, developed by Goldberg ass.). The FRACAS software used hereafter is a similar product, gradually developed at the Paris School of Mines by Cacas et al. (1990) and Bruel et al. (1994), in the framework of National and European research programmes dedicated to nuclear waste insulation, to geothermal projects in hard rocks (Bruel, 2002), and to the estimation of hydrogeological properties in the vicinity of mined areas. Some of the capabilities of the code were recently tested in an international benchmark exercise (Rejeb and Bruel, 2001).

Geometry

The FRACAS modelling approach is based on the assumption that fluid moves through a rock mass within a system of interconnected fractures and that flow in the rock matrix is negligible by comparison. To alleviate the problems faced in the interpretation of fractured rock geometry the following are adapted for a better representation and interpretation of the aquifer characteristics.

The three-dimensional hydraulically conductive network of planar, disc-shaped fractures is generated within a rectangular block of rock based on stochastic descriptions of fracture density (Poisson distribution), fracture orientation (Fisher von Mises distribution), and fracture diameter (log-normal distribution) for specific fracture sets. Fractures may arrange into five types of fracture systems for modelling purposes.

1. Pure random network of disk shaped fractures.
2. Fisher type set of disk shaped fractures, that is a directional set.
3. Sub-vertical, with no preferential strike, set of disk shaped fractures.
4. Planar structures of deterministic location, can be infinite or with a finite elliptical extension, partly glued/non-persistent.
5. For an array of discs, with a fully deterministic description.

Flow Rule

Time-dependant analysis requires assumptions to be made concerning the form of fluid flow within the fracture network. The general form of fluid flow assumed in each fracture is based on an analytical solution, known as the "cubic law", for fluid flow between approximately parallel surfaces (Witherspoon et al., 1980). For ground water purposes at shallow depth, in unconfined or semi-confined situations, a linear form is used. Transmissivity is proportional to the permeability and to the fracture thickness. It is also assumed that fractures are filled with a porous material of storativity *S*. However transmissivities and storativities are modified to account for the effects of pressure changes between fracture surfaces when the fracture becomes desaturated. Thus, in FRACAS, the volumetric flux (m^3s^{-1}) in the x-direction through a length *l* (m) of a fracture has the form:

$$Q = \frac{-a^3 glF}{12\upsilon}\frac{dh}{dx} \tag{1}$$

where *a* is the hydraulic aperture (m) of the fracture, *g* is acceleration due to gravity (ms^{-2}), υ is the kinematic viscosity (m^2s^{-1}), dh/dx is the hydraulic head gradient driving flow through the fracture, and *F* is a dimensionless function dependent on effective pressure.

Analytical and empirical expressions for *F*, in which *F* decreases as the effective pressure becomes negative ($F = 1$ under saturated conditions) are presented in the literature. As an example we adopt the Van Genuchten formalism: the water content θ and the fluid pressure ψ are linked by equation (2), where the residual water content θ_r, α and *k* are adjustable parameters to be calibrated. θ_s is the water content at the saturation ($\psi = 0$) and l = 1-1/k. In this case the *F* factor is derived as a power function of the water content, according to the Brooks and Corey formulation (3).

$$\theta_e = \frac{\theta - \theta_r}{\theta_s - \theta_r} = \frac{1}{\left[1 + (\alpha\psi)^k\right]} \tag{2}$$

$$F(\psi) = \theta_e^v \tag{3}$$

The FRACAS geometry underlying the fluid flow law is illustrated here below. For this geometry, the volumetric flux from the centre of fracture *i* to the centre of fracture *j* may be approximated by equation (4), where the geometric mean fracture hydraulic conductivity k_{ij} (m^3s^{-1}) is defined as:

$$Q_{ij} = k_{ij}\frac{h_i - h_j}{L_i + L_j},\ k_{ij} = \frac{k_i k_j (L_i + L_j)}{k_j L_i + L_j k_i} \tag{4}$$

in which, based on equation (1), the fracture hydraulic conductivities are defined as:

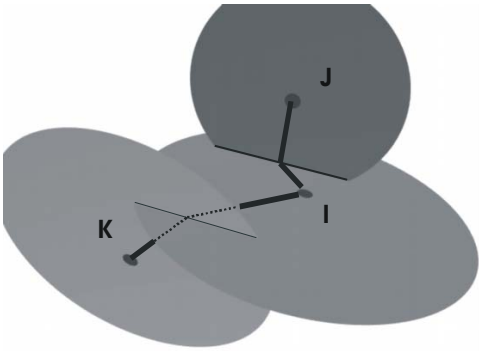

Figure 2. Geometry of the fracture network underlying the fluid flow law.

$$k_j = \frac{a^3 gly F_j}{12\upsilon}, \quad k_i = \frac{a^3 gly F_i}{12\upsilon},$$

If n_i fractures intersect fracture i, then the time dependent mass conservation equation for fracture i is given by:

$$\sum_{j}^{n_i} Q_y = V_i S_i \frac{dh_i}{dt}$$

The fracture volume term V_i (m^3) is:

$$V_i = \pi R_i^2 \alpha$$

and the specific storage of the S_i (m^{-1}) is a constant or, under unsaturated condition, a function of the water content:

$$S_i = \rho g \frac{1}{a} \frac{\partial \theta}{\partial \psi} \tag{5}$$

where R_i is the fracture radius (m) and ρ is the fluid density (kgm^{-3}).

In deriving the specific storage term, the rock stress has been assumed constant, such that changes are caused only by fluid pressure changes. Also, fluid compressibility is generally much smaller than fracture compressibility and, thus, has been neglected. The form of the term $d\theta/d\psi$, calculated at the centre of the fracture disc, depends on the assumed form of the relationship between the pore pressure and the water content that we use to describe the material infilling the fractures.

Modelling the Slug Tests Using the FRACAS DFN Approach

The objective of this section is to identify and calibrate a set of parameters suitable for modelling the observed spatial variability of the slug test responses, described in Fig. 1. Our working assumption is that the variability of the numerical responses resulting from statistically equi-consistent alternatives of the fracture network should be similar to the variability observed on the field. Therefore, our strategy will be (i) to built a set of fracture networks, using the same geometrical characteristics, (ii) simulate a transient hydraulic test, similar to a slug test, in each one of these networks and (iii) analyse the set of responses in terms of mean behaviour and deviation between the tested alternatives. This should be comparable with the in-situ corresponding curves in Fig. 1.

Determination of the Geometrical Fracture Network Parameters

Identification of Fracture Sets

Assuming that the rose diagram for the fracture orientations reflects the strike of sub-vertical fractures only, we define two fracture sets. First one representing sub-vertical fractures, striking to North +/– 30° and a second set, for the rest of the population. A third set is introduced for sub-horizontal fractures. There is much less constraint on this third set, since we only have visual indications in dry dug-wells and indirect indications of fluid occurrence in producing wells.

Densities of the Fracture Sets and Fracture Sizes

The determination of these parameters is highly empirical. At the scale of the visited excavated areas, there is no evidence of single sub-horizontal fractures that crosscut the domain. However, the sub-horizontal fractures may arrange into relay structures, therefore resulting at a larger scale in more continuous horizontal features. We assume that horizontal single elements have extensions ranging in between 5 and 10 m that is the size of a dug-well's side, with a mean value of 75 m. This in turn, indicates a mean fracture area of about 45 m^2. With a frequency of about 0.4 (i.e. one fracture in 2.5 m) we deduce the density, expressed in fracture centre/unit volume of rock, in the range of 0.4/45 = 0.0088. With a frequency of about 0.1 we end with a fracture density of about 0.0022. As a starting value for modelling purposes, the density of sub-horizontal fractures has been set to 0.005.

Concerning the sub-vertical structures, we arbitrarily assume a total density of about 0.01 and smaller sizes, ranging from 2 to 5 m. As the sub-vertical north striking fractures do not form the majority, we assume a density of 0.004 for this set. These numbers are starting numbers and will be subject to numerical tests to evaluate how sensible the model is to any significant variation.

The FRACAS model assumes a lognormal distribution for the fracture radius. Two parameters are required, a mean value μ and a deviation σ. The mean size in the real space, expressed in [m] is given by the expression $r = \exp(\mu + 0.5\,\sigma^2)$. The parameters used in the next sections are tabulated hereafter.

Table 1: Fracture Set Parameters

Fracture set	*Mean value*	*Deviation*	*Mean radius (m)*
Set 1: Sub-horizontal	1.20	0.5	3.75
Set 2: Sub-vertical, North-South	0.79	0.5	2.50
Set 3: Sub-vertical	0.79	0.5	2.50

Hydraulic Properties of the Different Sets of Fractures

Fracture Aperture, Fracture Permeability and Fracture Storativity

These parameters refer to single fracture and have to be calibrated. There is poor site specific information about realistic bracketing values, since no tests between packers are available, and since even the slug tests we are looking at refer to open hole sections that may intersect more than one fracture (2 to 5 intersections are frequently detected in the present numerical models). Fracture aperture are therefore set to 10^{-2} m, and we assume that the infilling materials, some weathering by products trapped in between the natural rough fracture walls, have a porosity of about 30%. We investigate fracture permeabilities ranging in between 10^{-2} ms^{-1} and 10^{-4} ms^{-1}. Dealing with storativity, we started with values close to that of confined aquifers, about 10^{-4} to 10^{-5}, and move towards values more appropriate to unconfined situations, i.e. some per cent.

Calibration Procedure and Model Outputs

Size and Shape of the Modelled Volume

The modelled volume of rock is a vertical cylinder, 50 m in diameter and 30 m in elevation. A vertical bore-hole is simulated along the vertical cylinder axis. The open hole section is 22 m, centered at the mid-height of the block. This value reflects the average aquifer thickness, which was observed on the 25 tested IFP wells.

Inner and Outer Prescribed Conditions at the Model Boundaries

The outer surface represents an open boundary where hydrostatic conditions prevail all the time. These conditions are applied at all the fractures (i.e. at the fracture centre in the numerics) that intersect this outer boundary. Along the central bore-hole is the inner boundary, where a transient chart is prescribed. Two phases are described. During the first two seconds, the hydraulic head at the well linearly increases from 0 to 0.49 m, the theoretical maximum value of the change in water level. Then from 2 to 2100 seconds, the well is subject to a 'no flow' condition and the head perturbation dissipates in the fracture network. The initial hydraulic head distribution is uniform and set to 0 m.

Calibration Strategy and Results

The scenario is applied and we present the period during which the pressure perturbation vanishes in the fracture network, in a normalized way, starting from 0 at the peak time and increasing to 1 as time increases. Series of 10 equi-consistent network alternatives are generated and we produce a set of

10 hydraulic drawdown curves. These curves are summed up into two curves, an average and a deviation curve respectively that can be compared to those derived from the *in situ* measurements. The first point is try to simulate the spatial variability of the responses, and then try to match the average behaviour. Hereafter (Figs 3 and 4), we show some of satisfactory results obtained using the parameters listed in Table 2. Obviously there is no unique solution to the problem and we only suggest set of values that produce an acceptable fit to the data, qualitatively and quantitatively.

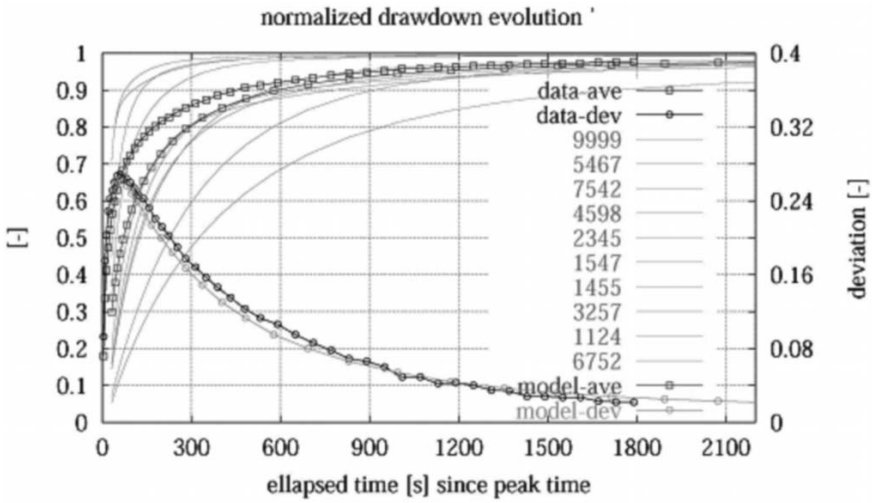

Figure 3. Calibration test, case 4.

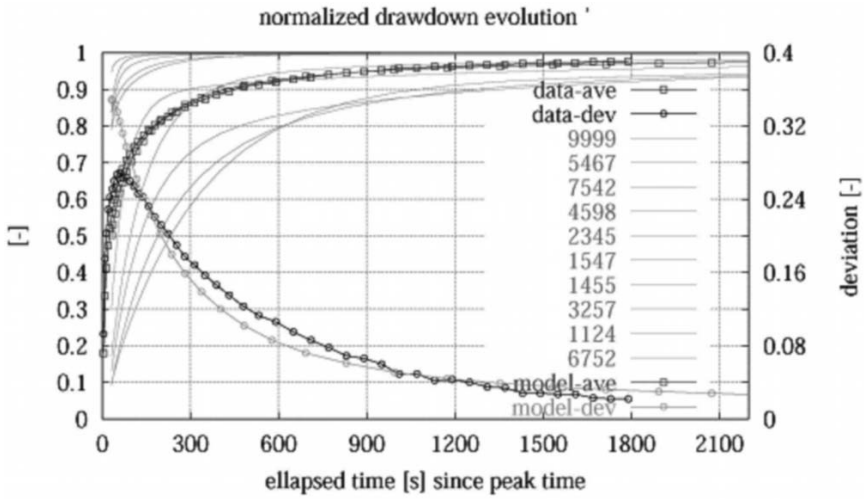

Figure 4. Calibration test, case 5.

Table 2: Parameters used to calibrate the slug test model, according to Figs 3 and 4

Calibration test	*Case 4*	*Case 5*
Density set 1 (frac/m^3)	0.004	0.0033
Density set 2 (frac/m^3)	0.004	0.0033
Density set 3 (frac/m^3)	0.006	0.005
K-1 (ms^{-1})	1.2×10^{-2}	1.0×10^{-2}
K-2 (ms^{-1})	1.2×10^{-2}	1.0×10^{-2}
K-3 (ms^{-1})	1.2×10^{-2}	1.0×10^{-2}
S-1(–)	1.0×10^{-3}	1.0×10^{-4}
S-2(–)	2.0×10^{-2}	8.0×10^{-3}
S-3(–)	2.0×10^{-2}	8.0×10^{-3}

UPSCALING THE TRANSMISSIVITY AND STORATIVITY PARAMETERS

Objectives

The upscaling phase of this study consists in a numerical derivation of equivalent hydraulic parameters at a spatial scale greater than the one investigated by the slug tests. The aim is to evaluate properties at the scale of an elementary cell of a global hydrogeological model based on standard porous media theory. The set of calibrated parameters, at the local scale, will be directly used for this purpose.

Method

The method consists in simulating parallel flow through a square cell of varying size. The size of this elementary cell is set successively to 50 m × 50 m × 30 m and 100 m × 100 m × 30 m, the sides of which are parallel to east-west and north south directions. Such a cell is filled with fracture elements, with geometrical properties directly inferred from the previous calibration phase. The flow is established across the cell, by assigning a head gradient between two opposite faces, the two others remaining closed to flow. The head gradient can be applied along X axis and Y axis in two successive runs.

Because the hydraulic regime is calculated in transient conditions, the numerical experience has to last until a quasi steady state situation is reached. Practical numerical prescriptions are as follows:

Initial head distribution: 0 m
Initial head value at the inlet face: + 5 m
Initial head value at the outlet face: – 5 m
Duration of the simulation: two days

Equivalent Transmissivity

The results of the tests are obtained for the two directions. They are obtained as the averaged value of the results produced by five equi-consistent networks, in a statistic sense. The five independent responses for a cell of 50 m × 50 m × 30 m for case 4 are listed hereafter:

Table 3: Flow in X and Y directions based on the parameters used for calibrating the slug test model in Table 2

Alternative	*Seed number*	*Flow in X direction (l/s)*	*Flow in Y direction (l/s)*
1	7571	2.76	3.49
2	3317	2.25	2.66
3	4531	2.31	3.04
4	9999	2.35	2.59
5	5703	1.92	2.91
Mean Value	-	2.32	2.93

From the calculated mean flux value combined with the geometry of the block and the applied head gradient, we derive an equivalent horizontal transmissivity, for both directions.

Because the cell has a square shape, the transmissivity is directly given when dividing the flux, expressed in m^3s^{-1} by the head difference, expressed in m. In the East-West direction (resp. along X axis), we obtain $T_{XX} = 2.3 \times 10^{-4}\ m^2s^{-1}$ and in the North-South direction (resp. along Y axis), we obtain $T_{YY} = 2.94 \times 10^{-4}\ m^2s^{-1}$. Therefore the equivalent porous media is likely to be slightly anisotropic, with a factor T_{XX}/T_{YY} close to 0.8. An equivalent isotropic horizontal permeability would be about $8.7 \times 10^{-5}\ ms^{-1}$. For case 5, there is no connection at a big scale, $T = 0$.

Equivalent Storativity

To derive an equivalent storativity factor suitable for hydraulic calculations at the regional scale, the calibrated fracture storativities are combined, using the densities of the fracture sets as weighting factors.

Table 2 shows that, to fit the data, the storativities values for the horizontal fracture set are smaller than the one for the sub-vertical and vertical fracture set. This can be due to the fact that because of the geometry, the vertical fractures are more in unconfined condition than the horizontal ones. In that case, the storativity calculated for the vertical and horizontal fracture set is

more representative of confined aquifer and more near from a storativity value. The storavities calculated for the vertical and sub-vertical fracture sets are a 'mix' between a storativity and a specific yield coefficient. That is why the resulting storativity value (no unit) is calculated as following according to the set of horizontal fracture parameters:

$$S = e.\pi.S_{set1}.(d_{set1}.R^2_{set1} + d_{set2}.R^2_{set2} + d_{set3}.R^2_{set3}) \quad (6)$$

where d_{seti} = density, set i (centres/m^2), e = fracture thickness (m), R_{seti} = fracture radius, set i (m^2) and S_{set1} = horizontal fracture storavity (1/m) and falls within the range of 3.89×10^{-6}, case 4 (Table 2) and 3.22×10^{-7}, case 5 (Table 2).

CONCLUSIONS

Numerical calibration was performed following a trial and error process. Although the solution may not be unique, we end with a combination of parameters that provides the set of responses shown in Fig. 1 when simulating a slug-test in a random fracture network. Total fracture density is about 0.02 m^{-3}, 30% of the fractures being sub-horizontal. Sizes are ranging in between 1 and 10 m, fracture thickness is about 0.01 m and porosity of the infilling material is set to 30%. Calibrated fracture permeability is close to 10^{-2} m/s, while the fracture storativity lies in between 10^{-3} and 10^{-4}m^{-1}.

Using these numbers to evaluate the permeability tensor by simulating parallel flow in a 100 m × 100 m × 30 m cell, in two perpendicular directions successively, leads to equivalent permeabilities ranging from 5.0×10^{-6} to 7.3×10^{-6} m/s, with a mean value of 6.2×10^{-6}m/s. An anisotropy factor of 1.25 is found in favour of the North/South direction, as a result of the existence of a set of north-south sub-vertical fractures.

REFERENCES

Ahmed, S. and Ledoux, E., 1999. Optimal Development and Management of Groundwater in Weathered Fractured Aquifers, CEFIPRA IFCGR Project no. 2013-1, 21 pp.

Bruel, D., 2002. Impact of Induced Thermal Stress During Circulation Tests. *Oil & Gas Science and Technology Rev. IFP*, **57(5):** 459-470.

Bruel, D., Cacas, M.C., Ledoux, E. and de Marsily, G., 1994. Modelling Storage Behaviour in a Fractured Rock Mass. *J. of Hydrology*, **162:** 267-278.

Cacas, M.C., Ledoux, E., Marsily, G.de, Barbreau, A., Tillie, B., Durand, E., Feuga, P. and Peaudecerf, P., 1990. Modeling Fracture Flow with a Discrete Fracture Network: Calibration and Validation, 1. The Flow Model, *Water Resources Research*, **26(3):** 479-489.

Rejeb, A. and Bruel, D., 2001. Hydromechanical Effects of Shaft Sinking at Sellafield Site. *Int. J. Rock of Mech and Min. Sci. & Geom. Abstr*, **38:** 17-29.

10 Groundwater Balance at the Watershed Scale in a Hard Rock Aquifer Using GIS

J.C. Maréchal, L. Galeazzi and B. Dewandel

Water Department, Unit "Water Resources, Discontinuous Media"
BRGM, Montpellier, France

INTRODUCTION

The high stress on ground water due to abstraction of large quantities of water through pumping for irrigation threatens the sustainability of agricultural development. This is mainly the case in hot and dry areas such as Hyderabad where the aquifers are located in hard rocks.

Therefore, it is necessary to adapt the exploitation of ground water to its availability. For that purpose, it is indispensable to have suitable tools able to assess either the water balance of the aquifer or its renewable reserve.

In this paper, a methodology for water balance evaluation using Geographical Information System is presented and applied to a study case. The different flows from or to the aquifer are listed and analysed in order to present a final spatial groundwater balance. The study area is a watershed centred on the village of Maheshwaram in Ranga Reddy district, Andhra Pradesh, India. The piezometric map of the aquifer indicates water level depletion in areas with high concentration of pumping wells (Fig. 1).

COMPONENTS OF THE GROUNDWATER BALANCE

Flows are divided in two categories: in- and out-flows (Fig. 2). First ones are flows coming in the watershed. They are positive and contribute to the recharge of the aquifer. The second ones correspond to water leaving the aquifer and contribute to the discharge of the aquifer.

Percolation flow (*INF*) from the ground to the aquifer through the soils and rocks can be diffused (through the whole surface area), or can take place at various specific places through preferential flows in cracks or fracture zones and from specific structures such as water tanks, trenches, old brick

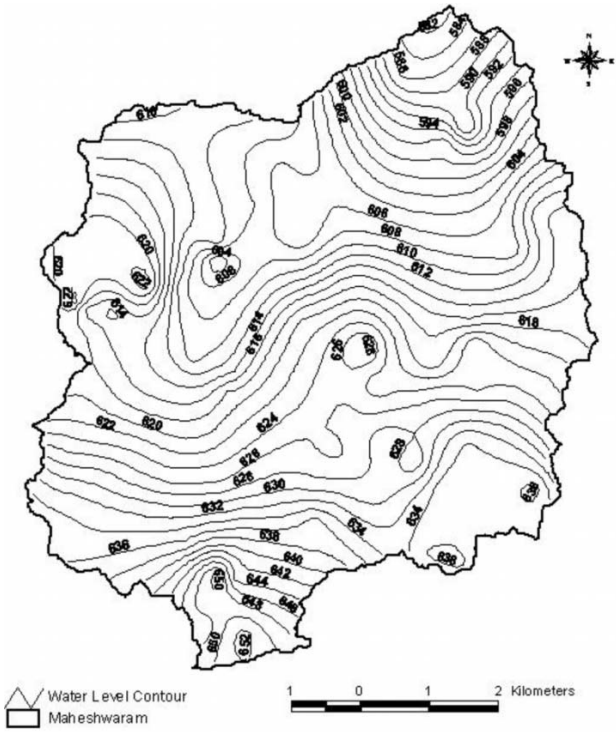

Figure 1. Piezometric map and pumping wells distribution in Maheshwaram watershed. Maheshwaram village (30 km south from Hyderabad) is at the centre of the map.

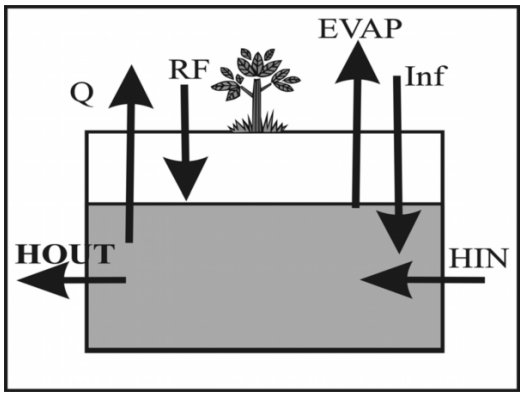

Figure 2. Simplified scheme of flow components.

factories, dug-wells. Return flow (*RF*) is the part of pumped flow that directly goes back to the aquifer. It is dependent on the irrigated crops type and the pumping volume. Horizontal In- (*HIN*) and Out-flows (*HOUT*) take place at the boundaries of the watershed only. They correspond to the exchanges of the watershed from outside and take place where the hydrological limit of

the watershed does not coincide with the hydrogeological limit of the aquifer comprised in the surface watershed. Pumping flow (Q) is the major negative component in such exploited basin. Water is mainly used for irrigation and domestic purposes. Evaporation (EVAP) from the groundwater table must be considered regarding the hot temperatures observed in this semi-arid area. Except when specially mentioned, the flows are expressed as rates in mm/yr.

The watershed is divided in a grid of 1324 cells of 200 × 200 metres size. The flows identified above are evaluated in each cell, except for HIN and HOUT, which are determined only along the boundary of the basin.

Pumping Flow

A database of the bore-wells present in the watershed has been constituted. In all 929 wells were located using GPS portable and their discharge rate measured. Information about daily duration of pumping and annual number of pumping days was gathered in order to assess annual abstracted volume. The discharge rates are comprised between 5 l/min and 700 l/min. A map of annual abstracted volume is presented (Fig. 3). Pumping is concentrated in low zones, on flat areas allowing agriculture.

Horizontal Flow Across the Boundaries of the Watershed

Because weathering cover of the geological profile is dry and permeability of the fresh basement is very low, horizontal flows in these layers of the aquifer can be neglected. They are only located in the fissured layer of the aquifer.

These flows are dependent on horizontal permeability, thickness of saturated zone and local hydraulic gradient. They were computed using a finite differences model in order to obtain a spatial distribution on a grid of squared cells. Modflow model was used with a grid corresponding to the one selected for the balance. A kriged grid of the altitude of the summit of the fresh basement, constituting the bottom of the aquifer, was imported along with the grid of water table. Hydraulic potentials were imposed on the four limits of the modelled domain. Flows are computed during a few days with an average horizontal permeability $K = 0.87 \times 10^{-5}$ m/s determined by upscaling (from slug-test scale to 200 × 200 metres cells) using a DFN (Discrete Fractures Network) model, on the basis of 25 slug-tests. The results are presented in Table 1.

Table 1: HIN—Horizontal In-Flow, HOUT—Horizontal Out-Flow

Flow	*Pre-monsoon*	*Post-monsoon*
HIN (m^3/d)	1997	1637
HOUT (m^3/d)	176	686
HIN-HOUT (m^3/d)	1821	951

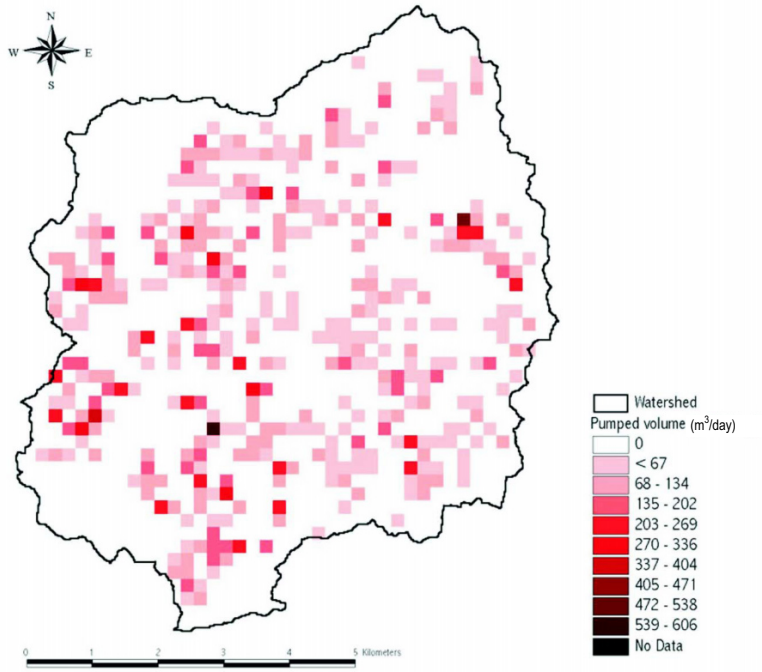

Figure 3. Abstracted volume (m^3/d) from the aquifer by pumping.

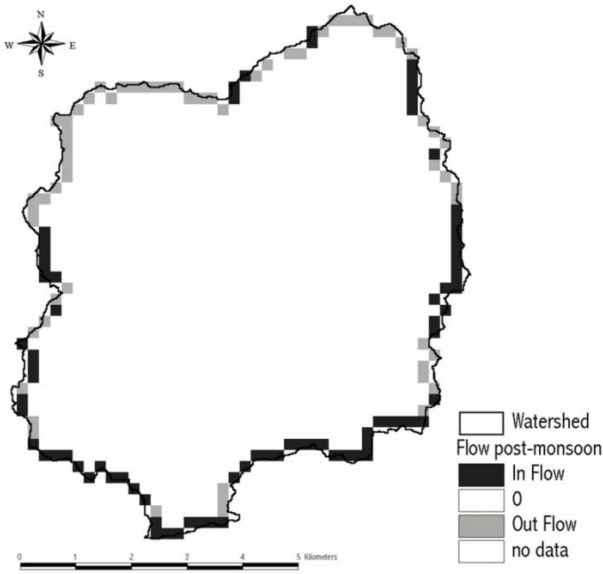

Figure 4. HIN and HOUT (m^3/d) at the boundaries of the watershed in November 2001.

In-flows mainly take place across the southern border of the watershed (Fig. 4) due to the regional south-north gradient linked to regional topographical slope. Other in-flows located west and east are due to the depletion of water table near the boundaries, due to pumping wells. The balance between horizontal in- and out-flows is finally positive due to the capture of water from outside. The balance is higher during pre-monsoon period according to higher water table depletion in such dry period.

Evaporation from Groundwater Table

This component is evaluated using the relation developed by Coudrain et al. (1998). Evaporation flux is expressed as an inverse power function of the piezometric depth below the soil surface, independently of the soil characteristics:

$$\mathrm{EVAP} = 71.9z^{-1,49} \tag{1}$$

where z is water table depth from soil (m).

It was calculated for both pre- and post-monsoon periods. Then, an average was determined. The value is about 1.7 mm/yr, very less compared to the other components of the water balance. This is due to high depth (18 m before the monsoon and 12 m after the monsoon) of depleted water table in the study area.

Return Flow from Irrigation

Most of the pumped water in the basin is used for irrigation, a large part of this volume returns back to the aquifer by direct infiltration in the irrigated lands. This can be written as: $RF = C \times Q$ with C = return coefficient ($0 < C < 1$), Q: pumping flow.

Because return coefficient is different from paddy fields to other crops, the global return coefficient is weighted by the repartition of crops:

$$A \times C = A_{\mathrm{RICE}} \times C_{\mathrm{RICE}} + A_{\mathrm{OTHER}} \times C_{\mathrm{OTHER}} \tag{2}$$

where A is the total irrigated surface, A_{RICE} = surface of irrigated paddy fields, A_{OTHER} = surface of other irrigated crops, C_{RICE} = return coefficient in paddy fields, C_{OTHER} = return coefficient in other crops.

The return coefficient for each crop is quite difficult to assess but some studies are available and mention that $0.55 < C_{\mathrm{RICE}} < 0.80$ for paddy fields. In granite areas encountered in Andhra Pradesh, the coefficient for paddy fields was evaluated to be 0.60 (APGWD, 1977). For other crops, the proposed coefficient is $C_{\mathrm{OTHER}} = 0.20$ (CGWB, 1998). With 79% of paddy fields and 21% of other crops, the obtained value is $C = 0.516$.

Percolation and Specific Yield

The satisfying knowledge of groundwater levels in the basin leads us to estimate the infiltration using the basic relationship between balance over a

given period and resulting water level fluctuations, better known as Water-Table Fluctuation Method (Healy and Cook, 2002):

$$\frac{\text{BAL}}{S} = \Delta h \tag{3}$$

where S = specific yield, BAL = balance result of the addition of all the components, Δh = water level fluctuation (same sign than BAL). This necessitates the accurate assessment of S at the catchment scale. This is done through the same way using (3) for a different period.

During the post-monsoon dry period (from November 2001 to June 2002), the percolation term can be neglected and the balance BAL becomes according to the budget defined by Schicht and Walton (1961), neglecting baseflow (groundwater discharge to streams or springs):

$$BAL_{\text{DRY}} = RF_{\text{DRY}} - Q_{\text{DRY}} - EVAP_{\text{DRY}} + HIN_{\text{DRY}} - HOUT_{\text{DRY}} \tag{4}$$

Including (3) in (4), it is obtained:

$$\text{S} = \frac{RF_{\text{DRY}} - Q_{\text{DRY}} - EVAP_{\text{DRY}} + HIN_{\text{DRY}} - HOUT_{\text{DRY}}}{\Delta h_{\text{DRY}}} \tag{5}$$

where all the terms are known (Table 2).

Table 2: Groundwater balance during dry period (all terms are expressed as rates in mm/yr)

RF_{DRY}	Q_{DRY}	$EVAP_{DRY}$	HIN_{DRY} - $HOUT_{DRY}$	$\Delta h_{DRY}(m)$	$S(-)$
69	135	1.0	4.9	–6.88	0.0089

The specific yield obtained is consistent with other approaches applied on this basin such as pumping tests (Maréchal et al., 2004) and global modelling (Engerrand, 2002).

Consequently, the same approach is applied to determine the percolation.

During the wet season (from June 2001 to November 2001), the BAL becomes:

$$BAL_{\text{WET}} = INF_{\text{WET}} + RF_{\text{WET}} - Q_{\text{WET}} - EVAP_{\text{WET}} + HIN_{\text{WET}} - HOUT_{\text{WET}} \tag{6}$$

Including (3) in (6), we obtain:

$$INF_{\text{WET}} \times \Delta h_{\text{WET}} \times S - RF_{\text{WET}} + Q_{\text{WET}} - EVAP_{\text{WET}} - HIN_{\text{WET}} + HOUT_{\text{WET}}$$

Application of this equation is illustrated in Table 3.

Table 3: Groundwater balance during wet period (flow terms are in mm/yr)

RF_{WET}	Q_{WET}	$EVAP_{\text{WET}}$	HIN_{WET}-$HOUT_{\text{WET}}$	Δh_{WET}(m)	INF_{WET}
49.6	96.1	0.7	3.5	+5.70	94.5

The percolation is quite coherent for such a hydrogeological context.

ANNUAL GROUNDWATER BALANCE

The annual groundwater balance was calculated from June 2001 to June 2002. The flows are easily determined using the following equation:

$$FLOW_{TOT} = FLOW_{WET} + FLOW_{DRY} \quad (7)$$

where $FLOW_{TOT}$ is the total flow along the year, the term $FLOW$ representing as well RF, Q, $EVAP$, HIN and $HOUT$.

Assuming that the percolation takes place only during the wet season (from June 2001 to November 2001 when the water levels are maximum):

$$INF_{TOT} = INF_{WET} \quad (8)$$

The annual balance on the whole watershed is described in Table 4.

Table 4: Groundwater balance during one hydrological cycle (flow terms are in mm/yr)

INF_{TOT}	RF_{TOT}	Q_{TOT}	$EVAP_{TOT}$	HIN_{TOT}-$HOUT_{TOT}$	BAL	Δh_{TOT}(m)
94.5	119	231	1.7	8.4	–10.5	-1.18

Considering the uncertainty on the components of the balance, this indicates that the balance is more or less in equilibrium. However, the total balance is a little bit negative, in accordance with an average water level decrease of about 1.18 metres on the watershed during this period, in spite of a normal monsoon (603 mm of rainfall). This clearly shows that, with such an abstraction rate on the basin, any bad monsoon as for example the monsoon of this year (2002), will induce a significantly negative balance followed by a depletion of water table.

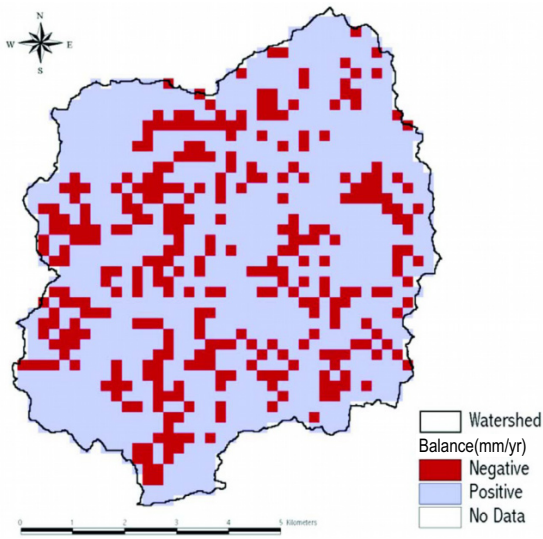

Figure 5. Spatial annual balance.

The map of water balance (Fig. 5) shows that negative balance areas only correspond to pumping areas due to the fact that pumping flows and return flows are respectively the main negative and positive components of the balance. In spite of the fact that they represent only 25% of the 1324 cells, the whole balance is negative.

CONCLUSIONS

The annual water balance of Maheshwaram watershed was calculated from June 2001 to June 2002. The global balance on the whole basin is a little bit negative, inducing a depletion of 1.18 metres for the water table in spite of the occurrence of a normal monsoon. The use of a Geographical Information System allows presenting a spatial budget.

The applied method gives very consistent results. It necessitates a good knowledge of pre- and post-monsoon groundwater levels. Thus, a network of observation of one hundred observation wells is necessary on this basin of 53 km^2 with monitoring twice a year. The accurate evaluation of pumping is also necessary for the determination of the balance and of the specific yield.

REFERENCES

APGWD, 1977. Studies on Hydrologic Parameters of Groundwater Recharge in Water Balance Computations, Andhra Pradesh. Government of Andhra Pradesh Ground Water Department, Hyderabad; Research Series no. 6, 151 pp.

CGWB, 1998. Detailed Guidelines for Implementing the Groundwater Estimation Methodology, 1997. Central Ground Water Board, Ministry of Water Resources, Government of India.

Coudrain-Ribstein, A., Pratx, B., Talbi, A. and Jusserand C., 1998. Is the Evaporation from Phreatic Aquifers in Arid Zones Independent of the Soil Characteristics? C.R. Acad. Sci. Paris, *Sciences de la Terre et des Planètes*, **326:** 159-165.

Engerrand, C., 2002. Hydrogéologie des socles cristallins fissures a fort recouvrement d'altérites en régime de mousson: Etude hydrogéologique de deux bassins versants situés en Andhra-Pradesh (Inde). PhD Thesis University Paris VI.

Healy, R.W. and Cook, P.G., 2002. Using Groundwater Levels to Estimate Recharge. *Hydrogeology Journal*, **10:** 91-109.

Maréchal, J.C., Wyns, R., Lachassagne, P. and Subrahmanyam, K., 2004. Vertical Anisotropy of Hydraulic Conductivity in the Fissured Layer of Hard-rock Aquifers due to the Geological Structure of Weathering Profiles. *Jr. Geol. Soc. of India*, **63(5):** 545-550.

Schicht, R.J. and Walton, W.C., 1961. Hydrologic Budgets for Three Small Watersheds in Illinois. Illinois State Water Surv Rep Invest 40, 40 pp.

11 Water Budgeting and Construction of Future Scenarios for Prediction and Management of Ground Water under Stressed Condition

Faisal K. Zaidi, Benoît Dewandel[1], Jean-Marie Gandolfi[1] and Shakeel Ahmed

Indo-French Centre for Groundwater Research, National Geophysical Research Institute, Uppal Road, Hyderabad-500007, India
[1]Water Division, Resource Assessment, Discontinuous Aquifers Unit BRGM, France

INTRODUCTION

The Indo-French Centre for Groundwater Research (IFCGR) has carried out intensive research for understanding the structure and functioning of the hard rock aquifers in granitic area by taking a small watershed at Maheshwaram, RR Dist of Andhra Pradesh and has developed a number of specific techniques during five years for aquifer characterization, groundwater balance both global and discretized including the technique of the "Double Water Table Fluctuation (DWTF)" (Maréchal et al., 2005), well suited for arid and semi-arid areas to improve the groundwater resource management in hard rock aquifers. This method has been implemented in the small pilot watershed of 53 km² area, a representative of the Southern Indian catchment in terms of overexploitation of the hard rock aquifers in semi-arid climate, cropping pattern, rural socio-economic context, etc. Between June 2001 and June 2004 three annual water budgets have been prepared. It is observed that both water balances for a "bad" and "good" monsoon could more or less be counterbalanced, the water balance is negative for a normal monsoon inducing a depletion of the Water Table at about 1 m/year due to consecutive deficit rainfall years. Due to this, in the long, medium, or short-term, drastic groundwater problems will inexorably occur if any realistic solution is not

found. Therefore, it is now essential that policy makers be equipped with accurate predictive tools for simulating the groundwater table in the coming years in order to better guide their future actions in total coherence.

The IFCGR has built up and developed a Decision Support Tool (DST) which can easily be used by everyone, and made under Excel Software interface which can be found everywhere on any computer. DST is now operational in Maheshwaram and can be applied to any other watershed with a similar context. The DST is designed for ground water scenarios under variable agro-climatic conditions, and focuses on the importance of changing cropping pattern and artificial recharge on groundwater levels. It is based on the Groundwater Budget method combined with the DWTF method. The DWTF method has been developed at the IFCGR and is specially applicable to hard rock aquifers in a semi-arid climate. For further details about this method, the readers are suggested to refer Maréchal et al., 2006.

The DST is composed of various active windows:

- the Groundwater budget method as memo,
- the various information about the studied watershed (geographical and geological contexts, land use, etc.) including all the data related to the components of the Groundwater budget and the different methodologies used,
- the ones for the input data related to the aquifer characteristics (specific yield, piezometric, surface area, etc.), the in- and out-flow balance, the irrigated crop characteristics (seasonal consumption, irrigation return flow for each crop, and for Rabi and Kharif season),
- the one to simulate the effect of different scenarios of rainfall on the groundwater levels,
- the one to simulate the effect of the changing cropping pattern and/or the artificial recharge on the groundwater levels,
- and a window for helping the user to build realistic scenarios through the support of socio-economic and socio-cultural data.

The DST enables to input rainfall scenarios for the coming years, calculate the corresponding recharge component, and simulate the consequences on groundwater levels at the watershed scale as well as the socio-economic consequences, like the impact on the population or the energy issues.

SCENARIOS USED IN DST

Considering no apparent climatic changes (same annual rainfall pattern since the last 20 years), two scenarios are presented in Fig. 1: 'current trend' with no change in both groundwater abstraction and cropping pattern, and 'present rate of agricultural development' where the irrigated area is increasing at a rate of ~1.3%/year according to FAO, 1997; cropping pattern remains also identical. In the first scenario, the mean groundwater resource limit, below which the aquifer cannot be exploited, will be reached by the year 2010 if

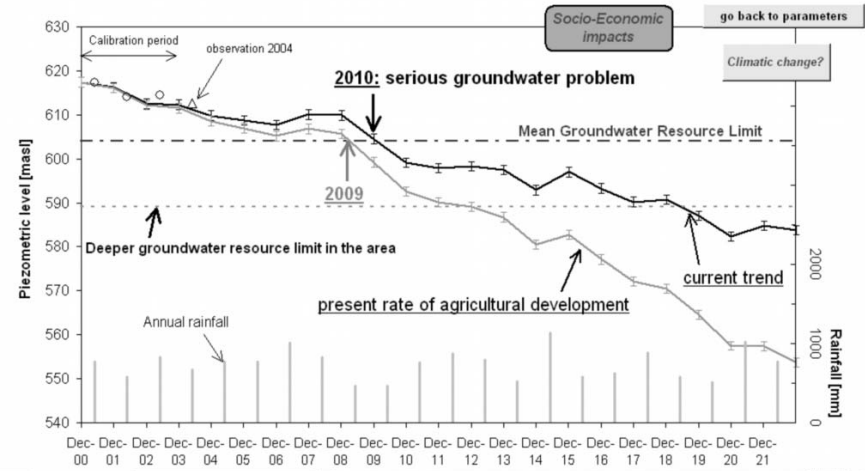

Figure 1. Simulation of water table levels in Maheshwaram watershed according to Rainfall scenario (substituting the 20 previous rainfall years for the coming 20 years).

the current pumping is maintained. This scenario will also entail the loss of about 50% of the bore-wells with accompanying serious socio-economic consequences that the reader can easily imagine (rural exodus, poverty, diseases, etc.). This limit will be reached by the year 2009 if the groundwater exploitation by pumping continues at the present rate of development. Unfortunately, recent information (complaints from the farmers and recent hydraulic tests) from the studied area is in accordance with the first scenario: strong decrease of the yield of numerous bore-wells and sometime drying-up.

Considering no change in both groundwater abstraction and cropping pattern, Fig. 2 presents simulations with two different climatic conditions: one with two consecutive weak monsoons (annual rainfall: for 2005 = 450 mm and for 2006 = 400 mm) and the other with two consecutive good monsoons (year 2005 = 1000 mm and year 2006 = 1100 mm). The simulated groundwater levels show that whatever the monsoon, the problems will occur sooner or later, and maybe faster than expected. Drying up of bore-wells are about 50% in 2006 in case of 'weak' monsoons and about 40% in 2014 in case of 'good' monsoons. These simulations as well as the ones presented in Fig. 1 show that immediate action is required.

Impacts of changing cropping pattern and artificial recharge on groundwater levels as well as groundwater budget clearly show that this catchment is overexploited. To avoid a dramatic situation in this area in the near future, decisions have to be taken to improve the groundwater management. As the area is overexploited, either the evapotranspiration of irrigated crops has to be reduced (decrease PG-RF) or/and additional artificial structures have to be implemented. However, the authors want to point out that building large

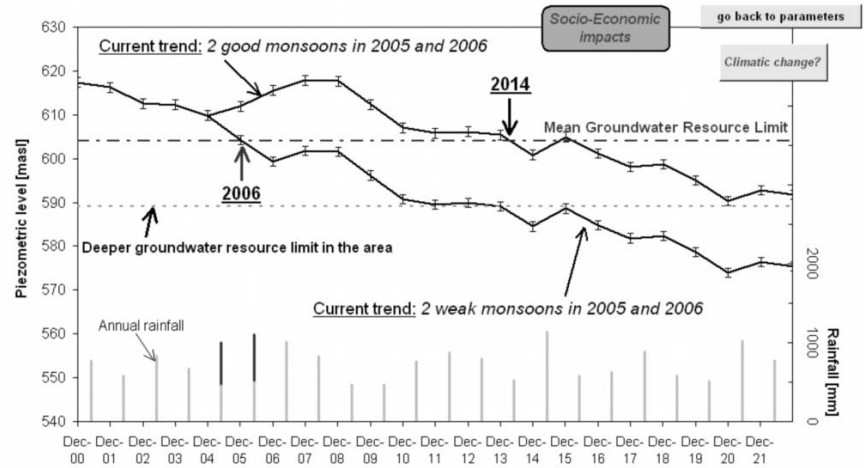

Figure 2. Simulation of water tables in Maheshwaram watershed according to Rainfall scenario (substituting the 20 previous rainfall years for the coming 20 years) and a 15-year action plan scenario (decreasing the rice surface area every two years by 5%, increasing vegetables and flowers surface areas by 10%, adding a package of solutions, 3 mm/year at the watershed scale).

number of rain harvesting structures (water tanks, dug-wells, etc.) may have serious negative impacts for the downstream areas.

One of the most interesting options of the developed tool is to assess the impact of both changing cropping pattern of irrigated culture scenarios and artificial recharge structure. DST enables the increase or decrease of surface area of irrigated crops present in the watershed (or other). In order to avoid non-realistic scenarios, which could not be accepted by the farmers because of profitability or cultural issues, the DST has been designed to enable the input of actions plan for several years under various socio-economic criteria.

Figure 3 presents two examples of scenario that considers a 15-year action plan scenario (from 2005 to 2019) where there is 6% decrease of the rice cultivated area every two years and at the same time 20% increase of vegetables and flowers cultivated area. In this scenario paddy field area is reduced by 40% and area of vegetables and flowers is increased by 30% at the end of the plan.

The first scenario (scenario 1) considers the changing cropping pattern only and in the second (scenario 2) artificial recharge structures have been added, the recharge rate being 2 mm/year at the watershed scale. This 2 mm/year may correspond to about 25 hectares of additional tanks or about 30 defunct dug-wells where run off is diverted (dug-well dimension: 10 × 10 × 13 m; supposed fully-filled up three times a year); moreover it might be the improvement of irrigation techniques or consequences of a public awareness programme (water conservation). While scenario 1 is just able to maintain the mean groundwater level above the mean groundwater resource limit,

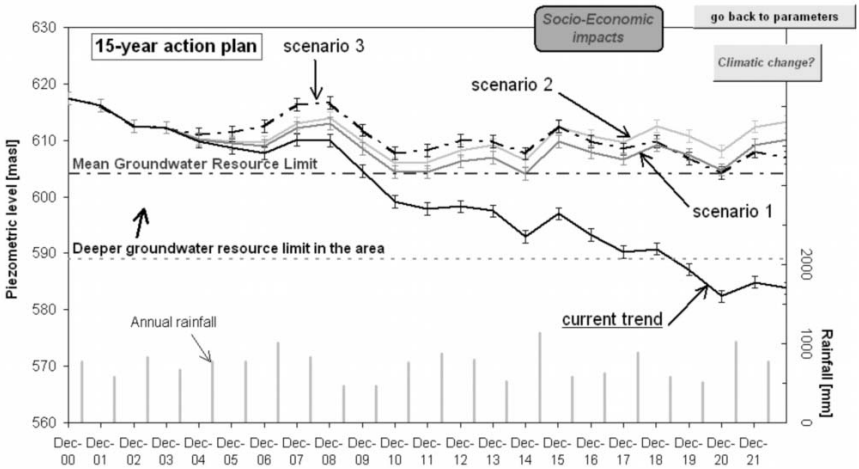

Figure 3. 15-year action plan scenario with changing cropping pattern and artificial recharge system - groundwater levels simulation. Scenario 1: changing cropping pattern - 6% decrease of the rice cultivated area every two years and at the same time 20% increase of vegetable and flower cultivated area. Scenario 2: scenario 1 + additional artificial recharge structures (+ 2 mm/year) (tanks, dug-wells, etc.). Scenario 3: artificial recharge only (dashed line) - 200 hectares of additional water tanks (efficiency of one hectare of tank: 0.1% of R).

adding some rain harvesting structures (scenario 2) now significantly maintained the water levels above. Drying up of bore-wells are also presented (Fig. 4); all scenarios clearly improve the current situation.

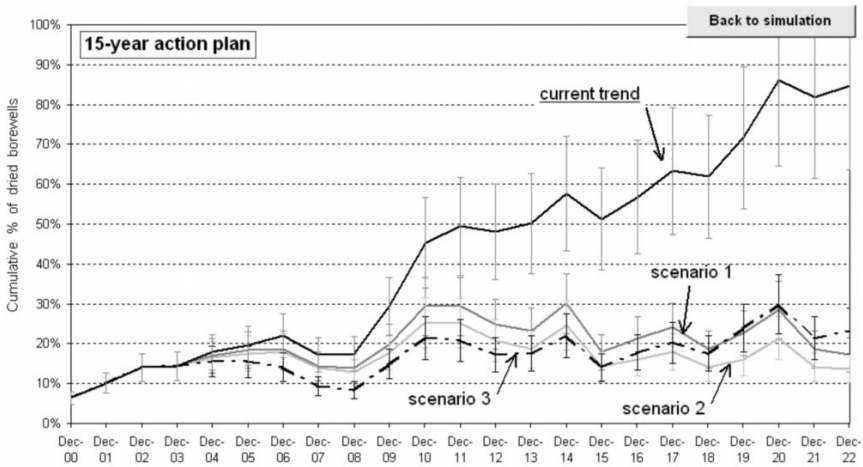

Figure 4. 15-year action plan scenario with changing cropping pattern and artificial recharge system - example of socio-economic impacts: drying-up of bore-wells. Results from the scenario 1, 2 and 3. The vertical bars depict the degree of uncertainty, which depends on the spatial variability of the aquifer thickness (about 25% of uncertainty).

Scenario 3 presents the results of a scenario where only rain harvesting structures are built to stabilize groundwater level decline (Fig. 3). However, about 230 hectares of tanks (or 270 dug-wells) are required. This non-realistic scenario shows that the artificial recharge cannot be considered as the only solution. One may question in such a semi-arid context the efficiency of groundwater management only based on such a solution.

One may conclude that in the present situation of Maheshwaram watershed, which is not an isolated case in the country and not an area recognized as an extremely or under overexploited area, reasonable solutions can be found by a package of solutions, i.e. combining changing cropping pattern, improving the irrigation techniques, new rain harvesting structure, etc. The water levels would be more or less maintained before getting back their original levels at the end of the plan; therefore this would induce a sustainable solution.

CONCLUSION

The DST is mainly based on changing cropping pattern solutions: that means trying to decrease the Real Evapo-Transpiration component of the water budget. It enables the increase or decrease of surface area of any crop present in the watershed. In order to avoid non-realistic scenarios, which could not be accepted by the farmers because of profitability or cultural issues, the DST has been designed to enable the input plan actions for several years under various socio-economic criteria.

As we have seen in Fig. 3, which considers a 15-year action plan scenario, decreasing the rice surface area every two years by 5%, at the same time increasing vegetable and flower surface area by 10%, and reasonably adding a package of solutions like the contribution of artificial recharge techniques to groundwater, or the improvement of irrigation techniques, or even a public awareness programme

This scenario shows that in any case the artificial recharge cannot be considered as the only solution. Its contribution to improve the situation is quite less than a changing cropping pattern solution. But a combination of both solutions could seriously improve the groundwater situation. Thus the only solution to get a sustainable groundwater management will come from a package of solutions.

The need of the hour is to adapt the exploitation of groundwater to its availability. Due to this, it is indispensable that policy makers be equipped with suitable predictive tools to better guide their coming actions.

The place of the DST (Fig. 5) is between policy makers and the experts, the experts helping them to build up realistic scenarios including the socio-economic aspects and the policy maker's own constraints as well. The results of simulations can be criticized, optimized or validated together, and it is only afterwards that the authorities can launch the actions. In addition, the package is entirely interactive and the scenarios could be built up by the

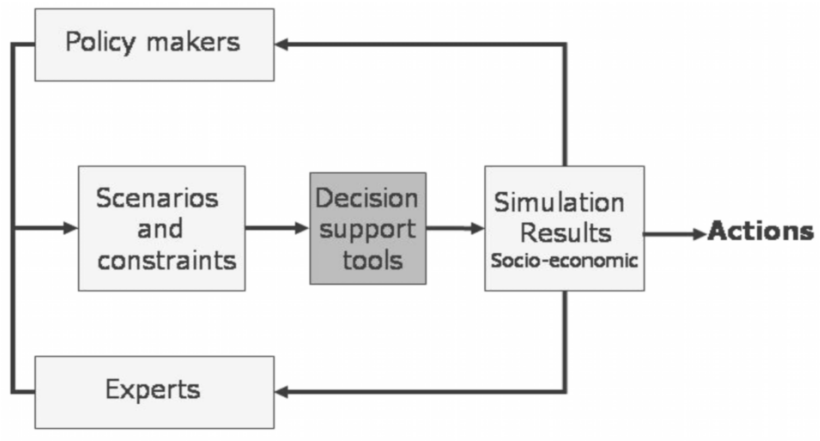

Figure 5. Scheme of assistance to policy makers.

farmers and the outcome be visualised. Thus the farmer's participation is ensured at one hand and on the other hand implementation of a particular scenario is also ensured as the scenarios are decided by mutual agreement rather than forcing it on the farmers.

REFERENCES

Acworth, R.I., 1987. The Development of Crystalline Basement Aquifers in a Tropical Environment. *Q. J. Eng. Geol.*, **20:** 265-272.

Ahmed, S., 2002. Groundwater Monitoring Network Design: Applications of Geostatistics with a Few Case Studies from a Granitic Aquifer from Semi-arid Region. *In:* Sherif M.M. et al. (eds.) Groundwater Hydrology, **2:** 37-57, A.A. Balkema Publishers.

APGWD, 1977. Studies on Hydrologic Parameters of Ground Water Recharge in Water Balance Computations, Andhra Pradesh. Government of Andhra Pradesh Ground Water Department, Hyderabad; Research Series no. 6, 151 pp.

Briz-Kishore, B.H., 1993. Assessment of Yield Characteristics of Granitic Aquifers in South India. *Ground Water*, **31(6):** 921-928.

CGWB, 1998. Detailed Guidelines for Implementing the Ground Water Estimation Methodology, 1997. Central Ground Water Board, Ministry of Water Resources, Government of India.

Chen, S-K., Liu, C.W. and Huang, H-C., 2002. Analysis of Water Movement in Paddy Fields (II) Simulation Studies. *Jour. of Hydrology*, **268:** 259-271.

Chilton, P.J. and Foster, S.S.D., 1995. Hydrogeological Characteristics and Water-Supply Potential of Basement Aquifers in Tropical Africa. *Hydrogeology Journal*, **3(1):** 3-49.

Coudrain-Ribstein, A., Pratx, B., Talbi, A. and Jusserand, C., 1998. Is the Evaporation from Phreatic Aquifers in Arid Zones Independent of the Soil

Characteristics? *C.R. Acad. Sci. Paris*, Sciences de la Terre et des Planètes **326:** 159-165.

Dewandel, B., Gandolfi, J-M., De Condappa, D. and Ahmed, S., 2006b. An Efficient Methodology for Assessing Coefficient of Irrigation Return Flow of Irrigated Cultures at Watershed and Seasonal Scale. Submitted to *Hydrological Process*.

Dewandel, B., Lachassagne, P., Wyns, R., Maréchal, J.C. and Krishnamurthy, N.S., 2006a. A Generalized 3-D Geological and Hydrogeological Conceptual Model of Granite Aquifers Controlled by Single or Multiphase Weathering. *Journ. of Hydrology*, in press.

FAO-Forestry, 1997. Aquasat: FAO's Information System on Water and Agriculture, available on *www.fao.org/ag/agl/aglw/aquasat/countries/india*

GEC, 1997. Report of the Ground Water Resource Estimation Committee; Ground Water Resource Estimation Methodology. Ministry of Water Resource, India.

Jalota, S.K. and Arora, V.K., 2002. Model-based Assessment of Water Balance Components Under Different Cropping Systems in North-West India. *Agricultural Water Management*, **57:** 75-87.

Maréchal, J.C., Dewandel, B., Ahmed, S., Galeazzi, L. and Zaidi, F.K., 2006. Combined Estimation of Specific Yield and Natural Recharge in a Semi-arid Groundwater Basin with Irrigated Agriculture. *Jour. of Hydrology* (in press).

Maréchal, J.C., Dewandel, B. and Subrahmanyam, K., 2004a. Use of Hydraulic Tests at Different Scales to Characterize Fracture Network Properties in the Weathered-fractured Layer of a Hard Rock Aquifer. *Water Resources Research*, **40:** W11508, 1-17.

Maréchal, J.C., Galeazzi, L., Dewandel, B. and Ahmed, S., 2003b. Importance of Irrigation Return Flow on the Groundwater Budget of a Rural Basin in India. *IAHS Red Book*, Pub. No. 278, 62-67.

Raj, P., 2001.Trend Analysis of Groundwater Fluctuations in a Typical Groundwater Year in weathered and fractured rock aquifers in parts of Andhra Pradesh. *Journal Geological Society of India*. **58:** 5-13

Raj, P., 2004. Classification and Interpretation of Piezometer Well Hydrographs in Parts of South Eastern Peninsular India. *Environmental Geology*, **46:** 808-819.

Rangarajan, R. and Athavale, R.N., 2000. Annual Replenishable Ground Water Potential of India - An Estimate Based on Injected Tritium Studies. *Jour. of Hydrology*, **234:** 38-53.

Schicht, R.J. and Walton, W.C., 1961. Hydrologic Budgets for Three Small Watersheds in Illinois, Illinois State Water Surv Rep Invest 40, 40 p.

Sukhija, B.S., Nagabhushanam, P. and Reddy, D.V., 1996. Ground Water Recharge in Semiarid Regions of India: An Overview of Results Obtained Using Tracers. *Hydrogeology Journal*, **4(3):** 50-71.

Uhl, V.W. and Sharma, G.K., 1978. Results of Pumping Tests in Crystalline-rock Aquifers. *Ground Water*, **16(3):** 192-203.

12 Applying Geostatistics: Basic Knowledge and Variographic Analysis with Exercises

P.S.N. Murthy, Tanvi Arora[1] and Shakeel Ahmed[1]

Ex-Head, Geostatistics Centre & Gen. Manager, NMDC Ltd., Hyderabad, India
(Presently) Adviser, Essar Ltd., Visakhapatnam, India
[1]National Geophysical Research Institute, Hyderabad-500007, India

INTRODUCTION

Any scientific study is based on a number of information on the system or processes through measurement of parameters defining one or more properties of the physical system. In most cases these parameters change their values in space and sometimes in time also and hence they are called variables. Rainfall, effective recharge, thickness of an aquifer, hydraulic head, transmissivity, permeability, storage coefficient, etc. are the examples in hydrogeology. Although, these parameters are often highly variables but this spatial variability is not purely random and, according to Matheron (1963), if measurements are made at two different locations, the closer the measurement points are to each other, the closer the measured values. These variables are given the name of Regionalized Variables (Re. V).

Although the characterization and estimation of a regionalized variable (Re.V.) can be made on a purely deterministic basis, it is more convenient and usual to introduce geostatistics in a probabilistic framework, bearing in mind that this artifact is only a tool for performing an estimation (Marsily, 1986).

In this article attempt has been made to include a few basic aspects that are often needed by a hydrogeologist to practise geostatistics and for others it will be a refreshing starting from basic definition and formulae of statistics, part of mathematics and algebra that are used.

BASIC STATISTICS AND MATHEMATICS USED

Data speak most clearly when they are organized. Much of statistics deals with the organization, presentation and summary of data.

Frequency Distribution

One of the most common and useful presentation of data sets is the frequency table and the histogram. A frequency table records how often observed values fall within certain intervals or classes. A typical data set is given in Table 1 (Isaaks and Srivastava, 1989).

Table 1: Values of a single variate data set observed on a regular grid.

81	77	103	112	123	19	40	111	114	120
•	•	•	•	•	•	•	•	•	•
82	61	110	121	119	77	52	111	117	124
•	•	•	•	•	•	•	•	•	•
82	74	97	105	112	91	73	115	118	129
•	•	•	•	•	•	•	•	•	•
88	70	103	111	122	64	84	105	113	123
•	•	•	•	•	•	•	•	•	•
89	88	94	110	116	108	73	107	118	127
•	•	•	•	•	•	•	•	•	•
77	82	86	101	109	113	79	102	120	121
•	•	•	•	•	•	•	•	•	•
74	80	85	90	97	101	96	72	128	130
•	•	•	•	•	•	•	•	•	•
75	80	83	87	94	99	95	48	139	145
•	•	•	•	•	•	•	•	•	•
77	84	74	108	121	143	91	52	136	144
•	•	•	•	•	•	•	•	•	•
87	100	47	111	124	109	0	98	134	144
•	•	•	•	•	•	•	•	•	•

The frequency table of the data set from Table 1 is given in Table 2.

Table 2 also shows, in its last column, the cumulative frequency distribution. For many Earth Science applications, such as pollution studies, the cumulative frequency above a lower limit is of more interest. Rather than recording the number of values within certain class, we record the total number of values below certain cut off. The second and third columns in the Table 2 can be represented graphically and they are called histogram and cumulative histogram respectively. The percent frequency and cumulative percent frequency forms are used interchangeably, since one can be obtained

from the other. The frequencies or the cumulative frequencies can be expressed in percentage. Incidentally, in the above example, since the total number of values is 100, the frequency and its percent are same. If a curve is plotted taking y-axis as the frequency, it is known as Probability Plot or Probability Distribution Function (PDF). A number of distribution function based on the shape of the curve are available. However, among the most common are the Gaussian/Normal and Log-normal distribution. Some of the estimation tools work better if the distribution of data values is close to a Gaussian or normal distribution.

Table 2: Frequency and cumulative frequency table

Class of values	*Number of observations/ Frequency*	*Cumulative Frequency*
0-10	1	1
10-20	1	2
20-30	0	2
30-40	0	2
40-50	3	5
50-60	2	7
60-70	2	9
70-80	13	22
80-90	16	38
90-100	11	49
100-110	13	62
110-120	17	79
120-130	13	92
130-140	4	96
140-∞	4	100

Summary Statistics

The centre of the distribution can be defined by mean, median and mode. The measure of spread can be defined as variance and standard deviation. The shape of the distribution is described by the coefficient of skewness and coefficient of variation. Taken together, these statistics provide feel of the data.

The mean, m, is the arithmetic average of the data values:

$$m = \frac{1}{n}\sum_{i=1}^{n} z_i \tag{1}$$

The number of data is n and z_1, ... z_n are the data values. The mean of the above presented 100 values is 97.55.

The median, M, is the midpoint of the observed values if they are arranged in increasing order. The median can easily be read from a probability plot. The mode is the value that occurs most frequently.

The variance, σ^2, is the average squared difference of the observed values from their mean and is given by:

$$\sigma^2 = \frac{1}{n}\sum_{i=1}^{n}\left(z_i - m\right)^2 \tag{2}$$

The standard deviation, σ, is simply the square root of the variance. This shows the spread of the values from the mean. The coefficient of skewness showing the symmetry of the distribution is defined as:

$$\text{Coeff. of Skewness} = \frac{\frac{1}{n}\sum_{i-1}^{n}\left(z_i - m\right)^3}{\sigma^3} \tag{3}$$

The coefficient of variation (CV) is a statistics that is often used as an alternative to skewness to describe the shape of the distribution. It is defined as the ratio of the standard deviation to the mean:

$$\text{CV} = \frac{\sigma}{m} \tag{4}$$

Some Remarks

The mean is quite sensitive to erratic extreme values. If the 145 ppm value in the above data set had been 1450 ppm, the mean would change to 110.6 ppm. The median, however, would be unaffected by this change because it depends only how many values are above and below it.

The variance, since it involves squared differences, is also quite sensitive to the extreme values. The variance of the 100 values is 688. Standard deviation is often used instead of the variance since its units are the same as the units of the variable.

The coefficient of skewness suffers even more than the mean and variance from sensitivity to erratic extreme values. A coefficient of variation greater than one indicates the presence of some erratic high sample values that may have a significant impact on the final estimates. The CV for the above data is 0.269, which reflects the fact that the histogram does not have a long tail of high values.

Bivariate Distribution

In the field of hydrogeology, due to scarcity of data, we always prefer to work on multivariable information. A typical data set for a two variable system is given in Table 3.

In the data set in Table 3, values of two variables are available at all the 100 locations. Values of the first variable are written above the circle (denoting the locations of measurement) and the values of the second variable are written below the circle in Italics. The basic statistics of the two sets of data are given in Table 4 for comparison.

Table 3: Values of a bi-variate data set observed on a regular grid

81	77	103	112	123	19	40	111	114	120
•	•	•	•	•	•	•	•	•	•
15	*12*	*24*	*27*	*30*	*0*	*2*	*18*	*18*	*18*
82	61	110	121	119	77	52	111	117	124
•	•	•	•	•	•	•	•	•	•
16	*7*	*34*	*36*	*29*	*7*	*4*	*18*	*18*	*20*
82	74	97	105	112	91	73	115	118	129
•	•	•	•	•	•	•	•	•	•
16	*9*	*22*	*24*	*25*	*10*	*7*	*19*	*19*	*22*
88	70	103	111	122	64	84	105	113	123
•	•	•	•	•	•	•	•	•	•
21	*8*	*27*	*27*	*32*	*4*	*10*	*15*	*17*	*19*
89	88	94	110	116	108	73	107	118	127
•	•	•	•	•	•	•	•	•	•
1	*18*	*20*	*27*	*29*	*19*	*7*	*16*	*19*	*22*
77	82	86	101	109	113	79	102	120	121
•	•	•	•	•	•	•	•	•	•
15	*16*	*16*	*23*	*24*	*25*	*7*	*15*	*21*	*20*
74	80	85	90	97	101	96	72	128	130
•	•	•	•	•	•	•	•	•	•
14	*15*	*15*	*16*	*17*	*18*	*14*	*6*	*28*	*25*
75	80	83	87	94	99	95	48	139	145
•	•	•	•	•	•	•	•	•	•
14	*15*	*15*	*15*	*16*	*17*	*13*	*2*	*40*	*38*
77	84	74	108	121	143	91	52	136	144
•	•	•	•	•	•	•	•	•	•
16	*17*	*11*	*29*	*37*	*55*	*11*	*3*	*34*	*35*
87	100	47	111	124	109	0	98	134	144
•	•	•	•	•	•	•	•	•	•
22	*28*	*4*	*32*	*38*	*20*	*0*	*14*	*31*	*34*

Table 4: Various statistics of the two data sets

Statistics	*Symbol*	*First variable V*	*Second variable U*
Population	n	100	100
Mean	m	97.6	19.1
Median	M	100.5	18.0
Mode		111.0	15.0
Standard Deviation	σ	26.2	9.81
Minimum	min	0.0	0.0
Maximum	max	145.0	55.0
Coeff. of Variation	CV	0.27	0.51

REFRESHING PRELIMINARY ALGEBRA AND MATHEMATICS

A few equations and expressions are reproduced below for refreshing and their applications in later part of the theory.

$$(x+y)^2 = x^2 + y^2 + 2xy \tag{5}$$

Similarly
$$(ax+by)^2 = a^2x^2 + b^2y^2 + 2abxy \tag{6}$$

Let us substitute x_1 for x and x_2 for y in the equation (5).

$$(x_1+x_2)^2 = x_1^2 + x_2^2 + 2x_1x_2 \tag{7}$$

Let us substitute λ_1, λ_2, x_1, x_2 for a, b, x and y respectively in the equation (6).

Then
$$(\lambda_1x_1+\lambda_2x_2)^2 = \lambda_1^2x_1^2 + 2\lambda_1\lambda_2x_1x_2 + \lambda_2^2x_2^2 \tag{8}$$

$(\lambda_1x_1 + \lambda_2x_2)$ can be written in the form of $= \sum_{i=1}^{2}\lambda_i x_i$ (9)

Then
$$(\lambda_1x_1+\lambda_2x_2)^2 = \lambda_1^2x_1^2 + \lambda_2^2x_2^2 + 2\lambda_1\lambda_2x_1x_2 = \sum_{i=1}^{2}\sum_{j=1}^{2}\lambda_i\lambda_jx_ix_j \tag{10}$$

This is because in the equation (10), when $i = j = 1$ the resulting term is $\lambda_1^2 x_1^2$; when $i = j = 2$ the term is $\lambda_2^2 x_2^2$; and when $i = 1, j = 2$ the term is $\lambda_1\lambda_2x_1x_2$. Similarly when $i = 2, j = 1$ the term $\lambda_2\lambda_1x_1x_2$ results.

Therefore, equation (10) can also be written as

$$\left(\sum_i \lambda_i x_i\right)^2 = \sum_{j=i}\lambda_i\lambda_jx_ix_j + \sum_{i\neq j}\lambda_i\lambda_jx_ix_j \tag{11}$$

The above formula can be simplified and written as

$$\left(\sum_i \lambda_i x_i\right)^2 = \sum_i\sum_j \lambda_i\lambda_jx_ix_j \tag{12}$$

This is an important derivation. Generally one is prone to confusion as to how the terms with j have come, when it is not there originally. This formula has got extensive application in statistics and geostatistics.

PROBLEM OF CALCULATING MEAN AND CONCEPT OF VARIOGRAM

Let us summarize again the most common statistics and their forms used in the development of geostatistical methods.

Expectation

If we can calculate the expected value of a distribution, it is known as Expectation and is denoted by E. It is also known as the first moment of the variable. Practically, one calculates the expected value of a variable using arithmetic mean keeping in mind that the number of values available can be approximated by $\propto$. However, we write an expected value of Z as follows:

$$m_z = E[z] \quad \forall z \tag{13}$$

Variance

The variance of the variable Z can be written in the following form:

$$\sigma_z^2 = E[(z_i - m_z)^2] \tag{14}$$

It is important to note that the variance in the general case is the variance of many realization available at a single location. However, the variance given by the equation (14) is the spatial variance of the variable and it does not depend on the location i.

Covariance

Similarly an expression for covariance of a variable Z between two points i and j in space can be given as:

$$C_{ij} = E[(z_i - m_x)(z_j - m_x)] \tag{15}$$

By definition the expected value m_z should not change by adding or removing one or a few values of the variable from the data. However, since we simply calculate an arithmetic mean, it will not be possible to ensure this. This means that a true mean or a true expected value can never be calculated from the data. Thus we can neither calculate a correct variance nor a correct covariance. We have to then introduce another hypothesis known as Intrinsic.

If we work on another variable y defined as:

$$y = z_i - z_j \tag{16}$$

i.e. the first order difference of the primary variable Z, then the expected value of the variable y can be shown to be 0 provided the variable Z has an unknown but constant mean m_z. Since the expected value of Y is 0, we need not calculate it from the data. If we calculate the variance of this new variable Y, we find the following expression.

$$\text{Var}\ (y) = E[(z_i - z_j)^2] \tag{17}$$

Though it is the variance of the new variable Y, it is a new function for the variable Z that does not depend on the location of points nor is affected by the value of m_z. This new function is called variogram of the variable Z between two points in space i and j and is denoted by

$$2\gamma_{ij} = E[(z_i - z_j)^2] \tag{18}$$

The variogram depends only on the separation vector between the two points i and j and not on the location of i and j. Here Z is called Intrinsic and more

precisely Intrinsic Random Function (IRF) of order zero because its first order difference has become stationary. Similarly if $(k + 1)^{th}$ order difference of a variable becomes stationary, the variable is called IRF-k, i.e. Intrinsic Random Function of order k. Most of the hydrogeological variables could be categorized as IRF-0 from the practical point of view. We will show in the subsequent text that the complete estimation theory can be developed using variograms and thus there is no need to calculate the mean.

STRUCTURAL ANALYSIS AND COMPUTATION OF COVARIANCE AND VARIOGRAM

As both the covariance and the variogram are the function of separation vector between two points i and j, values of separation vectors e.g., h_1, h_2 etc. are decided first such that

$$h = \left| x_i - x_j \right| \tag{19}$$

Depending upon the value of h, the data are grouped into pairs and some function as defined below are averaged to obtain a covariance (C_{ij}) or a variogram (γ_{ij}).

$$C^z(h) = \frac{1}{N_h}\sum_{i=1}^{N_h}\{z(x_i) - m_z\}\{z(x_i + h) - m_z\} \tag{20}$$

$$\gamma^z(h) = \frac{1}{2N_h}\sum_{i=1}^{N_h}\{z(x_i) - z(x_i + h)\}^2 \tag{21}$$

N_h is the number of pairs for a given h. It is usual to write $C(h)$ or C_{ij} or $C(x_i, x_j)$ etc. and correspondingly for the variogram also. If we consider equation (18), the expression in the equation (21) should be called semi-variogram. However, in practice only semi-variograms are used; hence for convenience we call it simply a variogram. It is now clear that in practice, we cannot calculate a true mean. Thus we prefer to work on variogram rather than covariance.

Properties of Covariance and Variogram

A relation between a variogram and a covariance can be established as follows if both the functions exist (i.e., the mean exist or the variable is stationary).

$$\gamma(h) = C(0) - C(h) \tag{22}$$

Here $C(0)$ is equal to the variance of the variable. Thus in case of stationary variables one function can be calculated from the other.

Behaviour of the Variogram for Large Separation Distance, *h*

As the distance h increases, $\gamma(h)$ increases. However, after a large distance, $\gamma(h)$ stabilizes around a constant value except sometimes when it increases

continuously. In case the variogram increases continuously with h, it is known as unbounded variogram and then no covariance exist. But if it stabilizes around a constant value (known as sill), it is called bounded variogram and both covariance and variogram exist [cf. equation (22)]. Unbounded variogram also shows the nonstationary nature of the variable.

Behaviour Close to Origin

Theoretically, $\gamma(h) = 0$ if $h = 0$ regardless of the type of variogram. However, often variograms exhibit a jump at the origin. This apparent jump is called nugget effect.

Anisotropy in the Variogram

Variogram can be calculated in different directions by taking the separation vector in particular direction. If variograms in different directions are different then the parameter is anisotropic but if variograms calculated in all possible directions are more or less same, the parameter can be considered as isotropic and so the variograms.

Parameters of the Variogram

A variogram function can be defined essentially by sill and range: sill is the constant value on the y-axis around which a variogram stabilizes after a large distance and range is the value at x-axis at which the variogram becomes constant or nearly constant. The sill value is usually very close to the variance of the variable. In addition, the sudden apparent jump near the origin that occurs in some cases is known as nugget effect. Also, the shape of the variogram between origin and the point of stabilization is different in different variables, which purely depends on its nature of variability. Depending on this shape, variograms are categorized into different type of variogram viz., *Linear, Spherical, Exponential, Gaussian, Cubic* etc.

Modelling a Theoretical Variogram

The variogram calculated from the field data is an erratic curve and known as an experimental variogram. It is not possible to use this variogram in the estimation purpose due to various reasons discussed later. Therefore, the curve of the experimental variogram is approximated by another theoretical curve with a defined mathematical expression. This smooth curve fitted to the experimental variogram is known as theoretical variogram. This fitting or modelling is performed in several ways mostly visual or using some form of difference between the two variograms but on a trial and error basis. Sometimes an automatic modelling has also been proposed but is not proved to be very useful. Mathematical functions for the common variogram type are given below. In all the expressions, c is the sill, a the range and h is the separation vector.

Model in h^2 including Linear Model

$$\gamma(h) = ch^{\lambda} \qquad \lambda<2 \tag{23}$$

If $\lambda = 1$ the variogram model is called Linear.

Spherical model

$$c\left[\frac{3}{2}\left(\frac{h}{a}\right)-\frac{1}{2}\left(\frac{h}{a}\right)^3\right] \qquad h \le a \tag{24}$$

$$c \qquad h > a \tag{25}$$

Exponential Model

$$c\left[1-\exp\left\{-\frac{h}{a}\right\}\right] \tag{26}$$

Gaussian Model

$$c\left[1-\exp\left\{-\left(\frac{h^2}{a^2}\right)\right\}\right] \tag{27}$$

Cubic Model

$$c\left[7\left(\frac{h}{a}\right)-8.75\left(\frac{h}{a}\right)^3+3.5\left(\frac{h}{a}\right)^s-0.75\left(\frac{h}{a}\right)^7\right] h \le a \tag{28}$$

$$c \qquad h > a \tag{29}$$

Difference between the approach of statistics and geostatistics

Statistics	Geostatistics
Statistics considers all the numerical values $Z(x)$, $Z(x')$ as independent realization of the same numerical function Z.	Geostatistics considers all the numerical values $z(x)$, $z(x')$ as the particular realizations of random variables $Z(x)$ and $Z(x')$
In other words it does not take into account the spatial auto-correlation between two neighbouring values $Z(x)$ and $Z(x + h)$	In other words it takes into account the spatial auto-correlation between two neighbouring values $z(x)$ and $z(x + h)$.
Statistics does not take the regionalization into consideration. In other words, the location of the samples is ignored.	Geostatistics takes the regionalization into consideration. Even when populations can have same parameters like mean, variance, skewness and kurtosis still they can differ considerably. Because the regionalizations can be different.
The variability with the distance and the anisotropies are not taken into consideration	Geostatistics also takes into consideration, the anisotropies, the correlation with the distance. In other words Geostatistics takes into account the holistic view.

EXERCISES IN LINEAR GEOSTATISTICS

1. Probabilities

Question 1.1

The variance of a random variable x is, by definition, $V(x) = E[x - \mu]^2$

where $\mu = E(x) = \int xf(x)dx$.

Show that $V(x) = E(x^2) - \{E(x)\}^2$

Answer

$$\begin{aligned}
\text{Var}(X) &= \int (x-\mu)^2 f(x)dx \\
&= \int x^2 f(x)dx - 2\mu\int xf(x)dx + \mu^2\int f(x)dx \\
&= E(x^2) - 2\ \mu\mu + \mu^2\ .1 \\
&= E(x^2) - \mu^2 \\
&= E(x^2) - \{E(x)\}^2
\end{aligned}$$

Question 1.2

Let x be a random variable and "a" a constant.

(a) Show that $E(ax) = a\ E(x)$.

(b) Show that $\text{Var}(ax) = a^2\ \text{Var}(x)$.

Answer

$$\text{(a) } E(ax) = \int (ax)f(x)dx = a\int xf(x)dx = a\mu = aE(x)$$

$$\begin{aligned}
\text{(b) Var}(ax) &= E[(ax)^2] - E[(ax)]^2 \\
&= a^2E(x^2) - a^2\mu^2 \\
&= a^2V(x)
\end{aligned}$$

Question 1.3

Let x, y and z be three random variables such that $z = x + y$.

Show that

$V(z) = V(x) + V(y) + 2\text{Cov}(x, y)$

Answer

$$\begin{aligned}
E(x + y) &= \int\int (x+y)f(x,y)dx.dy \\
&= \int\int xf(x,y)dx.dy + \int\int yf(x,y)dx.dy \\
&= \int\int x[f(x,y)dy]dx + \int\int f(x,y)dx.y.dy \\
&= \int\int x.f(x)dx + \int y.f(y).dy
\end{aligned}$$

$$E[(x + y) = E(x) + E(y)$$

Also $V(x + y) = E[(x + y)^2] - [E(x + y)]^2$

$$= E(x^2 + 2.x.y + y^2) - (\mu_x + \mu_y)^2$$
$$= E(x^2) + 2.E(x.y) + E(y^2) - \mu_x^2 - 2.\mu_x.\mu_y - \mu_y^2$$
$$= (E(x^2) - \mu_x^2) + (E(y^2) - \mu_y^2) + 2[E(x.y) - \mu_x.\mu_y]$$
$$= V(x) + V(y) + 2\text{Cov}(x, y)$$

In fact

$$\text{Cov}\ (x, y) = E[(x - \mu_x)(y - \mu_y)]$$
$$= E(x.y - \mu_x.y - \mu_y.x + \mu_x.\mu_y)$$
$$= E(x.y) - \mu_x.E(y) - \mu_y.E(x) + \mu_x\mu_y$$
$$= E(x.y) - \mu_x.\mu_y - \mu_x.\mu_y + \mu_x.\mu_y = E(x.y) - \mu_x.\mu_y)$$
$$\text{Cov}\ (x^2) = (\text{Cov}(x.x)) = E(x, x) - m^2 = E(x^2) - m^2$$
$$E(x^2) = \text{Cov}(x, x) + m^2$$

2. Properties of Variogram and Covariance Models

Question 2.1

Let $Z(x)$ be a stationary random function. Show that the co-variance that is equal to

$C(h) = E\{[Z(x + h) - m)[Z(x) - m]\}$ has the following properties:

(i) $C(0) \geq 0$

(ii) $C(h) = C(-h)$

(iii) $|C(h)| \leq C(0)$

Answer

(i) $C(h) = E\{[Z(x+h) - m][Z(x) - m]\}$

$C(0) = E\{[Z(x) - m]^2\} = V(x) \geq 0$

(ii) $C(-h) = E\{[Z(x-h) - m][Z(x) - m]\}$ Put $x - h = y$

$= E\{[Z(y) - m][Z(y+h) - m]\}$

$= C(h)$

Because the random variable is stationary.

(iii) It is to be shown that $-C(0) \leq C(h) \leq C(0)$

to show that $C(h) \leq C(0)$

$$0 \leq E\{[Z(x+h) - Z(x)]^2\} = E\{[(Z(x+h) - m) - (Z(x) - m)]^2\}$$

The expectation of a square is always ≥ 0

$$= E[Z(x+h) - m]^2 + E[Z(x) - m]^2 - 2E[Z(x+h) - m] \times E[Z(x) - m]\}$$
$$= 2C(0) - 2C(h) \geq 0 \Rightarrow C(h) \leq C(0)$$

to show that $-C(h) \geq C(0)$ again:

$$E\{[Z(x+h) - m) + (Z(x) - m)]^2\} \geq 0 \Rightarrow E[Z(x+h) - m]^2$$

$$\Rightarrow E\{[Z(x+h)-m]^2 + E[Z(x)-m]^2 + 2E[Z(x+h)-m]\times E[Z(x+h)-m]\} \geq 0$$

$$\Rightarrow 2C(0)+2C(h) \geq 0 \Rightarrow -C(0) \leq C(h)$$

Hence: $-C(0) \leq C(h) \leq C(0) \Rightarrow |C(h)| \leq C(0)$

Question 2.2

Let $Z(x)$ be a stationary random function. Show that the variogram that is equal to $\gamma(h) = \frac{1}{2}E[Z(x+h)-Z(x)]^2$ has the following properties:

$\gamma(0) = 0$

$\gamma(-h) = \gamma(h) \geq 0$

Answer

(i) $\gamma(0) = \frac{1}{2}E[Z(x)-Z(x)] = 0$

$\gamma(h)$ is the expectation of a square, hence it has to be positive.

$\gamma(-h) = \frac{1}{2}E[Z(x-h)-Z(x)]^2$

Let $y = x - h$ $\gamma(x,h) = \gamma(y,h)$, because it is intrinsic

$$\gamma(-h) = \gamma(y,h) = \tfrac{1}{2}E[Z(y)-Z(y+h)]^2 = \gamma(h) \Rightarrow \gamma(h) = \gamma(-h)$$

Question 2.3

Let $Z(x)$ be a stationary random function. Show that

$\gamma(h) = C(0) - C(h)$

Answer

$$\begin{aligned}
\gamma(h) &= \tfrac{1}{2}E\{[Z(x+h)-m]-[Z(x)-m]\}^2 \\
&= \tfrac{1}{2}\{E[Z(x+h)-m]^2 + E[Z(x)-m]^2 \\
&\quad -2E[(Z(x+h)-m)(Z(x)-m)]\} \\
&= \tfrac{1}{2}[2C(0)-2C(h)] \\
\gamma(h) &= C(0)-C(h)
\end{aligned}$$

Question 2.4

Let $Z^*(x)$ be a stationary random function.

$Z^*(x) = \sum_{i=1}^{n} \lambda_i Z(x_i)$ where λ_i are constants. Show that

$$V(Z^*(x)) = \sum_i \sum_j \lambda_i \lambda_j \text{ Cov}\,(Z(x_i), Z(x_j))$$

$$= -\sum_i \sum_j \lambda_i \lambda_j \gamma(Z(x_i), Z(x_j)) \text{ where } \sum \lambda_i = 0$$

Answer '

We know that $\text{Cov}(Z(x_i), Z(x_j)) = C(0) - \gamma(Z(x_i), Z(x_j))$

Hence $V(Z^*(x)) = \sum_i \sum_j \lambda_i \lambda_j [C(0) - \gamma(Z(x_i), Z(x_j))]$

$$= C(0) \sum_i \sum_j \lambda_i \lambda_j - \sum_i \sum_j \lambda_i \lambda_j \gamma(Z(x_i), Z(x_j))$$

$$= C(0)(\sum (\lambda_i)^2 - \sum_i \sum_j \lambda_i \lambda_j \gamma(Z(x_i), Z(x_j))$$

But $\sum \lambda_i = 0$ by the hypothesis.

Therefore: $V(Z^*(x)) = -\sum_i \sum_j \lambda_i \lambda_j \gamma(Z(x_i), Z(x_j))$ If $\sum \lambda_i = 0$

3. Standard Models

Spherical Model

$$\gamma(h) = \begin{cases} C\left(\frac{3}{2} \times \frac{h}{a} - \frac{1}{2} \times \frac{h^3}{(a)^3}\right) & \text{when } |h| < a \\ C & \text{when } |h| \geq a \end{cases}$$

Question 3.1

Trace the curve of $\gamma(h)$ when sill c = 2 and range a = 100 m.

Answer

The expression for $\gamma(h)$ when sill c = 2 and range a = 100 m will be

$$\gamma(h) = \begin{cases} \left(3 \times \frac{h}{100} - \frac{h^3}{(100)^3}\right) & \text{when } |h| < 100 \\ 2 & \text{when } |h| \geq 100 \end{cases}$$

The slope at the origin is equal to $\gamma'(h)$ when h = 0 which is equal to 3/100.

$$\gamma'(h) = \frac{d\gamma(h)}{dh} = \frac{3}{100} - \frac{3h^2}{100^3}$$

We will calculate $\gamma(h)$ when h takes values 0, 20, 40, 60, 80, 100, 120. Elaborate calculations are shown for two cases. Rest can be calculated in similar manner.

$$\gamma(0) = 3(0/100) - (0/100)^3 = 0$$
$$\gamma(20) = 3(20/100) - (20/100)^3 = 3 \times 0.2 - 0.008 = 0.59$$
$$\gamma(40) = 3 \times 0.4 - 0.064 = 1.14$$
$$\gamma(60) = 3 \times 0.6 - 0.216 = 1.58$$
$$\gamma(80) = 3 \times 0.8 - 0.512 = 1.9$$
$$\gamma(100) = 2$$
$$\gamma(120) = 2$$

Question 3.2

Trace the variogram which is a sum of two spherical variograms, the first variogram having sill = 1, range 50 m, and second variogram having a sill 1 and range 100 m. (Note the curvature at h = 50 m and at h = 100 m).

Answer

It may be remembered that variograms are additive. Sum of two spherical variograms with $c_1 = 1$, $a_1 = 50$, and $c_2 = 1$, $a_2 = 100$

$$\gamma(h) = \gamma_1(h) + \gamma_2(h) = \frac{3}{2} \times \frac{h}{50} - \frac{1}{2} \times \frac{h^3}{50^3} + \frac{3}{2} \times \frac{h}{100} - \frac{1}{2} \times \frac{h^3}{100^3}$$

When $h < a_1$: $\gamma_1(h) + \gamma_2(h) = \frac{3}{2} \cdot \frac{3h}{100} - \frac{1}{2}\left(\frac{8h^3}{100^3} + \frac{h^3}{100^3}\right) = \frac{1}{2}\left[\frac{9h}{100} - \frac{9h^3}{100^3}\right]$

$$= \frac{9}{2}\left[\frac{h}{100} - \frac{h^3}{100^3}\right] = \frac{9h}{200}\left(1 - \frac{h^2}{100^2}\right)$$

When $a_1 \le h \le a_2$..or..$h \in [a_1, a_2]$: $\gamma_1(h) + \gamma_2(h)$

$$= 1 + \gamma_2(h) = 1 + \frac{3}{2} \cdot \frac{h}{100} - \frac{1}{2} \cdot \frac{h^3}{100^3}$$

When $h > a_2$: $\gamma_1(h) + \gamma_2(h) = C_1 + C_2 = 2$

$\gamma'(h) = \frac{d\gamma(h)}{dh} = \frac{1}{2}\left[\frac{9}{100} - \frac{3h^2}{100^3}\right]$ Slope near the origin is when h = 0

$$\gamma'(0) = 9/200$$

$$\gamma(0) = \frac{9}{2}\left(0 - (0)^3\right) = 0$$

$$\gamma(10) = \frac{9}{2}\left(0.1 - (0.1)^3\right) = 0.445$$

$$\gamma(20) = \frac{9}{2}\left(0.2 - (0.2)^3\right) = 0.86$$

$$\gamma(30) = \frac{9}{2}\left(0.3 - (0.3)^3\right) = 1.23$$

$$\gamma(40) = \frac{9}{2}\left(0.4 - (0.4)^3\right) = 1.51$$

$$\gamma(50) = \frac{9}{2}\left(0.5 - (0.5)^3\right) = 1.69$$

$$\gamma(60) = 1 + \frac{3}{2} \times 0.6 - \frac{1}{2} \times (0.6)^3 = 1.79$$

$$\gamma(70) = 1 + \frac{3}{2} \times 0.7 - \frac{1}{2}(0.7)^3 = 1.88$$

$$\gamma(80) = 1 + \frac{3}{2} \times 0.8 - \frac{1}{2}(0.8)^3 = 1.944$$

$$\gamma(90) = 1 + \frac{3}{2} \times 0.9 - (0.9)^3 = 1.99$$

$$\gamma(100) = 1 + 1 = 2$$

$$\gamma(110) = 1 + 1 = 2$$

Question 3.3

Calculate the slope of the spherical variogram near the origin. Show that the tangent at the origin cuts the straight line $Y = c$ at $h = (2/3)a$.

Answer

The tangent at the origin cuts the straight line $Y = c$ at $h = (2/3)a$. The slope of the spherical variogram near origin is obtained by differentiating variogram function and substituting $h = 0$.

$$\gamma(h) = c\left(\frac{3}{2} \cdot \frac{h}{a} - \frac{1}{2} \cdot \frac{h^3}{a^3}\right)$$

$$\gamma'(h) = \frac{d\gamma(h)}{dh} = c\left(\frac{3}{2a} - \frac{3h^2}{2a^3}\right)$$

Substituting $h = 0$, $\gamma'(0) = \dfrac{3c}{2a}$ which is the slope near origin.

The equation of the tangent near the origin is $Y = \dfrac{3c}{2a} \cdot h$

When this tangent cuts the line $Y = c$ at the point of intersection, the values of (x, y) are common for both the lines, which can be obtained by equating them.

$$Y = c = \frac{3c}{2a}h \qquad \therefore h = \frac{2a}{3}$$

Question 3.4

Show that the spherical variogram has the same behaviour at the origin as the linear variogram with the following equation:

$$\gamma(h) = \frac{3c}{2a}|h|$$

Answer

At the origin, $\frac{h^3}{a^3}$ term is so small that it can be neglected for practical purposes. Hence the equation of the variogram can be considered as

$$\gamma(h) \cong c\left(\frac{3}{2}\cdot\frac{|h|}{a}\right) = \frac{3c}{2a}\cdot|h|$$

But this is nothing but the linear variogram. Hence it is proved that spherical variogram has the same behaviour at the origin as the linear variogram with the equation $\gamma(h) = \frac{3c}{2a}|h|$.

Exponential Model

$\gamma(h) = C[1 - \exp(-|h|/a)]$

Question 3.5

Trace the variogram curve when sill $c = 2$ and range $a = 30$ m. Make a comparison with those of the questions 3.1 and 3.2.

Answer

$$\gamma'(h) = \frac{d\gamma(h)}{dh} = c(-e^{-\frac{|h|}{a}})\cdot\left(-\frac{1}{a}\right) = \frac{c}{a}\left(e^{-\frac{h}{a}}\right)$$

We can get the slope near the origin by differentiating the Gamma function and substituting $h = 0$ in the differential.

$$\gamma'(0) = \frac{c}{a}\left(e^{-\frac{0}{a}}\right) = \frac{c}{a}\left(e^{-0}\right) = \frac{c}{a} = \frac{2}{30}$$

$$\gamma(0) = 2\left(1 - e^{-\frac{0}{30}}\right) = 0$$

$$\gamma(20) = 2\left(1 - e^{-\frac{20}{30}}\right) = 0.97$$

$$\gamma(40) = 2\left(1 - e^{-\frac{40}{30}}\right) = 1.47$$

$$\gamma(60) = 2\left(1 - e^{-\frac{60}{30}}\right) = 1.73$$

$$\gamma(80) = 2\left(1 - e^{-\frac{80}{30}}\right) = 1.86$$

$$\gamma(100) = 2\left(1 - e^{-\frac{100}{30}}\right) = 1.93$$

Note: The exponential variogram, in comparison to spherical variogram, rises very quickly in the beginning. On the contrary it increases very slowly and reaches the sill value very slowly. Since it is an exponential function, theoretically it reaches the sill value at infinity only. Therefore a practical range is defined below.

Question 3.6

Calculate the practical range of the model, i.e. the value of h, for which $\gamma(h)$ attains 95% of its sill value.

Answer

$$\gamma(h) = 95\% \times c = 0.95c = c\left(1 - e^{-\frac{h}{a}}\right) = 0.95 = \left(1 - e^{-\frac{h}{a}}\right)$$

$$e^{-\frac{h}{a}} = 1 - 0.95 = 0.05$$

$$h = -a \times \log(0.05) \Leftrightarrow h \cong 3a.$$

Note: One important point to be noted is that in spherical model, a represents the sill value at which the $\gamma(h)$ reaches the maximum value. Whereas in exponential model, theoretically, the sill value is reached when $h = \infty$. That is why we are forced to define a working sill value of 95% value.

Question 3.7

Calculate the slope of the variogram near the origin. Show that the tangent near the origin cuts the line $Y = c$ at $h = a$.

Answer

We can get the slope near the origin by differentiating the Gamma function and substituting $h = 0$ in the differential.

$$\gamma'(h) = \frac{d\gamma(h)}{dh} = c(-e^{-\frac{|h|}{a}}) \cdot \left(-\frac{1}{a}\right) = \frac{c}{a}\left(e^{-\frac{h}{a}}\right)$$

The slope near the origin = $\gamma'(0) = \frac{c}{a}\left(e^{-\frac{0}{a}}\right) = \frac{c}{a}\left(e^{-0}\right) = \frac{c}{a}$

The equation of the tangent near the origin is $Y = \frac{c}{a}h$

Since it cuts the line $Y = c$, both can be equated near point of intersection. In other words:

$$\frac{c}{a}h = c \quad \text{or} \quad h = a\,.$$

Gaussian Model

$$\gamma(h) = c\left(1 - e^{-\frac{h^2}{a^2}}\right) = c[1 - \text{Exp}(-h^2/a^2)]$$

Question 3.8

Trace the curve of the Gaussian variogram, when Sill c = 2 and the Range a = 50. Make a comparison of the curves in questions 3·5 and 3·1.

Answer

We can get the slope near the origin by differentiating the Gamma function and substituting h = 0 in the differential.

$$\gamma(h) = c\left(1 - e^{-\frac{h^2}{a^2}}\right)$$

$$\gamma' h) = \frac{d\gamma(h)}{dh} = c\left[-e^{-\frac{h^2}{a^2}} \times \left(-\frac{2h}{a^2}\right)\right] = c\left(\frac{2h}{a^2}\right) \times e^{-\frac{h^2}{a^2}}$$

$$\gamma'(0) = c\left(\frac{2 \times 0}{a^2}\right) \cdot e^{-\frac{0}{a^2}} = 0$$

$\gamma(0) = 2\left(1 - \text{Exp}\,(-0^2/50^2)\right) = 0$ $\quad$ $\gamma(10) = 2\left(1 - \text{Exp}\,(-1/25)\right) = 0.08$

$\gamma(20) = 2(1 - \text{Exp}\,(-4/25)) = 0.30$ $\quad$ $\gamma(30) = 2(1 - \text{Exp}\,(-9/25)) = 0.60$

$\gamma(40) = 2(1 - \text{Exp}\,(-16/25)) = 0.95$ $\quad$ $\gamma(50) = 2(1 - \text{Exp}\,(-25/25)) = 1.26$

$\gamma(60) = 2(1 - \text{Exp}\,(-36/25)) = 1.53$ $\quad$ $\gamma(70) = 2(1 - \text{Exp}\,(-49/25)) = 1.72$

$\gamma(80) = 2(1 - \text{Exp}\,(-64/25)) = 1.85$ $\quad$ $\gamma(90) = 2(1 - \text{Exp}\,(-81/25)) = 1.92$

$\gamma(100) = 2(1 - \text{Exp}\,(-100/25)) = 1.96$

Comparison

The Gaussian scheme presents a parabolic behaviour near the origin with a horizontal tangent. Hence it rises very slowly at the beginning, in comparison to either Exponential or Spherical Schemes. The Gaussian scheme also shows a concavity whereas the other two schemes are convex. Lastly, for the values of h nearer to the range, the Spherical and Gaussian schemes appear same.

Question 3.9

Show that the behaviour of the variogram is parabolic near the origin. Model in $|h|^{\alpha}$

$$\gamma(h) = |h|^{\alpha} \quad 0 \le \alpha < 2$$

Answer

The behaviour of the variogram is parabolic near the origin.
Behaviour of e^x at the origin is:

$$e^x = 1 + x + \frac{x^2}{2!} + \ldots\ldots\ldots\ldots\ldots + \frac{x^n}{n!} \quad (\text{for } x \approx 0)$$

Hence $\gamma(h) \approx c(1-(1-\frac{h^2}{a^2}+\frac{h^4}{2!a^4}+\ldots\ldots\ldots)) \approx c\frac{h^2}{a^2}$ (for $h \to 0$): This is because as $h \to 0$, the higher powers of h can be neglected. This represents the equation of a parabola of axis (0, y).

Hence the variogram has a parabolic behaviour near the origin. A few clarifications below:

Origin = h = 0 Behaviour near the origin means $h \approx 0$.

Model in $|h|^{\alpha}$

Question 3.10

Trace the curves for different values of α (for example α = ½, 1, 3/2).

Answer

The curves for different values of α (for example α = ½, 1, 3/2).

α = 0.5

h	0	1	2	3	5	10	15	20	25
$\gamma(h)$	0	1	1.41	1.73	2.24	3.16	3.87	4.47	5

α = 1

h	0	1	2	3	5	10	15	20	25
$\gamma(h)$	0	1	2	3	5	10	15	20	25

α = 1.5

h	0	1	2	3	5	10	15	20	25
$\gamma(h)$	0	1	2.83	5.2	11.18	31.62	58.1	89.4	125

Clarification: It may be clarified that α can not take values greater than or equal to 2. It can be 1.9 or 1.999, but cannot be equal to 2 or more.

4. Calculation of Experimental Variograms

Regular Grids in One Direction

Question 4.1

```
                1     3     5     7     9     8     6     4     2
Case I          I--------I--------I--------I------- I--------I-------I--------I--------I
                5     1     9     2     3     7     8     4     6
Case II         I--------I--------I--------I------- I--------I-------I--------I--------I
```

The above figures represent the value of $Z(x)$ at each point. Calculate the experimental variograms in both the cases.

Answer

The theoretical formula for the variogram is

$$\gamma(h) = \frac{1}{2} E\left[Z(x+h) - Z(x)\right]^2.$$

But to calculate practically $\gamma(h) = \frac{1}{2N}\sum\left(Z(x+h) - Z(x)\right),^2$ where N represents the number of pairs and h represents the lag. The variograms for the cases are calculated using the formula and presented in Table 5. The distance lag and the number of pairs for both the cases are same since the measurement points are same.

Table 5: Variograms of two data sets having same mean and variance

h	*γ(h)–Case I*	*γ(h)–Case II*	*Number of pairs*
1	1.81	10.44	8
2	6.43	8.29	7
3	11.92	4.58	6
4	14.80	5.40	5
5	10.50	11.75	4
6	5.83	4.50	3
7	2.50	6.50	2
8	0.50	0.50	1

It may be noted that though both data sets are numeral from 1 to 9 with the same mean and variance but have different variograms.

Question 4.2

```
10  12   36   72   91   38   31   50   69   07   21   18   71   08   40  82
I --- I --- I --- I --- I --- I --- I --- I --- I --- I --- I --- I --- I --- I--- I
```

Calculate the experimental Variogram for the above distribution.

Answer

h	γ(*h*)	*Number of pairs*	*h*	γ(*h*)	*Number of pairs*
1	647.7	15	9	707.8	7
2	962.7	14	10	834.6	6
3	896.2	13	11	543.4	5
4	615.7	12	12	481.6	4
5	810.7	11	13	484.0	3
6	1116.5	10	14	1450.0	2
7	861.5	9	15	2592.0	1
8	565.8	8			

Question 4.3

2.4 3.0 - 1.8 1.5 3.0 - 2.5
I-------- I-------- I-------- I-------- I-------- I-------- I-------- I

The numbers represent the tenors in percentage. Two values are missing. Calculate the experimental variogram.

Answer

Note: While calculating the variograms with missing values, the pairs with missing values is omitted and it is not taken into consideration while calculating the number of pairs.

h	0	1	2	3	4	5	6	7
γ(*h*)	0	0.45	0.52	0.60	0.22	0.18	0.13	0.01
Number of pairs	6	3	3	3	3	1	1	1

CONCLUSIONS

Geostatistical methods have found applications in many fields of Earth Sciences and much more in hydrogeology. In this article, efforts have been made to introduce the subject in a possible simple way by defining the basic statistics utilized to develop the method, the basic mathematical derivations required as well as a few critical comparisons between classical statistical methods and that of geostatistical methods. Variography, the most important component of the geostatistical methods, has been dealt with in details and finally a number of examples of computing the variograms are presented for demonstration purpose.

REFERENCES

Isaaks, H.E. and Srivastava, R.M., 1989. An Introduction to Applied Geostatistics, Oxford Universtity Press, USA.

Marsily, G.De., 1986. Quantitative Hydrogeology: Groundwater Hydrology for Engineers, Academic Press.

Matheron, G., 1963. Principles of Geostatistics, *Econ. Geol.* **58:** 1246-1266.

13 Kriging for Estimating Hydrogeological Parameters

Shakeel Ahmed and K. Devi

Indo-French Centre for Groundwater Research
National Geophysical Research Institute, Hyderabad-500007, India

INTRODUCTION

Geostatistics based on the theory of regionalized variables has found more and more applications in the field of groundwater hydrology. Now geostatistics has found applications in almost all domains of hydrogeology from parameter estimation to predictive modelling including the most important one: data network designing. Geostatistical estimation variance reduction, cross-validation techniques etc. are a few procedures that could study adequacy of a given monitoring network and could evolve an optimal monitoring network with some given constraints. The advantage of the geostatistical estimation technique is that the variance of the estimation error could be calculated at any point without having the actual measurement on that point (well). Thus the benefits to be accrued from an additional measurement could be studied prior to its measurement. Monitoring through an optimal network can reduce the amount of data required while providing the desired accuracy and a few simple procedures have been developed for a geostatistical optimization of the monitoring network in this study.

A number of geostatistical estimators have been developed and depending on the nature of the parameter, objectives of the result on precision etc. a particular method is applied. In this article development of the basic estimation method i.e. Ordinary Kringing as well as Universal Kriging; from the Kriging family are described in detail and remarks on them have been discussed.

BRIEF DESCRIPTION OF THE THEORY OF ESTIMATION

The kriging technique was originally developed by Matheron (1965, 1971) to estimate regionalized variable such as the grade of an ore body at known location in space, given a set of observed data. Its application to groundwater

hydrology has been described by a number of authors, viz. Delhomme (1976, 1978, 1979), Delfiner and Delhomme (1973), Marsily et al. (1984), Marsily (1986), Aboufirassi and Marino (1983, 1984), Gambolti and Volpi (1979 and 1979a) to name a few.

If $Z(x)$ represents any random function (for instance, the transmissivity field in an aquifer) with values measured at n locations in space $z(x_i)$, $i = 1 \ldots. n$ and if the value of the function Z has to be estimated at the point x_0, which has not been measured, the kriging estimate is defined as:

$$z^*(x_0) = \sum_{i=1}^{n} \lambda_i Z(x_i) \tag{1}$$

where $z^*(x_0)$ is the estimation of function $Z(x)$ at the points x_0 and λ_i are the weighting factors. Now we impose two conditions to equation (1), i.e. the unbiased condition and the condition of optimality.

The unbiased condition (also called universality condition) means that the expected value of estimation error or the difference between the estimated $z^*(x_0)$ and the true (unknown) $z(x_0)$ value should in the average be zero:

$$E[z^*(x_o) - z(x_o)] = 0 \tag{2}$$

The condition of optimality means the variance of the estimation error should be minimum.

$$\sigma^2 = \text{var } [z^*(x_o) - z(x_o)] \text{ minimum} \tag{3}$$

Note that the variance of estimation error $\sigma^2_{k,}$, is not a priori variance σ^2 of the random variable z. It is instead a measure of the uncertainty in the estimation of Z at an unmeasured location. By definition σ^2_k at a measured location is zero.

Using the expected value $E[Z(x)] = m$ and rewriting equation (2) with the help of equation (1) we get:

$$\sum_{i=1}^{n} \lambda_i = 1 \tag{4}$$

Developing equation (3) we get:

$$\sigma_k^2 = \sum_{i=1}^{n} \lambda_i \sum_{j=1}^{n} \lambda_j E[Z(x_i)Z(x_j)] + E[Z(x_o)^2] - 2\sum_{i=1}^{n} \lambda_i E[Z(x_i)Z(x_o)] \tag{5}$$

Introducing a coefficient called Lagrange multiplier μ and adding the term $-2\mu\left(\sum_{i=1}^{n} \lambda_i - 1\right)$ to the above equation we get:

$$Q = \sigma_k^2 - 2\mu \left(\sum_{i=1}^{n} \lambda_i - 1\right)$$

$$= \sum_{i=1}^{n} \lambda_i \sum_{j=1}^{n} \lambda_j C(x_i, x_j) + C(O) - 2\sum_{i=1}^{n} \lambda_i C(x_i, x_o) - 2\mu \sum_{i=1}^{n} \lambda_i + 2\mu \quad (6)$$

To minimize the above expression which is quadratic in λ and μ, we equate $\partial Q/\partial\lambda_i$, i = 1……$n$ and $\partial Q/\partial\mu$ to zero and obtain the following kriging equations:

$$\sum_{j=1}^{n} \lambda_j C(x_i, x_j) - \mu = C(x_i, x_o) \quad (7)$$

$$i = 1.....n$$

$$\sum_{j=1}^{n} \lambda_j = 1 \quad (8)$$

where $C(x_i, x_j)$ is the value of covariance between two points x_i and x_j. Now to express the value σ^2_k we multiply both sides of equation (7) by $\sum_{i=1}^{n} \lambda_i$ and put the value of $\sum_{i=1}^{n} \lambda_i \sum_{j=1}^{n} \lambda_j C(x_i, x_j)$ into equation (6) to get:

$$\sigma_k^2 = C(O) - \sum_{i=1}^{n} \lambda_i C(x_i, x_o) + \mu \quad (9)$$

which is the variance of the estimation error. Equations (7) and (8) are a set of (n + 1) linear simultaneous equations with (n + 1) unknowns and on solving them we get the values of λ_i, i = 1……n and which are later used to calculate the estimated value by equation (1) and the variance of the estimation error by equation (9). Therefore, the square root of the expression given by equation (9) gives the standard deviation σ_k, which means that with the 95% confidence true value will be within z^* $(x_0) \pm 2\sigma_k$.

When we deal with intrinsic case i.e. working with variogram, which is common in hydrogeology the kriging equations (7) to (9) are simply modified as follows:

$$C(x_i, x_j) = C(0) - \gamma(x_i, x_j) \quad (10)$$

$$C(x_i, x_0) = C(0) - \gamma(x_i, x_0) \quad (11)$$

Equations (10) and (11) hold good only when both the covariance and the variogram exist, i.e. in the case of stationary variables. In case the covariance cannot be defined we can derive the following kriging equations:

$$\sum_{j=1}^{n} \lambda_j \gamma(x_i, x_j) + \mu = \gamma(x_i, x_0) \quad (12)$$

$$i = 1.....n$$

$$\sum_{j=1}^{n} \lambda_j = 1 \tag{13}$$

and the variance of the estimation error becomes:

$$\sigma_k^2 = \sum_{i=1}^{n} \lambda_i \gamma(x_i, x_o) + \mu \tag{14}$$

Expression in a matrix form:

$$\begin{bmatrix} \gamma_{11}\gamma_{12}\gamma_{13}\cdots\cdots\cdots\gamma_{1n}1 \\ \gamma_{21}\gamma_{22}\gamma_{23}\cdots\cdots\cdots\gamma_{2n}1 \\ \gamma_{31}\gamma_{32}\gamma_{33}\cdots\cdots\cdots\gamma_{3n}1 \\ \\ \gamma_{n1}\gamma_{n2}\gamma_{n3}\cdots\cdots\cdots\gamma_{nn}1 \\ \\ 1\ldots\ldots1\ldots\ldots1\ldots\ldots\ldots\ldots\ldots\ldots1\ldots0 \end{bmatrix} \begin{bmatrix} \lambda_1 \\ \lambda_2 \\ \lambda_3 \\ \\ \lambda_{n\lambda} \\ \\ \mu \end{bmatrix} = \begin{bmatrix} \gamma_{10} \\ \gamma_{20} \\ \gamma_{30} \\ \\ \gamma_{n0} \\ 1 \end{bmatrix} \tag{15}$$

where γ_{nm} means $\gamma\ (x_n, x_m)$. In the short form it is written as:

$$[A][\lambda] = [B]$$

or

$$[\lambda] = [A]^{-1}[B] \tag{16}$$

We have seen previously that after a certain distance, called the range, which also shows the zone of influence, the variogram generally takes an asymptotic value. Thus for estimating any variable at a particular point, it is not very useful to consider the data points beyond the zone of influence, called the neighbourhood of the estimated point x_0. Therefore, if we consider the points, which lie inside the zone of influence for estimating the variable at any given point, a smaller matrix will be used. This procedure is called the 'moving neighbourhood'. However, when we used the moving neighbourhood for each point of estimation, a different matrix has to be inverted separately for calculating the situation and this becomes very time consuming. If we work with the so-called 'unique neighbourhood', where all the available data points are considered simultaneously, it is sufficient to calculate the inverse of matrix $[A]$ only once. A simple multiplication is needed to get the kriged estimate to any location.

It is also clear that the value of $z^*(x_0)$ is equal to $[\lambda]^T\ [Z]$ where $[Z]$ is the column matrix of the measured values at the measurement points; therefore we can easily write:

$$z^*(x_o) = [\lambda]^T\ [Z] = \{[A]^{-1}\ [B]\}^T\ [Z]$$

$$= [B]^T\ [A]^{-1}\ [Z] \tag{17}$$

Since $[A]$ is a square symmetric matrix, it is unchanged when transposed also $z^*(x_0) = [B]^T[C]$ where $[C] = [A]^{-1}\ [Z]$

So in the case of the unique neighbourhood, matrix $[C]$ is calculated once and used for the estimation of all the points.

Similarly the matrix equation for the variance of the estimation error can be written as follows:

$$\sigma_k^2 = [\lambda]^T\ [B] = [B]^T\ [A]^{-1}\ [B] \tag{18}$$

A few remarks about the Kriging

1. If we estimate the value of the variable Z at a point X_m, which also is one of the data locations, i.e. $x_m\ \varepsilon\ \{x_1 \ldots x_n\}$, the kriging system provides an estimated value $z^*\ (x_m)$ of the data and nil variance of estimation error. Hence the kriging estimator is called an "exact" estimator. It is also called a Best Linear Unbiased Estimator (BLUE) since it is indeed a linear estimator defined by the conditions of universality and of optimality.
2. Instead of working with the natural values of the variable, it is sometimes preferable to work with its logarithm; this is often the case with transmissivity, because when the natural values have a lognormal probability distribution the spatial structure, e.g. variogram or covariance, is better defined if the logarithms of the values are used. Moreover, the arithmetic mean of the logarithm gives, in fact, the geometric mean of the natural value, which is a better estimator of the true spatial average in the case of transmissivity (Matheron, 1967).
3. Very often the observed field data are approximate and unreliable but the kriging theory permits the use of data with uncertainties. For this we assume that the observed value of the variable z consists of two components T and e (true part and uncertainty).
4. The variogram calculated on the raw data uses the average variability of the variable for any particular separation h, and the theoretical model fitted through the experimental variograms makes it more approximate. Thus it is necessary to check the validity of the adjusted theoretical model. In other words, the variogram model and the kriging procedure should reproduce the observed data. To do so we remove one data point and estimate the variable at that point from the rest of the measured values and calculate the difference between the estimated and observed values (i.e. error).
5. The variance of the kriging estimation error depends on the geometry of the data network and on the structural model, i.e., the covariance or variogram but not on the measured value $z(x_i)$ at the measurement points. We have seen that the variance decreases as the number of points in the near-neighbourhood is increased.

Therefore, before deciding on a new location for a measurement point (or the deletion of an existing point) a variance can be calculated, and thus when the variogram or covariance is known, a better network of data can be designed based on the minimum variance, prior to any measurement.

UNIVERSAL KRIGING MOSTLY APPLIED TO WATER LEVEL ESTIMATION

Water levels generally being a non-stationary variable, Ordinary Kriging technique is not applicable and the technique of Universal Kriging is thus applied. The water level estimate at any point p (say a well) using Universal Kriging is written as follows:

$$h^*_{\mathrm{p}} = D^*_{\mathrm{p}} + \sum_{i=1}^{N} \lambda_i \, (h_{\mathrm{i}} - D_{\mathrm{i}}) \tag{19}$$

where h^*_{p} and D^*_{p} are the estimated water level and the drift respectively at any unmeasured well p; h_{i} and D_{i} are the values of water level and drift at well i and λ_{i} are kriging weights. The water levels h are split into a smoothly varying deterministic part D and the residual $(h - D)$. A bounded variogram could be obtained for the residual, as this is a stationary random function.

Modelling the drift correctly is difficult as it is not possible to estimate parameters of the drift and that of the variogram of residuals from a single data set. Drift depends on the nature of water level variation, and could be linear, quadratic or of higher order. Usually a drift is approximated by polynomials of the space coordinates. For example, a linear drift can be written as:

$$D_{\mathrm{i}} = a + bx_{\mathrm{i}} + cy_{\mathrm{i}} \quad \forall_{\mathrm{i}} \tag{20}$$

A quadratic drift can be written as:

$$D_{\mathrm{i}} = a + bx_{\mathrm{i}} + cy_{\mathrm{i}} + dx_{\mathrm{i}}^2 + ey_{\mathrm{i}}^2 + fx_{\mathrm{i}}y_{\mathrm{i}} \tag{21}$$

where a, b, c, d, e and f are the drift coefficients and are constants. It is possible to estimate a drift by ordinary kriging but it has got the indeterminacy problem, as that requires the knowledge of the variogram of residuals.

The kriging weights can be determined as follows:

$$\sum_{i=1}^{N} \lambda_i \gamma_{ij} + \mu_0 + \mu_1 x_{\mathrm{j}} + \mu_2 y_{\mathrm{j}} = \gamma_{\mathrm{jp}}$$

$$j = 1 \text{ -------- } N \tag{22}$$

$$\sum_{i=1}^{N} \lambda_i = 1 \tag{23}$$

$$\sum_{i=1}^{N} \lambda_i \, x_{\mathrm{i}} = x_{\mathrm{p}} \tag{24}$$

$$\sum_{i=1}^{N} \lambda_i \, y_i = y_p \tag{25}$$

and the variance of the estimation error is given by:

$$\sigma_p^2 = \sum_{i=1}^{N} \lambda_i \, \gamma_{ip} + \mu_0 + \mu_1 x_p + \mu_2 y_p \tag{26}$$

where γ are the variograms of residuals determined by the variographic analysis, i, j, p denote different points and μ_0, μ_1 and μ_2 are Lagrange multipliers.

REFERENCES

Aboufirassi, M. and Marino, M.A., 1983. Kriging of Water Levels in Souss Aquifer, Morocco. *J. Math. Geol.*, **15(4):** 537-551.

Aboufirassi, M. and Marino, M.A., 1984. Cokriging of Aquifer Transmissivities from Field Measurements of Transmissivity and Specific Capacity. *J. Math. Geol.*, **16(1):** 19-35.

Delfiner, P. and Delhomme, J.P., 1973. Optimum Interpolation by Kriging. In: Display and Analysis of Spatial Data, J.C. Davis and M.J. McCullough (eds.), 96-114, Wiley and Sons, London.

Delhomme, J.P., 1976. Application de la theorie des variables regionalisees dans les sciences de l'eau, Doctoral Thesis, Ecole Des Mines De Paris Fontainebleau, France.

Delhomme, J.P., 1978. Kriging in the Hydrosciences. *Advances in Water Resources*, 1 no. **5:** 252-266.

Delhomme, J.P., 1979. Spatial Variability and Uncertainty in Groundwater Flow Parameters: A geostatistical approach. *Water Resour. Res.* **15(2):** 269-280.

Gambolati, G. and Volpi, G., 1979(a). Groundwater Contour Mapping in Venice by Stochastic Interpolators, 1. Theory. *Water Resour. Res.*, **15(2):** 281-290.

Gambolati, G. and Volpi, G., 1979. A Conceptual Deterministic Analysis of the Kriging Technique in Hydrology. *Water Resour. Res.*, **15(3):** 625-629.

Marsily, G de., 1986. Quantitative Hydrogeology: Groundwater Hydrology for Engineers. Academic Press.

Marsily, G de., Lavedan, G., Boucher, M. and Fasanini, G., 1984. Interpretation of Interference Tests in a Well Field Using Geostatistical Techniques to Fit the Permeability Distribution in a Reservoir Model. Geostatistics for Natural Resources Characterization, part 2, edited by G. Verly et al., 831-849, D. Reidel, Hingham, Mass.

Matheron, G., 1965. Les variables regionalisèes et leur estimation. Masson, Paris.

Matheron, G., 1967. Elements pour une theorie des milieux poreux. Masson, Paris, 166 p.

Matheron, G., 1971. The Theory of Regionalized Variables and Its Application. Paris School of Mines, Cah. Cent. Morphologie Math., 5. Fontainebleau.

14 Application of Geostatistics in Optimal Groundwater Monitoring Network Design

Shakeel Ahmed, Dewashish Kumar and Aadil Nabi Bhat

Indo-French Centre for Groundwater Research
National Geophysical Research Institute, Hyderabad-500007, India

INTRODUCTION

Appropriate and adequate data are essential for the success of any scientific study such as groundwater hydrology. Scarcity of data and their collection on isolated location mainly in the field of hydrogeology makes it necessary to adopt special procedures such as geostatistical estimation technique for bridging the gap between field measurements and data requirements. However, these estimations are based on a crucial criterion of the structural analysis known as variography and obtaining a true and representative variogram is extremely ambiguous from limited field data. Cross-validation test to determine a representative and optimal variogram as well as to validate the other assumptions has been found very useful in case of hydrogeological parameters.

Ahmed (2001) used the application of Ordinary Kriging including variography in a case study on fluoride concentration. In addition to that, multivariate geostatistical techniques viz., Cokriging, Kriging with an external drift have found better applications. It is concluded that, depending upon the situation, geostatistical techniques could be applied at each step of hydrogeological modelling studies i.e., from data collection network design, parameter estimation to the fabrication and calibration of aquifer models.

According to Ahmed (2001), numerical simulation of flow and transport processes in an aquifer necessitates dividing and discretizing the natural heterogeneous system into a number of small volumes called mesh which are assumed to be uniform with almost no variation of the aquifer properties over it. To satisfy this condition, it is necessary to discretize the system into much finer and hence more number of grids. Although with the availability

of more powerful computers, computation with large number of grids/mesh is not a difficulty but the data preparation that is to assign the aquifer parameters to each grid/mesh becomes cumbersome. Thus an appropriate estimation procedure is required to provide an unbiased, minimum variance and with unique value over the entire area of the mesh.

Rouhani (1985) used composite programming with a combination of Geostatistics and multicriterion decision-making in optimizing network of measuring thickness and porosity of a two-layer aquifer system. Aspie and Barnes (1990) suggested the criterion by minimizing the expected cost of classification errors. Das (1995) developed an analytical method integrating the practical implementing aspects and applied to a multilayered groundwater flow system for contaminant detection. Agnihotri and Ahmed (1997) analyzed a number of ambiguities arising in the existing methods of data collection network design using a few worked examples. Hughes and Lettenmaier (1981) have suggested an algorithm to optimize the location of data collection points by minimizing the variance of the error in estimating the parameter over the entire area of the aquifer. Sophocleous et al. (1982) have applied the technique of Universal Kriging in analyzing the network of wells for water level measurement in Kansas, USA with respect to cost of the network and the accuracy obtained. However, it has been limited to the data regularly spaced along a square grid. Virdee and Kottegoda (1984) have proposed a map of kriging estimation error (σ_k) and located new measurement points at places where a high value of σ_k was calculated. They have applied this method to a network of transmissivity and water level measurements. This procedure has two drawbacks: (1) it is difficult to decide a limit to compare the σ_k values to, and (2) an additional point improves the estimation variance not only at that point but also at the neighbouring points forcing the procedure to work in an iterative way only. Carrera et al. (1984) proposed an iterative procedure based on non-linear programming to select the optimal location of measurement points and applied it to optimize monitoring fluoride concentration in the San Pedro River basin, Arizona. Bogardi et al.(1985) proposed a methodology combining two concepts: Geostatistics and Multicriterion decision making (MCDM) to design a regular observation network for spatially correlated and anisotropic parameter in a multiplayer aquifer system, where the composite solutions is quite robust with respect to variogram parameters and changes in the weight set assigned to the parameter. Dillon (1988), Rouhani (1985) and Rouhani and Hall (1988) have used the method of estimation variance reduction calculated at the centre of a set of discretized blocks in the area. Hudak and Loaiciga (1993) developed an analytical method integrating practical implementation aspects applied to a multilayered groundwater flow system for contaminant detection. Gao et al. (1996) presented a simple algorithm to rapidly compute the revised kriging estimation variance when new sample locations are added. Moreover, we believe that this algorithm is useful only if a network has to be improved

from a sparse one by adding additional measurement points. This algorithm may not be useful for optimizing a dense network either by deleting the measurement points or by shifting them. Bras and Rodriguez-Iturbe (1976) applied multivariate estimation theory to obtain the aerial mean precipitation of an event over a fixed area considering the spatial uncertainty and correlation of process, correlation in measurement errors and non-homogeneous sampling costs.

One of the challenges of monitoring network design in a fractured rock setting is the heterogeneity of the rocks. Nativ et al. (1999) summarize the activities and problems associated with the monitoring of contaminated groundwater in porous, low permeability fractured chalk in the Negev Desert, Israel. Mayer et al. (1994) have recently presented a related methodology for designing a monitoring network for plume detection that is based on finding an optimal design that considers three objectives: minimizing the number of monitoring wells, maximizing the probability of detecting a contaminant leak and minimizing the expected area of contamination at the time of detection. They develop examples based on a two-dimensional areal flow model and examine the factors influencing trade-offs between the three design objectives. The intention in their work is to illustrate a decision model for evaluating monitoring network designs at waste management facilities that overlie fractured bedrock.

There is a recent work also on Optimization techniques applied in solving groundwater flow management problems (Ahlfeld et al., 2002). Ahlfeld et al., in their work, used simple and advanced methods of linear optimization techniques and includes also sensitivity and range analysis. MODOFC software uses optimization techniques to find the best combination of pumping rates and well locations to achieve criteria specified by the user. The response of the groundwater system is modelled using the groundwater flow simulator. Design criteria can be specified that encompass construction and operation costs, pumping rates and volumes, water level elevations and groundwater flow directions. However, the use of hydraulic head surface is the simplest and quickest means of flow analysis and provide the most accurate flow representation.

According to Bogardi et al. (1985), the observation network design itself may involve the following interrelated factors: (1) observation effort (cost, time, instrumentation, etc.); (2) relative importance of the various parameters; (3) the different geostatistical properties of the parameters; and (4) estimation accuracy or error criteria for the various parameters. The key precondition for using geostatistics for observation network design is that the variograms be available for the design parameters. Clearly if no observation network exists, no variogram based on sample information over the entire area can be available. For any network design model, one must have some information on the overall areal variation of the parameter to be observed even if no "hard" data set, that is, sample information on such variation exists.

The applicability and usefulness of kriging as a tool for network design has been recognized. The success of kriging is primarily based upon taking into account the structural aspects, such as correlations of geological formations. One of the most interesting features of kriging, as pointed out by Matheron (1963), is that the variance of estimation, which measures the uncertainty of the estimate, can be computed before the actual measurements are available. This feature suggests its application to the design of measurement networks, namely to locate measurement points in such a way that the estimation variance is minimized. Hughes and Lettenmaier (1981) pointed out that kriging should be more useful for network design than for estimation. Frequently, measurement points are located by random search procedures. The estimation variance is computed for each set of measurement points and the set that gives the smallest estimation variance is accepted (Journel and Huijbregts, 1978).

ESTIMATION VARIANCE REDUCTION APPROACH IN OPTIMAL NETWORK DESIGN

Geostatistical estimation variance reduction, cross validation techniques etc. are a few procedures that could study adequacy of a given monitoring network and could evolve an optimal monitoring network with some given constraints. The advantage of the geostatistical estimation technique is that the variance of the estimation error could be calculated at any point without having the actual measurement on that point say a well. Thus the benefits to be accrued from an additional measurement could be studied prior to its measurements. A few new procedures have been developed using geostatistical technique so that the number of monitoring wells was reduced without loosing the scientific/ monitoring benefits. It is difficult to define or generalize the necessary and/ or sufficient data for a particular study but availability of adequate measurements to capture the variability of the parameter is the key for a successful scientific study. Large amount of measurements will make the study easy but the project extremely ill-favoured or uneconomic but less number of data will make the study gloomy. It is difficult but important to determine the optimal requirement of data for any study. Often it depends on the scientific objective of the study also. The main objectives of the geostatistical optimization of the monitoring network have been that the monitored parameter should:

- Represent the true variability of the parameter under study and,
- Provide its estimate on unmeasured locations with a desired accuracy in the form of the variance of the estimation error.

Thus the entire area is usually divided into reasonably finer grid and the variance of the estimation error are calculated through a suitable kriging technique and the same are compared with the pre-decided or desired limit of the variance of the estimation error. Thus depending on the outcome of

the comparison, a network is categorized into dense, sparse or near optimal. The network is iteratively optimized either by discarding, adding or shifting the measurement points.

The theory of regionalized variable using kriging was used to analyse the water level from 56 observation wells, with the grid size of 500 m × 500 m. Following norms are calculated by comparing the σ_c (cut off standard deviation) values with σ_i values all over the area.

Mean value of σ_i as $< \sigma_i >$ (1)

No. of grids (M) where $\sigma_i > \sigma_c$ (2)

Sum of the Squared Difference (SSD) = $\Sigma(\sigma_i - \sigma_c)^2$ where $\sigma_i > \sigma_c$ (3)

If the network is dense, the value of M and SSD will both be zero and measurement points can be discarded starting from the location with the least σ_i. If the network is sparse, M and SSD will be non-zero and positive and their magnitude directly relates to the sparseness of the network. New measurement points can be added at the highest σ_i areas. The monitoring network need not be dense or sparse but it may not be still optimal as per the desired accuracy/constraints. In that case values of M and SSD will be moderately positive and the network could be optimized by shifting the measurement points.

The following ordinary kriging equation was used in estimation:

$$Z(x_o) = \sum_{i=1}^{n} \lambda_i Z_i \tag{4}$$

$$\sum_{j=1}^{n} \lambda_j \gamma_{ij} + \mu = \gamma_{io},\ i = 1,\ldots\ldots\ldots n \tag{5}$$

$$\sum_{i=1}^{n} \lambda_i = 1 \tag{6}$$

$$\sigma_k^2 = \sum_{i=1}^{n} \lambda_i \gamma_{io} + \mu \tag{7}$$

where $Z(x_o)$ is the estimated value of the variable at the point x_o and x_o is the spatial coordinate. The λ, γ, σ_k^2 and μ are the kriging weight, variogram, kriging variance and Lagrange multiplier respectively. Krignet using ordinary kriging equation was used to analyze the 56 data points and based on the norms as shown in Table 1 and after comparing the different norms the particular well was not considered for monitoring purpose. The criterion for rejecting a well(s) was that the different norms should not differ much from the standard situation when all 56 wells were present. The procedure was repeated by removing a single well, two wells, three wells and four wells taken at a time (Table 1).

OPTIMAL MONITORING NETWORK DESIGN IN MAHESHWARAM WATERSHED FOR WATER LEVEL

Optimal water level monitoring network design is an important step for better analyzing the aquifer behaviour by using the geostatistical method in an unbiased way and to monitor the optimal network without loosing the scientific benefits. Water level data was used in optimizing the monitoring network of observation wells. A number of bore-wells (56) based on geomorphology, land use and other variations were selected to have a first hand network for measurement of water levels. The existing network consisted of 56 bore-wells (Fig. 1) out of which 25 (IFP) were specially drilled for monitoring the water levels and 31 (IFW) were selected from the existing irrigation wells. The analysis of the variance of the estimation error obtained using kriging technique on a suitably finer grid in the entire area has been the basis to discard some of the private irrigation wells. The wells were discarded in such a way that the variance of the estimation error does not

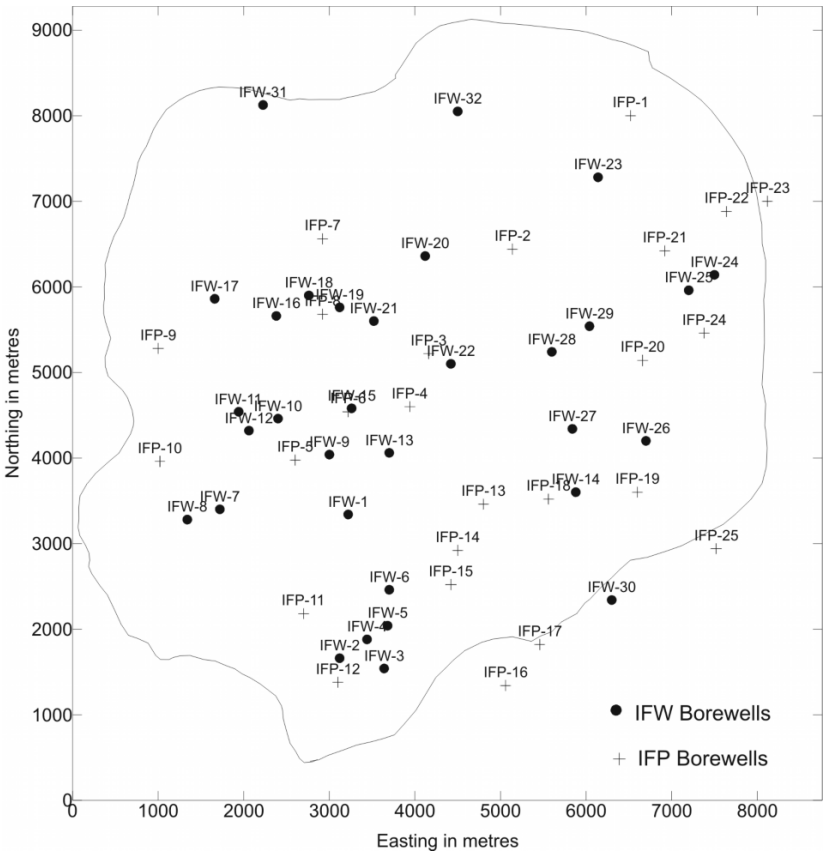

Figure 1. Location of bore-wells.

exceed a predecided value i.e., the network was designed based on ordinary kriging by analyzing the sum of square difference and the mean standard deviation, keeping the cut off standard deviation (σ_c) at the lowest i.e., σ_c = 3. Thus after a few iterations, a network of 40 monitoring wells have been evolved consisting all 25 specially drilled observation wells and 15 private irrigation wells keeping the variance of the estimation error within the desired limit. Monitoring through an optimal network can reduce the amount of data required while providing the desired accuracy and a few simple procedures have been developed for a geostatistical optimization of the monitoring network in this study. Also the use of common variogram reduces half of the estimation procedure for estimating water levels for various time periods. The network of 56 wells was thus modified in order to obtain optimum observation well for monitoring purpose taking into consideration the scientific importance so that the water level could be measured in least possible time and also to reduce the cost involved in water level data collection.

Table 1: Variogram, $\gamma(h) = 0 + 148$ sph(3500)

Sl. No.	*Sigma (σ)*	*Sigma(σ) Bar*	$S_K > S_C$	*For total nodes of 227*	*Deleted Well No.*	*Data Points*
1	3	5.03	1780	195	----	56
2	3	5.06	1800	196	IFW-3	55
3	3	5.04	1780	195	IFW-4	55
4	3	5.04	1780	195	IFW-5	55
5	3	5.05	1790	196	IFW-6	55
6	3	5.06	1800	196	IFW-3,4	54
7	3	5.05	1780	196	IFW-4,5	54
8	3	5.06	1790	196	IFW-5,6	54
9	3	5.07	1810	196	IFW-3,5	54
10	3	5.08	1810	197	IFW-3,6	54
11	3	5.05	1790	196	IFW-4,6	54
12	3	5.09	1820	197	IFW-3,5,6	53
13	3	5.08	1820	197	IFW-3,4,5	53
14	3	5.08	1810	197	IFW-3,4,6	53
15	3	5.12	1840	198	IFW-3,4,5,6	52
16	3	5.04	1780	196	IFW-10	55
17	3	5.05	1790	195	IFW-11	55
18	3	5.04	1780	195	IFW-12	55
19	3	5.06	1790	196	IFW-10,11	54
20	3	5.05	1780	197	IFW-10,12	54
21	3	5.07	1800	196	IFW-11,12	54
22	3	5.05	1790	196	IFW-16	55
23	3	5.10	1880	197	IFW-17	55
24	3	5.04	1780	195	IFW-18	55

(*contd.*)

Sl. No.	*Sigma (σ)*	*Sigma(σ) Bar*	$S_K > S_C$	*For total nodes of 227*	*Deleted Well No.*	*Data Points*
25	3	5.14	1910	197	IFW-16,17	54
26	3	5.06	1790	197	IFW-16,18	54
27	3	5.11	1880	197	IFW-17,18	54
28	3	5.04	1780	195	IFW-19	55
29	3	5.05	1780	195	IFW-21	55
30	3	5.05	1790	195	IFW-22	55
31	3	5.06	1790	196	IFW-19,21	54
32	3	5.05	1790	195	IFW-19,22	54
33	3	5.07	1800	195	IFW-21,22	54
34	3	5.06	1800	196	IFW-7	55
35	3	5.08	1860	197	IFW-8	55
36	3	5.16	1980	197	IFW-7,8	54
37	3	5.09	1840	196	IFW-23	55
38	3	5.05	1790	195	IFW-24	55
39	3	5.04	1780	196	IFW-25	55
40	3	5.07	1800	197	IFW-24,25	54
41	3	5.07	1800	196	IFW-28	55
42	3	5.06	1790	195	IFW-29	55
43	3	5.12	1850	196	IFW-28,29	54
44	3	5.07	1800	196	IFW-27	55
45	3	5.04	1780	196	IFW-14	55
46	3	5.08	1810	197	IFW-27,14	54
47	3	5.07	1810	197	IFW-26	55
48	3	5.10	1860	196	IFW-30	55
49	3	5.03	1780	196	IFW-15	55
50	3	5.08	1800	198	IFW-4,5,6	53
51	3	5.08	1810	197	IFW-14,28	54

It was therefore proposed that a systematic redesign of the network of 40 wells be undertaken in order to examine its adequacy for monitoring the wells within the watershed. This was achieved by optimizing the information gained from each observation well and modifying by decreasing the number of observation wells in order to upgrade the accuracy of the estimates.

MONITORING OF WELLS IN THE STUDY AREA

Water level monitoring was started during January 2000 from 31 wells; later 25 wells were also monitored for analyzing the water level variability in the fractured rock aquifer (Fig.1). These wells were monitored manually in the first week during each month. The water level measurements also tell us about the extent of exploitation of groundwater in a watershed. The water level decreases consistently in the watershed. In all 56 wells were monitored

regularly each month (Fig.1). The water level varies from 580 m to 640 m (amsl) which follows the topography of the area.

DISCUSSION AND CONCLUSIONS

The standard deviation maps (Figs 2 and 3) obtained by 56 observation wells and also the optimal number of 40 observation wells obtained after optimal network design from the area with grid size of 500 m × 500 m looks very similar which shows that the network so finally obtained after geostatistical optimization reproduce the complete water level fluctuation of the watershed. The statistics of standard deviation (σ) obtained after using krignet (Table 2) shows in good agreement with both cases i.e., when there are 56 and 40 observation wells. This has also been tested in a smaller grid of grid size 250 m × 250 m. The final map shows the optimized well location (Fig. 4). Similar work was carried out by Sophocleous et al. (1982). In their work the error analysis produced by universal kriging indicates that a significant reduction in the number of wells could be achieved by employing

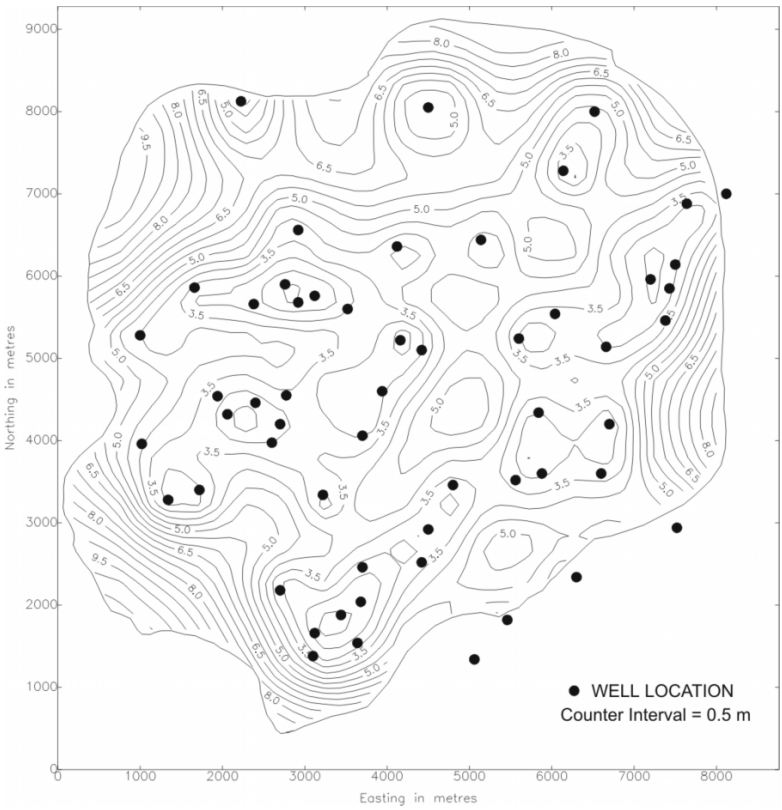

Figure 2. Contour map of sigma (in m) with 56 measurements points (500 m × 500 m).

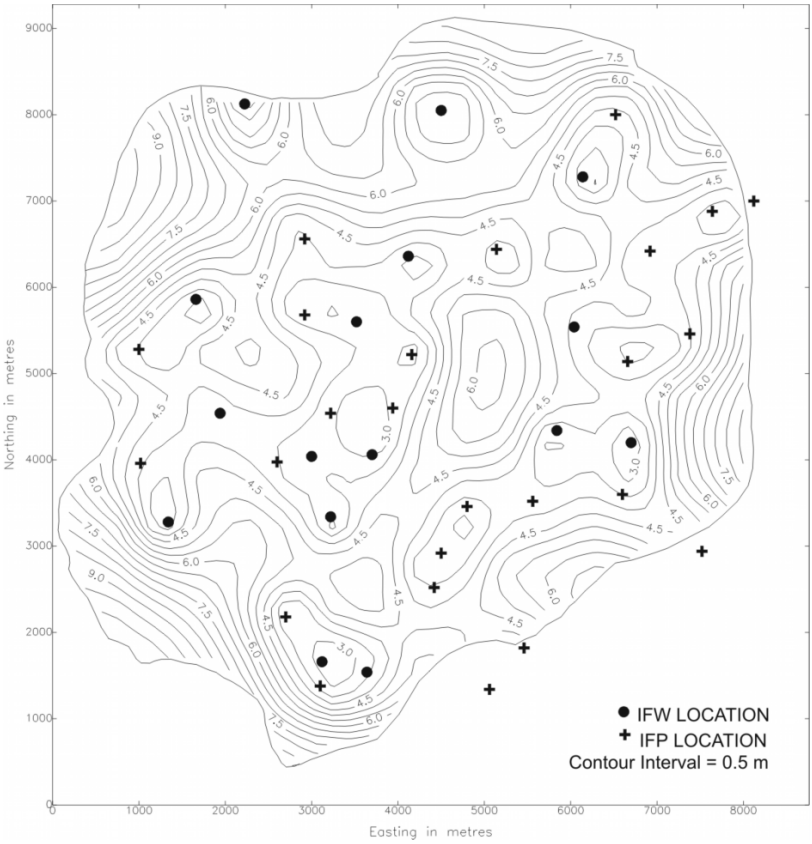

Figure 3. Contour map of sigma (in m) with 40 measurement points (500 m × 500 m)

a regular 4-mile (6.4 km) network, without affecting the present level of accuracy. It also indicates that it is not practical to reduce the estimation error in the water table surface uniformly throughout the region because to do so would increase the cost of monitoring wells drastically. For example, reducing the presently existing error by 50 percent throughout the area would require 16 times more wells than the currently existing well network.

Table 2: Comparison of σ_k for the existing and revised network

Grid Size	*Total Measurement Point*	*Min.*	*Max.*	*Mean*	*Variance*
500 m × 500 m	56	1.56	10.30	5.03	3.78
500 m × 500 m	40	2.34	10.17	5.32	3.19
250 m × 250 m	56	1.53	11.82	5.49	3.84
250 m × 250 m	40	1.57	11.56	5.77	3.26

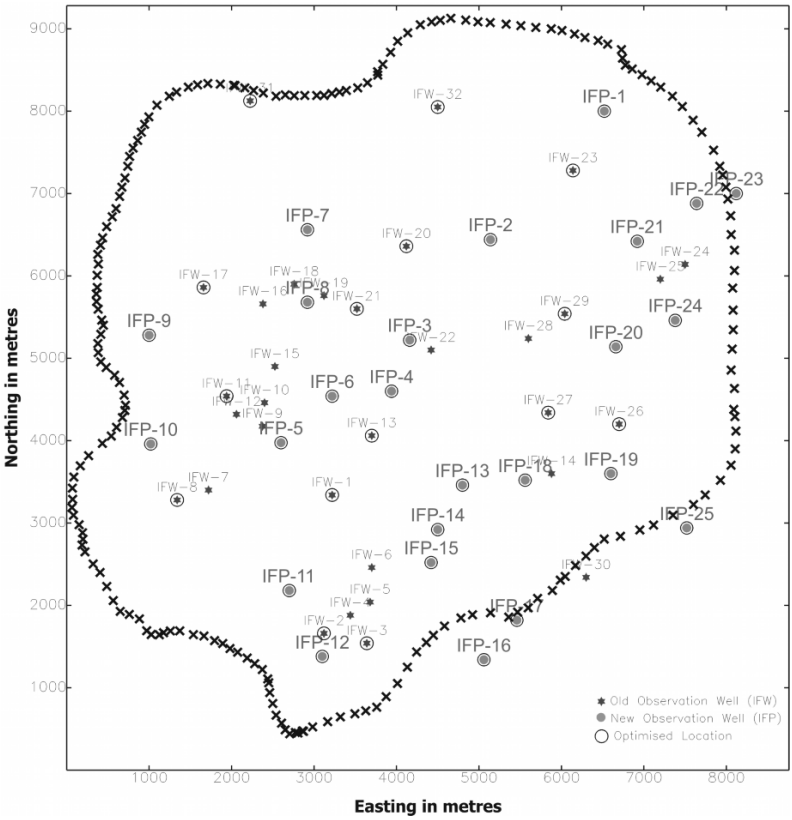

Figure 4. Optimized well location after geostatistical optimization.

It was also conveyed that the error analysis produced by universal kriging indicates that most of the increase in estimation error in the water table surface occurs within a short distance of the observation wells. The error map is a very powerful tool that can be used to evaluate the reliability of features on a map produced by universal kriging (Olea and Davis, 1977). The error map and the semivariogram also can be used to determine where more information is necessary to refine the map and to estimate the number of additional measurements that will be needed. In this way, regionalized variable theory provides criteria by which future measurements can be planned in order to achieve specified levels of reliability. The estimation error can be reduced to prescribed limit by taking more measurements in critical areas.

REFERENCES

Agnihotri, V. and Ahmed, S., 1997. Analyzing Ambiguities in the Data Collection Network Design by Geostatistical Estimation Variance Reduction Method. *Journal of Environmental Hydrology*, **5:** 1-13.

Ahlfeld, David P. and Mulligan, Ann E., 2002. Optimal Management of Flow in Groundwater Systems. *Hydrological Sciences-Journal-des Sciences Hydrologiques*, **47(3):** 538.

Ahmed, S., 2001. Rationalization of Aquifer Parameters for Aquifer Modelling including Monitoring Network Design. Modelling in Hydrogeology. UNESCO International Hydrological Programme. Allied Publishers Limited, 39-57.

Aspie, D. and Barnes, R.J., 1990. Infill Sampling Design and the Cost of Classification Errors. *Math. Geology*, **22(8):** 915-932.

Bogardi, I., Bardossy, A. and Duckstein, L., 1985. Multicriterion Network Design Using Geostatistics. *Water Resour. Res*. **21(2):** 199-208.

Bras, R.L. and Rodriguez-Iturbe I., 1976. Network Design for the Estimation of Areal Mean of Rainfall Events. *Water Resour. Research* **12(6):** 1185-1195.

Carrera, J., Usunoff, E. and Szidarovszky, F., 1984. A Method for Optimal Observation Network Design for Groundwater Management. *Journal of Hydrology*, **73:** 147-163.

Das, S., 1995. Manual: Hydrograph Network Stations, Central Groundwater Board, New Delhi.

Dillon, P.J., 1988. Quantitative Methods for Monitoring Network Design—Future directions. Hydrology and Water Resources Symposium, ANU, Canberra, 1-3 Feb.

Gao, H., Wang, J. and Zhao, P., 1996. The updated Kriging Variance and Optimal Sample Design. *Math. Geol*., **28(3):** 295-313.

Hudak, P.F. and Loaiciga, H.A., 1993. An Optimization Method for Monitoring Network Design in Multilayered Groundwater flow system. *Water Resour. Research*. **29(8):** 2835-2845.

Hughes, J.P. and Lettenmaier D.P., 1981. Data Requirements for Kriging: Estimation and Network design. *Water Resour. Research*, **17(6):** 1641-1650.

Journel, A.G. and Huijbregts, Ch J., 1978. Mining Geostatistics. Academic Press: London, 26-95.

Matheron, G., 1963. Traité de Géostatistique appliquée. Mémoires du BRGM, No. 14, Edition Technip.

Mayer, P.D., Valocch, A.J. and Eheart, J.W., 1994. Monitoring Network Design to Provide Initial Detection of Groundwater Contamination. *Water Resour. Res.*, **30(9):** 2647-2659.

Nativ, R., Adar, E.M. and Becker, A., 1999. Designing a Monitoring Network for Contaminated Ground Water in Fractured Chalk. *Groundwater*, **37(1):** 38-47.

Olea, R.A. and Davis, J.C., 1977. Regionalized Variables for Evaluation of Petroleum Accumulation in Magell Basin, South America. *American Association of Petroleum Geology Bulletin*, **61(4):** 558-572.

Rouhani, S., 1985. Variance Reduction Analysis, *Water Resources Research*, **21(6):** 837-846.

Rouhani, S. and Hall-Timothy-J., 1988. Geostatistical Schemes for Groundwater Sampling. *Jr. of Hydrology*, **103(1-2):** 85-102.

Sophocleous, Marios, E. Paschetto and Olea, R.A., 1982. Groundwater Network Design for Northwest Kansas, Using the Theory of Regionalized Variables. *Groundwater*, **20(1):** 48-58.

Virdee, T.S. and Kottegoda, N.T., 1984. A Brief Review of Kriging and Its Application to Optimal Interpolation and Observation Well Selection, *Hydrological Sciences Jr*. **29(4):** 367-387.

15 Reconstruction of Water Level Time Series in an Aquifer Using Geostatistical Technique

Dewashish Kumar and Shakeel Ahmed

Indo-French Centre for Groundwater Research
National Geophysical Research Institute, Hyderabad-500007, India

INTRODUCTION

Water level is the only parameter that is measured from the aquifer directly and also depicts the dynamics of the aquifer. It is measured normally in static condition but in spite of all precautions taken while measuring the water level there are data gaps. In aquifer modelling, particularly in the calibration of the model in transient condition, a sufficiently long time series of water level is required on all the wells that are used as control points. So to deal with two different situations that are to have a sufficiently long time series of water level at any well, geostatistics was applied to fill the data gap, at the time when the water level could not be measured. With this we obtained a mixed time series of water level at any well containing measured water levels without any error term and the estimated water level with estimation errors at uniform frequency.

A geostatistical technique from the theory of regionalized variables was first documented by Matheron (1963). The theory of regionalized variables very well applied to groundwater hydrology are by Delhomme (1978), Gambolati and Volpi (1979), Marsily (1986), Isaaks and Srivastava (1989) and Kitanidis (1997) and many others. This theory of regionalized variables has been applied here in analyzing time variant parameter, the water level data. As this parameter is very important in understanding the dynamics as well as stress-strain behaviour of the aquifer, it is of utmost importance that it should be available in adequate interval of time. This was used during calibration of the aquifer model.

In the present study, water level data from IFP wells (Fig. 1) was used from November 2000 to August 2003. The water level was monitored from

25 wells every month during the first week in one day. Due to unavoidable circumstances few wells were not monitored during some months. By this process after three years there were data gaps for some of the wells during various months (Fig. 2). But the water level had to be known for those wells for all months to have a complete time series of water level. The data gaps from January 2000 to October 2000 were completed by geostatistical estimation using unbiased kriging estimation variance (Best Linear Unbiased Estimator BLUE, Kitanidis, 1997). After the estimation of the water level was made along with variance of estimation, it was plotted with complete data set along with estimation variance and the water level now available from January 2000 to August 2003.

STUDY AREA

The study area, Maheshwaram watershed, falls between the geographical coordinate 17° 06' 20" to 17° 11' 00" North latitude and 78° 24' 30" to 78° 29' 00" East longitude and is situated in Ranga Reddy district at about 30 km south of Hyderabad, Andhra Pradesh, India and covering an area of 55 km^2, is a typical watershed in a granitic terrain with outcrops, structural features and fissure systems (Fig. 1). The average annual rainfall of the area

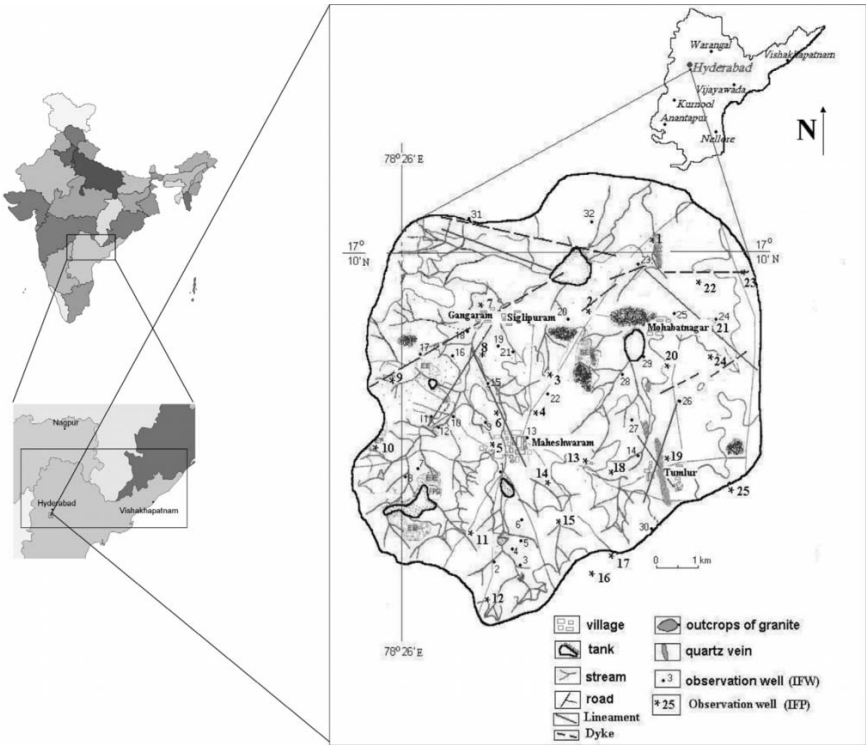

Figure 1. Study area and location of wells.

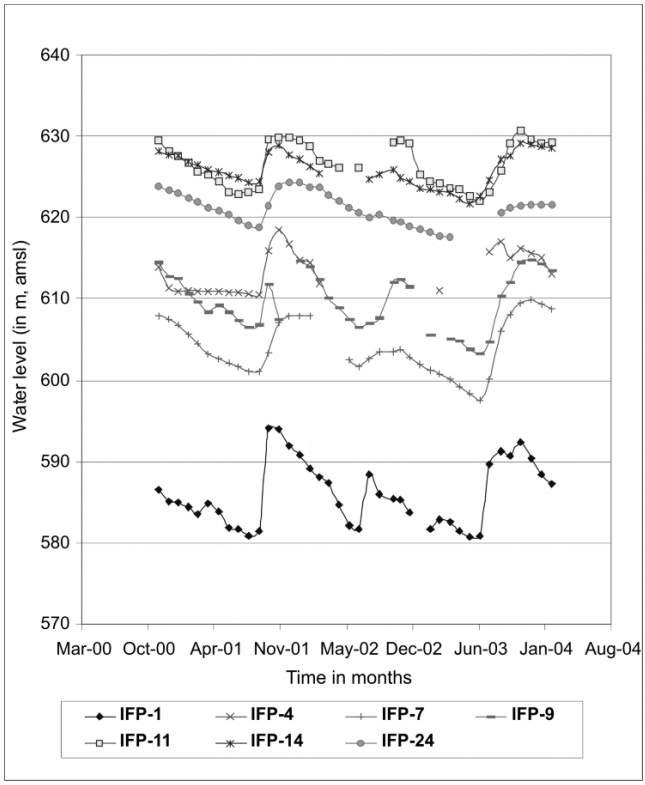

Figure 2. Hydrographs of observation wells showing data gap.

is 750 mm. The area lies at an elevation of 600 – 670 m above mean sea level. The area consists of hard crystalline rocks mainly pink and grey granites of Archaean age with variable density of fractures within the subsurface. Major part of the basin consists of biotite granite and some part of it consists of leucogranite. Foliation of the granites is traced on outcrops of granite. Granites with pegmatite show higher density of fractures/fissures. The area consists of dendritic drainage pattern. Major part of the basin is covered with pediplain having shallow weathering. Soil consisting of clay loam, red loam and sandy loam with variable thicknesses (0-1 m) form the top layer (Hashimi and Engerrand, 1999 and Krishnamurthy et al., 2000). Moderate thicknesses of weathered rocks are present and thus a two-tier system viz., weathered and fractured aquifers co-exist in the entire area. Due to over-exploitation of the groundwater resources, the water level has gone down and presently the groundwater occurrence is mainly in the fissured rock under unconfined conditions (Subrahmanyam et al., 2000; Maréchal et al., 2004).

Hydrogeology

Mostly horizontal fractures were prominent but vertical fractures are also contributing as a conduit for groundwater flow. Permeability in the fissured layer is greater than the laminated layer. In general the horizontal permeability is greater than the vertical permeability. Groundwater occurs mostly in fractured zone with water table varying between 11 and 20 m below ground level. The groundwater is mostly tapped by means of bore-wells in the fractured rock and the yield ranges between 1000-5000 gph (Subrahmanyam et al., 2000). High yields of some of the bore-wells are due to encountering of water bearing fractures at depths. Four sets of joints were mapped. The most prominent joint set strikes in N-S direction based on rose diagram plot. The strike varies between N10° E to N10° W. The joints are either vertical or dip very steeply towards west with angles 70° to 75°. The second set of joints strikes E-W with steep dips. The strike of this joint set varies between N80°W and N80°E. The third set of joints strike NE-SW direction with steep dips of 60°-75° towards SE. The fourth set of joints is more or less parallel to the surface of the topography. All these joints and its system help in the percolation of rainwater from the surface to the groundwater table. They also help to act as conduits for the transmission of groundwater. There are two sets of dykes and the strike of the first set is 90°-110° and the second set strikes 50° to 60°. There are joints and fractures in the dykes also but the surfaces are curved. These fracture also act as conduits for the transmission of surface water to the groundwater. The area is also traversed by lineaments, identified through the study of aerial photographs and land-sat imageries. The high yielding wells are aligned along these lineaments.

1-D Variogram of Water Level in Time

In the present study using the water level data from 25 experimental observation wells, the 1-D variogram analysis using Ahmed (1995, 2001) was carried out individually for each well to obtain the water level variability in time. The variogram was calculated and fitted with the theoretical variogram for all the monitoring wells (IFP's).

$$\gamma(\underline{d}) = \frac{1}{2N_{\mathrm{d}}} \sum_{i=1}^{N_{\mathrm{d}}} [h(t_{\mathrm{i}} + \hat{d}) - h(t_{\mathrm{i}})]^2 \tag{1}$$

where

$$d - \Delta d \le \hat{d} \le d + \Delta d \tag{2}$$

with

$$d = \frac{1}{N_{\mathrm{d}}} \sum_{i=1}^{N_{\mathrm{d}}} \hat{d}_{\mathrm{i}} \tag{3}$$

where $h(t)$ is water level, d is the initially chosen time interval between two measurement periods; t and $(t + d)$ with Δd as tolerance on time interval. d is actual time for the corresponding calculated variogram. N_d is the number of pairs for a particular time interval. The additional equation 3 avoids the rounding-off error of pre-decided time intervals (only multiples of the initial time is taken in conventional cases). It is very important to account for every term carefully while calculating variograms.

WATER LEVEL ESTIMATION IN TIME

Method of ordinary kriging was used for geostatistical estimation by Kitanidis (1997). Given the monsoon climate in the area and if there is no heavy pumping, the water level time series could be assumed stationary. The estimation were made at the month(s) for each well where the water level was not monitored due to some unavoidable cause e.g., due to the pumping in the nearby well. Thus the water level was estimated using the existing observed data and the corresponding best fitted variogram's model parameters. The estimation was made by ordinary kriging using equations 4-7 which gives the estimated water level along with the variance of the estimation error.

METHODOLOGY APPLIED

The theory of regionalized variable (Matheron, 1971) was used to analyze the water level data. The Ordinary Kriging equation used are as follows:

$$h^*(t_o) = \sum_{i=1}^{n} \lambda_i h(t_i) \tag{4}$$

$$\sum_{j=1}^{n} \lambda_j \gamma(t_i, t_j) + \mu = \gamma(t_i, t_o),\ i = 1, \ldots\ldots\ldots n \tag{5}$$

$$\sum_{i=1}^{n} \lambda_i = 1 \tag{6}$$

$$\sigma^2_{(t_o)} = \sum_{i=1}^{n} \lambda_i \gamma(t_i, t_o) + \mu \tag{7}$$

where $h^*(t_o)$ is the estimated value of water level at the point t_o and t_o is the particular time. The λ, γ, σ^2_o and μ are the kriging weight, variogram, kriging variance and Lagrange multiplier respectively.

RESULTS AND DISCUSSIONS

The estimated water level was combined with the existing (observed) water level data and the plot was made to view the trend of the water level fluctuations. The observed and the estimated water level were plotted along

with the standard deviation value at the estimated time. As an example two cases are shown (Figs 3 and 4). In the beginning the water level data was not available during the month of January 2000 to October 2000 for all the 25 wells as the wells were newly drilled and the regular monitoring was started from November 2000 and thus the estimated water level for this period shows higher standard deviation compared with the in-between estimated water level. In-between estimated water level for various wells for certain months shows good agreement with the observed water level and they follow the trend of the observed water levels. During aquifer modeling the output of the model is water level which has to be matched with the observed water levels and any deviation in the water level trend or abnormal behaviour of water level fluctuation can be justified by calibrating the model. These results were very useful during calibration of the numerical aquifer model in transient state with the updated data till July 2003 as the calibration

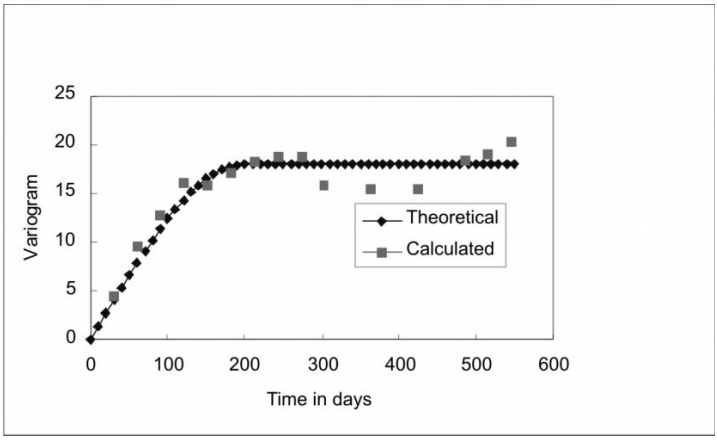

Figure 3a. 1-D variogram of water level for well IFP-1.

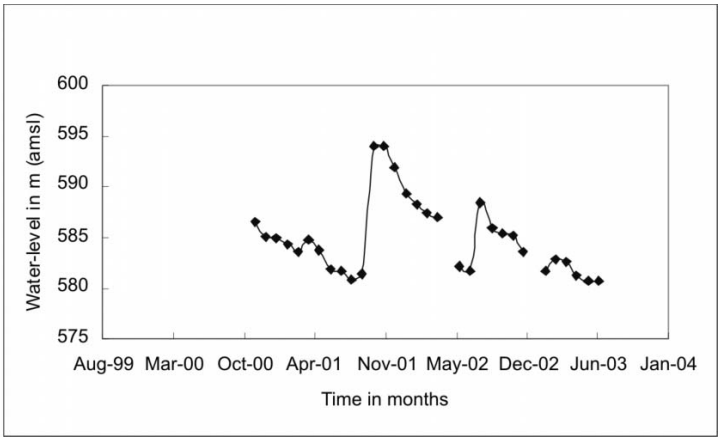

Figure 3b. Observed water level showing data gap for well IFP-1.

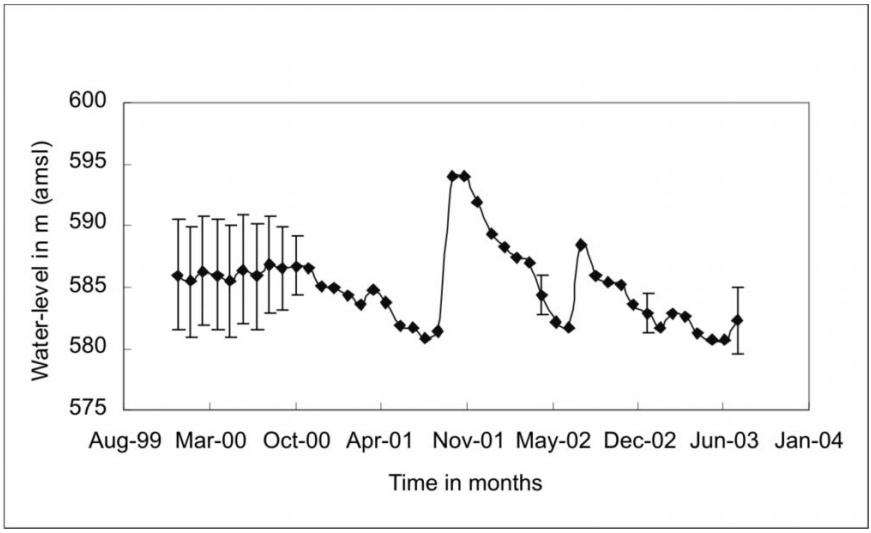

Figure 3c. Observed and estimated water level with standard deviation for well IFP-1.

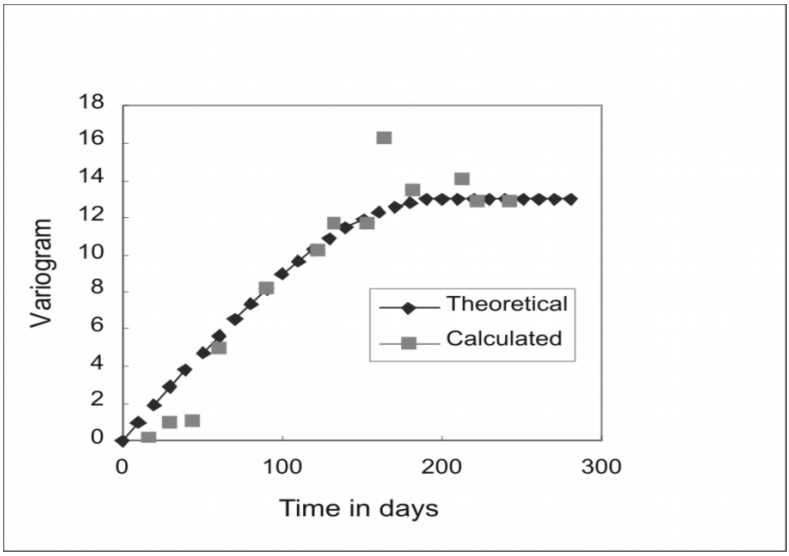

Figure 4a. 1-D variogram of water level for well IFP-9.

of the aquifer model in study area was completed up to July 2003 (Kumar, 2004). Thus these estimated water levels have helped for a reliable model

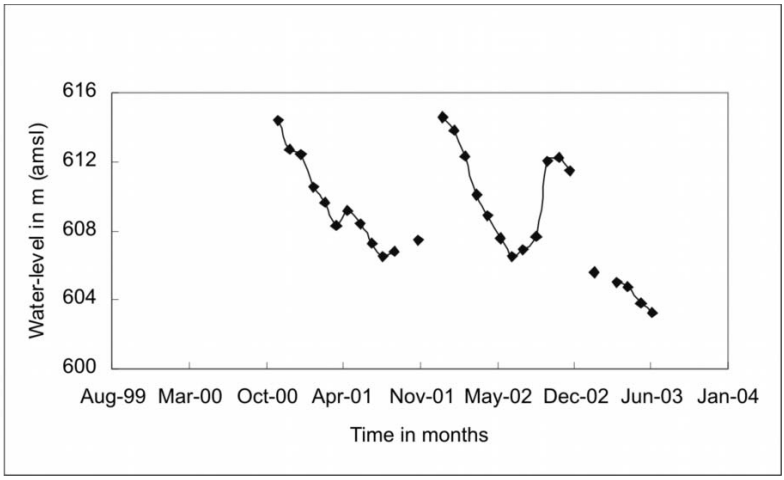

Figure 4b. Observed water level showing data gap for well IFP-9.

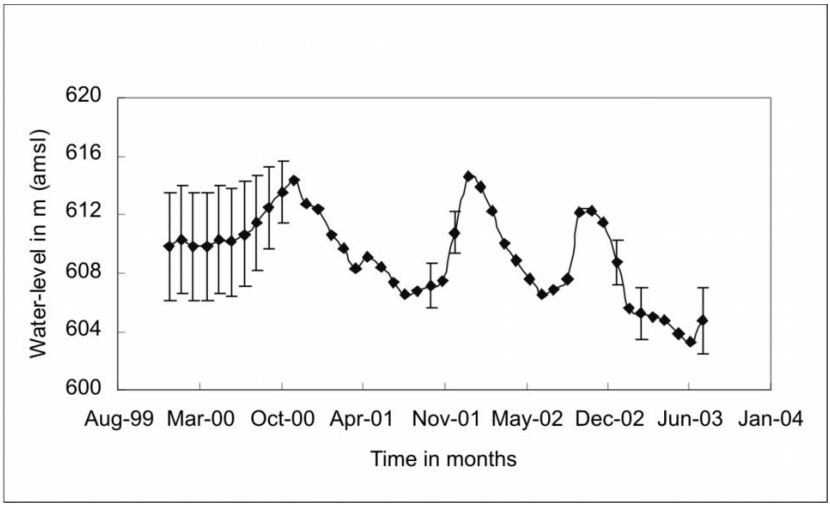

Figure 4c. Observed and estimated water level with standard deviation for well IFP-9.

calibration. Figure 5 shows the estimated water levels at three time steps well matched (very close to each other) with the calibrated water levels obtained from the aquifer model for well IFP-1. The estimation error bar helps in addition and suggests what percentage of various aquifer parameters should be increased or decreased in the aquifer model accordingly and also by keeping in mind the well condition in the field and its influence in the model. Similarly, Fig. 6 depicts that the estimated water levels are matched with the calibrated one but at one time step they are deviating. There could be many reasons for this type of situation.

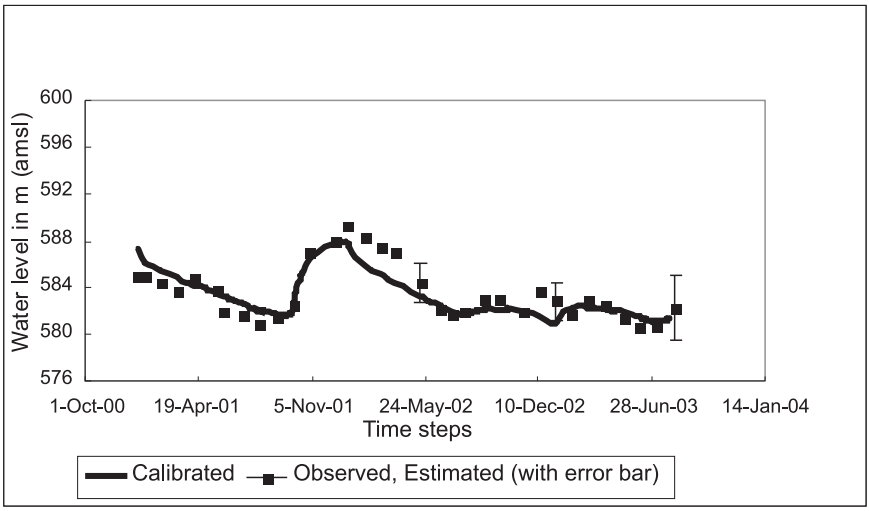

Figure 5. Calibrated, observed and estimated water levels with estimation error bar for well IFP-1.

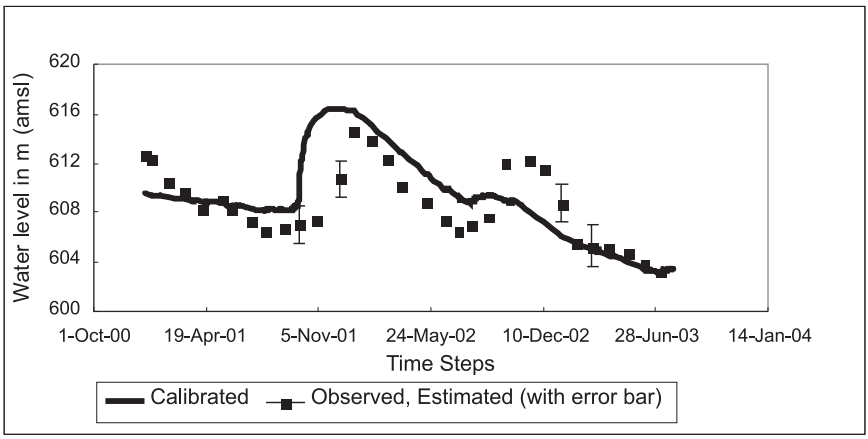

Figure 6. Calibrated, observed and estimated water levels with estimation error bar for well IFP-9.

CONCLUSIONS

Reconstructing of the time series of water levels in all the control wells has added value to the existing data sets. These estimated water levels value are plotted along with the variance of the estimation error (in the form of $\pm 2\sigma$, σ being the standard deviation of the estimated value) both in the form of upper and lower bound and with the observed water levels without error bar in the series as hydrographs. This study also helped or justified in an unbiased model calibration as the simulated hydraulic head obtained from

aquifer model could be verified against the value or a range that was absent otherwise. The plot of the error permits to check that the simulated heads are within the permissible limits. The water levels being non-stationary in nature, in general, are complicated applying geostatistical estimation in space. However, this problem is avoided in 1-D time domain as the same parameter shows recurring nature and until and unless extensive recharge or pumping conditions occur, the water level time series are stationary and provide a bounded variogram. Also the aquifer modelling provides water level as output at any time intervals often very close and theoretically the time interval should be kept close. However, in practice it is just not possible to monitor water levels at close intervals in the field and thus the present study provides a solution to match the two conditions.

REFERENCES

Ahmed, S., 1995. An Interactive Software for Computation and Modelling of a Variogram. *In*: Proc. of Conference on "Water Resources Management", Mousavi and Karamooz (eds), pp. 797-808, Isfahan University of Technology, Iran.

Ahmed, S., 2001. Program PLAYG, version 3.0, users guide, NGRI report.

Delhomme, J.P., 1978. Kriging in the hydrosciences. Advances in Water Resources, **1(5):** 252-266.

Gambolati, G. and Volpi, G., 1979. A Conceptual Deterministic Analysis of the Kriging Technique in Hydrology. *Water Resour. Res*., **15(3):** 625-629.

Hashimi, S.A.R. and Engerrand Carine, 1999. Groundwater Status Report for Maheshwaram Watershed, A.P., India. Technical Report No. APGWD - 1999.

Isaak, M. and Srivastava, R.M., 1989. An Introduction to Applied Geostatistics: Oxford Univ. Press, New York.

Kitanidis, P.K., 1997. Introduction to Geostatistics: Application to Hydrogeology. Cambridge University Press.

Krishnamurthy, N.S., Kumar, D., Negi, B.C., Jain, S.C., Dhar, R.L. and Ahmed, S., 2000. Electrical Resistivity Investigations in Maheswaram Watershed, Andhra Pradesh, India. Technical Report No. NGRI-2000-GW-287.

Kumar, D., 2004. Conceptualization and Optimal Data Requirement in Simulating Flow in Weathered-Fractured Aquifers for Groundwater Management, Ph.D. Thesis, Osmania University, Hyderabad, India, 263 pp.

Maréchal, J.C., Dewandel, B., Subrahmanyam, K., 2004. Use of Hydraulic Tests at Different Scales to Characterize Fracture Network Properties in the Weathered-fractured Layer of a Hard rock Aquifer. *Water Resour. Res*. **40:** W11508, 1-17.

Marsily, G de., 1986. Quantitative Hydrogeology: Groundwater Hydrology for Engineers. Academic Press: 286-329.

Matheron, G., 1971. The Theory of Regionalized Variables and Its Application. Paris School of Mines, Cah. Cent. Morphologie Math., 5. Fontainebleau.

Matheron, G., 1963. Traité de Géostatistique appliquée. Mémoires du BRGM, No. 14, Edition Technip.

Subrahmanyam, K., Ahmed, S. and Dhar, R.L., 2000. Geological and Hydrogeological Investigations in the Maheshwaram Watershed, R.R. Dist., Andhra Pradesh, India. Technical Report No. NGRI-2000-GW-292.

16 Governing Equations of Groundwater Flow and Aquifer Modelling Using Finite Difference Method

Shazrah Owais, S. Atal and P.D. Sreedevi

Indo-French Centre for Groundwater Research
National Geophysical Research Institute, Hyderabad-500007, India

INTRODUCTION

Groundwater, the term used for water occurring below the ground surface, is an important constituent of hydrological cycle and is the major source of water supply in various sectors. Due to over exploitation, mainly because of high population growth rates and extensive agricultural uses, there has been a growing concern about the water resources. For groundwater assessment and management it is essential to have a thorough understanding of complex processes viz., physical, chemical and/or biological occurring in the system. To understand these complexities groundwater model plays an important role. Groundwater models are simplified, conceptual representations of a part of the hydrologic cycle. They are primarily used for hydrologic prediction and for understanding hydrologic processes. During the last few decades there has been continuous improvement in the development of groundwater models. In the beginning groundwater models concentrated mainly on the flow behaviour in groudwater system while recent attempts are made to have full check on the water quality problem and to simulate the contaminant migration in groundwater. Now-a-days models range from simple two-dimensional analytical groundwater flow models to complex three-dimensional numerical groundwater flow and solute transport models.

DARCY'S LAW

More than a century ago, French Engineer Henry Darcy investigated the flow of water through a horizontal bed of sand to be used for filtration. In

1856 he published the mathematical law that is the basis for understanding all groundwater flow, and later named after him as *Darcy's Law*. Darcy's results were published consisting of 647 pages as a report titled "*Les Fontaines Publiques de la Ville de Dijon*". His experiment resulted in the formulation of a mathematical law that describes fluid motion in porous media. Darcy's law is the fundamental relationship that we use to understand the movement of fluids in the Earth's crust. He states, "The saturated flow of water through a column of soil is directly proportional to the head difference and inversely proportional to the length of the column".

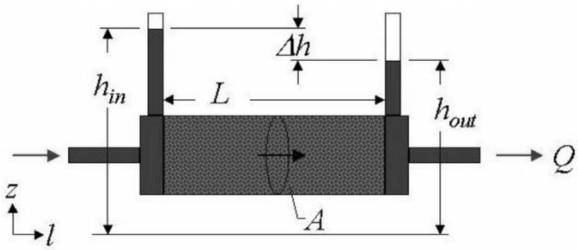

Figure 1. Experimental set-up for demonstrating Darcy's Law.

In mathematical form we can write as

$$Q \propto \Delta h$$

$$Q \propto 1/l$$

$$Q \propto A$$

So we can say, $Q \propto A\ \Delta h/l$

Now for 1-D flow

$$Q = -K(A\ \Delta h/l) \tag{1}$$

where Q = volumetric flow rate (m^3/s), A = flow area perpendicular to l (m^2), K = hydraulic conductivity (m/s), l = flow path length (m), h = hydraulic head (m), and Δ = denotes the change in h over the path l.

In differential form we can rewrite it as $Q = -K\ A\ (dh/dl)$ (2)

The minus sign on the right-hand term reflects that the hydraulic head always decreases in the direction of flow. In other words, fluid moves downhill from regions of high potential energy to regions of low potential energy.

Darcy's Velocity

The velocity v is known as Darcy velocity because it assumes that flow occurs through the entire cross section of the material without regard to solids and pores.

So $v = Q/A$

or $v = (-KA\ dh/dl)/A$

So $$v = -k\ dh/dl \quad (3)$$

Here the flow is limited to the pore space only so the average interstitial velocity

$$v = Q/\alpha A$$

where α is porosity.

Limits of Darcy's Law

Darcy's law has both upper and lower limits of applicability; it does not hold at very high fluid velocities. The nature of flow is quantified by the Reynolds Number. It is expressed as,

$$(\text{Re}) = \rho v d/\mu \quad (4)$$

(It is a dimensionless ratio)

where, v is the velocity (m/s), ρ is the fluid density (kg/m^3), μ is the fluid viscosity (kg/m/s), and d is the diameter of pipe (m).

Experimental evidence indicates that Darcy's Law is valid as long as Re does not exceed a critical value (between 1 and 10). The law holds for low velocity and high gradient.

EQUATIONS OF GROUNDWATER FLOW

Groundwater moves from areas of higher elevation or higher pressure/ hydraulic head (recharge areas) to areas of lower pressure or elevation/ hydraulic head. Permeable material contains interconnected cracks or spaces that are both numerous enough and large enough to allow water to move freely. In some permeable materials groundwater may move several metres a day; in other places, it moves only a few centimetres in a century. The direction of groundwater flow normally follows the general topography of the land surface. The groundwater movement is governed by established hydraulic principles.

Derivation of Groundwater Flow Equation

The groundwater flow equation is often derived for a small representative elemental volume (REV)—a cube, where the properties of the medium are assumed to be effectively constant. A mass balance is calculated on the water flowing in and out of this small volume, the flux terms in the relationship being expressed in terms of head by using the Darcy's law.

The volume of REV (V) = $\Delta X \Delta Y \Delta Z$ (5)

Let q be the specific discharge, so the rate of flow of water through this REV can be expressed in terms of three components viz., q_x, q_y, q_z. According to the Mass Balance equation outflow minus inflow is equal to the change in storage, i.e.,

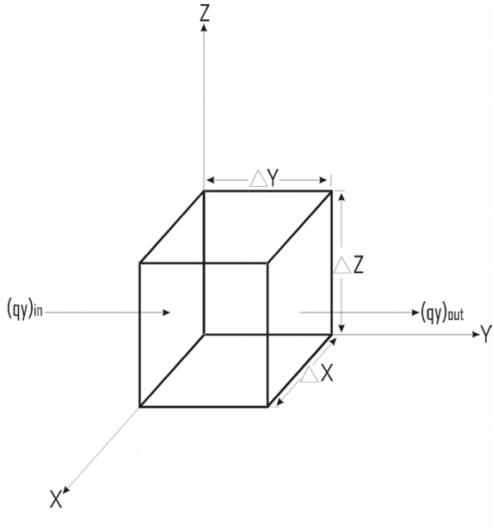

Figure 2. Mass Balance Diagram.

$$(q_{\text{out}} - q_{\text{in}}) = \text{Change in storage}$$

Now let us consider the flow along y-axis of the REV.

Influx to the elemental volume through the face, $\Delta X \Delta Z = (q_y)_{\text{in}}$

Flux out = $(q_y)_{\text{out}}$

Volumetric outflow rate – Volumetric inflow rate

$$= [(q_y)_{\text{out}} - (q_y)_{\text{in}}] \times \Delta X \Delta Z$$

Or

$$= \frac{[(q_y)_{\text{out}} - (q_y)_{\text{in}}] \times \Delta X \Delta Y \Delta Z}{\Delta Y}$$

So change in flow rate along y-axis is given as

$$= \frac{\partial q_y}{\partial y} \times \Delta X \Delta Y \Delta Z \tag{6}$$

Similarly change in flow rate along x-axis and z-axis is given as:

$$= \frac{\partial q_x}{\partial x} \times \Delta X \Delta Y \Delta Z \tag{7}$$

and

$$= \frac{\partial q_z}{\partial z} \times \Delta X \Delta Y \Delta Z \tag{8}$$

Now the *total change in flow rate = change in storage*

We can allow the possibility of source or sink of water within an elemental volume. The volumetric elemental volume is expressed as $R' \Delta X \Delta Y \Delta Z$, i.e.,

$$\left(\frac{\partial q_x}{\partial x}+\frac{\partial q_y}{\partial y}+\frac{\partial q_z}{\partial z}\right)\Delta X\Delta Y\Delta Z - R'\Delta X\Delta Y\Delta Z = \text{Change in storage} \tag{9}$$

The specific change in storage (Ss) is defined as the volume of water released from storage per unit change in head (h) per unit volume of aquifer.

i.e.,
$$Ss = -\frac{\Delta V}{\Delta h\Delta X\Delta Y\Delta Z} \tag{10}$$

Now the rate of change of storage is given by,

$$\frac{Ss}{\Delta t} = -\frac{\Delta V}{\Delta t\Delta h\Delta X\Delta Y\Delta Z}$$

Or,
$$\frac{\Delta V}{\Delta t} = -Ss\Delta X\Delta Y\Delta Z\frac{\Delta h}{\Delta t}$$

So
$$\frac{\Delta V}{\Delta t} = -Ss\Delta X\Delta Y\Delta Z\frac{\partial h}{\partial t} \tag{11}$$

where $\Delta V/\Delta t$ is rate of change in storage.

Now putting eq. (11) in eq. (9) we get;

$$\left(\frac{\partial q_x}{\partial x}+\frac{\partial q_y}{\partial y}+\frac{\partial q_z}{\partial z}\right)\Delta X\Delta Y\Delta Z - R'\Delta X\Delta Y\Delta Z = -Ss\Delta X\Delta Y\Delta Z\frac{\partial h}{\partial t}$$

Or,
$$\left(\frac{\partial q_x}{\partial x}+\frac{\partial q_y}{\partial y}+\frac{\partial q_z}{\partial z}\right) - R' = -Ss\frac{\partial h}{\partial t}$$

Or,
$$\left(\frac{\partial q_x}{\partial x}+\frac{\partial q_y}{\partial y}+\frac{\partial q_z}{\partial z}\right) = -Ss\frac{\partial h}{\partial t} + R' \tag{12}$$

R' is expressed as source or sink to aquifer.

Now from Darcy's Law we know that $q_x = -K_x\dfrac{\partial h}{\partial x}$

Similarly $q_y = -K_y\dfrac{\partial h}{\partial y}$ and $q_z = -K_z\dfrac{\partial h}{\partial y}$

Substituting for q_x, q_y, q_z in eq. (12) we get

$$\frac{\partial}{\partial x}\left(-K_x\frac{\partial h}{\partial x}\right)+\frac{\partial}{\partial y}\left(-K_y\frac{\partial h}{\partial y}\right)+\frac{\partial}{\partial z}\left(-K_z\frac{\partial h}{\partial z}\right) = -Ss\frac{\partial h}{\partial t} + R'$$

On solving L.H.S. of above equation we get,

$$\left[\frac{\partial h}{\partial x}\times\frac{\partial\left(-K_{\mathrm{x}}\right)}{\partial x}+\left(-K_{\mathrm{x}}\right)\frac{\partial}{\partial x}\left(\frac{\partial h}{\partial x}\right)\right]$$
$$+\left[\frac{\partial h}{\partial y}\times\frac{\partial\left(-K_{\mathrm{y}}\right)}{\partial y}+\left(-K_{\mathrm{y}}\right)\frac{\partial}{\partial y}\left(\frac{\partial h}{\partial y}\right)\right]$$
$$+\left[\frac{\partial h}{\partial z}\times\frac{\partial\left(-K_{\mathrm{z}}\right)}{\partial z}+\left(-K_{\mathrm{z}}\right)\frac{\partial}{\partial z}\left(\frac{\partial h}{\partial z}\right)\right]$$

Since K_{x}, K_{y}, K_{z} are very very small, their values can be neglected; therefore,

$$-\left(K_{\mathrm{x}}\frac{\partial^2 h}{\partial x^2}+K_{\mathrm{y}}\frac{\partial^2 h}{\partial y^2}+K_{\mathrm{z}}\frac{\partial^2 h}{\partial z^2}\right)=-Ss\frac{\partial h}{\partial t}+R'$$

or
$$\left(K_{\mathrm{x}}\frac{\partial^2 h}{\partial x^2}+K_{\mathrm{y}}\frac{\partial^2 h}{\partial y^2}+K_{\mathrm{z}}\frac{\partial^2 h}{\partial z^2}\right)=Ss\frac{\partial h}{\partial t}-R' \tag{13}$$

Equation (13) is the governing equation of the groundwater flow.

Partial Differential Equation of 2nd Order for Groundwater Flow

$$\frac{\partial}{\partial x}\left(K_{\mathrm{x}}h\frac{\partial h}{\partial x}\right)+\frac{\partial}{\partial y}\left(K_{\mathrm{y}}h\frac{\partial h}{\partial y}\right)+\frac{\partial}{\partial z}\left(K_{\mathrm{z}}h\frac{\partial h}{\partial z}\right)=\pm R'+Ss\frac{\partial h}{\partial t} \tag{14}$$

where s = storage coefficient; h = hydraulic head; and $\pm R$ = Input/Output.

For Confined Aquifer

The Groundwater flow equation for confined aquifer is

$$T_{\mathrm{x}}\frac{\partial^2 h}{\partial x^2}+T_{\mathrm{y}}\frac{\partial^2 h}{\partial y^2}=\pm R'+s\frac{\partial h}{\partial t} \tag{15}$$

where, T_{x} and T_{y} is transmissivity in x and y direction and is equal to

$$T = K{*}b = (\mathrm{m/day})(\mathrm{m}) = \mathrm{m}^2/\mathrm{day}$$

where b is the saturated thickness of the aquifer.

For Unconfined Aquifer

If the aquifer becomes unconfined, $b = h$, so $T{=}K{*}h$ and then the above equation reduces to:

$$K_x h \frac{\partial^2 h}{\partial x^2} + K_y h \frac{\partial^2 h}{\partial y^2} = \pm R' + Ss \frac{\partial h}{\partial t} \tag{16}$$

where h is the water level function of x, y.

Boundary Conditions

Boundary conditions specify how an aquifer interacts with the environment outside the model domain. To ensure a unique solution to a problem at least one unique boundary condition is specified. There are four basic types of boundary conditions:

No Flow Boundaries

There are physical or hydrological barriers that prevent water from flowing into or out of the model domain. No flow boundaries are specified either when defining the boundary of the model grid or by setting grid blocks as inactive (i.e. hydraulic conductivity = 0). This is a very special type of the prescribed flux boundary and is also referred to as no-flux, zero flux, impermeable, reflective or barrier boundary. In the analysis of model results, no flow boundaries are identical to streamlines. The natural groundwater divides or streamlines act as no flow boundaries.

Constant Head Boundary

A source of water has an invariant water level at the model boundary. This condition is used to model an aquifer in good communication with a lake, large river, or another external aquifer. This is also known as first type boundary condition, which is mathematically referred as Dirichlet boundary. The constant head boundary or prescribed boundaries can occur when surface water bodies such as rivers, lakes, canals, seacoast, impoundments and drains interact freely with the aquifer.

Mathematically, the constant head boundary condition is stated as

$$h(x) = h_0(x), \quad x \in \delta\Omega_1 \qquad \text{Dirichlet}$$

where h_0 is the specified head along the boundary segment $\delta\Omega_1$ of the modelled domain Ω.

Constant Flux Boundary

Entering or leaving the aquifer is constant/prescribed flux. This boundary condition is used to simulate rainfall or distributed discharge such as evaporation. It is also useful for specifying known recharge to the aquifer due to induced recharge or reticulation. This boundary condition is also referred to as second type boundaries, Neumann's condition or recharge boundaries.

$$\frac{\delta h(x)}{\delta n} = -K\frac{\delta h(x)}{\delta n}, x \in \delta\Omega_2 \qquad \text{Neumann}$$

where $\delta h(x)/\delta n$ is the specified outward normal gradient to the boundary segment $\delta\Omega_2$.

Stream or River Head Dependent Boundary

The rate of flow into or out of the aquifer is a function of the aquifer head, elevation of stream bed, and the leakage between the aquifer and the stream or river. This condition is used to model streams or small rivers in poor connection with the aquifer, upward leakage in artesian aquifers, drains and overlying aquitards. This is also known as third type boundary condition, mixed or Induced flux or mathematically Cauchi Condition/Robbins Condition.

$$\alpha h(x) + \beta\ \delta h(x)/\delta n = C_0, \quad x \in \delta\Omega_3 \qquad \text{Cauchi/Robbins}$$

where C_0 is specified function value along the boundary segment $\delta\Omega$ and α and β are specified functions.

GROUNDWATER MODELLING

Models are the tools or device that represents an approximation of a field situation or real system or natural phenomena. These models are applied to a variety of environmental problems especially for understanding and the interpretation of the issues having complex interaction of many variables in the system.

Groundwater flow models are used to calculate the rate and direction of movement of groundwater through aquifers and confining units in the subsurface. These calculations are referred to as simulations. The simulation of groundwater flow requires a thorough understanding of the hydrogeologic characteristics of the site. The hydrogeologic investigation should include a complete characterization of the following:

- Subsurface extent and thickness of aquifers and confining units (hydrogeologic framework),
- Hydrologic boundaries (also referred to as boundary conditions), which control the rate and direction of movement of groundwater,
- Hydraulic properties of the aquifers and confining units,
- A description of the horizontal and vertical distribution of hydraulic head throughout the modelled area for both beginning (initial conditions), equilibrium (steady-state conditions) and transitional conditions when hydraulic head may vary with time (transient conditions), and
- Distribution and magnitude of groundwater recharge, pumping or injection of groundwater, leakage to or from surface-water bodies, etc. (sources or sinks, also referred to as stresses). These stresses may be constant (unvarying with time) or may change with time (transient).

Groundwater modelling involves simulation of aquifer and its response to various input/output systems. Groundwater models have been applied to investigate a wide variety of hydrogeologic conditions. More recently, groundwater models are being applied to predict the fate and transport of contaminants for risk evaluation. Groundwater models represent or approximate a real system and are tools that help in the organization and understanding of hydrogeologic data or the prediction of future hydrogeologic events. Models are not substitute for field investigations, but should be used as supplementary tools.

Model Classification

Groundwater modelling helps in the analysis of many groundwater problems. In general, models are classified as Predictive, Interpretive and Generic types. Predictive model is used to understand the future availability of resources as well as aquifer responses under varied scenario and stress situation. Interpretive models are used to understand a system under different existing domain element such as how a system responds to different fracture densities and how a system would respond to recharge from a flood event? Generic type model helps in hypothesizing the situation. No calibration is required in case of such models.

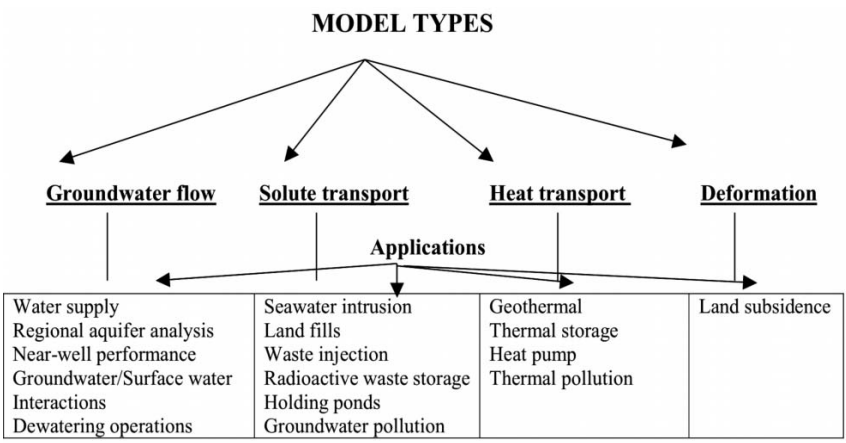

Figure 3. Types of groundwater models and typical applications

Further, on the basis of applications, four general types of groundwater models are identified (Fig. 3). The problem of water supply is normally described by one equation, usually in terms of hydraulic head. The resulting model providing a solution for this equation is referred to as *groundwater flow model*. If the problem involves water quality, then an additional equation to the groundwater flow equation must be solved for concentration of the chemical species. Such model is referred to as a *solute transport model*.

Problems involving heat also require an equation, similar to the solute transport equation, but now in terms of temperature. This model is referred to as a *heat transport model*. Finally, a *deformation model* combines a groundwater flow model with a set of equations that describe aquifer deformation. All of the models start with the basic equations of groundwater flow.

Models may be subdivided into those describing porous media and those describing fractured media. Large number of models have come up to resolve diverse type of hydrogeological problems. Some most widely used models are:

Physical Scale Model: is made from the same material as those of the natural system. Sand Models have been used for different types of hydrogeological studies such as dispersion, artificial recharge and seawater intrusion etc.

Analog Model: may be developed using electric circuits or viscous fluid flow as the governing equations of groundwater flow through porous media is similar to electricity through conductor. Two-dimensional groundwater flow can be analogous to the flow of a viscous fluid between two very closely spaced parallel plates. The model is known as Hele-Shaw model.

Fate and Transport Models: simulate the movement and chemical alteration of contaminants as they move with groundwater through the subsurface. These models require the development of a calibrated groundwater flow model or, at a minimum, an accurate determination of the velocity and direction of groundwater flow, which has been based on field data. Fate and transport models are used to simulate the following processes:

- Movement of contaminants by advection and diffusion,
- Spread and dilution of contaminants by dispersion,
- Removal or release of contaminants by sorption, or desorption, of contaminants onto, or from, subsurface sediment or rock, or
- Chemical alteration of the contaminant by chemical reactions, which may be controlled by biological processes, or physical chemical reactions.

In addition to a thorough hydrogeological investigation, the simulation of fate and transport processes requires a complete characterization of the following:

- Horizontal and vertical distribution of average linear groundwater velocity (direction and magnitude) determined by a calibrated groundwater flow model or through accurate determination of direction and rate of groundwater flow from field data,
- Boundary conditions for the solute,
- Initial distribution of solute (initial conditions),
- Location, history and mass loading rate of chemical sources or sinks,
- Effective porosity,
- Soil bulk density,

- Fraction of organic carbon in soils,
- Density of fluid,
- Viscosity of fluid,
- Longitudinal and transverse dispersivity,
- Diffusion coefficient,
- Chemical decay rate or degradation constant,
- Equations describing chemical transformation processes, if applicable, and
- Initial distribution of electron acceptors, if applicable.

Mathematical Models: are used to simulate the components of the conceptual model and include a single equation or set of governing equations that presents the processes occurring (e.g. groundwater flow, solute transport, etc.). The mathematical models rely upon the solution of the basic equations of groundwater flow, heat flow and mass transport. The simplest mathematical model of groundwater flow is Darcy's law. Darcy's law is an example of an Analytical Model.

Analytical Models: Analytical models are an exact solution of a specific, greatly simplified, groundwater flow or transport equation. The equation is a simplification of more complex three-dimensional groundwater flow or solute transport equations. Prior to the development and widespread use of computers, there was a need to simplify the three-dimensional equations because it was not possible to easily solve these equations. Specifically, these simplifications resulted in reducing the groundwater flow to one dimension and the solute transport equation to one or two dimensions. This resulted in changes to the model equations that include one-dimensional uniform groundwater flow, simple uniform aquifer geometry, homogeneous and isotropic aquifers, uniform hydraulic and chemical reaction properties, and simple flow or chemical reaction boundaries. Analytical models are typically steady state and one-dimensional, although selected groundwater flow models are two dimensional (e.g. analytical element models), and some contaminant transport models assume one-dimensional groundwater flow conditions and one-, two- or three-dimensional transport conditions. Well hydraulics models, such as the Theis or Neumann methods, are examples of analytical one-dimensional groundwater flow models. Because of the simplifications inherent with analytical models, it is not possible to account for field conditions that change with time or space. This includes variations in groundwater flow rate or direction, variations in hydraulic or chemical reaction properties, changing hydraulic stresses, or complex hydrogeologic or chemical boundary conditions.

Numerical Models: Numerical models are capable of solving the more complex equations that describe groundwater flow and solute transport. These equations generally describe multi-dimensional groundwater flow, solute transport and chemical reactions, although there are one-dimensional

numerical models. Numerical models use approximations (e.g. finite differences, or finite elements) to solve the differential equations describing groundwater flow or solute transport. The approximations require that the model domain and time be discretized. In this discretization process, a network of grid cells or elements represents the model domain, and time steps represent the time of the simulation.

The accuracy of numerical models depends upon the accuracy of the model input data, the size of the space and time discretization (the greater the size of the discretization steps, the greater the possible error), and the numerical method used to solve the model equations.

In addition to complex three-dimensional groundwater flow and solute transport problems, numerical models may be used to simulate very simple flow and transport conditions, which may just as easily be simulated using an analytical model. However, numerical models are generally used to simulate problems, which cannot be accurately described using analytical models.

Depending upon the numerical techniques employed in solving the mathematical model, there exists several types of numerical models such as Finite Difference Models, Finite Element Models, Boundary Element Models, Particle tracking models, Method of characteristic models, Random walk models and Integrated Finite Difference Models.

The main features of the various numerical models are:

- The solution is sought for the numerical values of state variables only at specified points in the space and time domains defined for the problems.
- The partial differential equations that represent balances of considered extensive quantities are replaced by a set of algebraic equation.
- The solution is obtained for a specified set of numerical values of the various model coefficients.

Because of the large number of equations that must be solved simultaneously, a computer programme is prepared.

Although a number of numerical techniques exist, only finite difference and finite element techniques have been widely used.

Finite Difference Method: L.F. Richardson, in his classic 1910 paper, introduced finite difference as a method to calculate approximately the solution of partial differential equations. A vast body of knowledge has been built up over the years concerning both the theoretical and applied aspects of these methods.

Fundamental to both the finite element and finite difference approaches to solving partial differential equations is the concept of discretization wherein a continuous domain is represented as a number of sub areas.

The basic idea of these finite difference methods is to replace derivatives at a point by ratios of the changes in appropriate variables over a small but finite interval.

Finite difference solution for partial differential equation: Anything moving on earth is governed by partial differential equation. To solve this partial differential equation we discretize the area into equal length area. There are two methods for solving this partial differential equations: the Explicit method and the Implicit method.

Here we will take the case of 1-D unsteady groundwater flow equation. It could be written as,

$$\frac{\partial u}{\partial t} = \frac{\partial^2 u}{\partial x^2} \tag{17}$$

$$\forall \leq 0\ x \leq 1,\ t \geq 0$$

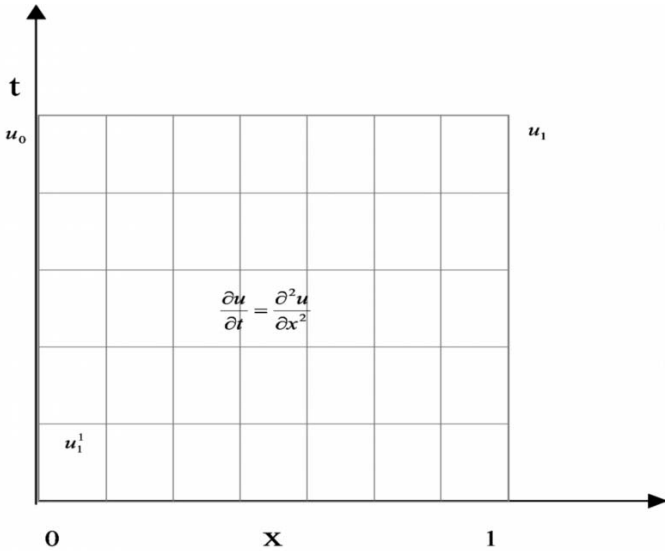

Figure 4. A grid for a finite difference solution.

Initial condition $u(x, 0) = u_0$

1st Boundary condition $u(0, t) = u_0$, $\forall\ t > 0$

2nd Boundary condition $u(1, t) = u_1$, $\forall\ t > 0$

Now we consider a function $f(a)$, which is smooth. Then, f may be expanded into Taylor series about a in the positive direction

$$f(a + h) = f(a) + hf'(a) + \frac{h^2}{2!} f''(a) + \text{----------}\ \infty \tag{18}$$

$$\frac{f(a+h) - f(a)}{h} = f'(a) + \frac{h}{2!} f''(a) + \frac{h^2}{3!} f''(a) + \text{---------}\ \infty$$

if $h << 0$ then,

$$f'(a) = \frac{f(a+h) - f(a)}{h} + O(h) \tag{19}$$

This is *forward difference approximation* with terms of order of h ($O(h)$). This term is known as truncation error having expressions (h^2) and higher power.

Similarly if we move to the negative direction then

$$f(a - h) = f(a) - hf'(a) + \frac{h^2}{2!} f''(a) - \text{----------}\infty \tag{20}$$

$$\frac{f(a-h) - f(a)}{h} = -f'(a) + \frac{h^2}{2!} f''(a) - \frac{h^2}{3!} f''(a) + \text{---------}\infty$$

or,
$$f'(a) = \frac{f(a) - f(a-h)}{h} + O(h) \tag{21}$$

This is *backward difference approximation.*

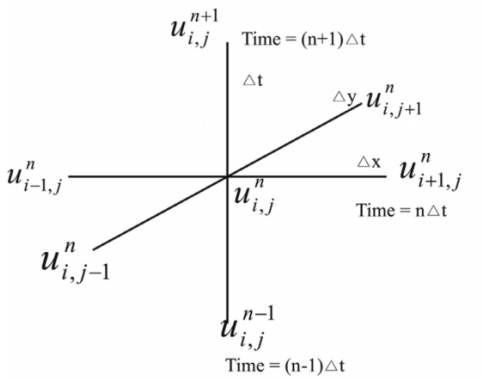

Figure 5. Notation for forward and backward simulation of the time derivative (modified after Bear, 1979).

Now by adding eqs. (18) and (20) we get

$$f(a + h) + f(a - h) = 2f(a) + \frac{2h^2}{2!} f''(a) + O(h^4)$$

or
$$\frac{f(a+h) + f(a-h) - 2f(a)}{h^2} = f''(a) + O(h^2)$$

$$f''(a) = \frac{f(a+h) + f(a-h) - 2f(a)}{h^2} + O(h^2) \tag{22}$$

And if we subtract eqs. (18) and (20) we will get

$$f(a+h) - f(a-h) = 2hf'(a) + \frac{h^3}{3!} f''(a) + \text{----------} \infty$$

So
$$f'(a) = \frac{f(a+h) - f(a)}{2h} + O(h^2) \tag{23}$$

This is the *central difference approximation.*

Now we have four equations with us:

$$f'(a) = \frac{f(a+h) - f(a)}{h} + O(h) \quad \text{forward difference approximation}$$

$$f'(a) = \frac{f(a) - f(a-h)}{h} + O(h) \quad \text{backward difference approximation}$$

$$f'(a) = \frac{f(a+h) - f(a-h)}{2h} + O(h^2) \quad \text{central difference approximation}$$

$$f''(a) = \frac{f(a+h) + f(a-h) - 2f(a)}{h^2} + O(h^2)$$

So finite difference formulas for the first- and second-order derivatives at (i, j) is,

$$f'(a) = \frac{f_{i+1,j} - f_{i,j}}{h} + O(h) \tag{24}$$

$$f'(a) = \frac{f_{i,j} - f_{i-1,j}}{h} + O(h) \tag{25}$$

$$f'(a) = \frac{f_{i+1,j} - f_{i-1,j}}{2h} + O(h^2) \tag{26}$$

$$f''(a) = \frac{f_{i-1,j} - 2f_{i,j} + f_{i+1,j}}{h^2} + O(h^2) \tag{27}$$

Method of Solution

The first step in obtaining a finite difference solution to eq.(17) is to superpose a grid on the region of interest in the *x-t* plain. Each intersection is called a 'node' or a mesh point.

An Explicit Approximation: Let us take a nodal point (u_i^n) anywhere on the grid, where '*n*' is the time interval and '*i*' is the space interval. Now using forward difference approximation method we have

$$\frac{u_i^{n+1} - u_i^n}{\Delta t} = \frac{u_{i+1}^n - 2u_i^n + u_{i-1}^n}{(\Delta x)^2} + O(\Delta t + \Delta x^2) \tag{28}$$

Now,
$$u_i^{n+1} = u_i^n + \frac{\Delta t}{(\Delta x)^2}\left[u_{i+1}^n - 2u_i^n + u_{i-1}^n\right]$$
$$= u_i^n + r\left[u_{i+1}^n - 2u_i^n + u_{i-1}^n\right] \tag{29}$$

where
$$r = \Delta t/(\Delta x)^2$$
$$u_i^{n+1} = r u_{i+1}^n + (1 - 2r)\, u_i^n + r u_{i-1}^n \tag{30}$$

This r will depend on interval levels which we assign for Δx and Δt. This is the Explicit method where the values unknown can be calculated from the known values of previous levels.

Stability Criterion: The Explicit method is stable if

$$\frac{\Delta t}{(\Delta x)^2} = 1/2$$

or,
$$0 < r < 0.5$$

One can see from the above conditions that Δt must be very small since $\Delta t \leq 1/2(\Delta x)^2$, and the number of computations required to reach a time level 't_m' are extremely large.

An Implicit Approximation: Here instead of forward difference approximation we use backward difference approximation. So we will have

$$\left(\frac{\partial u}{\partial t}\right)_i^n = \left(\frac{\partial^2 u}{\partial x^2}\right)_i^n$$

where, 'n' is the time interval and 'i' is the space interval.

Now writing the equation of backward difference approximation at $t = (n + 1)\Delta t$, we obtain for constant Δx

$$\frac{u_i^{n+1} - u_i^n}{\Delta t} = \frac{u_{i+1}^{n+1} - 2u_i^{n+1} + u_{i-1}^{n+1}}{(\Delta x)^2} O(\Delta t + \Delta x^2) \tag{31}$$

Here only one value is associated with previous time level and the three are associated with the present time level unlike Explicit method. Now assuming that the values u_i^n are known at all nodes at time $n\Delta t$, eq. (31) is a single equation containing three unknowns u_i^{n+1}, u_{i+1}^{n+1}, and u_{i-1}^{n+1}. We can, however, write equations for each node in the flow domain like eq. (31). Then since there is one unknown value of head, for time $(n+1)\Delta t$, at each node, we shall have a system of equations in which the total number of equation is equal to the total number of unknowns. Therefore now we can

be able to solve the entire set of equations, obtaining the new value u_i^{n+1} at each node i, therefore it is called Implicit method.

It has been deduced by comparing these two methods of solution, that though implicit method requires much more work in solving the set of simultaneous equations, it is unconditionally stable, regardless of the size of the time step Δt.

Crank-Nicolson Method

In an Implicit method, Δt can be chosen independent of Δx. Another refinement is possible. Generally the smaller the truncation error, the faster is the convergence of the finite difference equations to the differential equation. In Explicit and Implicit methods for the time derivative $\partial u/\partial t$ the truncation error was of the order of $0(\Delta t)$. If $\partial u/\partial t$ is replaced by the central difference, the truncation error associated with the time term would be reduced from $O(\Delta t)$ to $O\{(\Delta t)^2\}$. This was done by Crank-Nicolson and later on known as Crank-Nicolson method.

The Crank-Nicolson method is obtained by averaging the approximations $\partial^2 u/\partial x^2$ at n and n+1 time levels. Sometimes a weight λ ($0<\lambda<1$) is used here. We then obtain value for $\partial u/\partial t$ evaluated at (n+1/2)

$$\text{So} \quad \frac{u_i^{n+1}-u_i^n}{\Delta t}=\frac{\lambda\left(u_{i-1}^{n+1}-2u_i^{n+1}+u_{i+1}^{n+1}\right)+\left(1-\lambda\right)\left(u_{i-1}^n-2u_i^n+u_{i+1}^n\right)}{\left(\Delta x\right)^2} \tag{32}$$

The Explicit approximation is obtained by setting $\lambda = 0$ in eq. (12) and $\lambda = 1$ gives the *Implicit scheme*.

The Crank-Nicolson approximation is given by setting eq. (12) with $\lambda = ½$

$$\frac{u_i^{n+1}-u_i^n}{\Delta t}=\frac{1/2\left(u_{i-1}^{n+1}-2u_i^{n+1}+u_{i+1}^{n+1}\right)+1/2\left(u_{i-1}^n-2u_i^n+u_{i+1}^n\right)}{\left(\Delta x\right)^2} \tag{33}$$

This equation can be modified to treat the problems of unsaturated flow as well as saturated flow. Extension to more than one space dimension causes no difficulty.

CONCLUSION

The groundwater modelling is an efficient tool for the assessment and management of groundwater potential as well as pollution due to anthropogenic and/or natural causes. Model may be used to predict some future groundwater flow or contaminant transport condition. The model may also be used to evaluate different remediation alternatives, such as hydraulic containment, pump-and-treat or natural attenuation, and to assist with risk evaluation. In order to perform these tasks, the model, whether it is a

groundwater flow or solute transport model, must be reasonably accurate, as demonstrated during the model calibration process. However, because even a well-calibrated model is based on insufficient data or oversimplifications, there are errors and uncertainties in a groundwater-flow analysis or solute transport analysis that make any model prediction no better than an approximation. For this reason, all model predictions should be expressed as a range of possible outcomes, which reflect the uncertainty in model parameter values.

REFERENCES

Anderson, M.P. and Woessner, W.W., 1992. Applied Groundwater Modelling. Academic Press, New York.

Bear, J., 1979. Hydraulics of Groundwater. McGraw-Hill, New York. 576 pp.

Bear, J., Beljin, M.S. and Ross, R.R., (1992). Fundamentals of Groundwater Modelling. U.S. EPA.

Crank, J. and Nicolson, P. (1947). A Practical Method for Numerical Evaluation of Solutions of Partial Differential Equations of the Heat Conduction type. Proc. Camb. Phill. Soc., **43:** 50-67.

De Marsily, G. 1986. Quantitative Hydrogeology—Groundwater Hydrology for Engineers. Academic Press, inc., Paris.

Elango, L., 2005. Numerical Simulation of Groundwater Flow and Solute Transport. Allied Publishers, Chennai.

Fetter, C.W., 1992. Applied Hydrogeology. Prentice Hall.

Richardson, L.F. 1910. The Approximate Arithmetical Solution by Finite Differences of Physical Problems Involving Differential Equations, with an Application to the Stresses in a Masonry Dam. *Phil Trans. Royal Soc*. **A 210:** 307-357.

Rai, S.N., 2004. Role of Mathematical Modeling in Groundwater Resources Management. Sri Vinayaka Enterprises, Hyderabad

Richtmeyer, R.D. and Morton, K.W., 1967. Difference Methods for Initial Value Problems. New York, Interscience.

Todd, D.K., 1980. Groundwater Hydrology, second edition. John Wiley and Sons, New York. 535 pp.

17 Simulation of Flow in Weathered-Fractured Aquifer in a Semi-Arid and Over-Exploited Region

Shakeel Ahmed and P.D. Sreedevi

Indo-French Centre for Groundwater Research
National Geophysical Research Institute, Hyderabad 500 007, India

INTRODUCTION

The granites in and around Hyderabad, India, form part of the largest of all granite bodies recorded in Peninsular India. Alcaline intrusions, aplite, pegmatite, epidote, quartz veins and dolerite dykes traverse the granite. There are three types of fracture patterns (Fig. 1) in the area, viz. (i) mineralised or weathering fractures, (ii) fractures traversed by dykes, and (iii) late-stage fractures represented by joints. The vertical fracture pattern is partly responsible for the development of the weathered zone and the horizontal fractures are the result of the weathering. Hydrogeologically, the aquifer occurs both in the weathered zone and in the underlying weathered-fractured zone. The Maheshwaram watershed of about 53 km^2 in the Ranga Reddy district (Fig. 2) of Andhra Pradesh, India, is underlain by granitic rocks. This watershed is a representative Southern India catchment in terms of over-exploitation of its weathered hard rock aquifer, its cropping pattern, rural socio-economy, agricultural practices and semi-arid climate. The objective of this study is to develop and test well-suited modelling approaches to simulate the flow in the existing aquifer system that consist of two layers with any separating strata.

However, due to deep drilling and heavy groundwater withdrawal, the weathered zone has now become dry. About 150 dug-wells were examined and the nature of the weathering was studied. The weathered-zone profiles range in thickness from 1 to 5 m below ground level (bgl). They are followed by semi-weathered and fractured zones that reach down to 20 m bgl. Joints

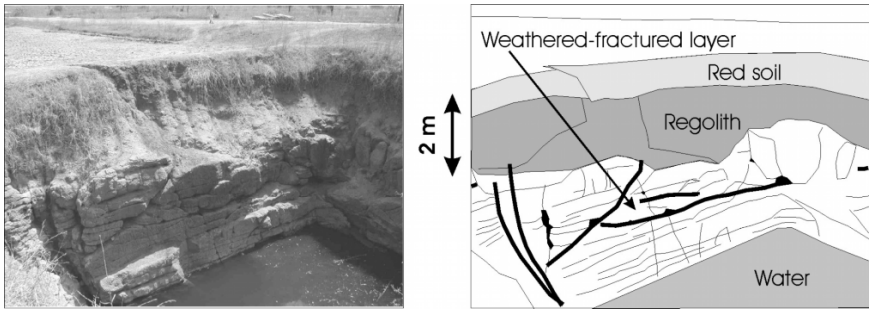

Figure 1. Cross-section of the typical substratum in a dug-well.

are well developed in the main directions: N 0°–15°E, NE-SW, and NW-SE that vary slightly from place to place. The groundwater flow system is local, i.e. with its recharge area at a topographic high and its discharge area at a topographic low adjacent to each other. Intermediate and regional groundwater flow systems also exist since there is significant hydraulic conductivity at depth. Aquifers occur in the permeable saprolite (weathered) layer, as well as in the weathered-fractured zone of the bedrock and the quartz pegmatite intrusive veins when they are jointed and fractured. Thus only the development

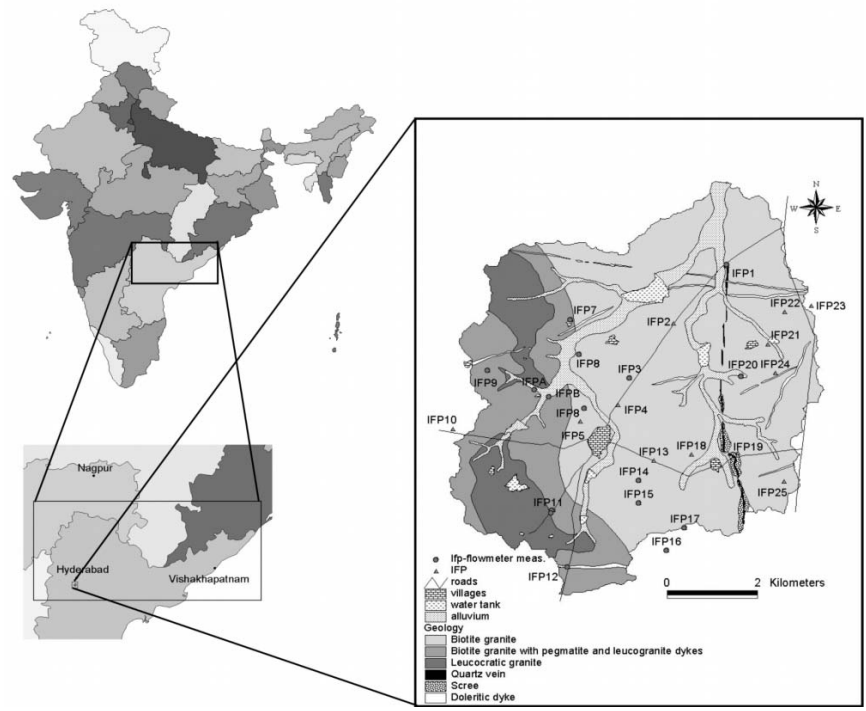

Figure 2. Maheshwaram hard rock watershed in Ranga Reddy Dist., Andhra Pradesh.

of the saprolite zone and the fracturing and interconnectivity between the various fractures allow a potential aquifer.

Mean annual rainfall is about 750 mm, the mean annual temperature is about 26 °C, although in summer, the maximum temperature can reach 45 °C. The resulting potential evaporation transpiration is 1,800 mm/year. The annual rainfall is around 750 mm and the recharge around 10-15 %.

NUMERICAL MODELLING OF AQUIFER FLOW IN MAHESHWARAM WATERSHED

The Maheshwaram watershed was modelled with the MARTHE software developed at the BRGM (French Geological Survey, Thiery, 1993). MARTHE is a transient hydrodynamic modelling code, representing three-dimensional and/or multi-layer flow in aquifers. The solution method uses finite differences with a rectangular grid and offers the possibility of having a free surface in a mesh of any layer.

Model Fabrication

The studied aquifer was represented by a two-layer aquifer flow system. The upper layer for the weathered zone, the lower one in the weathered-fractured granite represented as an equivalent porous medium. Each layer was divided into 5,272 square meshes with a 100-m side (Fig. 3). Layer 1 is unconfined and layer 2 is confined but may become unconfined when layer 1 becomes dry. The MARTHE code is used with its coupled climatic-balance model (GARDENIA: Thiéry and Boisson, 1991). The groundwater flow in the Maheshwaram watershed is simulated in transient regime in order to represent the piezometric variations observed in the wells in the studied area from January 2001 to July 2003.

The thickness of the weathered layer was estimated by kriging from the measurements made in the 25 existing lithologs and the Vertical Electrical Sounding (VES) interpretations (Krishnamurthy et al., 2000). The geometry of the weathered-fractured granite layer was deduced jointly from the total depth of the 900 inventoried wells in the watershed after removing the wells with a total depth of more than 70 m and from the result of the VES. Figure 4 shows the aquifer geometry with bottom of each layer above mean sea level.

Boundary Conditions

The topographical limits of the watershed were taken as the groundwater divides (no-flow boundaries), except at the northern limit where a non-perennial stream at the outlet of the watershed can evacuate the surface

water. At this location, the hydraulic heads were prescribed and set the average of the 2000-2002 measured field values.

The streams flow only during heavy rainfall for a few hours in a year due to very rare runoff. That is why, as a first approximation, the role of the hydrographic network in recharging the aquifer is assumed to be negligible. The hydrographic network in the study area includes a few low order ephemeral streams connected to a surface storage tank. The assumption of a negligible recharge is justified in this study as the flow in the streams are rare and fast as well as the vertical hydraulic conductivity of the tank beds are almost zero due to thick silting.

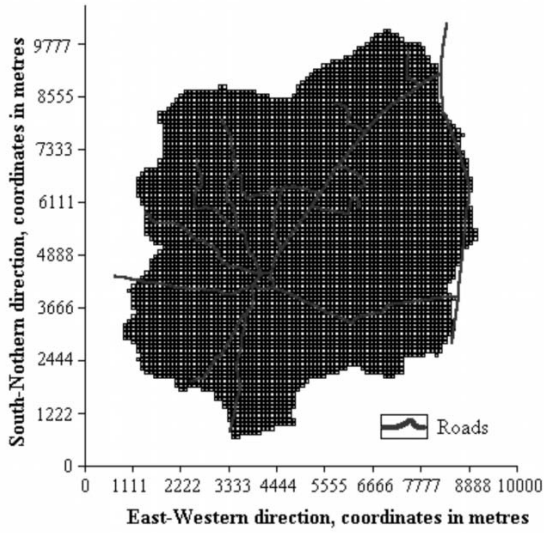

Figure 3. Grid of the watershed, layer 1 is similar to layer 2.

Aquifer Characteristics

No hydraulic tests could be carried out in the first layer because, during the project period (1999 to 2003), the water table was constantly deeper than the bottom of the weathered zone. Thus the hydraulic parameters for that layer were estimated from the literature. The hydraulic conductivities chosen for the weathered layer were selected according to two assumptions:

- The hydraulic conductivity values must be in the range of the ones found in the literature for the same type of geology;
- The variability in hydraulic conductivity is based on the conceptual model of the hydrogeological functioning of weathered-rock/hard rock aquifers in Africa proposed by Chilton and Foster (1995).

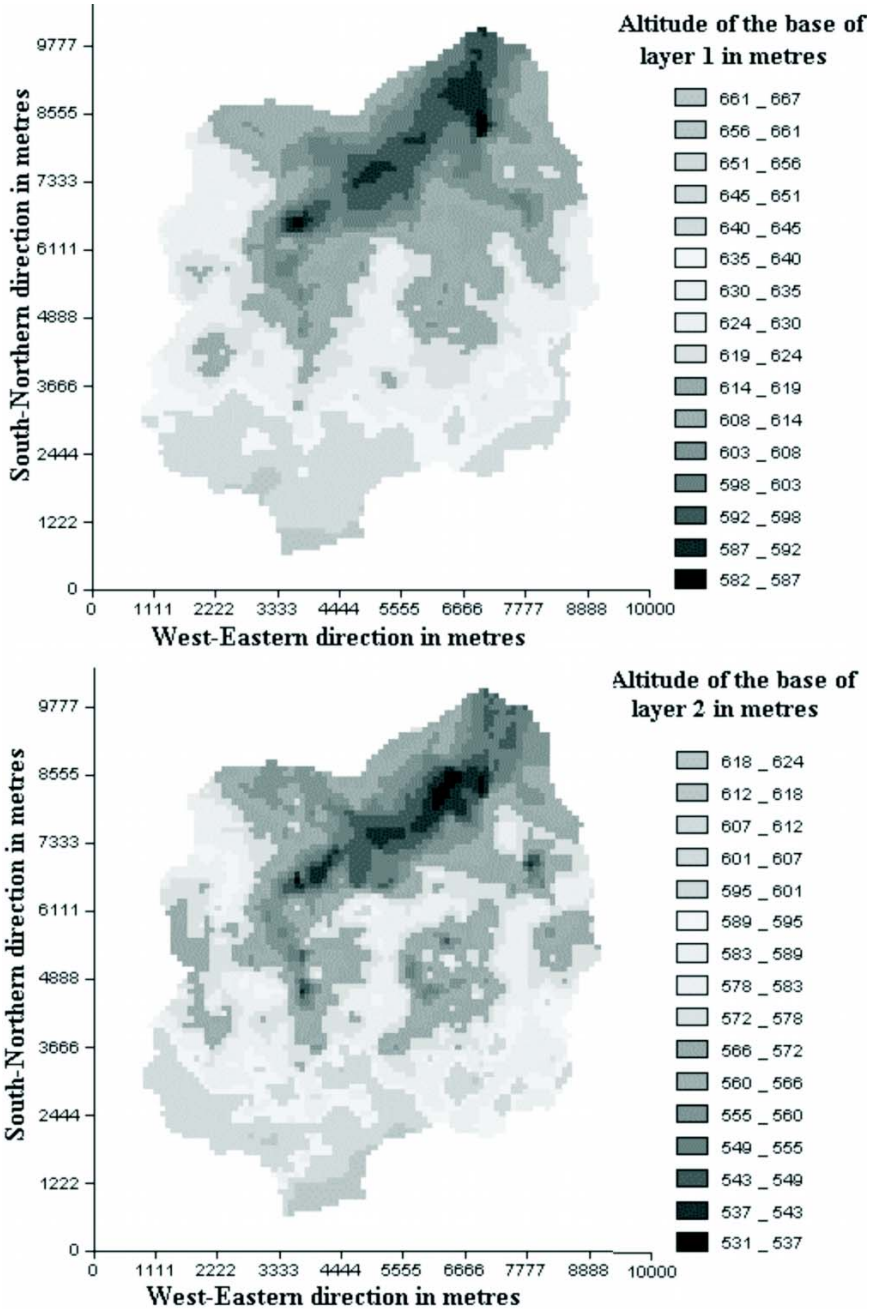

Figure 4. Aquifer bottom of layers 1 and 2 (asl, in m).

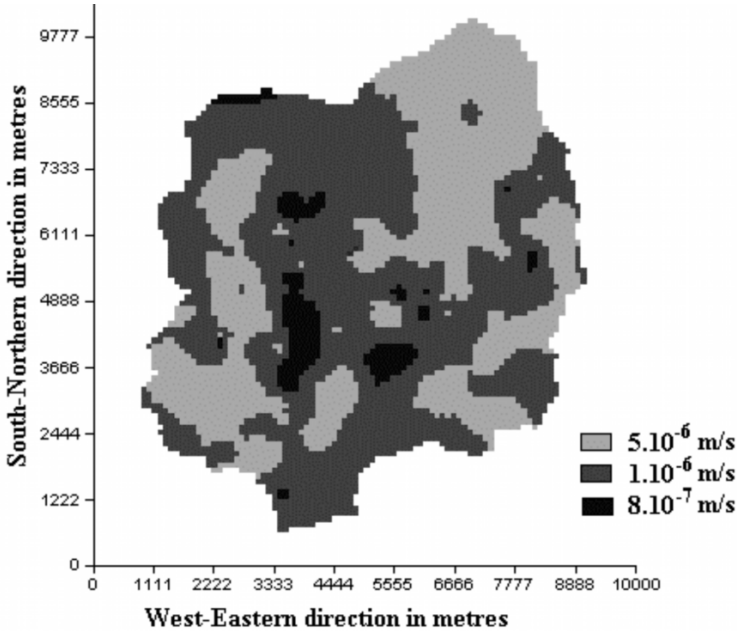

Figure 5. Hydraulic conductivities in the weathered layer, after calibration.

Figure 5 shows the distribution of the calibrated hydraulic conductivities for the weathered layer. They range between 8.10^{-7} m.s^{-1} and 5.10^{-6} m.s^{-1}. The transmissivities were calculated from the results of 34 aquifer tests in the weathered-fissured granite layer. But the high variability observed in the field and the difficulties of matching the simulated heads with the measured ones led to additional manual calibration of the hydraulic conductivities in the model.

Average hydraulic conductivity obtained by calibration was compared with the equivalent horizontal hydraulic conductivity calculated by the FRACAS model (Bruel et al., 2002), a "discrete fracture network" model, which was used to interpret 25 slug tests. The hydraulic conductivities in the weathered-fissured granite layer are shown in Figure 6. They exhibit large variability (1.10^{-7} to 3.10^{-5} m.s^{-1}) from one place to another because of the heterogeneity of the rocks.

In the weathered-fissured granite layer, linear heterogeneities (impervious vertical barriers) had to be introduced into the model because this was the only way to take into account the observed piezometric data. These heterogeneities were attributed to the dykes that crop out in the studied area, to a South-North quartz reef crossing the watershed and to some assumed extensions of dykes (Fig. 6).

The specific yield was taken to be 2.4% in the weathered rocks. This value is an average of the specific yields observed in the weathered rocks

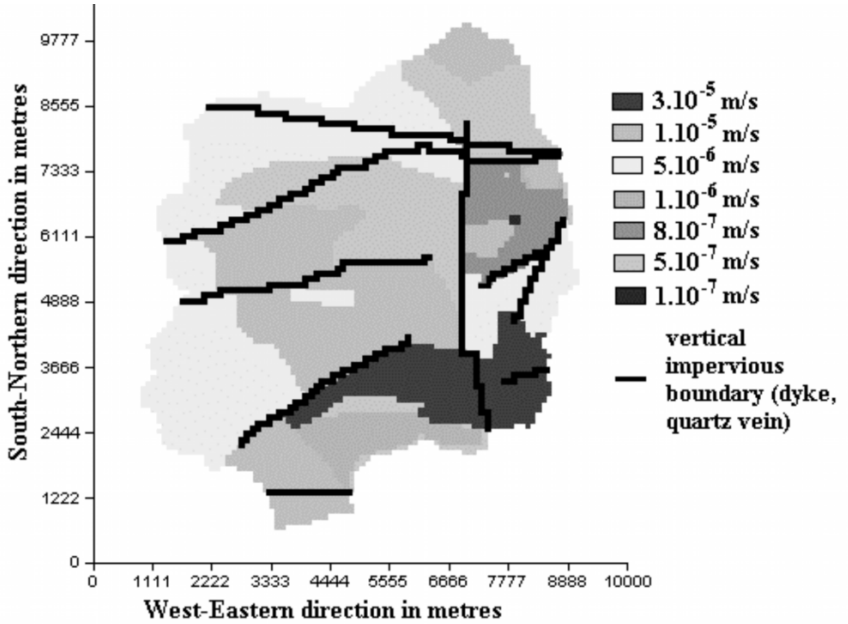

Figure 6. Hydraulic conductivities in the weathered-fissured granite layer, after calibration.

of similar watersheds (Rangarajan and Prasada Rao, 2001). The specific yield of the weathered rocks was also used for the calculation of preferential recharge. This value lies within the orders of magnitude given by the Proton Magnetic Resonance (PMR) measurements carried out in the watershed (Legchenko and Baltassat, 1999). In the fissured granite, this specific yield is assumed constant at a value of 1%, which is close to the value deduced from the discrete-fracture network interpretation (0.8%, Bruel et al., 2002), from pumping test interpretations (0.63%; Maréchal et al., 2004) and water-table fluctuation interpretations (1.4%; Maréchal et al., 2006). Some sensitivity tests were made by decreasing the specific yield in layer 2 by one order of magnitude. This led to a lowering of the simulated water levels due to the effect of pumping.

Storativity of the weathered layer (as a confined aquifer) plays a role in the flow calculations only when this layer becomes saturated (Engerrand, 2002). Its value was taken as 8.10^{-5}. For layer 2, the storativity value was set at 1.10^{-5}.

Aquifer Flows: Recharge, Discharge and Irrigation Return

Total recharge can be divided into three main components (Lerner et al., 1990): direct recharge (by direct vertical percolation through the vadose zone - saprolite), indirect recharge (percolation to the water table through the beds of surface-water courses, almost nil in the study area due to absence of

water in surface streams) and local recharge (various scale pathways such as those due to cracks, roots and trenches, dug-wells, brick factories and major landscape features) as preferred path.

The direct recharge was calculated on the basis of tritium injection tests that were carried out in 1999 and 2000. The interpretation by piston flow of the tests indicated that between the end of July 1999 and November 1999, the direct recharge was 22.2 mm (Rangarajan and Prasada Rao, 2001) and that during the 2000 monsoon, the direct recharge was 42 mm. The GARDENIA code was used at a daily time-step to calculate the balance between:

- Rainfall (daily data from a rain gauge located in Maheshwaram village).
- Potential evapotranspiration, calculated from the evaporation in a Pan A and multiplied by a factor of 0.9 (Monteith et al., 1989). The data are daily when collected at Maheshwaram village and weekly, from an average of six years of monitoring at the CRIDA farm (CRIDA, 1991-2000), when they are not available at Maheshwaram.
- Run-off. For the Musi basin, the Central Water Commission calculated a run-off/rainfall ratio of 11.2 % for the period 1989-1994.
- Available water capacity of the soil. The most common soils in the area have an available water capacity ranging from 75 to 110 mm (CRIDA, 1990).

The parameters of the GARDENIA code (run-off and available water capacity) were calibrated for 1999 and 2000 to obtain the measured 22.2 mm and 42 mm of recharge, respectively, for these periods, as obtained by tritium injection. The same parameters were then used in the code to estimate the recharge for the years 2001 and 2002.

Indirect and local recharge was calculated from the groundwater level rise in the weathered rocks during the tritium experiments of 1999. In 2000, most of the dug-wells located near the tritium injection points were dry, preventing us from estimating the preferential recharge. It was thus calculated only for 1999 with the specific yield value of the weathered layer that was known for similar watersheds (Rangarajan and Prasada Rao, 2001) and the groundwater level fluctuations measured in the dug-wells within this layer.

Table 1 shows the calculated direct, indirect and local recharge for the years 1999, 2000 and 2001.

Table 1: Direct, indirect and local recharge for years 1990-2001

Year	*Direct recharge (mm)*	*Indirect and local recharge (mm)*	*Total recharge (mm)*
1999	22.2	13.8	36
2000	42	25	67
2001	83	35	118

The major part of the groundwater withdrawal from the system is due to pumping from the wells. Various means were used to cross-check the estimates; two quite independent methodologies, viz. a direct one based upon the well inventory including the location of the wells, their discharge and pumping duration etc., and an indirect one based upon the demand using data on irrigated areas, cropping pattern and crop water requirements were applied.

Evaluation of the discharge rates due to pumping from the well inventory survey is a direct method of estimation and also provides the grid-wise information as the wells pumping the groundwater can be plotted on the grids. For the years 2000, 2001 and 2002, all the wells drilled up to 2000, 2001 and 2002 respectively were taken into account. The total yearly amount of groundwater withdrawal from the aquifer is given in Table 2. The groundwater pumping is mainly from the 2nd layer due to water level declines but the return flow from the irrigated fields occurs in the 1st layer. It was deduced from the pumping according to:

- Andhra Pradesh Groundwater Department (APGWD) (personal communication, 2000) report on Maheshwaram land use, and
- APGWD (1977) report on hydrologic parameters of groundwater recharge in Andhra Pradesh.

that 86% of the pumped water is used for the rice and 14% for other crops.

In the APGWD report (1977), experiments on the return flow from the rice in a nearby watershed showed that 55 to 88% of the irrigation water returned to the aquifer. After calibration, 60% of return flows from the rice and 20 % from the other crops were assumed. In the model, we do not distinguish between the locations of the rice and the other crops, because they are not known. The average return flow of one crop (rice/other) is then taken as:

$$0.86 \times 60 + 0.14 \times 20 = 54.4 \text{ or } \approx 55\% \text{ of return flow from the withdrawals.}$$

Simulation and Calibration of the Model

The time-steps of the hydrodynamic calculation in transient flow are 14 days during the dry season and one week in the rainy season (they are daily when it rains). The MARTHE code uses GARDENIA to calculate the hydroclimatic balance; this balance is calculated with a weekly time-step during the dry season and a daily one during rainy days throughout the year.

The fitting of the model was carried out by calibrating the following parameters:

- the hydraulic conductivities of the two layers; and
- the return flow from withdrawals.

The fitting criteria were based on:

- probable orders of magnitude of the fitting parameters; and
- the similarity between the hydraulic heads observed in the project wells in the field and the simulated ones.

Groundwater Balance

In 2000, the balance (storage variation) is negative (Table 2). The withdrawals are greater than the recharge and the storage decreases. The pumping wells are in operation at 99.9% of normal capacity. The discharge from the prescribed head-boundaries is 1.3% of the recharge, which is negligible. The overflows are nil.

For 2001, the balance is positive. The recharge is greater than the withdrawals and the stock increases. The pumping wells are in operation at 99.7%. The discharge from the prescribed heads is 1.8% of the recharge, which again is negligible. The overflows are 0.2% of the recharge, which is also negligible. The aquifer overflows are located near the draining meshes, which seems logical.

In 2002, the balance is strongly negative. The recharge is weaker compared to the other years and the withdrawals have increased. The pumping wells are in operation at 97.6%. But the return flow is calculated on the basis of the maximum demand and not on the basis of the actual withdrawals; in this case, because the quantity of water that cannot be pumped is not negligible compared to the demand for water, the prescribed return flow is slightly over-estimated and the balance is optimistic. In fact, the return flows range between 6,720,000 m^3 and 6,560,000 m^3. The discharge from fixed heads is 3.1% of the recharge. The overflows are 0.2% of the recharge, which is negligible and also located near the draining meshes.

Table 2. Annual water balance in Maheshwaram watershed

	1/1/–31/12/2000	*1/1/–31/12/2001*	*1/1/–31/12/2002*
Recharge ($m^3.y^{-1}$)	3,521,000	6,213,000	2,372,000
Return flow ($m^3.y^{-1}$)	5,214,000	6,228,000	6,720,000
Outlet from fixed heads ($m^3.y^{-1}$)	–46,000	–110,000	–74,000
Withdrawals ($m^3.y^{-1}$)	–9,469,000	–11,293,000	–11,927,000
Groundwater overflows ($m^3.y^{-1}$)	0	–13,000	–5,000
Storage variation ($m^3.y^{-1}$)	–780,000	1,026,000	–2,912,000
Balance deviation (%)	–0.02	–0.02	0.42

Analyses of the Simulation/Calibration and Prediction

A comparison between the simulated heads and the measured ones for January 2001 under steady state conditions shows that most of the water levels are well simulated and are falling on the 450 line. The comparison between the

simulated groundwater levels in the transient condition shows a satisfactory calibration as the differences (Fig. 8) are more or less in the tolerance limit.

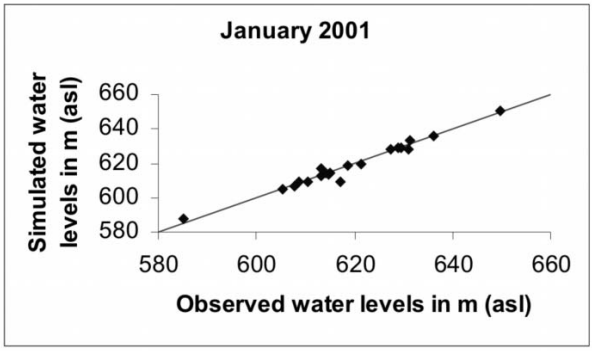

Figure 7. Comparison between simulated and calculated heads for January 2001 in Steady State Simulation.

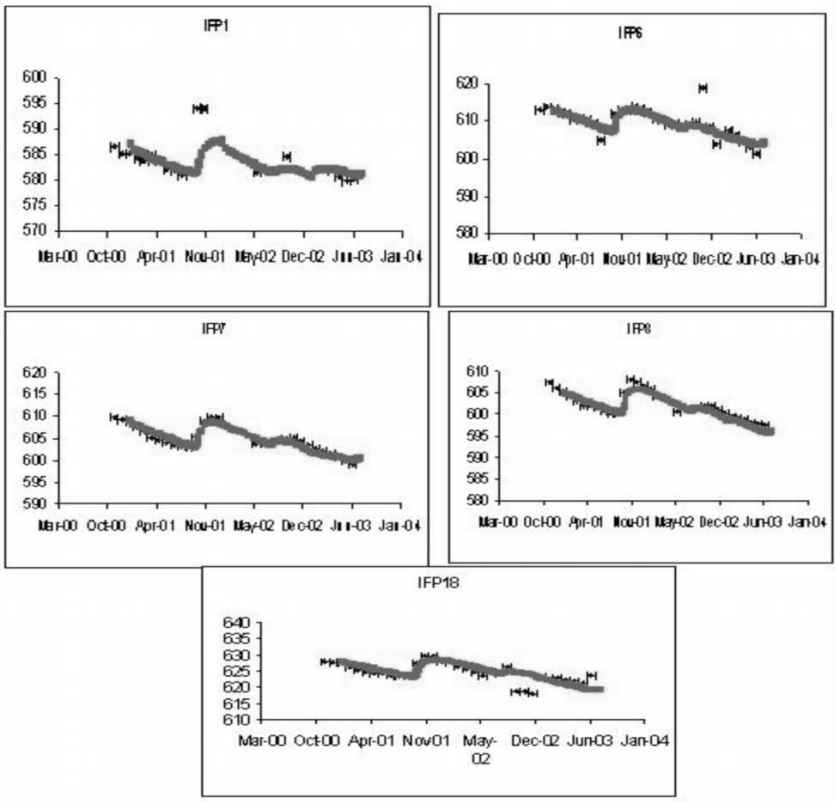

Figure 8. Comparison of the simulated groundwater levels (continuous line) and observed ones (stars).

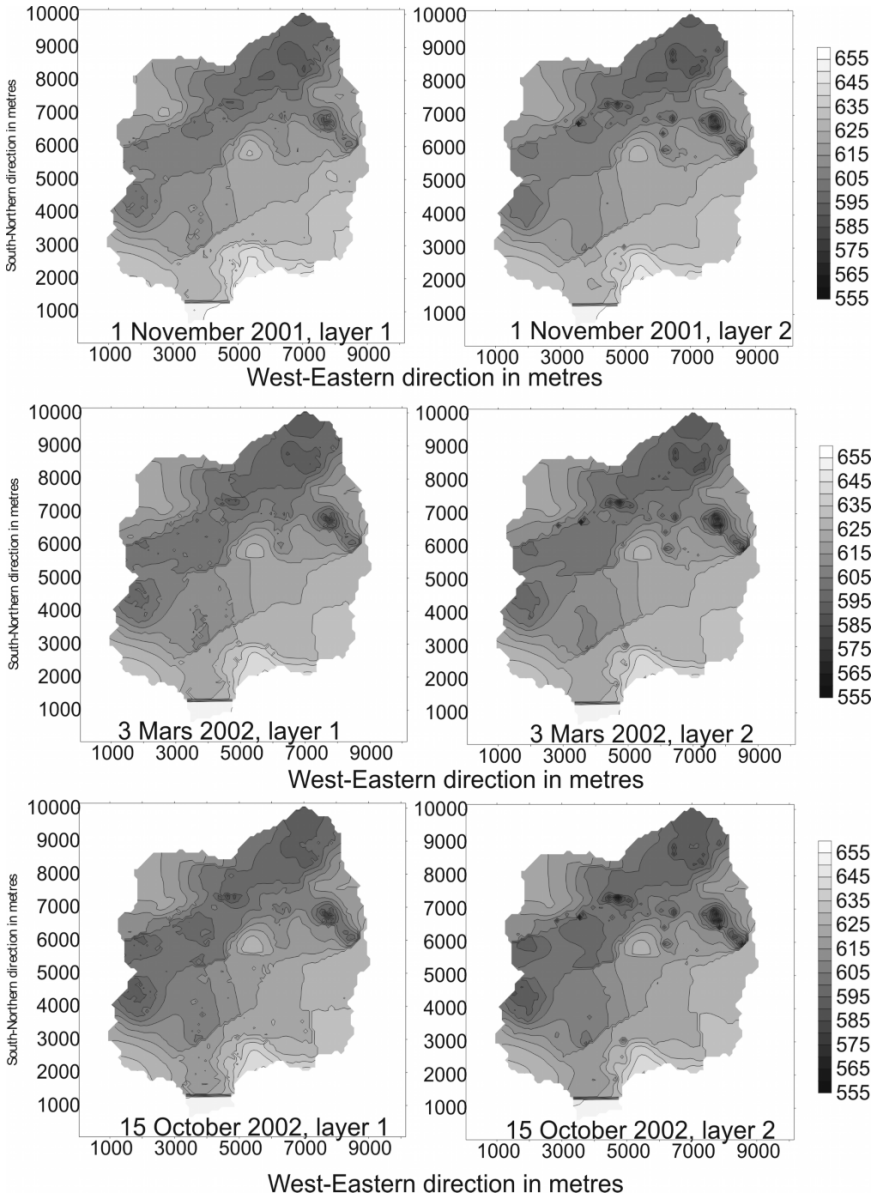

Figure 9. Simulated water levels for layers 1 and 2.

Figure 9 presents some simulated water-level maps for both layers. There is not much difference in the water levels between layer 1 and layer 2 except in the zone of large groundwater withdrawals where layer 2 shows lower hydraulic heads than layer 1.

Some predictive scenarios were tested until the year 2023 assuming:

- that the recharge was set at a constant value equivalent to the average of the recharge calculated between 1986 and 2002; and

- that the recharge varied as it had done between 1986 and 2002.

In both scenarios, the water demand was set constant and equal to the one in 2002.

If the water demand increases, the scheme is different. Figure 10 shows an extrapolation of the water demand over the next 20 years. This figure is only an example. It proposes a logarithmic increase in the water demand justified by the assumption that the yearly increase of the number of wells will decrease due to a saturation of the land use. With this figure, the number of wells located in the watershed will have increased from 709 to 1004 in January 2023.

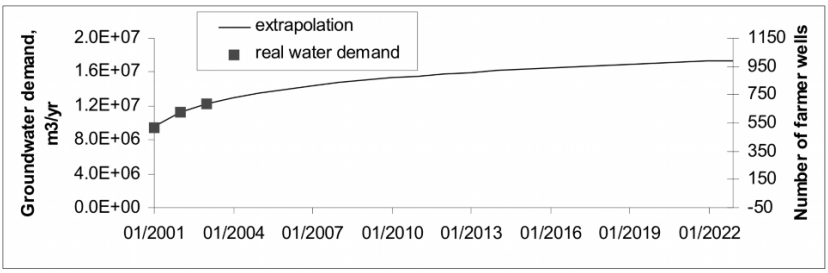

Figure 10. Anticipated water demand for the next 20 years.

Predictions were made with this new scenario. The groundwater level decreases rapidly (Figure 11). In the longer term (a few more years), the

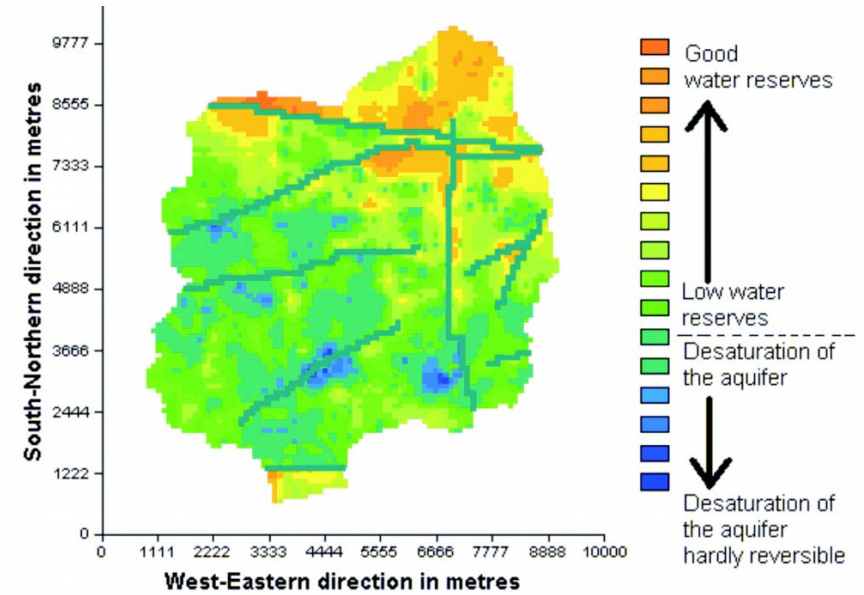

Figure 11. Groundwater status in 2023.

groundwater storage will be directly equivalent to the recharge. The monsoon will allow the aquifer to recharge but the irrigation will, within one year or less, empty the aquifer until the next monsoon season. In these conditions, the farmers will be more vulnerable to dry years than at present and may not be able to grow two or even one crop in these years. This will lead to economic instability and hardship for the farmers.

CONCLUSION

The flow in a weathered-fractured coupled system of aquifers was simulated using two layers model. Such situation is quite representative of the aquifers in granitic terrains. The special condition in this particular case has been that in most of the simulation period the aquifer in the weathered layer has been dry. In the two-layer aquifer model the upper layer being the weathered rocks was simulated as porous medium with comparatively low variability in hydraulic property but in the lower layer the weathered-fractured rocks was simulated as equivalent porous medium with highly variable hydraulic properties and contrast. The special case is also due to the fact that no separating layer exists nor is simulated between the weathered and fractured layers. For a majority of wells, hydraulic head simulations are in accordance with the water levels observed in the project wells for the years 2001 and 2002. Hydraulic heads that are not in accordance with the field observations are located in areas where the withdrawals have been intensive and are to be verified. The average hydraulic conductivity and the specific yield of the weathered-fissured layer are in accordance with those found with the "Discrete Fracture Network" model used to interpret the pumping tests in the aquifer (Bruel et al., 2002). The model has to be further improved and calibrated for the heterogeneities in the hydraulic properties by accurately estimating other input parameters. The return flow from the irrigation water is very difficult to validate. It is an approximate parameter that can also be calibrated with the model. Although the model was calibrated only for two years for which the data existed, some predictive scenarios were tested for further 20 years.

The results of the predictive model with the anticipated scenario show that if the water demand increases, the water levels in the watershed will decrease drastically everywhere. More and more wells will become dry and the groundwater storage at the beginning of a given year will be entirely dependent on the recharge of that year. In other words, there will not be any more reserves in the aquifer (Custodio, 2002) to even out the temporal variability of recharge from year to year. This will lead to difficulties for the farmers and economic instability.

REFERENCES

Andhra Pradesh Groundwater Department (APGWD), 1977. Studies on Hydrologic Parameters of Groundwater Recharge in Water Balance Computations, Andhra Pradesh. Government of Andhra Pradesh Ground Water Department, Hyderabad. Research series no. 6, 151 p.

Bruel, D., Engerrand, C., Ledoux, E., Maréchal, J-C., Touchard, F., Subrahmanyam, K. and Ahmed, S., 2002. The Evaluation of Aquifer Parameters in Maheshwaram Mandal, RR dist., AP., India. Ecole des Mines de Paris, CIG, technical report LHM/RD/02/28, July 2002, updated November 2002, 27 p.

Chilton, P.J. and Foster, S.S.D., 1995. Hydrogeological Characteristics and Water-Supply Potential of Basement Aquifers in Tropical Africa. *Hydrogeology J.*, **3(1):** 36-49.

CRIDA, 1990. Soil Map of Hayathnagar Farm and Appendix. Centre for Research in Dry-land Agriculture, Ranga Reddy District, Andhra Pradesh, India.

CRIDA (1991-92; 1993-94; 1994-95; 1997-98; 1998-99; 1999-2000). Annual Reports. Centre for Research in Dry-land Agriculture, Ranga Reddy District, Andhra Pradesh, India.

Custodio, E., 2002. Aquifer Overexploitation: What does it mean? *Hydrogeology J.*, **10(2):** 254 - 277.

Legchenko, A. and Baltassat, J.M., 1999. Application of the "Numis" Proton Magnetic Resonance Equipment for Groundwater Exploration in a Fractured Granite Environment 30 km south of Hyderabad, India. BRGM, Internal report—December 1999. R40925, 44 p.

Lerner, D.N., Issar, A. and Simmers, I., 1990. A Guide to Understanding and Estimating Natural Recharge. Int. Contribution to hydrogeology, I.A.H. Publ., 8, Verlag Heinz Heisse, 345 p.

Maréchal, J.C., Dewandel, B., Ahmed, S., Galeazzi, L. and Zaidi, F.K., 2006. Combined Estimation of Specific Yield and Natural Recharge in a Semi-arid Groundwater Basin with Irrigated Agriculture. *J. Hydrol.*, in press.

Maréchal, J.C., Dewandel, B. and Subrahmanyam, K., 2004. Use of Hydraulic Tests at Different Scales to Characterize Fracture Network Properties in the Weathered-fractured Layer of a Hard-rock Aquifer. *Water Resour. Res.*, **40:** W11508, doi:10.1029/2004WR003137.

Marsily, G. de, 1986. Quantitative Hydrogeology: Groundwater hydrology for Engineers. Academic Press, Orlando, Fl.

Rangarajan, R. and Prasada Rao, N.T.V., 2001. Natural Recharge Measurements in Maheshwaram Granitic Watershed, Ranga Reddy district, Andhra Pradesh, India - 1999 Monsoon. Technical Report No. NGRI-20001-GW-298, National Geophysical Research Institute, Hyderabad, India, 14 p.

Thiéry, D. and Boisson, M., 1991. Logiciel GARDENIA modèle Global A Réservoirs pour la simulation des DEbits et des NIveaux Aquifères. Guide d'utilisation (version 3.2). BRGM, R32209.

Thiéry, D., 1993. Logiciel Marthe: Modélisation d'Aquifères par un maillage Rectangulaire en régime Transitoire pour le calcul Hydrodynamique des Ecoulements Version 4.3. Rapport BRGM.

18 Regional Simulation of a Groundwater Flow in Coastal Aquifer, Tamil Nadu, India

L. Elango and C. Sivakumar

Department of Geology, Anna University
Chennai, India

INTRODUCTION

Increasing demand for groundwater due to ever increasing population has initiated the need for effective management of available groundwater resources. During the past two decades, the water level in several parts of India has been falling rapidly due to increase in pumping of ground waters. Proper management of aquifer systems is necessary as groundwater is the major source for domestic and industrial purposes, especially in urban and semi urban areas. Groundwater modelling is a powerful management tool which can serve multiple purposes such as providing a framework for organising hydrologic data, quantifying the properties and behaviour of the systems and allowing quantitative prediction of the responses of those systems to externally applied stresses. A number of groundwater modelling studies have been carried out around the world for effective groundwater management (Corbet and Bethke, 1992; Storm and Mallory, 1995; Gnanasundar and Elango, 2000; Senthil Kumar and Elango, 2004). Such a study was carried out in the coastal aquifer located south of the city of Chennai, India. In addition to this, local residents also pump water from this aquifer. This aquifer is under stress due to pumping of groundwater to meet the ever increasing water needs of the city. The present study was carried out with the objective of developing a numerical model for this area in order to understand the behaviour of the system with the changes in hydrological stresses. The finite difference computer code MODFLOW (Modular 3-d finite difference flow) with Groundwater Modelling System (GMS) as pre- and post-processor was used to simulate the groundwater flow in this study.

DESCRIPTION OF THE STUDY AREA

The study area lies just south of Chennai city and extends from Adyar river in the north to Muttukkadu estuary in the south. It covers an area of 20 km in length and 3 km in width. The eastern side of this area is bounded by the Bay of Bengal as shown in Fig. 1. Climate of this area is characterised by an oppressive hot summer, dampness in atmosphere nearly throughout the year and good seasonal rainfall. The summer season is from April to June which is followed by the southwest monsoon season from June to September. October to December constitutes the northeast monsoon season with the associated rains being confined to November and December. Average total rainfall is about 1260 mm/year.

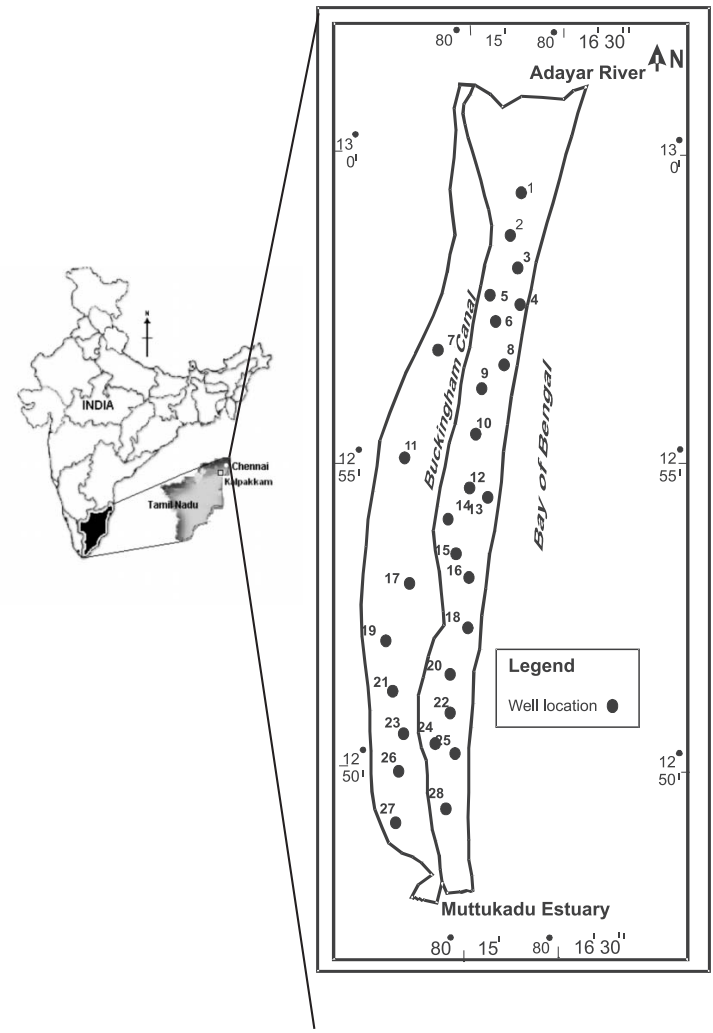

Figure 1. Study area with location of monitoring wells.

Geology and Hydrogeology

The study area exhibits varied physiographic features with elevation ranging from 1.0 to 11.5 m above MSL. The ground surface slopes towards the east and west from the central elevated portion. The region which lies towards the west of the Buckingham Canal has topographic elevation varying between 1.0 and 8.0 m above MSL. Western boundary of the study area has the highest elevation of 8.0 m above MSL. Geologically, the area comprises unconsolidated sandy formation of different depositional environments belonging to Quaternary age. The alluvial deposits are comprised of interlayered clay, silt, sand, gravel and pebble beds. These formations overlie the charnockites of Archean age. Charnockites occuring below this sandy formation function as impermeable strata or bed rock. The total depth of the aquifer system ranges between 3 and 23 m (Gnanasundar and Elango, 2000). The hydraulic conductivity of the aquifer lying west of the Buckingham Canal has values between 25 and 35 m/day, while the sub basin along the east of the canal has high hydraulic conductivity with values ranging between 45 and 75 m/day. The specific yield of the aquifer ranges from 0.17 to 0.23.

GROUNDWATER MODELLING

The computer software programme MODFLOW, Groundwater Modelling System (GMS), (McDonald and Harbaugh, 1998) developed by the United States Geological Survey was used for the present study to give input data and process the model output. This equation describes the groundwater flow under non-equilibrium and anisotropic medium, provided the principal axes of hydraulic conductivity are aligned with x-y Cartesian coordinates axes. The computer programme uses finite-difference technique and block-centered formulation to solve the groundwater flow equation for the three dimensional steady and transient flow in heterogeneous media of the South Chennai aquifer.

Model Formulation

The conceptual model of the hydrogeologic system was derived from a detailed study of the geology, borehole lithology and water level fluctuations in wells. Groundwater of the study area was found to occur in both alluvial formations and in the underlying weathered rocks. The measured groundwater head in monitoring wells, screened in the alluvial and weathered formation, is about the same. Based upon this information, the alluvial and the weathered fractured rocks can be considered as a single, unconfined layered system.

Grid Design and Boundary Conditions

The scanned map of the study area was imported in the MAP module of GMS with proper geographical registration. Boundaries and canal of this

map were digitised as polygons in the MAP module. This digitised map automatically generated grid pattern for use in the MODFLOW.

The gird pattern was developed by assigning a constant spacing 400 × 600 m. This spacing resulted in dividing the area into 40 rows and 30 columns (Fig. 2). A part of the area was discretised into a relatively finer mesh size as they comprised numerous pumping wells. Vertically this region was divided into a single layer of varying thickness. The Bay of Bengal, Muttukadu Estuary and the Adyar River were taken as constant head boundaries as the water levels in these water bodies are generally at mean sea level throughout the year. The Buckingham Canal was taken as internal constant head boundary with the constant head at mean sea level. The western boundary of the area was considered as a no flow boundary as shown in Fig. 2.

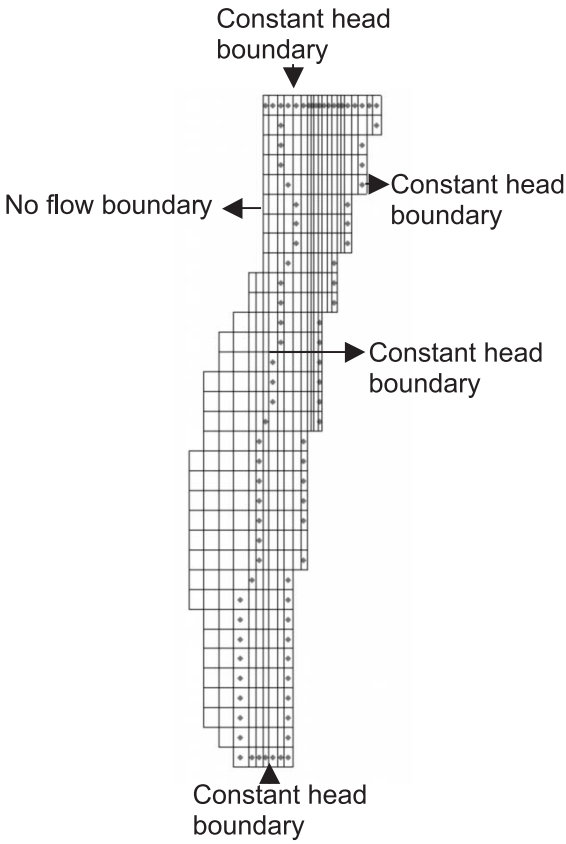

Figure 2. Model grid pattern and boundary conditions.

INPUT PARAMETERS

Aquifer Characteristics

Horizontal hydraulic conductivity of the sandy aquifer ranges between 25 and 75 m/day. Aquifer lying west of the Buckingham Canal has values between 45 and 75 m/day. The low K value along west of the canal is attributed to the presence of sandy clay and clay. The specific yield of the alluvial aquifer ranges from 0.17 to 0.23. The specific yield of the aquifer existing between the coast and the canal ranges between 0.21 and 0.23, while the other portion has values ranging between 0.17 and 0.19.

Groundwater Abstraction

The groundwater of the study area is abstracted for domestic, industrial and irrigational purposes. The average annual pumping is about 4.25 MGD. This has been obtained from the government agencies such as the Public Works Department and Metro Water. Pumping rate by private agencies was estimated through field visits. The pumping rate of wells that exist within the housing complexes in the northern part of the study area was also taken into account and pumping rates from these wells were estimated from well inventory survey by collecting data on pumping duration in a day. About 90% of the total pumping occurs within the regions lying between the Buckingham Canal and the coast. The pumping activity on western side of the canal is limited only to domestic purposes mainly for drinking and other household purposes due to poor groundwater quality.

Groundwater Recharge

The rate of rainfall recharge varies within the study area. Two recharge zones, A and B, have been demarcated based on the soil types, geomorphic pattern, land use and topography. The rainfall recharge rate in zone A is around 40-48% and in zone B it is around 25-35% as shown in Table 1. High recharge occurs in Zone A where sand and sand dunes occur. Recharge rate in the areas of zone B is quite less due to the presence of sandy clay/clayey soil.

Table 1. Recharge value incorporated in the model

Zone	*Recharge %*
Zone A (Sand)	40-48%
Zone B (Sandy clay/Clayey soil)	25-35%

Model Calibration

The calibration strategy was initially to vary the best known parameters as little as possible, and vary the poorly known or unknown values the most to achieve the best overall agreement between simulated and observed datasets. Transient state model calibration was carried out to minimize the difference between the computed and field water level conditions with the water level data of January 2000 in 28 wells distributed over the study area. Out of all the input parameters, the hydraulic conductivity and specific yield are the poorly known. Based on the data, it was decided to vary hydraulic conductivity, specific yield values up to 10% to get a good match of the computed and observed heads (Fig. 3). Table 2 shows the initial and calibrated hydraulic conductivity values of the simulated head. The root mean square error and mean error were minimised through numerous trial runs. Transient-state simulation was carried out for a period of six years from January 2000 to January 2006, with monthly stress periods and 24 hr time steps. The trial and error process by which calibration of the transient model was achieved included several trials until a good match was achieved between computed and observed heads over space and time.

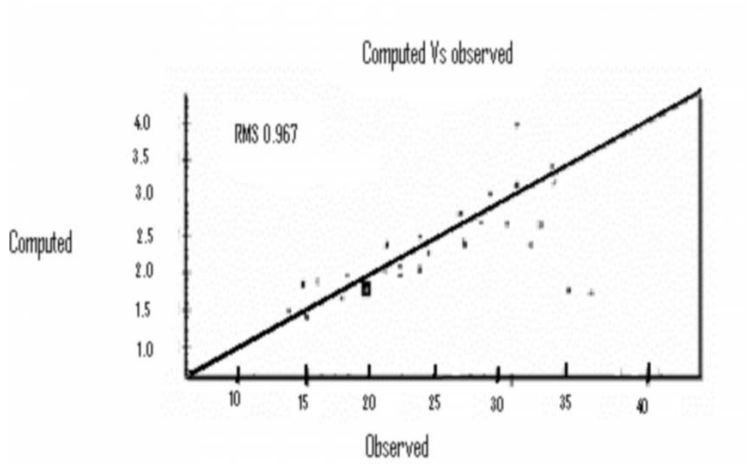

Figure 3. Computed and observed head in transient state calibration.

Table 2. Initial and calibrated hydraulic conductivity and specific yield of the simulated head

Geology of the area	*Hydraulic conductivity (m/day)*		*Specific yield*	
	Initial	*Calibrated*	*Initial*	*Calibrated*
Sand	75	81	0.22	0.31
Clayey sand	25	21	0.17	0.23

SIMULATION RESULTS

The model was simulated with the regional groundwater head and it was compared with the observed data of 28 wells. The predicted regional head generally follows the observed regional groundwater head. The regional groundwater head for the months of January 2000 and January 2006 is shown in Figs 4 and 5 respectively. In general, the simulated results indicate that this aquifer system is stable under the present pumping rate, excepting for a few locations along the coast where groundwater level has gone up to 1 m above sea level. The regional groundwater flow direction is towards east. There is fairly good agreement between the computed and observed heads. A comparison between the observed and computed head values for the observation well no. 8 is shown in Fig. 8. The computed head values mimic the observed head values.

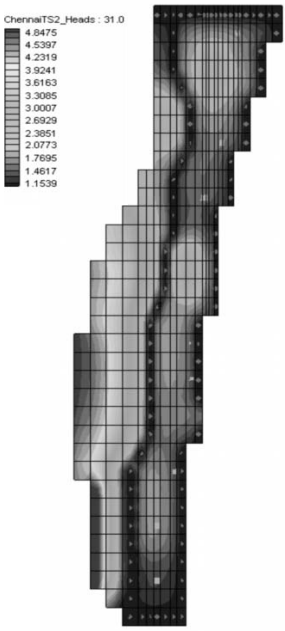

Figure 4. Computed regional groundwater head (Jan 2000).

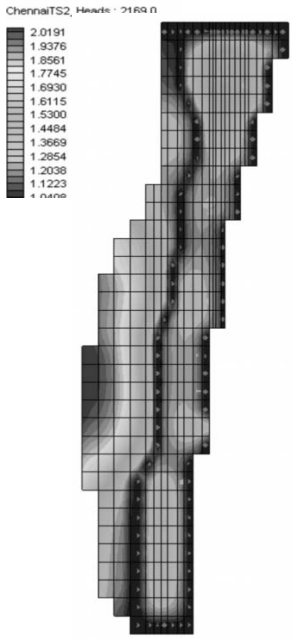

Figure 5. Computed regional groundwater head (Jan 2006).

Increase in Pumping

As groundwater is the major source of water for the cities from this region, there has been increase in pumping over the years. Hence, it is essential to know the behaviour of the system under increased hydrological stress. The model was simulated for the increase in pumping of 10% along the coastal region. The regional groundwater heads for the months of January 2000 and January 2006 are shown in Figs 6 and 7, respectively. A comparison between the observed and computed head values for the observation well no. 8 is

shown in Fig. 9. In well No. 8, the groundwater head is lowered by 0.5 to 1.5 m. The result clearly indicates that the aquifer is not stable and increase in 10% pumping in the coastal region does affect this aquifer system.

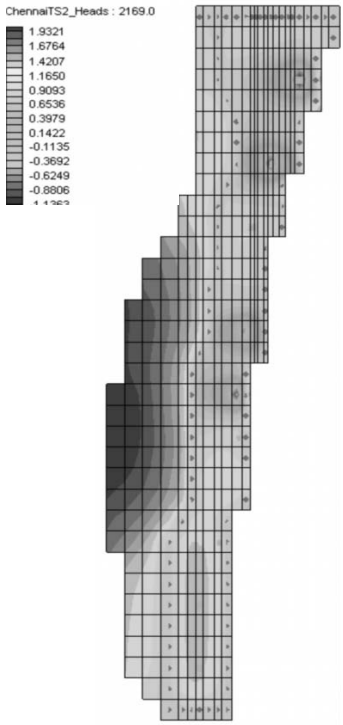

Figure 6. Computed regional groundwater head after 10% increase in pumping (Jan 2000).

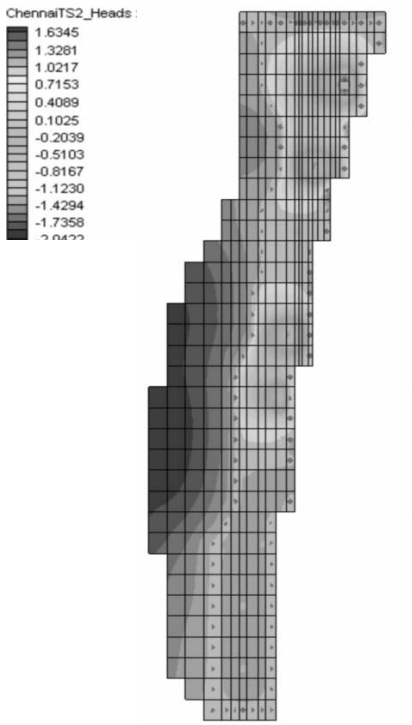

Figure 7. Computed regional groundwater head after 10% increase in pumping (Jan 2006).

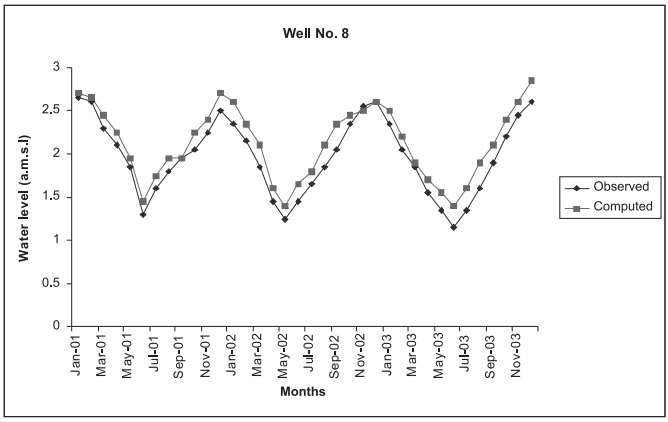

Figure 8. Computed and observed water heads at normal pumping in well no. 8.

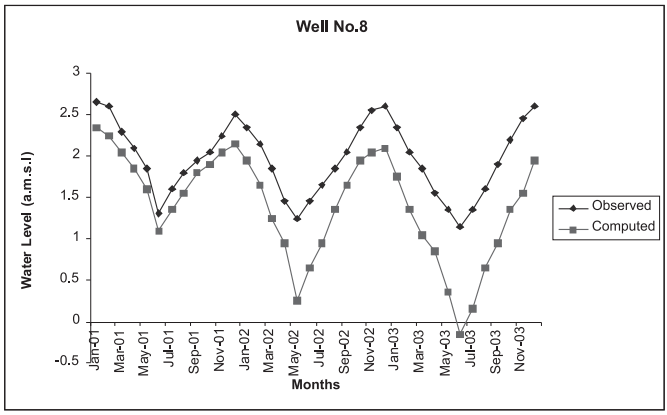

Figure 9. Computed and observed water heads at 10% increase in pumping in well no. 8.

CONCLUSION

Simulation of groundwater flow by three-dimensional mathematical model indicates that this aquifer system is stable under the present pumping rate. The computed groundwater head over space and time matches reasonably with the observed groundwater head with a difference of 0.4 m. Sensitivity analysis revealed that the developed model is very sensitive to recharge and, to some extent, hydraulic conductivity and specific yield. Increase in 10% pumping rate will lead to lowering of the groundwater head by 0.5 to 1.5 m. This will result in seawater intrusion in coastal regions of this aquifer system. The study indicates that the total abstraction from this aquifer has to be restricted to 4.25 mgd to prevent seawater intrusion.

REFERENCES

Corbet, T.F. and Bethke, C.M., 1992. Disequilibrium fluid pressures and ground water flow in western Canada sedimentary basin. *J. Geophys. Res.*, **97(B5):** 7203-7217.

Gnanasundar, D. and Elango, L., 2000. Groundwater flow modelling of a coastal aquifer near Chennai city, India. *Journal of Indian Water Resources Society*, **20(4):** 162-171.

McDonald, M.G. and Harbaugh, A.W., 1998. User's documentation for MODFLOW-98, an update to the U.S. Geological Survey modular finite-difference groundwater flow model, U.S. Geological Survey Open-File Report 96-485, pp56 ISBN 90 54 10 942 4.

Storm, E.W. and Mallory, M.J., 1995. Hydrogeology and simulation of groundwater flow in the Eutaw-Mcshan aquifer and in the Tuscaloosa aquifer system in northeastern Mississippi: U.S Geological Survey Water Resources Investigations Report 94-4223, 83.

Senthilkumar, M. and Elango, L., 2004. Three-dimensional mathematical model to simulate groundwater flow in the lower Palar River basin, southern India. *Hydrogeology Journal*, **12(4):** 197-208.

19 Hydrogeology of Hard Rock Aquifer in Kashmir Valley: Complexities and Uncertainties

G. Jeelani

Department of Geology and Geophysics
University of Kashmir, Srinagar, India

INTRODUCTION

Groundwater occurs in varied geological formations. Its occurrence in geological system is controlled mainly by the lithology (porosity and permeability) and structure (fractures, faults, dykes). The unconsolidated sediments referred to as continuous media, although vulnerable to contamination under shallow conditions, always form important source of water due to appreciable porosity and permeability. However, the water supply from these aquifers is dwindling worldwide due to overexploitation, global warming, easy exploitation, poor management etc. As the demand of freshwater exceeds rapidly than its renewal, the groundwater levels have gone down rendering a good number of wells dry. Hard rocks can also be good aquifers only if the secondary porosity is developed in the form of fractures or solution cavities and/or weathering. Fortunately all consolidated subsurface rocks are fractured to some degree with a scale ranging from microcracks to crustal rifts (Bonnet et al., 2001). The fractures generally increase the hydraulic conductivity of the rocks if the discontinuities are more permeable than the parent rock. Sometimes fractures may form barriers to flow if the contained material is less permeable than the host rock. Geological formations with fractures, solution cavities and large openings are referred to as discontinuous media. The occurrence, exploration and exploitation of groundwater in these media continue to intrigue and challenge hydrogeologists (Narasimhan, 2005) due to very high heterogeneity and anisotropy. Karst is commonly considered as the result of the solution process of carbonate rocks, viz., limestone and dolomite (Bakalowicz, 2005). Generally, fractured media do not constitute highly productive aquifers due

to limited fracture dimensions. However, most carbonate rocks are karstified during geological time, with the development of poljes, sinkholes, dolines, caves etc. thereby forming highly productive aquifers. Generally less than 50 ky are required for development of an integrated karst network (Atkinson et al., 1978; Dreybrodt, 1998).

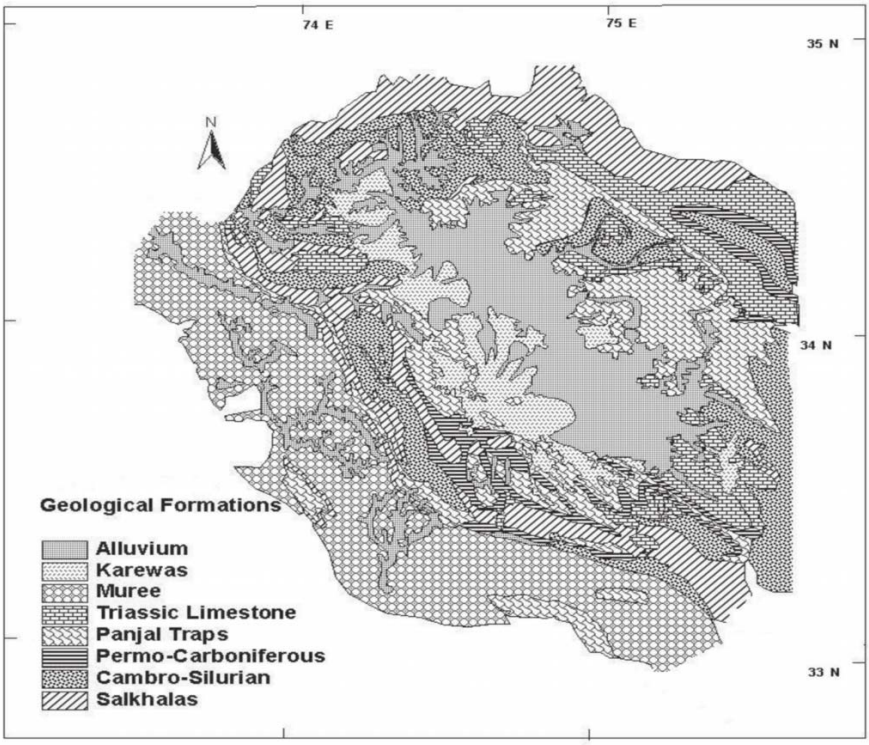

Figure 1. Geological map of Kashmir (modified after GSI, 1977)

Kashmir Valley (Jhelum basin), one of the many NW-SE oriented depressions of regional dimensions of Himalayan mountain system is an intermontane valley bounded by four major ranges; Pir Panjal Range towards SW, Saribal Range SE, Great Himalayan Range towards NE and Qazinag Range towards NW. The valley is about 135 km long and 40 km wide with a floor which in the Jhelum floodplain is only 1585 m above sea level, covering an area of about 12,757 km^2. It lies between the longitudes 33°25′N and 34°32′N and latitudes 74°0′E and 75°30′E. The Valley has been described as a great synclinal (de Terra and Paterson, 1939; Wadia, 1975), seated on the back of a vast nappe, Kashmir nappe (Wadia 1931). Spate and Learmonth (1976) described the complexity of physiographic features of Kashmir Valley as "predominance of majestic mountain ranges with snow clad peaks, large longitudinal valleys of subsequent streams occupying deep gorges, transverse gorges cut across the ranges by antecedent streams, strategic mountain passes

alluvial plains, preponderance of glaciers and patches of snow fields, plateau like features developed in thick accumulations of the Pleistocene glacial moraines (Karewas) and numerous glacial lakes". Geomorphologically the area is represented by a valley, high structural hills, small mounds of Karewa in the valley portion and colluvial fans below the hill slopes (Singh and Sharma, 1999). This complexity of physiographic units with numerous faults gives rise to complex aquifer system. However, in this article an attempt is made to describe the possibility of occurrence of groundwater in geological formations on a broader scale.

Diversified geological formations, lithological variations, tectonic complexity and geomorphological dissimilarities of Kashmir give rise to a variety of groundwater situations. The Valley is filled with soft rocks, unconsolidated sediments of Quaternary and Recent age, garlanded by and rested on hard rocks mostly volcanics and limestones (Fig. 1). Being part of the Himalayas, it has a complex tectonic history, consisting of diversified rocks that are folded, faulted and jointed. Groundwater occurs in both soft as well as hard rocks.

SOFT ROCK AQUIFERS

The Quaternary to Recent rocks comprising the alluvium and Karewa deposits are the important continuous media or unconsolidated formations. These sediments are comprised of clays, silts, sands, gravels etc. and may be good aquifers.

1. Karewas

The Karewas preserve a record of sediment deposition in a lake formed during the Late Neogene to Quaternary period (Bhatt, 1975, 1976; Singh, 1982; Burbank and Johnson, 1983) covering an area of about 5000 km^2. These unconsolidated fluvio-lacustrine deposits are exposed in the river valleys and the plateau margins of the Kashmir Valley, comprising alternations of clays, silts, sands with occasional boulder beds. The gravity surveys supported by refraction surveys, carried out in the Valley, indicate their maximum thickness as 2000 m resting on Triassic Limestone or Panjal Traps (Datta, 1983). Exploratory drilling carried out by ONGC in search of hydrocarbon; at Chattargam (very close to Yachigam, Pulwama) where the Karewa sediments encountered up to the depth of only 515 m below which 600 m of Triassic Limestone have been drilled and at Narbal where Karewa sediments directly overlie Panjal Traps at a depth of only 550 m. This indicates the narrowing of the Karewas towards the peripheral areas. Isolated exposures of Karewas form minor hillocks in the Valley. The frequent alternations of clay with sand and boulders, sub-horizontal disposition, almost gradational character and undulating nature of the Karewa deposits minimizes the possibility of occurrence of potential aquifers in these deposits. Groundwater

in the Karewa aquifers are mostly Mg(Ca)-HCO_3 type and have characters of interaction with volcanics indicating their reservoir in Panjal Traps (Jeelani 2004, 2005).

2. Alluvium

The central part of the Valley, which mostly covers the flood plains of the river Jhelum and adjoining streams, is filled with Recent alluvium. These deposits include alluvial tracts, flood plains, river terraces and talus and scree fans. The deposits are mostly water logged. The groundwater at some places along Jhelum River has evolved to chloride type and the total dissolved solids have increased to ~1500 mg/L. Besides, the groundwater is mostly associated with methane gas. The wells sunk in these deposits were abandoned by the people. However, towards the periphery the quality of groundwater is excellent of Ca-HCO_3 type. The groundwater in these areas has signatures of interaction with carbonates reflecting Triassic Limestone as the reservoir.

The exploratory drilling operations carried out by ONGC, CGWB and Directorate of Geology and Mining, Jammu & Kashmir, suggest that the aquifers are highly erratic, mostly lenticular with lesser aerial and vertical extent.

HARD ROCK AQUIFERS

The soft rocks are surrounded and underlaid by hard rocks. Broadly hard rocks of Kashmir can be divided on the basis of their distribution and dimensions into two broad divisions; Panjal Traps and Triassic Limestones. These rocks have been subjected to tectonic disturbances through geological time with the evolution of Himalayas, resulting into the deformation in the form of fractures. The fractures in the Triassic Limestone have progressively developed to karst due to solution action.

1. Panjal Traps

The Panjal Traps are upper Middle Carboniferous to Permian basic volcanic rocks of Kashmir. These are fine grain, generally light coloured, massive and hard block lavas with columnar and conjugate joints (Middlemiss, 1910; Bhat et al., 1881). The Panjal Traps are extensively developed with estimated thickness of about 2500 m. Active tectonics have developed the secondary porosity in the Formation, making it a productive aquifer. A number of perennial springs with a discharge of not exceeding 20 L/s emanate through it. The perennial and less fluctuating discharge of the springs reflects the productivity of the aquifer. The famous Chashma-Shahi spring emanate through this aquifer. The water is sweet and digestive, and was used by people from time immemorial. Pandit Jawahar Lal Nehru used to get this water to Delhi. The groundwater of this formation is really a mineral water

of Ca(Mg)-HCO_3 type. Presence of a number of trace elements, Fe, Cr, Cu, Mn, Zn, Co, Ni, F etc., although within the drinking water quality standards prescribed by World Health Organisation (WHO) and Indian Standards Organisation (ISO) has categorized the groundwater within this aquifer into the excellent quality.

2. Triassic Limestones

Of the three epochs of the Mesozoic era, only Triassic is well developed and lies conformably over Paleozoic. Triassic limestone consists of a thick series of compact blue limestone, argillaceous limestone and dolomitic limestone and covers a large area of Kashmir, with a thickness of about 850 m (Middlemiss, 1910; Wadia, 1975). The groundwater effluence takes place as natural springs through Triassic limestone with fairly high rate of discharge ranging from a few L/s to 1800 L/s (Jeelani, 2005). The perennial nature and high and fluctuating discharges of these springs are indicative of the extent of development of karstification and productivity of the formation. Historical famous springs beautified by Mughals include Verinag, Kokernag, Achabal, Andernag, Martandnag, etc. The groundwater of this formation is of Ca-HCO_3 type.

Groundwater Development

Although groundwater development in Kashmir Valley is at its first stage, the demand for groundwater is increasing due to unreliable and/or inadequate surface water or supplied water. The people started groundwater exploitation to meet their demands but abandoned the wells due to poor quality and/or association of clay and silt particles and/or drying within a small period in alluvium and/or Karewas as the wells were drilled on non-scientific basis. Due to scanty precipitation, mostly in winter, the Valley has witnessed drought from 1999 to 2004. Some springs and wells totally dried up. There was a drastic reduction (about one-third) of discharges of all perennial springs. Most of the areas were without water for drinking and other domestic purposes. The agriculture was the main to suffer. Because of increased water demand, the abstraction of the scarce groundwater resources from shallow aquifers, that are generally lenticular with less aerial and vertical extent, has led to the drying up of wells in many parts of the area, and the farmers could not sustain their agricultural activities.

REFERENCES

Atkinson, T.C., Harmon, R.S., Smart, P.L., Waltham, A.C., 1978. Paleoclimatic and geomorphic implications of $^{230}Th/^{234}U$ dates on speleothems from Britain. *Nature* **272:** 24-28.

Bakalowicz, M., 2005. Karst groundwater: A challenge for new resources. *Hydrogeol, J.,* **13:** 148-160.

Bonnet, E., Bour, O., Odling, N.E., Davy, P., Main, I., Cowie, P., Berkowitz, B., 2001. Scaling of fracture systems in geologic media. *Rev Geophys,* **39(3):** 347-383.

Bhat, M.I., Zinuddin, S.M., Rais, A., 1981. Panjal Trap chemistry and the birth of Tethys. *Geol Mag,* **118(4):** 367-375.

de Terra, H. and Paterson, T., 1939. Studies on the ice age in India and associated human culture. Carnegie Inst of Washington, DC p 354.

Dreybrodt, W., 1998. Limestone dissolution rates in karst environments. *Bulletin d'Hydrogeologie*, Centre d'Hydrog^eologie, Universite de Neuchâtel, **16:** 167-183.

GSI, 1977. Geology and mineral resources of the states of India, part X Jammu and Kashmir state. *Geol Sur Ind,* **30:** 1-71.

Jeelani, G., 2004. Effect of subsurface lithology on springs of a part of Kashmir Himalaya. *Himal Geol,* **25(2):** 145-151.

Jeelani, G., 2005. Chemical quality of Anantnag springs, Kashmir, India. *J. Geol Soc of Ind,* **66(4):** 453-462.

Middlemiss, C.S., 1910. Revision of Silurian-Trias sequence of Kashmir. *Rec Geol Surv India,* **40(3):** 206-260.

Narasimhan, T.N., 2005. Hydrogeology in North America: Past and future. *Hydrogeol J,* **13:** 7-24.

Singh, R. and Sharma, V.K., 1999. Geoenvironmental appraisal of Kashmir region. *Rec Geol Sur Ind,* **131(8).**

Spate, O.H.K. and Learmonth, A.T.A., 1967. India and Pakistan: A general and regional geography. Methuen Co, London. 439p

Wadia, D.N., 1931. The syntaxis of north west Himalayas: Its rocks, tectonics and orogeny. *Rec Geol Sur Ind,* **65:** 189-220.

Wadia, D.N., 1975. Geology of India. Tata McGraw Hill Co, New Delhi. 344pp.

Index

Abstraction 94, 238
Abstraction Rate 140
Alluvium 11, 13, 246
Analytical Models 211
Anisotropy 48, 50, 52, 57, 102, 103, 105
Apparent Resistivity 66
Aquifer Parameter Estimation 31
Aquifer Performance Test (APT) 93
Artesian Aquifers 7
Artificial Recharge 15, 16, 17, 57, 144

Backward Difference Approximation 215
Barker Theory 101, 108
Bessel Function 69
Best Linear Unbiased Estimator (BLUE) 176
Boundary Conditions 207, 221

Calibration 224, 227, 228
Cauchi Condition 208
Central Difference Approximation 215
Coefficient of Skewness 153
Cokriging 179
Compressive Stress 22
Conductive Fissure Zones (CFZ) 48, 51
Conduits 33, 194
Consolidated Formations 8, 9
Consolidated Sandstones 8, 9
Constant Flux Boundary 207
Constant Head Boundary 207
Continuous Stratiform Aquifer 42
Covariance 174
Crank-Nicolson Method 217
Cross-Validation Test 179
Cubic Law 21, 25, 126
Cubic Model 159

Dar Zarrouk Curves 70
Darcy Law 24, 201
Darcy Velocity 202
Dead Water 115
Decision Support Tool (DST) 58, 143
Deltaic Tracts 8
Depletion Effect 119
Digital Elevation Model (DEM) 51, 54
Dirichlet Boundary 207
Discharge 4, 40, 105, 118, 225, 227
Discontinuous Aquifer 7, 40, 41
Discrete Fracture Network 26, 28, 125
Dispersion 13
Double Porosity Model 26, 106
Double Water Table Fluctuation 142
Drainage Linearities 90
Drift 177
Drift Coefficients 177
Dupuit Formula 120

Electrical Profiling 67
Electrical Resistivity Tomography (ERT) 73
Electromotive Force 74
Equivalent Porous Medium (EPM) Model 26, 28
Evaporation 4, 16, 221, 226
Evaporation Flux 138
Evapotranspiration 2, 226
Evapotranspiration Component 147
Expectation 156
Explicit Approximation 215
Exponential Model 159

Finite Difference Method 212
Fisher Von Mises Distribution 125
Fissured Aquifer 41
Fissured Layer 44, 45, 47, 232
Foliation 21, 22, 33

Forward Difference Approximation 214
Fracas Software 125
Fracture Aperture 22, 28, 129
Fracture Skin 24, 26
Fractured Zone 219, 220

Gamma Ray Log 80
Gardenia 227
Gaussian Model 159
Geostatistical Optimization 172
Geothermal Gradients 21
Global Composite Aquifer 43, 44, 54
Granite 9, 13, 16, 29, 31, 33, 40, 43, 44, 48, 100, 221
Gringarten Method 104
Groundwater Balance 228
Groundwater Budget 57, 60, 143, 144
Groundwater Flow Equations 203
Groundwater Modelling 32, 208, 236
Groundwater Potential 4, 5, 13, 17, 41
Gyromagnetic Ratio 76

Hard Rock Aquifers 20, 32, 36, 57, 61, 123, 245
Homogeneity 21
Horizontal In- and Out-Flows 135
Horizontal Permeability 104, 132, 194
Hydraulic Characteristics 31, 36
Hydraulic Conductivity 9, 10, 28, 32, 41, 52, 108, 112, 114, 117, 119, 126, 222, 224, 232, 236, 238
Hydrodynamic Properties 41, 47, 57
Hydrogeology of Hard Rocks 21
Hydrogeomorphology 88, 89

Implicit Approximation 217
Injection Pulse 116
Intermontane Valley 8, 244
Intracratonic Basins 7
Intrinsic Hypothesis 156
Intrinsic Random Function 157
Intrusive Lineaments 72
Irrigation Return 57, 225
Isape Software 119
Isotropy 21

Jacob's Straight-Line Method 98

Karstified Rocks 244
Kriging Variance 195
Kriging with an External Drift 179

Lagrange Multiplier 173, 195
Larmor Frequency 76
Lenticular 246
Lineaments 8, 21, 22, 34, 49, 90
Linear Model 159
Log-Normal Distribution 125

Magnetic Resonance Sounding 75
Magnetic Susceptibility 74
Magnetometer 74
Marthe 221, 227
Mathematical Models 211
Mise-à-La-Masse Method 82
Modflow 234
Molecular Diffusion 13
Moving Neighbourhood 175
Multicriterion Decision Making (MCDM) 180
Multielectrode Resistivity 71

Neuman Method 102
Neumann Boundary 208
No Flow Boundaries 207
Non-Parallelism 22
Non-Stationary 200
Numerical Modelling 23, 61, 221
Numerical Models 26, 211

Ordinary Kriging 177, 183

Palaeowaters 14
Paleo-Landscape 54
Paleoweathering 54
Panjal Traps 246
Pediments 8, 89
Percolation 4, 16
Percolation Flow 134
Permeability 8, 22, 24, 25, 29, 43, 48, 53, 94, 105, 120, 129, 243
Photolineaments 90
Phreatic Aquifer 16
Pleistocene Glacial Moraines (Karewas) 245
Plutonic Rock 42, 43
Point Resistance (PR) Logging 79
Poisson Distribution 125
Porosity 8, 9, 10, 43, 53, 94, 129, 243
Precipitation 4, 13, 30
Prediction 228

Primary Porosity 9
Probability Distribution Function (PDF) 152
Pumping Pulse 116
Pumping Test 28, 31, 32, 48, 50, 93, 225, 232

Radon Methodology 58
Rainfall Recharge 13, 238
Recharge 4, 7, 13, 15, 21, 35, 36, 57, 220, 225, 226
Regionalized Variables 150
Resistivity Logging 80
Return Flow 14, 57, 135
Rock Discontinuities 21
Rose Diagram 128

Saprolite 43, 57
Schlumberger Array 67
Seawater Intrusion 14, 242
Secondary Porosity 8
Self-Potential Logging 79
Semi-consolidated Formations 10
Semivariogram (*see also* Variogram) 189
Sheeting Joints 29
Simulation 227, 228
Slug Test 31, 49, 50, 113, 124, 127, 224
Soft Rock Aquifers 245
Sounding Curve 69
Specific Yield 48, 57, 103, 224, 225, 236, 238, 239, 242
Spherical Model 159
Stability Criterion 216
Standard Deviation 187
Stefanesco Kernel Function 69
Step-Draw Down Test (SDT) 93
Storage Coefficients 93, 97, 119
Storativity 27, 44, 131, 132
Stream or River Head Dependent Boundary 208
Streaming Potential 82

Theis Method 32, 98
Theory of Regionalized Variables 183, 191
Transient State Model 239
Transmissivity 24, 27, 50, 93, 97, 106, 119, 126, 131, 132
Triassic Limestones 247
Tritium Injection Method 13, 36

Unconsolidated Fluvio-Lacustrine Deposits 245
Unconsolidated Formations 12
Unique Neighbourhood 175
Universal Kriging 177
Unsaturated Zone 13, 37
Unsteady State Radial Flow 118
Upscaling 131

Valley Fills 11, 89
Van Genuchten 126
Variogram 156, 194
Variography 178, 179
Vertical Electrical Sounding 69
Vertical Permeability 194
Vesicular Horizons 7
Volumetric Flux 126

Warren and Root Method 106
Water-Table Fluctuation Method 139
Weathered Zone 23, 46, 123, 219, 220, 221, 222
Weathered-Fissured Granite 224, 225
Weighted Index Overlay Analysis 90
Wenner Array 67

Zeta Potential 82